2019

Glial cell mechanisms regulate alcohol sedation in Drosophila melanogaster

Kristen M. Lee
Virginia Commonwealth University

Glial cell mechanisms regulate alcohol sedation in *Drosophila melanogaster*

A dissertation submitted in partial fulfilment of the requirements for the degree of Doctor of Philosophy at Virginia Commonwealth University.

by

Kristen Mary Lee
Bachelor of Science, Wagner College, 2014

Director: Mike Grotewiel, PhD
Assistant Graduate Dean
Associate Professor, Department of Human & Molecular Genetics

Virginia Commonwealth University
Richmond, Virginia
March, 2019

ACKNOWLEDGEMENT

First and foremost, I would like to thank my mentor, Dr. Mike Grotewiel, who has been extremely supportive of my research endeavors. When I walked into your office five years ago, I never would have imaged that a small screen would have blossomed into a dissertation project. Thank you for not only letting me pursue this project, but for being just as excited about it as I am. I feel extremely grateful to have you as a mentor, and I truly appreciate all of your advice, it has shaped me into a better scientist.

I would also like to thank Dr. John Bigbee. Thank you for being a haven of support and guidance throughout my time at VCU. And thank you for being the advisor, and so supportive, of the NeuroNerds. This organization has allowed me to form so many new friendships and has given me a sense of community outside of the lab.

I would like to thank my committee members, Drs. Dupree, Fuss, Davies and Lister who have been extremely enthusiastic at all my committee meetings. Thank you for providing helpful critiques and experimental ideas, and for always having an open door when I needed any additional guidance. I have appreciated all your support.

I would like to thank my F31 co-sponsor, Dr. Knapp, for being so present and responsive. Thank you for coming to my committee meetings and providing advice on my fellowship application. You guidance was vital for my fellowship's success.

A huge thank you also goes out to (Silly) Rebecca Schmitt, who has managed to be in the seat next to me almost every day these last five years. I could say a lot of weird stuff here, but to put it simply – thank you for turning a very small office into a home. I also thank all the Grotewiel lab members pass and present – Ian, Jena, Laura, and especially Brandon – you have all been awesome people that I have looked forward to spending each day with.

I am extremely grateful to have Christopher Dean in my life. Thank you for filling my free time with adventure, good food, and cute animals. I appreciate your endless encouragement.

Last but certainly not least, I would like to thank my family. My parents, Tom and Kathy, have been a constant source of support throughout my life. Thank you for being present and active in all my endeavors, I wouldn't be here today without you both. My brother and sister, Matt and Monica, are two of the best and funniest people I know. Thank you for always being a phone call away, and for knowing how to make me smile and laugh. I thank my family for coming to visit me in Richmond so frequently, and for making New Jersey such a hard place to leave every time I visit home. Your support has meant the world to me.

Table of Contents

List of Tables

List of Figures

List of Abbreviations

ADH: Alcohol Dehydrogenase

AKAP200: A kinase anchoring protein 200

ATP: Adenosine Tri-Phosphate

AUD: Alcohol Use Disorder

axo: axotactin

BBB: Blood Brain Barrier

Ca^{2+}: calcium

CCL2: Chemokine C-C motif Ligand 2

CNS: Central Nervous System

Cp1: Cysteine proteinase 1

DAG: Diacylglycerol

DBH: Dopamine Beta Hydroxylase

DREADDs: Designer Receptors Exclusively Activated by Designer Drugs

DSM: Diagnostic and Statistical Manual of Mental Disorders

EAAT: Excitatory Amino Acid Transporter

elav: embryonic lethal abnormal vision

Ent2: Equilibrative nucleoside transporter 2

ER: Endoplasmic Reticulum

GA25021: Cysteine proteinase 1 orthologue

GABA: Gamma-Aminobutyric Acid

Gal4: Galactose 4

Gal80: Galactose 80

GAT: Gamma-Aminobutyric Acid (GABA) transporter

GFAP: Glial Fibrillary Acidic Protein

GFP: Green Fluorescent Protein

GLAST: Glutamate-Aspartate transporter

GLT-1: Glutamate transporter 1

GPCR: G-Protein Coupled Receptor

GS: GeneSwtich

GT: Gliotransmitter

HCX: hydrogen/calcium exchanger

Iba-1: Ionized calcium-binding adapter molecule 1

IL1R: Interleukin 1 Receptor

IP_3: Inositol triphosphate

Jhl-21: Juvenile hormone Inducible 21

K^+: potassium

Kir: inwardly rectifying K^+ channel

LacZ: bacterial β-galactosidase Z

MAG: Myelin Associated Glycoprotein

MBP: Myelin Basic Protein

mCD8:GFP: membrane bound GFP

MCT: Monocarboxylate Transporter

MCU: Mitochondrial Calciume Uniporter

mGluR: metabotropic glutamatergic receptor

mRNA: messenger ribonucleic acid

Na^+: sodium

NCKX: sodium/calcium, potassium exhanger

nemy: no extended memory

NF-kB: nuclear factor kappa-light-chain enhancer of activated B cells

NMDA: N-methyl-D-aspartate

NPF: Neuropeptide F

NPY: Neuropeptide Y

n-syb: neuronal synaptobrevin

NT: neurotransmitter

Oct-TyrR: Octopamine-Tyramine Receptor (same as TAR1)

P2Y: purinoreceptor 2Y

P2X: purinoreceptor 2X

PIP_2: Phosphatidylinositol biphosphate

PLC: Phospholipase C

PLP: proteolipid protein

PNS: Peripheral Nervous System

PTP: Permeability Transition Pore

repo: reverse polarity

RNAi: ribonucleic acid interference

ROS: Reactive Oxygen Species

RU486: mifepristone

SNARE: Soluble N-ethylmaleimide sensitive factor Attachment Protein Receptor

ST50: Sedation time 50

TAR1: Tyramine receptor 1 (same as Oct-TyrR)

Tbh: Tyramine beta hydroxylase

Tdc2: Tyramine decarboxylase 2

TeTx: Tetanus Toxin

Th: Tyrosine hydroxylase

TLR: Toll-Like Receptor

TRAP-seq: targeted purification of polysomal messenger ribonucleic acid sequencing

TRP: Transient Receptor Potential

ts: temperature sensitive

TyrR: Tyramine Receptor

TyrRII: Tyramine Receptor 2

UAS: Upstream Activation Sequence

VGCC: Voltage Gated Calcium Channel

VMAT: Vesicular Monoamine Transporter

xCT: cysteine glutamate anti-transporter

Abstract

GLIAL CELL MECHANISMS REGULATE ALCOHOL SEDATION IN *DROSOPHILA MELANOGASTER*
Kristen Mary Lee

A dissertation submitted in partial fulfillment of the requirements for the degree of Doctor of Philosophy at Virginia Commonwealth University.

Virginia Commonwealth University, 2019.

Major Director: Mike Grotewiel, PhD
Assistant Graduate Dean
Associate Professor, Human & Molecular Genetics

Approximately 16 million people in America are diagnosed with Alcohol Use Disorder (AUD) but no efficacious medical treatments exist. Alcohol-related behaviors can be studied in model organisms, and changes in these behaviors can be correlated with either (i) a risk for alcohol dependence or (ii) a symptom/feature of AUD itself. Although AUD is a disease of the central nervous system, a majority of research has focused on the neuronal underpinnings, leaving glial contributions largely undescribed. We used *Drosophila melanogaster* (fruit fly) to identify genes whose expression in glia regulates alcohol sedation. Mammals and *Drosophila* have conserved behavioral responses to alcohol and functionally similar adult glial cells, especially astrocytes. Since previous research in mammals and flies has demonstrated that glia respond to alcohol

administration, we hypothesized that glia are important regulators of alcohol-related behaviors. To pursue this, we characterized a pan-glial steroid-inducible GeneSwitch transgenic fly, which allows gene manipulation within glia during adulthood. We performed a targeted screen and manipulated genes that were known to be expressed within *Drosophila* glia and measured their alcohol sedation sensitivity using the ethanol sedation assay. We identified the genes *Cysteine proteinase 1* (*Cp1*) and *Tyramine decarboxylase 2* (*Tdc2*). Knocking down Cp1 in cortex glia, as well as all glia during adulthood, increased alcohol sedation sensitivity and may also enhance rapid tolerance development. We could not identify what pathway Cp1 was functioning within to mediate this response, suggesting that Cp1 may have a unique function within glia. Knockdown or overexpression of Tdc2 in glia increased or decreased alcohol sedation sensitivity, respectively. Tdc2 functions upstream of the vesicular monoamine transporter (VMAT) and the SNARE complex to regulate alcohol sedation. These results were specific to astrocytes, as well as all glia during adulthood. These results suggest that tyramine synthesis via Tdc2 and its release via vesicular exocytosis regulates alcohol sedation. Taken together, these results suggest that glia are important regulators of alcohol-related behaviors in flies. Interestingly, fly cortex glia and astrocytes are functionally similar to mammalian astrocytes, indicating that these results may be translatable to mammals.

CHAPTER 1: INTRODUCTION

A. ALCOHOL ABUSE AND ALCOHOL USE DISORDER

Approximately 86% of people have drunk alcohol at some point in their lifetime, and roughly 2.4 billion people are currently alcohol drinkers worldwide[1]. While these statistics may not be surprising, 2.8 million deaths were caused by alcohol use in 2016, making alcohol the leading cause of premature death of people ages 18-49 worldwide[1,2]. Continued, problematic and severe alcohol consumption can lead to the diagnosis of an alcohol use disorder (AUD). Although AUD is a spectrum disorder, it is largely characterized by a (i) compulsive and uncontrolled use of alcohol and (ii) a negative emotional state when not using alcohol[3]. Depending on the number of DSM-5 criteria met, AUDs can be classified as mild, moderate or severe[3]. In 2015, it was estimated that 16 million people in the United States were living with AUD. However, only 7% of this population received any medical treatment[1]. No new pharmacotherapies for AUD have been approved in over a decade, and the only Food and Drug Administration approved drug is naltrexone[4]. Together, these statistics highlight the need to better understand the biological progression from alcohol use to AUD so more efficacious treatments can be discovered.

Alcohol use impacts central nervous system (CNS) function, and AUD is a disease of the central nervous system[5]. Since many parallels have been made between alcohol-related behaviors and alcohol abuse and dependence, there is a continuing effort to use

model organisms to identify genes and mechanisms underlying alcohol-related behaviors to better understand the role of the CNS during alcohol use, abuse and dependence. Identifying novel genes and mechanisms may facilitate the discovery of novel treatments for humans with AUD. Although the central nervous system contains both glia and neurons, the majority of research to date has focused on the role of neuronal mechanisms in alcohol-related behaviors. Thus, there is likely much to be learned by investigating the role of glia in behavioral responses to alcohol.

The model organism *Drosophila melanogaster* is a well-established model for identifying novel genes and mechanisms that regulate alcohol-related behaviors. Considering that flies and mammals have conserved behavioral responses to alcohol, as well as functionally homologous glial cells, we postulate that the fly is an excellent model to investigate how glial cells influence alcohol-related behaviors (reviewed in sections B and C). Additionally, previous research has demonstrated that glia in human alcoholic post-mortem tissue, rodents and flies are altered in the presence of alcohol (reviewed in section D). While there is still much to be learned, this body of work supports the notion that glia do respond to alcohol administration and influence alcohol-related behaviors.

B. *DROSOPHILA MELANOGASTER* AS A MODEL TO STUDY ALCOHOL-RELATED BEHAVIORS

In both humans and flies, lower doses of alcohol produce a stimulant effect, characterized by hyperactivity[6,7]. Conversely, higher doses of alcohol lead to depressant effects, such as motor impairment and sedation[7,8]. Flies and humans can

both develop tolerance to alcohol, but rapid tolerance and chronic tolerance are typically measured in the fly. Flies can develop tolerance in the presence of a brief exposure to a high, sedating, dose of ethanol (rapid tolerance) or in the presence of a long exposure to a non-sedative dose of alcohol (chronic tolerance)[9]. It is largely accepted that chronic ethanol exposure can result in long term changes in the brain, and this is thought to be a sign of dependence, and can lead to withdrawal symptoms. In the absence of ethanol, as a sign of withdrawal, humans experience dysphoria, anxiety, cognitive impairment and seizures[10]. By electrically stimulating the brain and recording seizure like activity in the flight muscle, seizures can be studied in the fly[11]. The threshold for inducing seizures is lower in flies previously exposed to ethanol[11]. Another hallmark feature of alcohol dependence is uncontrolled use and continued consumption despite aversion[7]. Ethanol consumption can be measured in the fly, and when given a choice between food with or without ethanol, flies develop a preference for the ethanol containing food[12]. This preference persists when the aversive, bitter tasting compound quinine is added to the ethanol containing food[12]. Interestingly, by associating ethanol vapor with an odor, flies will even undergo an electric shock for the alcohol associated cue[13].

Additionally, there are conserved molecular mechanisms regulating alcohol-related behaviors in flies and mammals. For example, the same alcohol metabolism machinery exists in flies and mammals and it is essential to avoid ethanol toxicity[14,15]. Specifically, alcohol is converted to acetaldehyde by alcohol dehydrogenase (ADH), and acetaldehyde is converted to acetate by aldehyde dehydrogenase[16]. Mutations in the ADH gene reduce hyperactivity in response to a low dose of ethanol and increase

sensitivity to a high dose in flies[6,17]. In humans, ADH variants produce an inactive form of the enzyme, and protect against AUD development[5].

Various neurotransmitters have also been implicated in alcohol abuse, including γ-Aminobutyric Acid (GABA), dopamine and neuropeptide Y. Antagonizing the GABA-B receptor in flies blunts the loss of postural control associated with a high dose of alcohol[18]. Interestingly, the GABA-B receptor has been associated with alcohol consumption and motivation in rats and alcohol withdrawal and cravings in humans[19]. Additionally, knocking out the dopamine D1-like receptor in flies decreases ethanol-induced hyperactivity, suggesting that dopamine contributes to the stimulant effect of alcohol in flies[20]. In mammals, dopamine mediates the rewarding properties of drugs of abuse, including alcohol[21] and the stimulating effect of alcohol is reported as rewarding[7]. Neuropeptide Y (NPY) has also been implicated in alcohol consumption and dependence in mammals[22]. The fly orthologue to NPY is neuropeptide F (NPF), and flies with decreased NPF signaling are resistant to alcohol sedation[23]. Together, this research supports that flies have a conserved behavioral response to alcohol, and that many genes that alter alcohol-related behavior in flies have also been implicated in mammalian, and even human, alcohol use and abuse.

Additionally, many tools exist in the fly to manipulate gene expression, which makes it feasible to screen large sets of genes to determine if any influence alcohol behavior. For example, the Gal4-UAS system allows constitutive transgene expression in specific tissues or cell types[24]. The Gal4 “driver” is expressed via tissue-specific promoters, and only Gal4 can bind to and activate a specific upstream activator sequence (UAS) that is followed by a transgene of choice. Once the UAS is activated, that transgene is

transcribed[24]. Commercially available UAS-transgenes include RNAi's to knockdown specific genes, dominant negatives to functionally silent genes, and duplicate copies to overexpress a specific gene. Similar systems exist with different "driver" proteins (i.e. LexA or Q), which recognize their own "UAS" sequences (i.e. LexAop or QUAS)[25,26]. When used together, unique manipulations can be made in different cell types at the same time[27]. These systems can also be temporally controlled by temperature shifts and drug treatments. For example, Gal80 proteins repress Gal4 proteins and can be temperature sensitive (Gal80ts)[28]. In the Gal4 restrictive temperature (18°C) the Gal80 protein is activated, and the Gal4 protein is repressed. At the Gal4 permissive temperature (30°C) the Gal80 protein is inactive and the Gal4 protein is functional. Additionally, GeneSwitch (GS) drivers are tissue specific, steroid-inducible Gal4 drivers, which allow temporal control over UAS-transgene induction[29]. Utilizing this system, when the steroid is not present, the Gal4 protein is inactive and expression of the UAS-transgene is not induced. When the steroid is present, however, the Gal4 protein is activated and can induce expression of the UAS-transgene. The steroid (RU486 or mifepristone) can be administered to flies through their food. Therefore, flies with GS- and UAS-transgenes fed steroid during adulthood will have the UAS-transgene expressed during adulthood. Conveniently, many tools exist to manipulate glia and glial cell subtypes in flies.

C. *DROSOPHILA MELANOGASTER* AS A MODEL TO STUDY ADULT CNS GLIAL CELLS

The adult mammalian CNS has three major glial cell subtypes: oligodendrocytes, microglia and astrocytes, as well as other glial cells like NG2 cells and polydendrocytes. A core function of oligodendrocytes is forming myelin sheath around neuronal axons in the CNS, allowing fast conductance of action potentials and trophic support[30]. Microglia are the primary immune cell in the mammalian brain; they are constantly surveying their microenvironment for foreign pathogens or danger signals, and can secrete pro- or anti-inflammatory molecules in response[31]. Astrocytes can interact with the blood brain barrier (BBB), other glia and neurons, and play a role in maintaining overall brain homeostasis[32].

The adult fly CNS contains five glial cell subtypes: subperineural glia, perineural glia, ensheathing cells, cortex glia and astrocytes. The subperineural and perineural glia (also termed surface glia) make up the BBB of the fly. While they express similar proteins found in the mammalian BBB[33], they do not share any functional or molecular similarities with mammalian CNS glia. Like their name implies, ensheathing glia encapsulate axon bundles[34]. Ensheathing glia can also regulate neuronal excitability by metabolizing glutamate[35], as well as engulf neuronal debris[36-38]. Cortex glia surround neuronal cell bodies and maintain the microenvironment[39]. Additionally, fly astrocytes extend processes into the synapse and maintain the synaptic environment[27]. In the fly CNS, macrophages are the primary immune cell and it is currently believed that flies do not have microglia[40].

In a healthy brain, fly ensheathing glia and mammalian oligodendrocytes share some similarities: they are both closely associated with neuronal axons and provide some support[30,35]. However, the fly CNS does not contain myelin[40] and during trauma, ensheathing glia become highly phagocytic[36], when oligodendrocytes typically become damaged and can die[41-43]. This suggests that ensheathing glia and oligodendrocytes are fundamentally different, and that studies using fly glia may not be translatable to mammalian oligodendrocytes. However, mammalian astrocytes share many morphological and functional similarities with fly cortex glia and fly astrocytes, suggesting that studying these cell types in flies may be translatable to mammals. Mammalian astrocytes and their fly counterparts will be reviewed in sections 1 and 2 below.

C.1 A FUNCTIONAL OVERVIEW OF MAMMALIAN ASTROCYTES

Astrocytes are the most abundant cell type in the mammalian CNS and tile the entire CNS with fine processes in a non-overlapping manner[44]. One astrocyte can contact approximately 100,000 and 2,000,000 synapses in rodents and humans, respectively[45]. This allows astrocytes to function in close proximity with neurons, blood vessels, and other glial cells, therefore allowing these cells to regulate overall brain homeostasis. Astrocytes provide support to neurons through ion homeostasis, transmitter clearance and recycling, direct modulation of neuronal signaling and provide metabolites and nutrients[32]. Astrocytes also participate and maintain the BBB, where their perivascular end feet directly contact blood vessels and transfer metabolites from the blood to neurons[46,47]. Additionally, astrocytes function in a network and can communicate with

each other through gap junctions. In the hippocampus, there are approximately 15 astrocytes per network in the rat[48], and 18 astrocytes per network in the mouse[49]. While not electrically excitable like neurons, astrocytes display a form of excitability based on intracellular calcium variations[50]. Intracellular calcium can be transferred between gap junctions, allowing one calcium event which originated in one astrocyte to reach thousands of synapses[51]. These calcium events are in response to neurotransmitters, neuromodulators and changes in the extracellular space[52], and can lead to the release of gliotransmitters. Astrocytes also respond to pathological insults, a process known as astrogliosis, which can alter their functions. Astrocyte functions in a healthy mature brain, as well as under pathological insults, will be reviewed in detail below.

Among others, two ways astrocytes regulate synaptic activity is through neurotransmitter uptake and ion homeostasis. One of the defining features of astrocytes is their enrichment for glutamate and GABA transporters, which efficiently clear the respective neurotransmitters (NTs) from the extracellular space after neuronal activity[53,54]. Astrocyte expression of the excitatory amino acid transporters (EAAT) glutamate transporter 1 (GLT-1) and glutamate-aspartate transporter (GLAST), as well as the cysteine glutamate anti-transporter (xCT), prevents glutamate-derived neuronal excitotoxicity[55,56]. These transporters also control glutamate spillover outside of the synapse, allowing glutamate to function solely in the synapse it was released into[57]. Additionally, once glutamate has been transported into the astrocyte, it can be converted to glutamine via glutamine synthetase and recycled back to the neuron[58]. The GABA transporters (GATs) 1 and 3 are expressed in astrocytes. GAT-1 reduces GABA spillover outside the synapse and GAT-3 regulates extracellular GABA

concentrations, consequently regulating tonic synaptic inhibition[59]. In the hippocampus, activation of GAT-3 leads to an increase in intracellular sodium (Na^+) concentrations, and a sequential increase in calcium (Ca^{2+}) via Na^+/Ca^{2+} exchangers[60].

When neurons are undergoing an action potential, they release a large amount of potassium (K^+) into the extracellular environment. To maintain neuronal activity, astrocytes engage in K^+ buffering. While astrocytes express multiple K^+ channels[56], the most studied is the inwardly rectifying K^+ (Kir) channel, Kir4.1, which controls the hyperpolarized resting potential of astrocytes[61]. Expression of Kir4.1 on astrocyte processes allows a rapid uptake of K^+ from the synapse[62] and reduced Kir4.1 expression in astrocytes is associated with elevated extracellular K^+ and an increase in neuronal membrane depolarization[63]. Interestingly, the aquaporin-4 water channel is also highly expressed in the same subcellular regions as Kir4.1 on astrocytes. It is believed that K^+ uptake via Kir4.1 generates a parallel water influx through aquaporin-4, which regulates osmotic changes within the astrocyte[64]. However, K^+ clearance from the synaptic cleft is not limited to Kir4.1; astrocytic Na+/K+ ATPase activity in the hippocampus and optic nerve is also important for K^+ buffering during neuronal activity[65,66].

Astrocyte membranes also express many calcium channels and exchangers which are important for Ca^{2+} mediated events. For example, transient receptor potential (TRP) channels allow Ca^{2+} influx in response to various changes in the environment. TRPA1 mediated Ca^{2+} influx contributes to the astrocytes' resting cytosolic Ca^{2+} levels[67]. Mechanical stimulation can activate Ca^{2+} influx via TRPC1[68], TRPC3[69] and TRPV4 channels[70]. *In vivo* mechanical stimulation of astrocytes can occur in response to blood

flow, allowing astrocytes to be sensitive to local changes in vasomotion[71]. Temperature changes also activate Ca^{2+} influx via TRPV1 channels[72]. Local brain temperature can change in response to metabolic heat produced by physiological activity or pathology[73,74]. Additionally, astrocytes express voltage-gated Ca^{2+} channels (VGCCs) *in vivo*[75,76]. While VGCCs do not contribute to internal Ca^{2+} concentrations at rest, they may be recruited to the membrane to function under depolarizing or pathological conditions[77,78], but this is controversial[79]. Although TRP channels and VGCCs are important for Ca^{2+} influx, the Na^{+}/Ca^{2+} exchanger is important for Ca^{2+} efflux. This exchanger brings three Na^{+} into, and one Ca^{2+} out, of the cell. However, when astrocytic intracellular Na^{+} is elevated, NCX can function in the opposite mode, and thus cause Ca^{2+} influx[80].

Astrocytes also express many NT receptors and their activation can lead to increases in intracellular calcium. These NTs include acetylcholine, ATP, GABA, endocannabinoids, and glutamate[81]. There is also evidence that astrocytes respond to the neuromodulators norepinephrine[82,83] and dopamine[84] as well as neuroendocrine molecules[85]. Activation of the ionotropic N-methyl-D-aspartate (NMDA) glutamate receptor and ionotropic purinergic P2X(1/5) ATP receptor causes an influx of cations, such as Ca^{2+}[86]. Additionally, many of these receptors are G-protein coupled receptors (GPRC), and activation of $G_{\alpha q}$ GPRCs can lead to increases in intracellular calcium indirectly through increases in phospholipase C (PLC) production. PLC converts phosphatidylinositol biphosphate (PIP_2) to diacylglycerol (DAG) and inositol triphosphate (IP_3). The endoplasmic reticulum (ER) in astrocytes has IP_3 receptors, which require Ca^{2+} and IP_3 as co-agonists[87,88]. Upon activation, the IP_3 receptors

release Ca^{2+} from the ER, thus raising intracellular Ca^{2+} levels within the astrocyte[89]. $G_{\alpha q}$ GPCRs expressed on astrocytes include the metabotropic glutamatergic receptor 5 (mGluR5)[90], the purinergic P2Y receptor[91], the serotonergic 5HT2A receptor[92] and the adrenergic α1A receptor[93].

Outside of the ER, the mitochondria also regulate intracellular Ca^{2+} in astrocytes through the mitochondrial H^+/Ca^{2+} exchanger (HCX), the mitochondrial Ca^{2+} uniporter (MCU) and the permeability transition pore (PTP)[94]. Although HCX and MCU both remove intracellular Ca^{2+} from the astrocyte cytosol, HCX is sensitive to nanomolar concentrations of Ca^{2+}[95] and MCU is sensitive to micromolar concentrations[96]. PTP, on the other hand, can produce spontaneous Ca^{2+} events when the IP_3 receptors are not activated[97].

When the intracellular Ca^{2+} concentration reaches a certain threshold[98,99], the astrocyte can release gliotransmitters (GTs). The widely accepted and frequently studied gliotransmitters are glutamate, D-serine, GABA, ATP and adenosine[32]. While still debated, evidence suggests that GTs can be released from astrocytes through (i) Ca^{2+} dependent vesicle release, (ii) transporters or (iii) the opening of channels, specifically hemichannels or pannexons. In astrocytes, GT release via vesicular exocytosis is a relatively slow process and is dependent on Ca^{2+} and SNARE proteins[100,101]. Interestingly, unique elements of the SNARE complex appear to regulate independent SNARE-dependent vesicular release pathways. Glutamate-containing vesicles require synaptobrevin II for their release, while neuropeptide Y containing vesicles require cellubrevin[102]. These data suggest that there is diversity within the astrocyte SNARE protein pathways. There is also evidence that transporters may be

able to release GTs under pathological and non-pathological conditions. Transporters can reverse their directionality and release gliotransmitters, specifically glutamate and GABA, into the synapse[101,103]. Lastly, astrocytes can release GTs through hemichannels and pannexons. Hemichannels are channels compromised of connexins, while pannexons are channels made of pannexins[104]. Both these channels are found in similar domains on the astrocyte[105] and they both allow ions and small molecules, including ATP, glutamate, D-serine and possibly other GTs, to pass[104,106,107]. Despite these similarities, the two channels have different opening properties. Hemichannels exhibit a low open probability under resting conditions[108], whereas pannexons have a high open probability under resting conditions[109].

Once released, GTs can influence nearby neurons and glial cells. However, astrocyte communication with each other through GT is temporally limited by GT diffusion in the extracellular space, and is therefore relatively slow. A faster mechanism of astrocyte communication with their immediate neighbors is through gap junctions[110]. Gap junctions form from the docking of two hemichannels, creating a pore that connect the cytoplasm of the two cells[106]. Thus, ions, second messengers and small molecules up to 1.8 kiloDalton, including Ca^{2+}, K^{+}, Na^{+}, cyclic adenosine monophosphate, inositol-1,4,5 triphosphate, glutamate, ATP and energy metabolites can pass between the cells[111,112]. This allows metabolic and electric coupling and coordination of the astrocytes.

Overall, astrocytes preform these functions to maintain their microenvironment and promote normal neuronal firing. Due to this, it is not surprising that astrocytes are a highly heterogeneous cell type. However, it is debated whether astrocyte heterogeneity

stems from distinct molecular differences during development or adaptations to the microenvironment. In a healthy adult brain, astrocytes are morphologically distinct based on their location. Fibrous astrocytes are found in the white matter of the CNS and have numerous long branches that wrap around neuronal cell bodies and contact nodes of Ranvier on the axon. They can also extend their end-feet to blood vessels. Protoplasmic astrocytes are found in the grey matter and typically have shorter and stubbier processes. These processes surround virtually every synapse, and also contact blood vessels[44]. However, astrocytes also display heterogeneity in their protein expression in normal, healthy adult brains. For example, astrocytes have been identified as “passive” or “active” based on whether they express glutamate transporters or receptors. Passive astrocytes express glutamate transporters but not receptors, while active astrocytes express glutamate receptors but not transporters. Passive and active astrocytes can be found in the same brain region[113].

Research also suggests that layer-specific astrocytes exist as well. For example, astrocytes from cortical layer 2/3 take up a larger volume compared to astrocytes from cortical layers 1, 4, 5 and 6[114]. Likely due to their expansive processes, cortical layer 2/3 astrocytes also surround more synapses than other cortical astrocytes[114]. *In vivo* analysis revealed that cortical layer 1 astrocytes have twice as much Ca^{2+} activity compared to cortical layer 2/3 astrocytes[115]. Additionally, cortical layer 2/3 and 5 astrocytes express higher levels of the K^+ channel Kir4.1 compared to astrocytes in other cortical layers[116]. Taken together, these data suggest that astrocyte functions may reflect the needs of their neighboring neurons and that astrocytes can, therefore, differentially influence surrounding synapses.

Astrocytes also differ between brain regions. Astrocytes isolated from mouse cerebellum, thalamus, brainstem, olfactory bulb and cortex could be separated into five different subpopulations based on their immunoreactivity to several antibodies[117]. Additionally, astrocyte mRNA expression patterns from the cortex, hippocampus, thalamus, hypothalamus, caudate-putamen and nucleus accumbens revealed three molecularly distinct subpopulations with different, and sometimes complete opposite, profiles between regions[118]. A similar study found astrocyte transcriptome differences to be region and age dependent[119]. Besides RNA and protein expression differences, astrocytes in the hippocampus, striatum and ventral tegmental area also display difference in their K^+ currents, spontaneous and evoked Ca^{2+} events, morphology and synapse proximity[120,121].

Not surprisingly, astrocytes also actively, and heterogeneously, respond to CNS insults, diseases and disorders. Under these conditions, astrocytes become activated and alter their morphology and gene expression, a process termed astrogliosis[31]. Activated astrocytes take on an A1 or A2 profile. A1 astrocytes exacerbate disease progression by killing neurons and oligodendrocytes, resulting in a largely negative effect on CNS function and recovery. However, A2 astrocytes upregulate neurotrophic genes and promote neuronal survival[122]. Interestingly, astrocytes also react uniquely in different disease states, and this heterogeneity has been heavily studied[123]. However, since this research focuses on alcohol use and AUD, astrocytic contributions to this will be reviewed below (Section D).

C.2 A FUNCTIONAL OVERVIEW OF *DROSOPHILA MELANOGASTER* CORTEX GLIA AND ASTROCYTES

In *Drosophila melanogaster*, cortex glia and astrocytes are morphologically and functionally similar to mammalian astrocytes. These parallels will be highlighted below. The basic anatomy between the mammalian and fly brain is very different, however. There are few structural similarities and the fly brain is divided into two major regions: the cortex and the neuropil. The fly cortex contains neuronal cell bodies and no synapses. The neuropil, on the other hand, contains neuronal axons and is a synaptic rich region.

Cortex glia, as their name implies, reside in the cortex region of the *Drosophila* CNS[124]. However, one cortex glia cell can extend its fine processes to surround approximately 100 neuronal cell bodies[125] and make significant contact with the BBB[126]. Through their non-overlapping spatial domains, cortex glia surround virtually every neuronal cell body in the adult fly brain[124]. Genetic ablation of these cells results in developmental lethality[127] and disruption of cortex glial secretion of the neurotrophin Spätzle 3 leads to neuronal cell death[39], demonstrating that these cells are important for neuronal health and maintenance, like their mammalian astrocyte counterparts.

Given that cortex glia are positioned between the BBB and neuronal cell bodies, it has been assumed that cortex glia shuttle important metabolites to neurons[39,128] similarly to mammalian astrocytes, but this relationship has never been experimentally demonstrated. However, components of the mammalian astrocyte neuron lactate shuttle are conserved in *Drosophila* glial cells, but the exact glial cell subtype(s) remain unidentified. For example, the monocarboxylate transporter (MCT) Chaski, which

shuttles lactate and pyruvate, is enriched in fly glia but is also expressed in neurons[129]. The mammalian MCT1 and MCT2 are also expressed on glia and neurons[129], although these transporters are known to be expressed on mammalian astrocytes and oligodendrocytes[130-132]. Taken together, these data suggest that fly cortex glia may be equipped to provide trophic support to neurons.

Additionally, like their mammalian counterparts, cortex glia display rapid, near membrane Ca^{2+} oscillations[133]. The change in intracellular Ca^{2+} is mediated by TRPA1 channels, as well as zydeco, a Na^{+}/Ca^{2+}, K^{+} exchanger (NCKX)[133]. This suggests that cortex glia (i) have similar machinery as mammalian astrocytes to alter intracellular Ca^{2+} levels and (ii) can respond to and regulate ion concentrations in the extracellular space. *Drosophila* zydeco is homologous to mammalian NCKX2, which regulates intracellular Ca^{2+} in astrocytes, oligodendrocytes and neurons[134,135]. Knockdown of zydeco in cortex glia decreased Ca^{2+} influx and increases seizure susceptibility[133]. Interestingly, several mammalian studies have correlated astrocyte Ca^{2+} oscillations with seizure initiation[136-138], suggesting that glial Ca^{2+} dysregulation may be a conserved seizure pathology. Cortex glial cells also contribute to seizure susceptibility when their plasma membrane structure is compromised, causing neuronal cell bodies to be abnormally encapsulated[139]. While this exact mechanism is unknown, these data further suggest that cortex glia can regulate neuronal excitability.

Drosophila astrocytes, like their mammalian counterparts, maintain ion homeostasis, remove neurotransmitters from the synapse, produce Ca^{2+} oscillations and release gliotransmitters[40,140]. These cells also are morphologically similar; however, fly astrocytes are unique in that their fine processes are only found in synaptic rich

regions[141]. The approximately 4,600 fly astrocytes exist and tile to form a dense meshwork with very little overlap to cover the entire synaptic space[124,125].

Fly astrocytes express the EAAT1 (also known as GLAST) and GAT for the uptake of glutamate and GABA from the synapse. As seen in mammals, this allows the balance of excitatory and inhibitory synapses in the adult fly brain[142,143]. Previous work in the fly has demonstrated that EAAT1 and GAT expression on astrocytes is physiologically relevant. Loss of EAAT1 in fly astrocytes leads to neuronal firing dysregulation, axon degeneration, and a shortened lifespan[141,144]. Additionally, an increase in EAAT1 on fly astrocytes has been correlated with increased seizure susceptibility[145]. Conversely, downregulation of GAT endocytosis in astrocytes, and therefore an increase in GABA in the synaptic cleft, has been associated with a rapid onset of paralysis in flies[146]. Under normal conditions, astrocyte GAT expression on the plasma membrane is regulated by neuronal activity levels, indicating that flies engage in glia-neuron crosstalk[147]. Neuronal activity can increase astrocyte Ca^{2+} levels, leading to endocytosis of GAT[146]. Interestingly, mutations in EAAT's and GAT have also been associated with seizures and paralysis in mammals[148,149]. Moreover, fly astrocytes, like mammalian astrocytes, express the enzymes and proteins necessary to break down glutamate and GABA into intermediates and recycle them back to neurons[142-144].

In mammals, astrocytes display Ca^{2+} oscillations, which can modulate the synaptic environment and neuronal function. Similar processes have been identified and studied in depth in *Drosophila*. Fly astrocytes can function in a tripartite synapse[150], display Ca^{2+} transients [27,40,146], and directly modulate neuronal function[27]. Under normal conditions, fly astrocytes display spontaneous Ca^{2+} transients which are regulated by

synaptic activity and TRP channels[27,146]. Specifically, the invertebrate catecholamines octopamine or tyramine binding to the Octopamine-Tyramine receptor (Oct-TyrR) on astrocytes leads to an increase in intracellular Ca^{2+}. This Ca^{2+} transient stimulates adenosine release from the astrocyte, which binds to the adenosine receptor on a neighboring dopaminergic neuron to inhibit its function and alter locomotor behavior[27]. Mammalian astrocytes' Ca^{2+} levels are modulated by the catecholamine norepinephrine[83,151,152] demonstrating the utility of *Drosophila* to understand astrocyte-neuronal communication and its physiological relevance *in vivo*.

The *Drosophila* CNS also expresses innexins, which are structurally and functionally similar to mammalian pannexins and connexins, and they form hemichannels and gap junctions[153]. 8 innexins exist in flies, and innexin-2 and ogre are strongly expressed in glial cells[153]. Fly astrocytes can form gap junctions with each other[141] and with cortex glia[58]. These couplings have been implicated in glutamate metabolism and sleep[58]. These data suggest that fly glia may be a useful model to study the physiological relevance of astrocyte communication through gap junctions.

Fly astrocytes also express multiple inflammatory mediators, such as TNFα and NF-$\kappa\beta$ homologues[109,154]. Due to this, fly models of Alzheimer's disease, amyotrophic lateral sclerosis and Huntington's disease have been developed and research has implicated astrocyte contributions to disease progression[140]. While activated profiles of astrocytes in flies have not been fully characterized, these data begin to suggest that *Drosophila* astrocytes can respond to pathology similarly to their mammalian counterparts.

As mentioned previously, mammalian astrocytes display robust heterogeneity[123]. Recently, fly astrocytes have been proposed as a model to study astrocyte heterogeneity as well[155]. For example, within the visual cortex of the adult fly, astrocyte morphology and orientation vary depending on the depth of the cell in the lamina and 4 specific astrocyte subtypes in this region have been classified[156,157]. Additionally, different Gal4 drivers have been used to induce UAS-transgene expression in unique astrocyte populations, indicating that certain Gal4 promoters are specific to certain fly astrocytes[24,125].

Drosophila cortex glia and astrocytes are functionally homologous to mammalian fibrous and protoplasmic astrocytes, respectively[39,40]. Although heterogeneity within individual cortex glial cells has yet to be explored, fly astrocytes are emerging as a diverse cell type[155]. Taken together, this invites the speculation that *Drosophila* cortex glia and astrocytes have a common origin with mammalian astrocytes.

D. GLIAL RESPONSES TO ALCOHOL ADMINISTRATION AND THEIR ROLE IN ALCOHOL-RELATED BEHAVIORS

To date, the role of glial cells in alcohol use, abuse and dependence is not fully understood. However, previous literature has demonstrated that mammalian astrocytes, microglia, oligodendrocytes, as well as fly surface glia, can respond to adolescent and adult alcohol exposure and influence alcohol-related behaviors. This body of literature will be reviewed below.

D.1 MAMMALIAN ASTROCYTES AND ALCOHOL

Astrocytes are robustly altered in human alcoholic post-mortem brain tissue samples. Increases in glial fibrillary acidic protein (GFAP) in the pre-frontal cortex[158], as well as decreased astrocyte density in the pre-frontal cortex[159,160] and hippocampus[158] have been observed, along with overall changes in astrocyte morphology[161]. Additionally, there is less connexin 43, a hemichannel precursor, in alcoholic brain tissue[162]. Microarray data also demonstrated that alcoholic postmortem brain tissue has upregulated immune-related genes, and microglia and astrocytes are historically major contributors to the neuroimmune response[163-165]. These data suggest that astrocytes are robustly altered in the presence of chronic alcohol.

Studies in the rodent have further demonstrated that astrocytes are altered in the presence of alcohol. For example, neurotransmitter uptake in astrocytes is influenced by alcohol administration. Acute ethanol blocks glutamate uptake[166-168] and chronic ethanol downregulates the expression of the glutamate transporter GLT-1 and xCT[169,170]. Conversely, chronic ethanol treatment increased GLAST and GLT1 in cultured astrocytes[171]. Manipulating glutamate uptake *in vivo* also influences alcohol related behaviors. When GLAST was knocked out, mice had reduced voluntary alcohol consumption and did not exhibit motivation for alcohol[172]. Pharmacologically blocking glutamate uptake with dihydrokainic acid reduced binge drinking[173], while pharmacologically enhancing GLT1 and xCT with N-acetylcysteine and clavulanic acid decreased ethanol consumption, ethanol seeking and ethanol reacquisition after abstinence[174,175]. Additionally, upregulation of GLT1, but not GLAST, was seen in the nucleus accumbens core astrocytes following voluntary ethanol consumption[176,177].

These results indicate that astrocytes may differentially regulate glutamate uptake as a response to alcohol.

Transcriptomic data have revealed changes in astrocyte Ca^{2+} signaling in response to chronic ethanol consumption[178]. In cultured astrocytes, the presence of alcohol increases intracellular Ca^{2+} transients[179,180]. Increases in astrocytic Ca^{2+} are indicative of GT release[32], suggesting that GT may be released in response to alcohol. In support of this, hemichannels, which release GTs, are also altered by alcohol treatment[104]. Interestingly, hemichannels are opened in the presence of alcohol, specifically, connexin 43 and pannexin 1 in hippocampal astrocytes[181,182]. Blocking hemichannels in the nucleus accumbens core increased ethanol seeking behavior, while activating these same astrocytes reduced motivation for ethanol after abstinence[183].

Research has also implicated that GTs respond to alcohol administration. For example, ethanol administration increases extracellular levels of the GT adenosine[184]. Increased adenosine activates the astrocyte-specific equilibrate nucleoside transporter, ENT1, which decreases glutamate uptake by downregulating GLT-1[185].

Ethanol also promotes immune signaling, specifically through the toll-like receptor 4 (TLR4) and interleukin 1 receptor (IL1R), which increases expression of inflammatory cytokines[186-190]. Microglia and astrocytes regulate the neuroimmune response[191] and this response can also influence alcohol related behaviors. The chemokine C-C motif ligand 2 (CCL2) is increased in alcohol post-mortem brains[163] as well as in mice after alcohol exposure[192,193]. Increased CCL2 expression in astrocytes led to increases in whole-brain CCL2 and reduced ethanol consumption, impaired spatial learning and improved associative learning in alcohol dependent mice[194]. However, increasing CCL2

with transgenics in astrocytes also increases endogenous CCL2 secretion from microglia, which complicates any conclusions about astrocytes directly modulating behavior[194].

D.2 MAMMALIAN MICROGLIA AND ALCOHOL

Microglia typically become activated when they sense threats, leading to morphological changes and the secretion of pro- or anti-inflammatory molecules[195]. In human alcoholic post-mortem brain tissue, markers of microglia activation are upregulated, including the Ionized calcium-binding adapter molecule 1 (Iba-1) and the antigen CD11b[196], suggesting that microglia may regulate toxicity and neurodegeneration associated with chronic alcohol exposure[197]. Similar results were seen in the mouse brain following chronic and binge alcohol exposures[186,198,199]. Interestingly, after alcohol administration microglia in the prefrontal cortex[200] and hippocampus[201] were activated but there was no increase in inflammatory markers, suggesting that microglia may have a protective or homeostatic role in these brain regions after alcohol exposure.

Alcohol is predicted to activate microglia through the TLRs. Specifically, alcohol administration upregulates TLR4 and TLR2 and promotes the release of neuroinflammatory mediators[202]. In TLR4 knockout mice, alcohol administration did not increase Iba-1 and neurotoxicity development was blunted[186]. Interestingly, microglia activation is associated with the nuclear factor kappa-light-chain enhancer of activated B cells (NF-κB) signaling and reactive oxygen species (ROS) production, which has also been correlated with neurodegeneration following ethanol treatment[203].

Pharmacologically inhibiting microglial activation with minocycline decreased alcohol self-administration in mice[204] and alcohol relapse after abstinence in rats[205]. Chemically depleting microglia with the colony-stimulating factor 1 receptor antagonist, PLX33397, blocks the expression of anti-inflammatory genes that are typically unregulated during alcohol withdrawal, but did not alter alcohol induced motor impairment[206]. Taken together, these data suggest that microglial activation occurs in response to alcohol administration, and that this process may mediate alcohol-related behaviors, as well as ethanol-induced neurodegeneration and toxicity.

D.3 MAMMALIAN OLIGODENDROCYTES AND ALCOHOL

Oligodendrocytes are characterized by forming myelin sheath around axons. Markers for myelin include myelin basic protein (MBP), proteolipid protein (PLP) and myelin associated glycoprotein (MAG), among others[207]. In human alcoholic post-mortem brain, mRNA levels for MBP, PLP and MAG were decreased compared to non-alcoholic brain samples[163,208]. Interestingly, these reductions were also significant in alcoholics with cirrhosis compared with alcoholics without cirrhosis[208], suggesting nutritional or metabolic impairments caused by chronic alcohol consumption enhance myelin degeneration.

In adult mice, chronic alcohol exposure is correlated with reduction of myelin components in multiple brain regions, eventually leading to neurodegeneration. However, the addition of calpain inhibitors prevented Ca^{2+} activation of calpain and significantly blunted myelin reduction and neurodegeneration associated with alcohol administration[209]. Another proposed regulator of alcohol-associated myelin loss and

neurodegeneration is the alcohol metabolite acetaldehyde[210]. Although alcohol administration clearly leads to myelin pathology, more research is needed to determine how alcohol reduces myelin and how this process influences alcohol-related behaviors.

D.4 *DROSOPHILA MELANOGASTER* SURFACE GLIA AND ALCOHOL

Two studies using *Drosophila* as a model organism have demonstrated a causal relationship between the surface glial cells and alcohol sedation and tolerance[211,212]. The fly blood brain barrier is a layer of two glial cells, also known as the surface glia, which are comprised of the subperineural and the perineural glia[213]. The GPCR, Moody, is expressed in the BBB glia in fly larva and a mutation in the *Moody* gene blocks alcohol-induced motor impairments in adult flies[211]. While interesting, the gene *Moody* was never specifically altered in the BBB glia, and the Moody GPCR expression pattern wasn't investigated in the adult brain as well as throughout the rest of the body. This is a concern, given that a mutation in the gene *Moody* causes a ubiquitous knock down, and not just reduced expression in the BBB. Taken together, how Moody functions specifically in the BBB to influence alcohol sedation remains elusive. An additional study indicated that expression of the A kinase anchoring protein AKAP200 in perineural glia is required for alcohol tolerance[212]. Similar results were observed when protein kinase A, actin and calcium signaling were manipulated in perineural glia, leading to conclusions that AKAP200 is coordinating these to control alcohol tolerance[212]. While possible, these molecular interactions were not tested formally, making this conclusion premature. These studies, however, begin to demonstrate the utility of the fly to manipulate glia *in vivo* and investigate the resulting behavioral changes to alcohol.

E. SIGNIFICANCE

Previous research has demonstrated that adult CNS glia robustly respond to alcohol administration and can influence alcohol related behaviors. This supports our overarching hypothesis that adult CNS glia are important regulators of alcohol-related behaviors. However, to date, a causal relationship between any glial cell molecular pathway and an alcohol related behavior has not been demonstrated fully. Given that flies and mammals have (i) conserved behavioral responses to alcohol, (ii) conserved molecular responses to alcohol and (iii) conserved astrocyte function, we decided to use *Drosophila melanogaster* as a model to identify novel genes whose expression in glia regulates alcohol sedation. In pursuit of this, we characterized a novel GeneSwitch driver, GliaGS, to manipulate gene expression specifically in glia during adulthood (Chapter 3). Through targeted screens, we identified the genes cysteine proteinase 1 (Cp1) and tyrosine decarboxylase 2 (Tdc2) as novel regulators of alcohol sedation sensitivity. Cp1 functions in cortex glia to regulate alcohol sedation (Chapter 4). Tdc2 is involved in the synthesis and release of tyramine in astrocytes, which mediates alcohol sedation (Chapter 5). This research demonstrates that glia are integral for normal alcohol-related behaviors, and could therefore be regulating alcohol abuse and dependence progression.

CHAPTER 2: MATERIALS AND METHODS

A. UNIVERSAL METHODS

Fly husbandry. All flies were reared under standard conditions as described previously[214,215]. Flies were grown on food medium containing 10% sucrose, 3.3% cornmeal, 2% yeast, 1% agar, 0.2% Tegosept, and antibiotics (0.1 g/L ampicillin, 0.02 g/L tetracycline, 0.125 g/L chloramphenicol) with active dry yeast on top in 6-ounce polypropylene *Drosophila* bottles (Fisher Scientific, Hampton, NH). Flies were housed in an environmental chamber kept at 25°C and 60% relative humidity with a 12-hour light/dark cycle. All comparisons between groups were based on studies with flies that were grown, handled, and tested side by side.

Fly stocks. UAS-transgenic and Gal4 driver strains were obtained from either (i) other laboratories or (ii) one of the following commercial/public resources: Vienna *Drosophila* Resource Center (VDRC), Vienna, Austria and Bloomington *Drosophila* Stock Center (BDSC), Bloomington, IN. A w^{1118} reference stock from the VDRC (stock number 60000) was used to control the genetic background of all flies obtained from this stock center. Any UAS-transgene marked with *y*+ was backcrossed to a w^1y^1 strain (stock number 1495, BDSC) for seven generations to normalize the genetic background. All Gal4 stocks (marked with mini-*w*) were backcrossed to our standard reference strain, *w*[A]

(*w*^{1118} in an isogenic background; BDSC, stock number 5905) for seven generations to normalize the genetic background. All fly strain information is listed below.

Ethanol sedation sensitivity. One day before behavioral studies, adult flies (1-4 days old) were placed under light CO_2 anesthesia and sorted for sex. Eleven adult female flies were placed into fresh non-yeasted food vials (standard food medium without active dry yeast on top). Flies recovered in food vials stored upside down (food side up) overnight at 25°C and 60% relative humidity. Each vial of flies corresponded to n=1; up to 24 vials were tested in each single ethanol sedation experiment.

Ethanol sedation studies were performed at 23-25°C and 55-65% relative humidity under standard office lighting as previously described[214,215]. Flies, after a 1-2 hour acclimation period in the testing room, were transferred to empty polystyrene food vials (VWR, Radnor, PA) and trapped in the vials with a cellulose acetate Flug (FlyStuff, San Diego, CA) inserted approximately 2 cm into each vial. The number of inactive flies was recorded for each vial (typically 0-1 flies/vial). One mL of 85% ethanol (made fresh weekly) was added to each Flug, and the vials were immediately sealed with a silicone stopper. Once every 6 minutes, each vial was tapped gently on a table 3 times and the number of sedated flies (i.e. still on the bottom of the vial) was recorded 30 seconds later. The ethanol sedation experiments were terminated when all flies were sedated, typically after 60-90 minutes. The percentage of active flies was calculated for each vial at each time point, and the time required for 50% of the flies in each vial to become sedated (sedation time 50, ST50) was interpolated from sigmoidal curve fits using Excel (Microsoft, Redwood, WA)[214,215].

Internal ethanol. Flies were exposed to vapor from 85% ethanol as described for measuring ethanol sedation[8]. After exposure to ethanol vapor for a duration equivalent to the ST50, flies were transferred to 1.5 mL snap-cap tubes and frozen at -80°C. Frozen flies were homogenized in 200 µL ice-cold ddH_20 and then centrifuged at 14,000 rpm at 4°C for 20 minutes. The internal ethanol concentration of the supernatant was determined using Alcohol Reagent Set (Pointe Scientific Inc., Canton, MI) according to the manufacturer's instructions.

GeneSwitch induction. 100 µl of 1 mM Mifepristone (RU486; Sigma Aldrich, St. Louis, MO) or vehicle (100% ethanol) was added to the surface of solidified food in vials and allowed to dry overnight. Flies were provided food medium topped with RU486 (induced) or vehicle (control) for 6 days total. Flies were transferred to fresh drug- or vehicle-treated food vials after 3 days.

Whole brain imaging and immunodetection. Whole brains from adult (4 day-old) female flies were dissected in 0.3% Phosphate buffer Triton X-100 (PBT) under a dissecting microscope. Dissected brains were fixed in 0.5 mL snap cap tubes containing 4% paraformaldehyde on ice and then for 20 minutes at room temperature on a tube rotator. Brains were then washed with 0.3% PBT and blocked with 5% normalized goat serum (NGS). Primary antibodies diluted in 5% NGS were added and brains were placed on a tube rotator at 4°C for 36-48 h. Brains were washed with 0.3% PBT and exposed to the secondary antibodies diluted in 5% NGS at 4°C for 36-48 h. Brains were

then washed with 0.3% PBT and mounted onto glass slides in SlowFade mounting medium (Invitrogen, Carlsbad, CA)[216].

Statistics. All statistical analyses (Student's t-test, one-way ANOVA, two-way ANOVA and Bonferroni's multiple comparison tests) were performed with Prism 6.04 (GraphPad Software, San Diego, CA, USA). Numerical data are mean ± S.E.M.

B. CHAPTER SPECIFIC METHODS

Chapter 3: GliaGS identification

Fly stocks.

Annotation/Gene	Supplier; stock number (if applicable)	Genotype
da-Gal4	-	w[1118];; da-Gal4
elav-Gal4	-	w[1118], elav-Gal4;;
repo-Gal4	-	w[1118];; Repo-Gal4/TM3Sb
UAS-LacZ	BDSC; 6452	y[1] w[*];; P{w[+mC]=UAS-GFP::lacZ.nls}30.1
GliaGS	BDSC; 59929	w[*];; P{w[+mW.hs]=Switch2}GSG7293-1/TM6B, Tb[1]
40262	BDSC; 40262	w[*];; P{w[+mW.hs]=Switch2}GSG1821/TM6B, Tb[1]

β-Galactosidase activity. β-galactosidase activity was measured in whole body extracts of flies as previously described[217]. Three adult (4 day-old) female flies were homogenized in 250 µL buffer (1 X PBS with 1 X protease inhibitor cocktail (Sigma Aldrich, St. Louis, MO)). An additional 500 µL of extraction buffer was added, the extracts were vortexed and then centrifuged at 14,000 rpm for 5 minutes at room temperature. 100 µL of the resulting supernatant was added to 900 µL of 1 mM chlorophenol red-β-d-galactopyranoside (Sigma Aldrich, St. Louis, MO). β-

galactosidase activity was observed as the change in absorbance at 562 nm over 6 minutes in a Ultraspec 2000 spectrophotometer (Pharmacia Biotech, Piscataway, NJ).

Chapter 4: Cysteine proteinase 1 regulates *Drosophila* alcohol sedation by functioning in adult cortex glia

Fly stocks.

Annotation/Gene	Supplier; stock number (if applicable)	Genotype
akap200	VDRC; v5647	w[1118]; P{GD1207}v5647;
loco	VDRC; v9248	w[1118]; P{GD1282}v9248;
nrv1	VDRC; v46542	w[1118] P{GD959}v46542;;
unc5	VDRC; v8138	w[1118]; P{GD3510}v8138;
unc5	VDRC; v8137	w[1118];; P{GD3510}v8137
draper	VDRC; v4833	w[1118];; P{GD2628}v4833
draper	VDRC; v27086	w[1118]; P{GD14423}v27086;
CG6218	VDRC; v35069	w[1118];; P{GD11863}v35069
Jhl-21	VDRC; v45190	w[1118];; P{GD3466}v45190
Jhl-21 RNAi	VDRC; v45191	w[1118];; P{GD3466}v45191
Jhl-21	VDRC; v45192	w[1118];; P{GD3466}v45192
Jhl-21	VDRC; v45193	w[1118];; P{GD3466}v45193
argk	VDRC; v34037	w[1118];; P{GD10436}v34037/TM3
DAT	VDRC; v12082	w[1118]; P{GD2034}v12082;
axo RNAI #1	VDRC; v18866	w[1118]; P{GD6017}v18866;
axo RNAi #2	VDRC; v18867	w[1118];; P{GD6017}v18867
nemy RNAi	VDRC; v40803	w[1118];; P{GD15732}v40803
ent2 RNAi	VDRC; v7618	w[1118]; P{GD953}v7618;
Cp1 RNAi #1	VDRC; v13959	w[1118];; P{GD5803}v13959
Cp1 RNAi #3	VDRC; v110619	w[1118]; P{KK107765}VIE-260B;
Cp1 RNAi #2	BDSC; HMS00725	y[1]w[1]; P{TRiP.HMS00725}attP2;
Cp1 OE	BDSC; 15957	y[1]w[1]; P{Cp1[EY05806]};
Crammer RNAi #1	VDRC; v22751	w[1118]; P{GD12961}v22751/CyO;
crammer RNAi #2	VDRC; v22752	w[1118];; P{GD12961}v22752
cut RNAi #1	VDRC; v4138	w[1118];; P{GD1237}v4138
cut RNAi #2	VDRC; v5687	w[1118];; P{GD1237}v5687
syb RNAi #1	BDSC; 39067	y[1] sc[*] v[1]; P{y[+t7.7] v[+t1.8]=TRiP.HMS01987}attP40/CyO;
syb RNAi #2	BDSC; 38234	y[1] sc[*] v[1];; P{y[+t7.7] v[+t1.8]=TRiP.HMS01678}attP2/TM3, Sb[1]

elav-Gal4	-	w[1118], elav-Gal4;;
repo-Gal4	-	w[1118];; Repo-Gal4/TM3Sb
GliaGS	BDSC; 59929	w[*];; P{w[+mW.hs]=Switch2}GSG7293-1/TM6B, Tb[1]
TIFR-Gal4	Mary Logan, Oregon Health Science University	w^{1118};;TIFR-Gal4
MZ0709-Gal4	Marc Freeman, Oregon Health Science University	w^{1118};;mz0709-Gal4
CtxGlia Split-Gal4	Jaeda Coutinho-Budd, University of Vermont	w; sp/+; wrapper-DBD, Nrv2-AD/Tm6B
NP2222-Gal4	Mary Logan, Oregon Health Science University	w^{1118};NP2222-Gal4
Gli-Gal4	Doris Kretzschmar, Oregon Health Science University	w^{1118};Gli-Gal4
Indy-Gal4	Fred Wolf, University of California - Merced	w^{1118};;Indy-Gal4
NP2222-Gal4; GFP	Mary Logan, Oregon Health Science University	w1118; NP2222, UAS-mCD8::GFP/cyo;
UAS-GA25021 #1	-	w1118; pUAST-GA25021
UAS-GA25021 #2	-	w1118; pUAST-GA25021
UAS-GA25021 #3	-	w1118; pUAST-GA25021
UAS-GA25021 #4	-	w1118; pUAST-GA25021
UAS-GA25021 #5	-	w1118; pUAST-GA25021
UAS-GA25021 #6	-	w1118; pUAST-GA25021
UAS-GA25021 #7	-	w1118; pUAST-GA25021
repo-Gal4, UAS- Cp1 RNAi #2	-	w1118; HMS00725/cyo; repo-Gal4/TM3Sb

Trans-species rescue of the Cp1 RNAi in glia. FlyBase and NCBI were used to determine that *D.melanogaster* Cp1 and *D. pseudoobscura* GA25021 were orthologous. Fly stocks that express *D. pseudoobscura* GA25021 under UAS control were created via standard P-element-mediated transgenesis using pUAST[218]. The *D. pseudoobscura* GA25021 cDNA was cloned into the pUAST vector by GenScript (Piscataway, NJ, USA) and injected in w[A], our standard lab stock, by Rainbow Transgenic Flies (Camarillo, CA, USA). We mapped the independent UAS-GA25021 insertions to autosomes. Flies

constitutively expressing the HMS00725 *Cp1* RNAi transgene in all glia via *repo*-Gal4 were generated through standard crosses.

Rapid tolerance. Rapid tolerance to ethanol was assessed as the change in sensitivity to ethanol sedation due to a prior exposure to the drug. Flies were tested for ethanol sedation during a first ethanol exposure as described above (E1), returned to food vials to recover for 4 h, and then tested for ethanol sedation during a second ethanol exposure (E2)[214]. The development of rapid tolerance was quantitated as the ratio between the ST50 during E2 and the ST50 during E1.

Locomotor behavior. Flies were collected as described above for ethanol sedation. On the test day, flies were transferred to empty polystyrene food vials. The positive control group vials (Gal4/+) were vortexed for four minutes prior to the experiment. Thereafter vials were handled as described for ethanol sedation studies, except for the following changes: (i) no ethanol was placed on the flug and (ii) no plug was used to seal the vial. The percentage of active flies was calculated for each vial at each time point.

Immunodetection. The following primary antibodies at the indicated concentrations from the listed sources were used: polyclonal guinea pig anti-cp1 (1:250; donated from Patrick Dolph, Dartmouth College, NH); monoclonal mouse anti-repo (1:100, Developmental Studies Hybridoma Bank, Iowa City, IA); polyclonal rabbit anti-LacZ (1:25, Fisher Scientific). The following secondary antibodies were used: goat anti-

guinea pig Alexa 568, rabbit anti-mouse Alexa 488 and chicken anti-rabbit Alexa 647 (all at 1:1000; ThermoFisher, Waltham, MA).

All images were collected using a Zeiss LSM 510 multi-photon microscope (Carl Zeiss Microscopy, LLC, Thornwood, NY) or a Zeiss LSM 700 confocal microscope (Carl Zeiss Microscopy, LLC, Thornwood, NY) housed in the VCU Department of Anatomy and Neurobiology Microscope Facility. Confocal images using a pin hole of 1 Airy disc unit and Nyquist sampling were collected from each adult brain. Images were taken with a 10X objective with a numerical aperture of 0.3 or a 63X oil-immersion objective with a numerical aperture of 1.4. The gain and offset values were kept constant for all images compared within an experiment.

All images taken on the Zeiss LSM 510 multiphoton microscope were processed using Zeiss LSM Image Browser Version 4,2,0,121 and Inkscape 0.92 was used to adjust image orientation. All images taken on the Zeiss LSM 700 confocal microscope were processed using Zeiss Zen 2.3. Colocalization between glia (via endogenous repo expression) and LacZ was quantified using Volocity™ 3D Image Analysis Software version 6.3. All thresholds were automatically set and Pearson Correlation was reported. Mean pixel intensity of Z-stacks was quantified using ImageJ (NIH, Bethesda, MA, USA).

Chapter 5: Tyramine decarboxylase 2

Fly stocks.

Annotation/Gene	Supplier; stock number (if applicable)	Genotype
Sod 1	BDSC; 24493	w[*]; P{w[+mC]=UAS-Sod.IR}F103/SM5
	VDRC; v31552	w[1118]; 2[VDRC]; UAS-Sod1-IR[31552]/Sb
Sod2	John Phillips, University of Guelph	w[1]; UAS-Sod2-IR-15/SM6
	John Phillips, University of Guelph	w[1]; UAS-Sod2-IR-24/SM6; 3[?]
AdoR	VDRC; v1385	w[1118];; P{GD380}v1385
	VDRC; v1386	w[1118];; P{GD380}v1386
Nos	BDSC; 56829	P{w[+mC]=UAS-Nos.L}1, w[*];;
src42a	BDSC; 6410	w[1118];; P{w[+mC]=UAS-Src42A.CA}5
Eaat1	BDSC; 8202	y[1] w[1118];; P{w[+mC]=UAS-Eaat1.Exel}3/TM6B, Tb[1]
nrg	BDSC; 24169	w[*];; P{w[+mC]=UAS-nrg[180]}28b
	BDSC; 24172	w[*];; P{w[+mC]=UAS-nrg[167]}2/TM6B, Tb[1]
Htl	BDSC; 5366	y[1] w[*];; P{w[+mC]=UAS-htl.DN.M}33-B40; P{w[+mC]=UAS-htl.DN.M}33-B61
serca	BDSC; 63228	w[1118]; P{w[+mC]=UAS-SERCA.F}8
Rab27	BDSC; 23267	y[1] w[*];; P{w[+mC]=UASp-YFP.Rab27.T25N}nsl1[02]
mor	BDSC; 59074	w[*];; P{w+mC]=UAS-mor.DN}A3
pros	BDSC; 32244	P{w[+mC]=UAS-pros.L}L3a, w[*];;
Gαi	BDSC; 44600	P{w[+mC]=UAS-Galphai.L}1, w[*]; P{ry[+t7.2]=neoFRT}82B Df(3R)Gprk2/TM6B, Tb[1];;
RabX4	BDSC; 9849	y[1] w[*];; P{w[+mC]=UAST-YFP.RabX4.T40N}02/TM3, Sb[1]
	BDSC; 9850	y[1] w[*]; P{w[+mC]=UAST-YFP.RabX4.T40N}03
syx1A	BDSC; 51618	P{w[+mC]=UAS-Syx1A.B}2, y[1] w[*];;
repo-Gal4	BDSC; 7415	w^{1118};;Repo-Gal4/TM3 Sb
GliaGS	BDSC; 59929	w*; P{w[+mW.hs]=Switch2}GSG7293-1/TM6B, Tb[1]
Tdc2 RNAi #1	BDSC; 25871	y^1w^1;;TRiP.JF01910
Tdc2 RNAi #2	VDRC; v330541	w^{1118};P{VSH330541}attP40
UAS-Tdc2 #1	BDSC; 9316	w^{1118};;UAS-Tdc2
UAS-Tdc2 #2	BDSC; 9315	w^{1118};;UAS-Tdc2

alrm-Gal4	Mark Freeman, Oregon Health Science University	w^{1118};; alrm-Gal4 #2
VMAT RNAi # 1	VDRC; v4856	w^{1118};; P{GD1982}v4856
VMAT RNAi # 2	VDRC; v104072	w^{1118};KK112993/cyo
VMAT RNAi #1, UAS-Tdc2 #1	-	w^{1118};; P{GD1982}v4856, UAS-Tdc2, TM3SB
UAS-TeTx	BDSC; 28837	w*; P{w[+mC]=UAS-TeTxLC.tnt}E2
UAS-TeTx, UAS-Tdc2 #1	-	w^{1118}; P{w[+mC]=UAS-TeTxLC.tnt}E2, Cyo; UAS-Tdc2, TM3Sb
elav-Gal4	BDSC; 8760	w^{1118},elav-Gal4
UAS-Tbh	Henrike Scholtz, University of Koln	w^{1118}, UAS-Tbh
Tbh RNAi #1	VDRC; v51667	w^{1118}; P{GD6449}v51667
Tbh RNAi #2	VDRC; v107070	w^{1118};P{KK102670}VIE-260B
Tbh RNAi #3	BDSC; 27667	y^1v^1; P{y[+t7.7] v[+t1.8]=TRiP.JF02746}attP2
Tbh RNAi #4	BDSC; 67968	$y^1sc^*v^1$; P{y[+t7.7] v[+t1.8]=TRiP.HMS05829}attP40
Th RNAi #1	VDRC; v108879	w^{1118};;P{KK101660}VIE-260B
Th RNAi #2	BDSC; 25796	y^1v^1; P{y[+t7.7] v[+t1.8]=TRiP.JF01813}attP2
Th RNAi #3	BDSC; 65875	$y^1sc^*v^1$; P{y[+t7.7] v[+t1.8]=TRiP.HMC06137}attP2
Th RNAi #4	VDRC; v3308	w^{1118}; P{GD1181}v3308
Th OE	BDSC; 37539	w*; P{w[+mC]=UAS-ple.T}331f2
TIFR-Gal4	Mary Logan, Oregon Health Science University	w^{1118};;TIFR-Gal4
MZ0709-Gal4	Marc Freeman, Oregon Health Science University	w^{1118};;mz0709-Gal4
NP2222-Gal4	Mary Logan, Oregon Health Science University	w^{1118};NP2222-Gal4
Gli-Gal4	Doris Kretzschmar, Oregon Health Science University	w^{1118};Gli-Gal4
Indy-Gal4	Fred Wolf, University of California - Merced	w^{1118};;Indy-Gal4
repo-Gal4; GFP	Mary Logan, Oregon Health Science University	w^{1118}; +/Sco; UAS-mCD8::GFP, repo-Gal4/TM#, Sb, ftz-Lacz
syt1	BDSC; 31289	y[1] v[1];; P{y[+t7.7] v[+t1.8]=TRiP.JF01234}attP2
	VDRC; v100608	w[1118]; P{KK108653}VIE-260B
SNAP25	BDSC; 27306	y[1] v[1];; P{y[+t7.7] v[+t1.8]=TRiP.JF02615}attP2
	BDSC; 34377	y[1] sc[*] v[1];; P{y[+t7.7] v[+t1.8]=TRiP.HMS01367}attP2
syx1	BDSC; 25811	y[1] v[1];; P{y[+t7.7] v[+t1.8]=TRiP.JF01829}attP2
	VDRC; v33112	w[1118];; P{GD564}v33112
Syb	BDSC; 38234	y[1] sc[*] v[1];; P{y[+t7.7] v[+t1.8]=TRiP.HMS01678}attP2/TM3, Sb[1]
	BDSC; 39067	y[1] sc[*] v[1]; P{y[+t7.7] v[+t1.8]=TRiP.HMS01987}attP40/CyO
	BDSC; 44014	y[1] sc[*] v[1]; P{y[+t7.7] v[+t1.8]=TRiP.HMS02728}attP40
Rob	BDSC; 28929	y[1] v[1];; P{y[+t7.7] v[+t1.8]=TRiP.HM05140}attP2
	BDSC; 51925	y[1] v[1]; P{y[+t7.7] v[+t1.8]=TRiP.HMC03422}attP40/CyO
ykt6	BDSC; 50937	y[1] v[1]; P{y[+t7.7] v[+t1.8]=TRiP.HMJ21032}attP40
	VDRC; v19329	w[1118]; P{GD8927}v19329/CyO
	BDSC; 38314	y[1] sc[*] v[1]; P{y[+t7.7] v[+t1.8]=TRiP.HMS01778}attP40
	VDRC; v105648	w[1118]; P{KK101343}VIE-260B
snapin	BDSC; 40837	y[1] v[1]; P{y[+t7.7] v[+t1.8]=TRiP.HMS02003}attP40
syt4	BDSC; 26730	y[1] v[1];; P{y[+t7.7] v[+t1.8]=TRiP.JF02272}attP2/TM3, Sb[1]
	VDRC; v33317	w[1118];; P{GD2842}v33317
TyrR	VDRC; v2857	w[1118];; P{GD691}v2857/TM3
	BDSC; 25857	y[1] v[1];; P{y[+t7.7] v[+t1.8]=TRiP.JF01878}attP2

	BDSC; 57496	y[1] sc[*] v[1];; P{y[+t7.7] v[+t1.8]=TRiP.HMC04811}attP2
TyrRII	VDRC; v51387	w[1118] P{GD690}v51387;;
	BDSC; 27670	y[1] v[1];; P{y[+t7.7] v[+t1.8]=TRiP.JF02749}attP2
	BDSC; 64964	y[1] sc[*] v[1];; P{y[+t7.7] v[+t1.8]=TRiP.HMC05838}attP2
TAR1	VDRC; v26876	w[1118]; P{GD13188}v26876;
	BDSC; 28332	y[1] v[1];; P{y[+t7.7] v[+t1.8]=TRiP.JF02967}attP2

Tyramine feeding. 100 mL of 100 mg/mL tyramine (tyramine hydrochloride; Sigma Aldrich, St. Louis, MO) or vehicle (5% sucrose in diH_2O) was added to the surface of solidified food in vials and allowed to dry overnight in an environmental chamber. Adult flies were collected and placed on food topped with tyramine or vehicle (control) for 2 days total.

Yohimbine feeding. Adult flies were collected and starved in empty food vials for 17 hours. Whatman #1 filter papers (Cat. No 1001 125; Whatman International Ltd., Maidstone, England) were placed at the bottom of empty food vials, and the drug treatment was administered onto the filter paper. Vials were treated with either 1 mg/mL yohimhine (yohimbine hydrochloride; Sigma Aldrich, St. Louis, MO) or vehicle (5% sucrose in diH_2O). Starved flies were transferred onto the drug treated vials for 1 hr and 45 min.

Immunodetection. The following primary antibodies at the indicated concentrations from the listed sources were used: rabbit anti-Tdc2 (1:200; Covalab, Villeurbanne, France), rabbit anti-VMAT (1:2000, David Krantz, University of California - Los Angeles.). The following secondary antibody was used: chicken anti-rabbit Alexa 647 (1:1000; ThermoFisher, Waltham, MA).

All images were collected using a Zeiss LSM 700 confocal microscope (Carl Zeiss Microscopy, LLC, Thornwood, NY) housed in the VCU Department of Anatomy and Neurobiology Microscope Facility. Confocal images using a pin hole of 1 Airy disc unit and Nyquist sampling were collected from each adult brain. Images were taken with a 10X objective with a numerical aperture of 0.3. The laser power, gain and offset values were kept constant for all images compared within an experiment. All images were processed using Zeiss Zen 2.3. Mean pixel intensity of individual Z-stacks were quantified using ImageJ (NIH, Bethesda, MA, USA).

CHAPTER 3: CHARACTERIZATION OF A CNS-GLIA SPECIFIC GENESWITCH FLY STOCK

A. INTRODUCTION

Development is an extremely sensitive time in any species, including in the fruit fly *Drosophila melanogaster*. Molecular expression changes can result in robust alterations in the neuronal circuitry, which can have an impact on the adult fly lifespan and behavior[27,139,153]. Glia are major regulators of neuronal migration and circuitry assembly[27,153]. While changes to CNS development are relevant for alcohol use disorder[219-221], we were interested in investigating alcohol-related behavioral changes due to acute molecular mechanisms within glia, and not due to glia-dependent CNS developmental changes. Therefore, to bypass any developmental changes associated with glial gene manipulation, we utilized the GeneSwitch system[29]. The GeneSwitch protein is a steroid-inducible Gal4 driver, and therefore allows temporal control of UAS-transgene expression. In the presence of steroid (mifepristone, referred to as RU486 throughout), the GeneSwitch Gal4 driver is changed to an active confirmation, and is able to bind to the upstream activator sequence (UAS) and induce expression of the associated transgene. However, when RU486 is not present, the Gal4 driver is in an inactive confirmation, and therefore cannot bind to the UAS and induce transgene expression[29]. To bypass development and manipulate gene expression during adulthood, flies are fed RU486 during adulthood and not during development. This

system has been used extensively previously to manipulate gene expression during adulthood in ubiquitous and pan-neuronal manners[222-224], although when we started this project no glial-specific GeneSwitch reagent had been characterized. However, Nicholson and colleagues screened approximately 3,000 publically available GeneSwitch flies[29]. Each of these flies had a randomly inserted GeneSwitch p-element, and therefore the GeneSwitch expression pattern for many lines was unknown. In third-instar larvae, 433 GeneSwitch lines induced GFP expression in neurons, glia or muscles[29]. Using this expression data, we selected candidate fly lines that induced GFP expression in larval glia, and not in other tissues. We wanted to determine if (i) the GeneSwitch induced transgene expression in adult flies fed 1 mM RU486 for 6 days, (ii) the GeneSwitch induced transgene expression in glia during adulthood and (iii) the RU486 feeding regimen did not influence alcohol sedation behavior in control flies. In total, we tested two transgenic lines: 59929 (GeneSwitch ID 7293) and 40262 (GeneSwitch ID 1821).

B. RESULTS

B.1 IDENTIFYING GENESWITCH REAGENTS THAT INDUCE LACZ TRANSGENE EXPRESSION DURING ADULTHOOD

Given that each GeneSwitch fly is unique, we wanted to determine if the candidate GeneSwitch transgenic flies were capable of inducing robust transgene expression. To measure relative amounts of transgene induction, we utilized the β-galactosidase activity assay to quantify the amounts of LacZ protein produced via UAS-LacZ transgene induction. To validate this assay, we measured LacZ activity in flies

expressing a UAS-LacZ transgene ubiquitously (via *da*-Gal4), in all neurons (via *elav*-Gal4) and in all glia (via *repo*-Gal4). As anticipated, we found that flies with both *da*-Gal4 and UAS-LacZ had the most LacZ activity (Fig 1; green line, slope = 0.05). Flies with both *elav*-Gal4 and UAS-LacZ had a median amount of LacZ activity (Fig 1; purple line, slope = 0.03) and flies with both *repo*-Gal4 and UAS-LacZ had the least amount of LacZ activity (Fig 1; red line, slope = 0.005). Since the amount of LacZ activity correlated with size of the tissue represented by each Gal4 driver (i.e. presumably *da*-Gal4 induces in the most cells, *elav*-Gal4 induces in the second highest and *repo*-Gal4 induces in the smallest population of cells), we felt comfortable using this technique to measure how much LacZ each GeneSwitch driver induced when flies were fed RU486.

We investigated whether flies expressing a GeneSwitch candidate transgene and the UAS-LacZ transgene had increased LacZ activity when fed RU486 compared to controls. For all experiments, flies were fed 1 mM RU486 for 6 days. Flies with the 59929 GeneSwitch transgene and the UAS-LacZ transgene fed RU486 had an increase in LacZ activity (Fig 2A; black line, slope = 0.03) and control flies had no LacZ activity (slopes indistinguishable from zero). Control flies either had the 59929 GeneSwitch transgene and UAS-LacZ transgene and were fed vehicle, the UAS-LacZ transgene alone fed RU486 or vehicle and the 59929 GeneSwitch transgene alone fed RU486 or vehicle (Fig 2A). The 59929 GeneSwitch transgene induced LacZ activity well above the background of the controls, so we decided to characterize this reagent further. Additionally, flies with the 40262 GeneSwitch transgene and the UAS-LacZ transgene fed RU486 had an increase in LacZ activity (Fig 2B; black line, slope = 0.003) and control flies had no LacZ activity (slopes indistinguishable from zero). Control flies either

had the 40262 GeneSwitch transgene and UAS-LacZ transgene and were fed vehicle, the UAS-LacZ transgene alone fed RU486 or vehicle and the 40262 GeneSwitch transgene alone fed RU486 or vehicle (Fig 2B). However, the 40262 GeneSwitch transgene did not induce LacZ activity above the background of the controls, making this GeneSwitch transgene unattractive for use in behavioral studies; therefore, we decided not to move forward with characterizing this reagent.

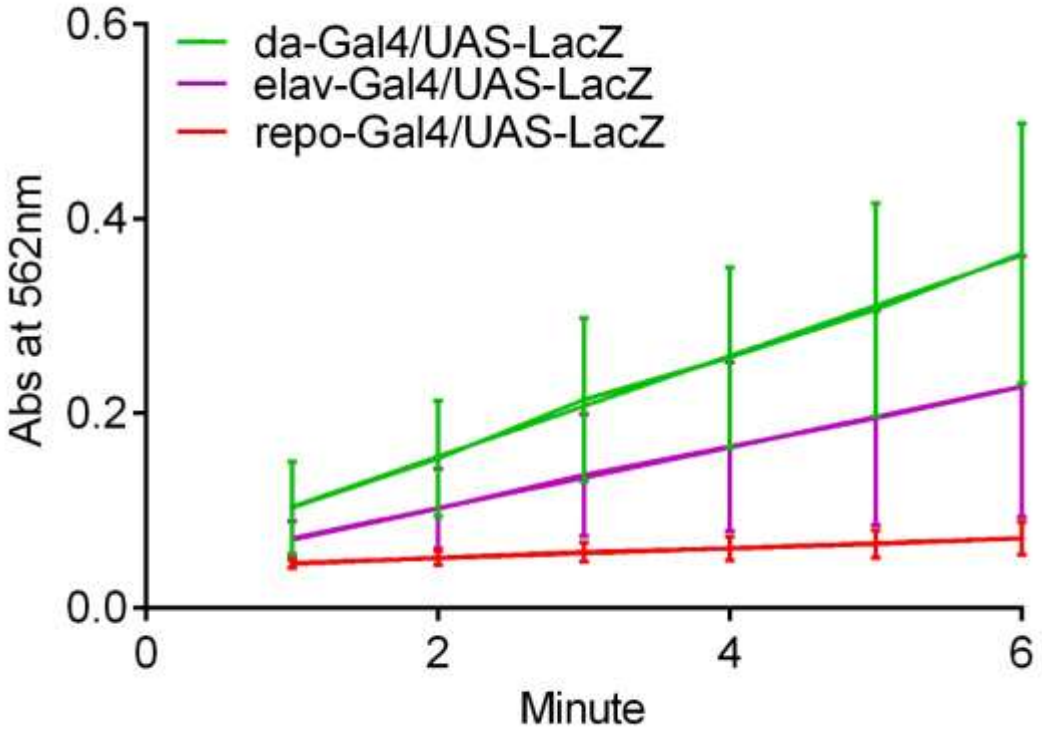

Figure 3.1. LacZ induction can be measured in a tissue-size dependent manner. Using the β-galactosidase activity assay, flies expressing UAS-Lacz ubiquitously via *da*-Gal4 had the largest amount of LacZ activity (green line: slope = 0.05 ± 0.04, p = 0.0003, n = 3). Flies expressing UAS-LacZ in all neurons via *elav*-Gal4 had the second largest amount of LacZ activity (purple line: slope = 0.03 ± 0.01, p = 0.0073, n = 3). Flies expressing UAS-LacZ in all glia via *repo*-Gal4 had the least amount of LacZ activity (red line: slope = 0.005 ± 0.001, p = 0.0021, n = 3). P-values represent how different the slope is from zero. β-galactosidase activity was measured for 6 minutes.

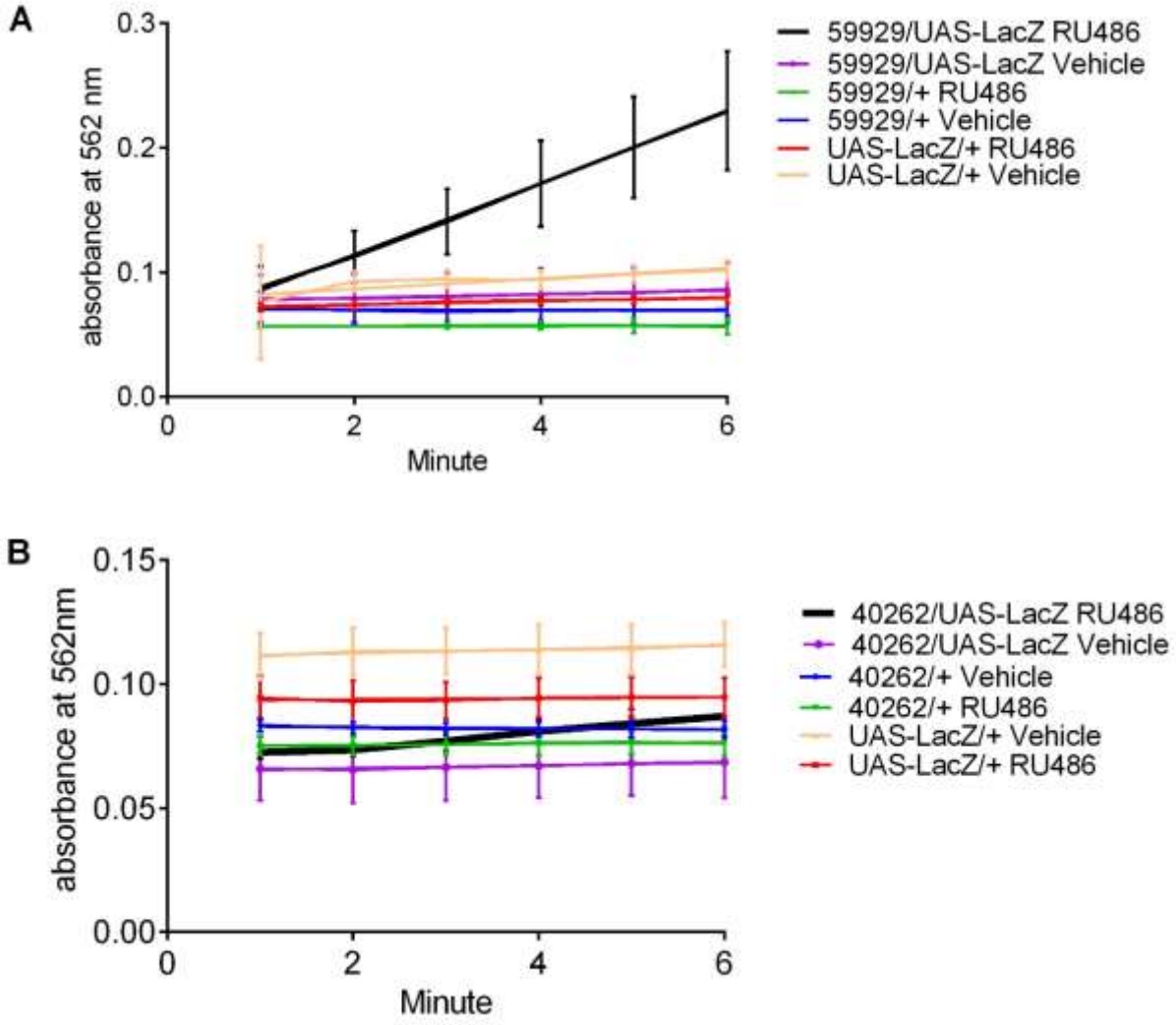

Figure 3.2. GeneSwitch transgenes induce different amount of UAS-LacZ. (**A**) Using the β-galactosidase activity assay, flies expressing the 59929 GeneSwitch transgene and UAS-LacZ transgene fed 1mM RU486 for 6 days had significant LacZ activity (black line: slope = 0.03 ± 0.004, $p < 0.0001$, n = 5). All other groups were controls and had insignificant slopes, indicating that there was no LacZ activity. (**B**) Using the β-galactosidase activity assay, flies expressing the 40262 GeneSwitch transgene and UAS-LacZ transgene fed 1mM RU486 for 6 days had significant LacZ activity (black line: slope = 0.003 ± 0.0009, $p = 0.008$, n = 5). All other groups were controls and had insignificant slopes, indicating that there was no LacZ activity. P-values represent how different the slope is from zero. β-galactosidase activity was measured for 6 minutes.

B.2 THE 59929 GENESWITCH TRANSGENE INDUCES UAS-TRANSGENE EXPRESSION IN CNS GLIA

Flies with the GeneSwitch 59929 transgene and UAS-LacZ transgene were fed either RU486 or vehicle during adulthood. After exposure to RU486, we dissected their brains and labeled endogenous glial cells (in green via anti-repo; Fig 3A) and induced LacZ (in red via anti-LacZ; Fig 3B). Colocalization is represented in yellow (Fig 3C). When quantified, approximately 96 percent of green pixels expressed a red pixel, indicating that approximately 96 percent of glia also expressed LacZ (Mander's correlation = 0.957; n = 7). Additionally, flies fed vehicle expressed no LacZ, suggesting that the 59929 GeneSwitch transgene induces UAS-transgene expression when RU486 is present. Given that the 59929 GeneSwitch transgene induces transgene expression in glia, we termed this reagent "GliaGS".

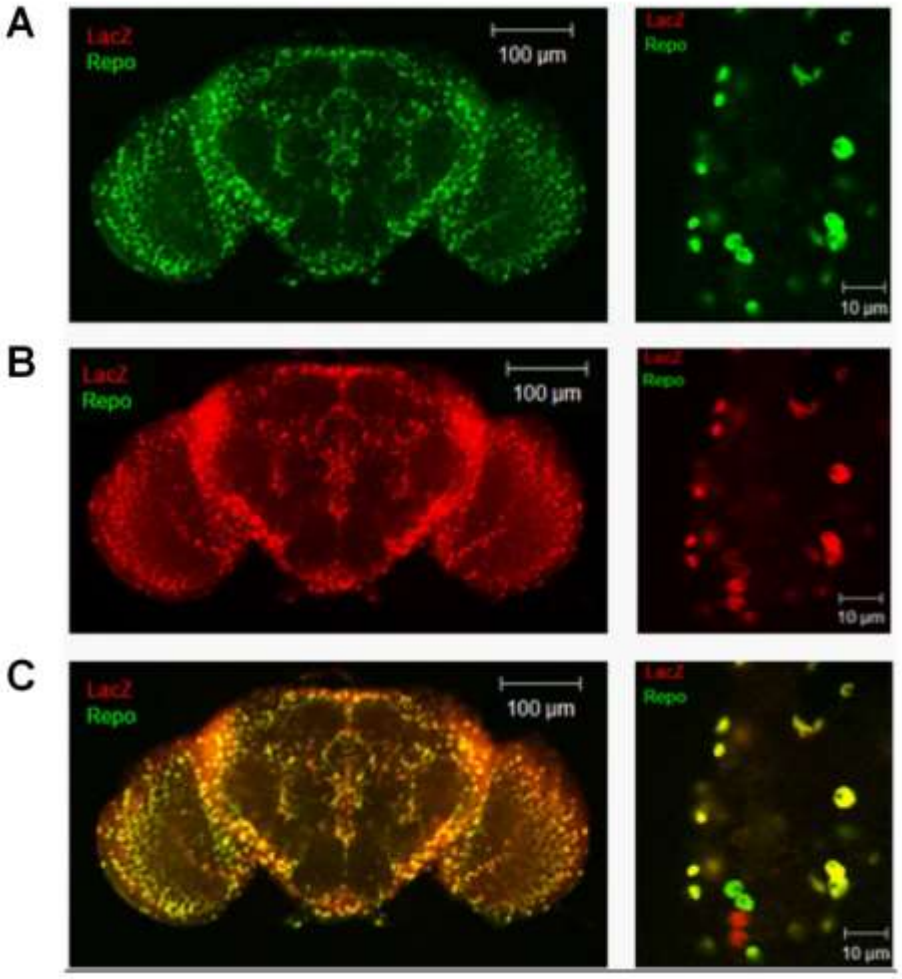

Figure 3.3. GliaGS drives expression in CNS glia during adulthood. Flies with the 59929 GeneSwitch transgene and the UAS-LacZ transgene were fed 1 mM RU486 for 6 days prior to brain dissection and immunolabeling. (**A**) Endogenous repo expression (green) indicating CNS glia (anti-repo 1:100, Alexa 488 1:1000) (**B**) GliaGS-driven LacZ expression labeled red (anti-LacZ 1:500, Alexa 568 1:1000) (**C**) Merged images of panels A and B; yellow indicates co-localization of repo and LacZ. Representative images from 10X and 63X oil.

B.3 THE RU486 FEEDING REGIMENT DOES NOT ALTER ALCOHOL SEDATION SENSITIVITY IN CONTROL FLIES

To determine if feeding 1 mM RU486 to flies for 6 days altered their behavioral responses to alcohol in control flies, we measured the ST50's of flies with the GliaGS transgene alone fed vehicle or RU486, a universal control for any behavioral experiment utilizing GliaGS. Compared to vehicle control, GliaGS/+ flies fed RU486 had no change in ST50, indicating that this regimen of RU486 exposure, which can induce transgene expression, does not impact ethanol sedation in control animals.

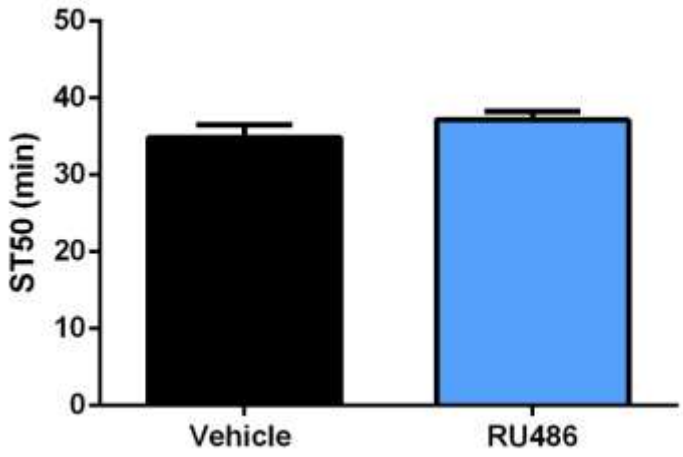

Figure 3.4. RU486 feeding regiment does not alter alcohol sedation sensitivity. Flies with the GliaGS transgene (59929) alone were fed vehicle or 1mM RU486 for 6 days. Treatment did not alter ST50 values (student's t test, $p = 0.264$, $n = 8$).

CHAPTER 4: CYSTEINE PROTEINASE 1 REGULATES *DROSOPHILA* ALCOHOL SEDATION BY FUNCTIONING IN ADULT CORTEX GLIA

A. INTRODUCTION

In largely naïve alcohol drinkers, the initial level of response to alcohol correlates with their likelihood of becoming alcohol dependent[225], a significant phenotype associated with AUD[3]. For example, men with an initially low sensitivity to alcohol are four times more likely to be an alcoholic by age thirty[225]. Therefore, investigating molecular-genetic mechanisms that influence alcohol sensitivity is a potentially promising approach for understanding the molecular underpinnings of AUD.

The fruit fly *Drosophila melanogaster*, the nematode *C. elegans* and rodents have been used extensively to investigate the genetics of alcohol-related behaviors, including alcohol sedation. Numerous genes involved in alcohol-related behaviors in model organisms have human orthologues that have been implicated in human alcohol abuse, suggesting mechanistic connections between alcohol-related behaviors in model organisms and alcohol abuse in humans[226,227]. A majority of these genes are known or predicted to function in neurons[226], leaving the contribution of glia and glial cell mechanisms to alcohol-related behavior largely unexplored. To the best of our knowledge, only three studies have investigated the direct contribution of glia in alcohol-related behaviors. One study found that activation of calcium signaling in rat nucleus accumbens core astrocytes via DREADDS decreases motivation for alcohol after a

three week long alcohol abstenance[183]. Another study found that *Drosophila* with a mutation in the gene *moody*, a gene expresssed in surface glia as well as other cell types, have reduced sensitivity to ethanol-induced loss of postural control[211]. An additional study in *Drosophila* found that surface glia also contribute to alcohol tolerance[212]. Despite these pioneering studies, our understanding of the role of glia in alcohol-related behavior is woefully incomplete.

The *Drosophila* central nervous system (CNS) is compartmentalized into two gross anatomical regions: an outer cortex (containing neuronal cell bodies) and a more central neuropil (containing neurites and synapses). Like mammals, the *Drosophila* CNS is composed of both neurons and glia. *Drosophila* CNS glia are functionally and molecularly similar to mammalian CNS glia[27,40,142,228,229]. Cortex glia, astrocytes and ensheathing cells are the main subtypes of CNS glia in adult flies[40]. Additionally, perineural and subperineural glia, often referred to as surface glia, surround the entire CNS and compose the blood brain barrier in flies[128,230]. *Drosophila* cortex glia and astrocytes are intimately associated with neurons in the CNS[125]. Cortex glia are located in the cortex region of the brain and encapsulate virtually all neuronal cell bodies with fine processes[124]. A single adult cortex glial cell is thought to be able to encapsulate up to 100 neurons[125]. Cortex glia aid in gas exchange, neuronal firing and nutrient transfer to neurons, similarly to mammalian protoplasmic astrocytes[40,124,231]. Cortex glia also exhibit calcium transients near membranes close to neurons, which appear to regulate neuronal cell function[133]. Physical associations between cortex glia and neurons are essential for normal nervous system function and behavior in *Drosophila*[39]. In contrast to cortex glia, the cell bodies of astrocytes reside at the cortex-neuropil interface and

extend processes into the neuropil[36]. Like mammalian astrocytes, *Drosophila* astrocytes are important for synapse formation and maintenance, clearing and recycling neurotransmitters from the synapse, and modulating neuronal physiology[141,232]. *Drosophila* astrocytes release gliotransmitters, which are regulated by transient intracellular calcium signaling; this mechanism can directly influence nearby cells and influence behavior[27,143,146]. The cell bodies of ensheathing glia are also located at the interface of the brain cortex and neuropil[36]. Under normal physiological conditions, ensheathing glia encase the entire neuropil region in the CNS and occasionally wrap axonal segments between the neuropil and the periphery[34]. Ensheathing glia can regulate neuronal excitability by metabolizing glutamate, and disruptions in this function can alter behavior[35]. Under pathological conditions, these cells extend processes into the neuropil to phagocytize debris[36-38]. *Drosophila* surface glia (i.e. subperineural and perineural glia) are less similar to mammalian glia, but they have been associated with alcohol-related behavior in flies[211,212]. Subperineural glia mediate most of the blood brain barrier chemoprotective functions, similar to mammalian brain vascular endothelial cells[33]. Interestingly, subperineural glia can extend processes which function at PNS synapses[150]. As their name implies, perineural glia reside on top of the subperineural glia, and protect against the entrance of larger molecules[213]. With macrophages, these cells secrete a dense lamella that covers the CNS and peripheral nerves[213]. Despite being extensively investigated in numerous experimental settings, a role for glia in fly alcohol-related behavior has not been comprehensively explored.

Here, we demonstrate that RNAi-mediated knockdown and rescue of the gene *cysteine proteinase 1* (*Cp1*) constitutively in all CNS glia regulates alcohol sedation.

This behavioral effect appears specific to Cp1 expression in cortex glia, as well as all glia during adulthood. Cp1 is a hydrolase involved in protein degradation that is functionally and structurally homologous to mammalian Cathepsin L[233]. Our data suggest a novel role for cortex glia and Cp1 in the adult *Drosophila* CNS: regulation of sedation in response to acute administration of alcohol.

B. RESULTS

B.1 IDENTIFYING GLIAL GENES THAT INFLUENCE ALCOHOL-RELATED BEHAVIOR IN DROSOPHILA

To begin exploring the role of central nervous system (CNS) glia in alcohol behavior, we performed a targeted screen in which we (i) compiled genes previously reported to be expressed in glia[142], (ii) obtained RNAi reagents to manipulate the expression of those genes, and (iii) determined whether constitutive expression of RNAi targeting of those genes in glia influenced alcohol sedation. In total, we screened 13 genes by RNAi and identified 5 genes whose expression in glia influenced alcohol sedation sensitivity (Table 4.1).

Flies with pan-glial Gal4 (via *repo*-Gal4) driven expression of the *Cp1* RNAi #1 transgene had significantly decreased sedation time 50 (ST50) values compared to control flies containing the Gal4 or an RNAi transgene alone (Fig. 4.1A). Similar results were obtained with flies containing *repo*-Gal4 and an RNAi transgene for the genes *axo* (Fig 4.1B, 4.1C), *Jhl-21* (Fig 4.1D), *nemy* (Fig 4.1E) and *Ent2* (Fig 4.1F).

To characterize the role of these genes in alcohol sedation further, we (i) determined if expression of RNAi against these genes in glia altered alcohol metabolism and (ii) determined if expression of RNAi against these genes in neurons influenced

alcohol sedation. To determine if these genes influenced alcohol metabolism, we measured the internal alcohol levels in these flies after an 30-minute alcohol exposure (approximating the ST50). We found no significant difference in the internal alcohol concentrations between flies expressing an RNAi transgene in glia (via *repo*-Gal4) compared to controls that expressed the respective RNAi transgene or *repo*-Gal4 transgene alone (Table 4.2). These results suggest that *Cp1, axo, Jhl-21, nemy* and *Ent2* might influence a pharmacodynamic mechanism that impinges on alcohol sedation. To determine if expression of RNAi against these genes in neurons influenced alcohol sedation, we compared the ST50 values of flies with both pan-neuronal Gal4 (via *elav*-Gal4) and an RNAi transgene to control flies that had the *elav*-Gal4 transgene or the respective RNAi transgene alone. We found no significant difference in ST50 between flies expressing an RNAi transgene individually for *Cp1, axo, Jhl-21, nemy* and *Ent2* in neurons (via *elav*-Gal4) compared to controls (Table 4.3). While not fully conclusive, these data begin to suggest that expression of *Cp1, axo, Jhl-21, nemy* and *Ent2* in glia, but not neurons, is important for alcohol sedation.

Lastly, we aimed to determine whether expression of RNAi against these genes during adulthood influenced alcohol sedation because CNS glia play important roles during both development[229,234,235] and adulthood[125,229,236]. To express the RNAi transgenes against *Cp1, axo, Jhl-21, nemy* and *Ent2* in glia during adulthood, we used the steroid-inducible GeneSwitch (GS) system[29]. Specifically, we utilized GliaGS, a driver that induced transgene expression in glia. Flies with both the GliaGS driver and an RNAi transgene, and control flies with either GliaGS or the respective RNAi transgene alone, were reared to adulthood in the absence of the steroid mifepristone

(RU486) and then switched to food medium containing steroid (RU486) or vehicle for 6 days, allowing induced transgene expression exclusively for 6 days during adulthood. Compared to vehicle control animals of the same genotype, flies containing both GliaGS and the *Cp1* RNAi #1 transgene fed RU486 had significantly decreased ST50 values (Fig 4.2A). Exposure to RU486 in flies with either the GliaGS alone or the Cp1 RNAi transgene alone did not alter ST50 values (Fig 4.2A). However, compared to vehicle control animals of the same genotype, flies containing both GliaGS and an RNAi transgene against *Axo, Jhl-21, nemy* or *Ent2* transgene fed RU486 had similar ST50 values (Fig 4.2B-F). Taken together, these data suggest a role for *Cp1* expression in adult glia. While follow-up experiments would be needed, our data begin to suggest that expression of *axo, jhl-21, nemy* and *Ent2* function in glia during development to influence alcohol sedation.

Since expression of the *Cp1* RNAi transgene in glia during adulthood altered alcohol sedation, we postulated that Cp1 is likely functioning through an acute molecular pathway in glia to alter alcohol sedation. Due to this, we decided to pursue research on Cp1 further. *Cysteine Proteinase 1* (*Cp1*) is known to function in *Drosophila* midgut, garland cells, salivary glands, macrophages, gonads and PNS neurons[233,237-240] and is expressed in glia[142], but prior to our results no studies have demonstrated a functional role for Cp1 in glia. Cp1 is the only *Drosophila* cysteine proteinase that has been described and is functionally and structurally homologous to mammalian Cathepsin L[238,241]. Although cysteine proteinases play key roles in the lysosomes of phagocytic cells[240] and mammalian Cathepsin L has been associated with multiple diseases including cancer[242,243], Alzheimer Disease[244] and retinal degeneration[238], no

previous studies implicate this family of genes in alcohol-related behavior. In subsequent experiments, we aimed to (i) validate our previous findings by repeating experiments and/or using different methods to manipulate Cp1, (ii) determine which glial cell subtype Cp1 expression is required in for normal alcohol sedation and (iii) investigate whether Cp1 expression in glia is important for any other alcohol related behaviors.

Table 4.1. Screen results: expressing RNAi against genes known to be expressed in glia and measuring alcohol sedation sensitivity.

Gene	reagent (identifier)	Group	ST50	ANOVA	Bonferonni mult. comparisons (to Gal4/RNAi)
axo	RNAi (v18866)	Gal4/+	30.38 ± 1.05[#]	F (4, 35) = 19.13, p < 0.0001[#]	p < 0.0001
		RNAi/+	33.1 ± 1.28		p < 0.0001
		Gal4/RNAi	21.16 ± 1.07		n/a
	RNAi (v18867)	Gal4/+	32.49 ± 1.29[$]	F (5, 42) = 17.45, p < 0.0001[$]	p < 0.0001
		RNAi/+	34.43 ± 0.99		p < 0.0001
		Gal4/RNAi	20.26 ± 0.81		n/a
akap200	RNAi (v5647)	Gal4/+	32.49 ± 1.29[$]	F (5, 42) = 17.45, p < 0.0001[$]	p = 0.107
		RNAi/+	33.26 ± 1.28		p = 0.253
		Gal4/RNAi	37.08 ± 2.35		n/a
loco	RNAi (v9248)	Gal4/+	30.38 ± 1.05 [#]	F (4, 35) = 19.13, p < 0.0001[#]	p = 0.577
		RNAi/+	33.11 ± 1.16		p > 0.9999
		Gal4/RNAi	32.85 ± 1.35		n/a
nrv1	RNAi (v46542)	Gal4/+	32.19 ± 1.12[@]	F (4, 33) = 2.243, p = 0.08[@]	n/a
		RNAi/+	33.65 ± 2.54		n/a
		Gal4/RNAi	31.86 ± 2.17		n/a
unc5	RNAi (v8138)	Gal4/+	26.23 ± 0.98[~]	F (4, 33) = 7.076, p = 0.0003[~]	p = 0.0004
		RNAi/+	30.65 ± 1.13		p = 0.27
		Gal4/RNAi	33.95 ± 2.07		n/a
	RNAi (v8137)	Gal4/+	23.49 ± 0.82	F (2, 20) = 0.32, p = 0.726	n/a
		RNAi/+	23.19 ± 0.78		n/a
		Gal4/RNAi	24.39 ± 1.57		n/a
Cp1	RNAi (v13959)	Gal4/+	26.43 ± 1.064	F (2, 21) = 3.94, p = 0.035	p = 0.045
		RNAi/+	26.33 ± 1.40		p = 0.05
		Gal4/RNAi	21.69 ± 1.57		n/a
draper	RNAi (v4833)	Gal4/+	32.61 ± 1.54[%]	F (4, 33) = 1.354, p = 0.271[%]	n/a
		RNAi/+	31.78 ± 1.25		n/a
		Gal4/RNAi	30.09 ± 1.94		n/a
	RNAi (v27086)	Gal4/+	32.61 ± 1.54[%]	F (4, 33) = 1.354, p = 0.271[%]	n/a
		RNAi/+	33.66 ± 1.13		n/a
		Gal4/RNAi	34.71 ± 1.66		n/a

CG6218	RNAi (v35069)	Gal4/+	28.38 ± 1.21	F (2, 21) = 3.52, p = 0.04	p = 0.041
		RNAi/+	27.70 ± 0.97		p = 0.11
		Gal4/RNAi	24.83 ± 0.77		n/a
Jhl-21	RNAi (v45190)	Gal4/+	28.60 ± 1.57^	F (4, 34) = 6.461, p = 0.0006^	p > 0.9999
		RNAi/+	24.19 ± 0.58		p = 0.35
		Gal4/RNAi	27.20 ± 1.76		n/a
	RNAi (v45191)	Gal4/+	28.60 ± 0.77^	F (4, 34) = 6.461, p = 0.0006^	p = 0.001
		RNAi/+	28.56 ± 1.18		p = 0.001
		Gal4/RNAi	21.80 ± 0.36		n/a
	RNAi (v45192)	Gal4/+	20.63 ± 0.87+	F (4, 32) = 2.108, p = 0.102+	n/a
		RNAi/+	21.64 ± 0.88		n/a
		Gal4/RNAi	21.05 ± 1.09		n/a
	RNAi (v45193)	Gal4/+	20.63 ± 0.87+	F (4, 32) = 2.108, p = 0.102+	n/a
		RNAi/+	24.29 ± 1.14		n/a
		Gal4/RNAi	21.73 ± 0.81		n/a
argk	RNAi (v34037)	Gal4/+	24.16 ± 2.49	F (2, 21) = 2.32; p = 0.122	n/a
		RNAi/+	25.89 ± 2.76		n/a
		Gal4/RNAi	26.86 ± 0.83		n/a
nemy	RNAi (v7909)	Gal4/+	26.23 ± 0.98~	F (4, 33) = 7.076, p = 0.0003~	p > 0.9999
		RNAi/+	29.64 ± 1.01		p = 0.16
		Gal4/RNAi	26.20 ± 0.76		n/a
	RNAi (v40803)	Gal4/+	26.6 ± 0.81=	F (4, 35) = 14.89, p < 0.0001*	p = 0.05
		RNAi/+	27.56 ± 1.51		p = 0.01
		Gal4/RNAi	22.73 ± 1.02		n/a
Ent2	RNAi (v7618)	Gal4/+	26.2 ± 0.81=	F (4, 35) = 14.89, p < 0.0001*	p < 0.0001
		RNAi/+	24.38 ± 0.78		p = 0.0001
		Gal4/RNAi	17.21 ± 0.98		n/a
DAT	RNAi (v12082)	Gal4/+	32.19 ± 1.24@	F (4, 33) = 2.243, p = 0.08@	n/a
		RNAi/+	36.21 ± 0.91		n/a
		Gal4/RNAi	28.23 ± 1.94		n/a

Table 4.1. Each gene and the RNAi reagent used to presumably manipulate gene expression are listed in the first two columns. The ST50 ± SEM are listed for each genotype: Gal4/+ (*repo*-Gal4/+), RNAi/+ (the respective RNAi transgene/+) and Gal4/RNAi (repo-Gal4/RNAi transgene). If the ANOVA is significant, we reported the Bonferonni multiple comparisons adjusted p-value. To determine if expression of the RNAi transgene in glia (via *repo*-Gal4) influences alcohol sedation, we compared the Gal4/RNAi group to the Gal4/+ group and the RNAi/+. $, #, @, ~, %, ^, + and = symbols represent common Gal4/+ controls ST50 and ANOVA values, due to multiple genotypes being tested in the same experiment.

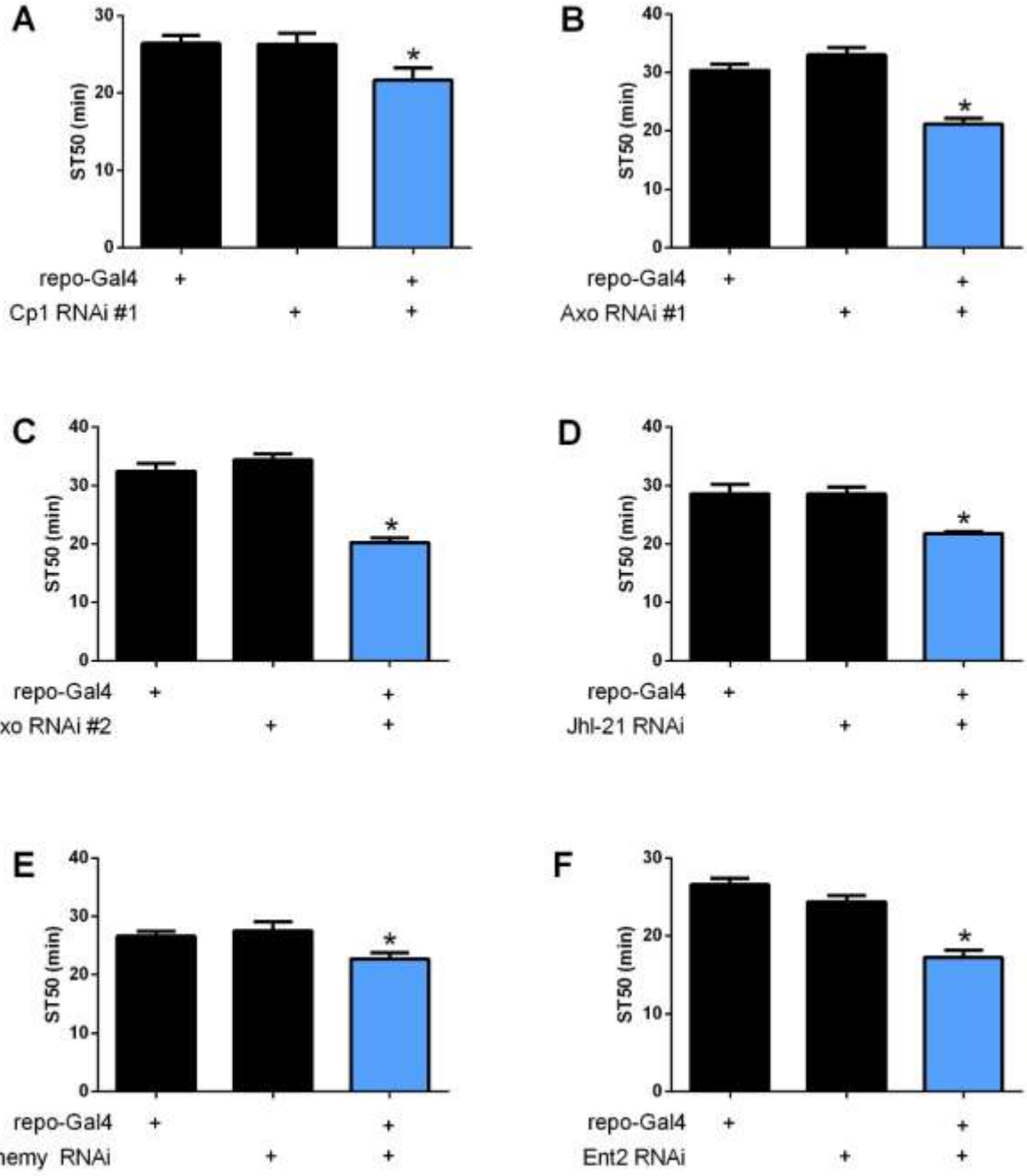
A
ST50 (min)
30
20
10
0
*
repo-Gal4 + +
Cp1 RNAi #1 + +
B
ST50 (min)
40
30
20
10
0
*
repo-Gal4 + +
Axo RNAi #1 + +
C
ST50 (min)
40
30
20
10
0
*
repo-Gal4 + +
Axo RNAi #2 + +
D
ST50 (min)
40
30
20
10
0
*
repo-Gal4 + +
Jhl-21 RNAi + +
E
ST50 (min)
40
30
20
10
0
*
repo-Gal4 + +
nemy RNAi + +
F
ST50 (min)
30
20
10
0
*
repo-Gal4 + +
Ent2 RNAi + +

Figure 4.1. Expression of RNAi against Cp1, axo, Jhl-21, nemy and Ent2 in glia alters alcohol sedation. (**A**) ST50 values were reduced in flies expressing the *Cp1* RNAi #1 transgene in glia (blue bar: *repo*-Gal4/*Cp1* RNAi #1) compared to control flies with either *repo*-Gal4 alone (black bars: *repo*-Gal4/+) or the RNAi transgenes alone (black bars: *Cp1* RNAi #1/+) (one-way ANOVA, $p = 0.0352$; *Bonferroni's multiple comparison vs controls, $p < 0.05$; $n = 8$). (**B, C**) ST50 values were reduced in flies expressing *axo* RNAi transgenes in glia (blue bars: *repo*-Gal4/*axo* RNAi #1, panel B; *repo*-Gal4/*axo* RNAi #2, panel C) compared to control flies with either *repo*-Gal4 alone or the respective RNAi transgene alone (black bars) (Panel A: one-way ANOVA, $p < 0.0001$; *Bonferroni's multiple comparison vs controls, $p < 0.05$; $n = 8$; Panel B: one-way ANOVA, $p < 0.0001$; *Bonferroni's multiple comparison vs control, $p < 0.05$; $n = 8$). (**D**) ST50 values were reduced in flies expressing a *Jhl-21* RNAi transgene in glia (blue bar: *repo*-Gal4/*Jhl-21* RNAi) compared to control flies with either *repo*-Gal4 alone or the RNAi transgene alone (black bars) (one-way ANOVA, $p = 0.0004$; *Bonferroni's multiple comparison vs controls, $p < 0.05$; $n = 8$). (**E**) ST50 values were reduced in flies expressing a *nemy* RNAi transgene in glia (blue bar: *repo*-Gal4/*nemy* RNAi) compared to control flies with either *repo*-Gal4 alone or the RNAi transgene alone (black bars) (one-way ANOVA, $p = 0.018$; *Bonferroni's multiple comparison vs controls, $p < 0.05$; $n = 8$). (**F**) ST50 values were reduced in flies expressing a *Ent2* RNAi transgene in glia (blue bar: *repo*-Gal4/*Ent2* RNAi) compared to control flies with either *repo*-Gal4 alone or the RNAi transgene alone (black bars) (one-way ANOVA, $p < 0.0001$; *Bonferroni's multiple comparison vs controls, $p < 0.05$; $n = 8$).

Table 4.2. Expression of RNAi against Cp1, axo, Jhl-21, nemy and Ent2 in glia does not alter internal alcohol concentrations.

Gene	reagent (identifier)	Group	Internal EtOH (nM)	ANOVA	Bonferonni mult. comparisons (to Gal4/RNAi)
Cp1	RNAi (v13959)	Gal4/+	152.4 ± 12.46#	F (2, 15) = 1.25, p = 0.31	n/a
		RNAi/+	128.3 ± 9.87		n/a
		Gal4/RNAi	148.8 ± 6.33		n/a
axo	RNAi (v18866)	Gal4/+	130.4 ± 7.72@	F (2, 12) = 2.73, p = 0.11	n/a
		RNAi/+	135.3 ± 7.04		n/a
		Gal4/RNAi	112.1 ± 2.6		n/a
	RNAi (v18867)	Gal4/+	130.4 ± 7.72@	F (2, 12) = 9.98, p = 0.003	p = 0.18
		RNAi/+	160.1 ± 7.02		p = 0.002
		Gal4/RNAi	110.4 ± 7.34		n/a
Jhl-21	RNAi (v45191)	Gal4/+	152.4 ± 12.46#	F (2, 15) = 0.36, p = 0.71	n/a
		RNAi/+	140.0 ± 12.10		n/a
		Gal4/RNAi	139.0 ± 14.32		n/a
nemy	RNAi (v40803)	Gal4/+	130.4 ± 7.72@	F (2, 12) = 3.16, p = 0.07	n/a
		RNAi/+	106.3 ± 7.87		n/a
		Gal4/RNAi	106.0 ± 8.66		n/a
Ent2	RNAi (v7618)	Gal4/+	130.4 ± 7.72@	F (2, 12) = 0.68, p = 0.52	n/a
		RNAi/+	115.8 ± 10.68		n/a
		Gal4/RNAi	119.3 ± 10.55		n/a

Flies expressing individual RNAi against *Cp1, axo, Jhl-21, nemy* and *Ent2* in glia via *repo*-Gal4 (the Gal4/RNAi group) had similar internal alcohol concentrations compared to controls with either *repo*-Gal4 alone (the Gal4/+ group) or the respective RNAi transgene alone (the RNAi/+ group). The mean internal EtOH concentration for each group is reported ± SEM. Results from individual one-way ANOVAs and (when appropriate) Bonferroni's multiple comparisons are reported. @ and # represent common Gal4/+ controls.

Table 4.3. Expression of RNAi against Cp1, axo, Jhl-21, nemy and Ent2 in neurons does not alter alcohol sedation sensitivity.

Gene	reagent (identifier)	Group	ST50	ANOVA	Bonferonni mult. comparisons (to Gal4/RNAi)
Cp1	RNAi (v13959)	Gal4/+	26.84 ± 1.62	F (2, 20) = 0.44, p = 0.65	n/a
		RNAi/+	24.98 ± 1.54		n/a
		Gal4/RNAi	25.74 ± 0.97		n/a
axo	RNAi (v18866)	Gal4/+	36.91 ± 1.16#	F (4, 35) = 1.99, p = 0.11#	n/a
		RNAi/+	34.39 ± 1.48		n/a
		Gal4/RNAi	31.14 ± 1.31		n/a
	RNAi (v18867)	Gal4/+	36.91 ± 1.16#	F (4, 35) = 1.99, p = 0.11#	n/a
		RNAi/+	34.31 ± 1.85		n/a
		Gal4/RNAi	33.21 ± 1.49		n/a
Jhl-21	RNAi (v45191)	Gal4/+	28.46 ± 1.19$	F (4, 35) = 8.15, p = 0.0001$	p = 0.37
		RNAi/+	26.78 ± 0.93		p > 0.9999
		Gal4/RNAi	24.80 ± 0.7		n/a
nemy	RNAi (v40803)	Gal4/+	30.13 ± 3.47	F (2, 20) = 1.43, p = 0.26	n/a
		RNAi/+	32.19 ± 1.62		n/a
		Gal4/RNAi	34.79 ± 2.73		n/a
Ent2	RNAi (v7618)	Gal4/+	28.46 ± 1.19$	F (4, 35) = 8.15, p = 0.0001$	p = 0.11
		RNAi/+	34.71 ± 2.19		p > 0.9999
		Gal4/RNAi	33.36 ± 1.92		n/a

Flies expressing individual RNAi against *Cp1, axo, Jhl-21, nemy* and *Ent2* pan-neuronally via *elav*-Gal4 (the Gal4/RNAi group) had similar ST50 values compared to controls with either *elav*-Gal4 alone (the Gal4/+ group) or the respective RNAi transgene alone (the RNAi/+ group). The ST50 for each group is reported ± SEM. Results from individual one-way ANOVAs and (when appropriate) Bonferroni's multiple comparisons are reported. $ and # represent common Gal4/+ controls and one-way ANOVA values, because the genotypes were tested in the same experiment.

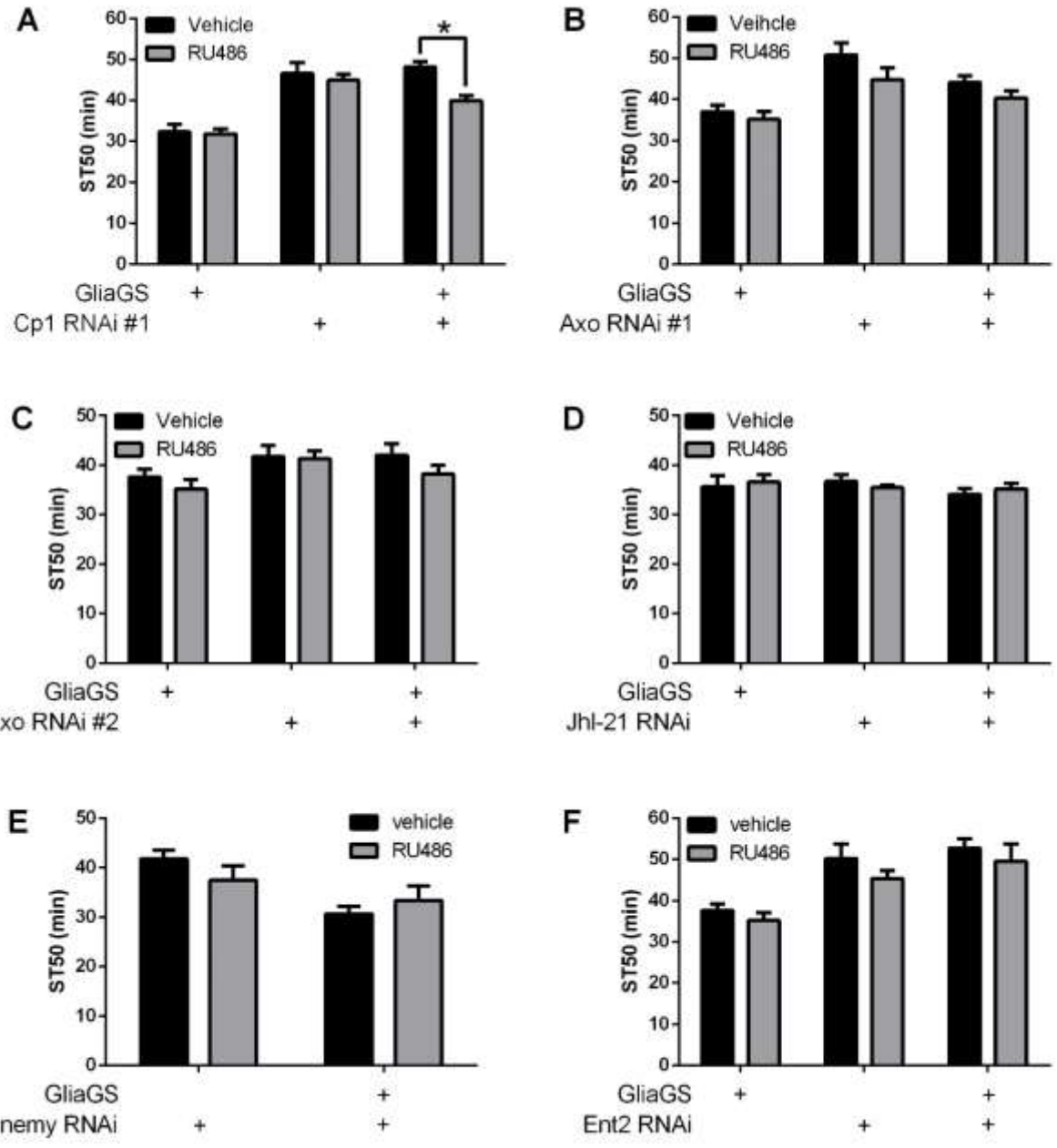
A
Vehicle
RU486
ST50 (min)
*
GliaGS
Cp1 RNAi #1
B
Veihcle
RU486
ST50 (min)
GliaGS
Axo RNAi #1
C
Vehicle
RU486
ST50 (min)
GliaGS
Axo RNAi #2
D
Vehicle
RU486
ST50 (min)
GliaGS
Jhl-21 RNAi
E
vehicle
RU486
ST50 (min)
GliaGS
nemy RNAi
F
vehicle
RU486
ST50 (min)
GliaGS
Ent2 RNAi

Figure 4.2. Expression of RNAi against Cp1, axo, Jhl-21, nemy and Ent2 in glia during adulthood. (**A**) Compared to vehicle, treatment with 1 mM RU486 for 6 days decreased ST50 values in flies with the GliaGS driver and Cp1 *RNAi* #1 transgene (GliaGS/*Cp1* RNAi #1), but not in control flies with either GliaGS or the RNAi transgene alone (two-way ANOVA; RU486, $p = 0.019$; genotype, $p < 0.0001$; interaction, $p = 0.089$; *Bonferroni's multiple comparisons between vehicle and RU486, $p < 0.05$; $n = 8$). (**B-F**) Compared to vehicle, treatment with 1 mM RU486 for 6 days did not alter ST50 values in flies with the GliaGS driver and an RNAi transgene against either *axo* (Panels B, C)*, Jhl-21* (Panel D)*, nemy* (Panel E) or *Ent2* (Panel F) (tested individually). There were also no differences in ST50 between vehicle and drug treated control flies (GliaGS/+ and RNAi/+). (Panel B: two-way ANOVA; RU486, $p = 0.03$; genotype, $p < 0.0001$; interaction, $p = 0.62$; Bonferroni's multiple comparisons between vehicle and RU486, $p > 0.05$; $n = 8$; Panel C: two-way ANOVA; RU486, $p = 0.68$; genotype, $p = 0.029$; interaction, $p = 0.16$; Bonferroni's multiple comparisons between vehicle and RU486, $p > 0.05$; $n = 8$; Panel D: two-way ANOVA; RU486, $p = 0.84$; genotype, $p = 0.51$; interaction, $p = 0.65$; $n = 8$; Panel E: two-way ANOVA; RU486, $p = 0.75$; genotype, $p = 0.005$; interaction, $p = 0.17$; Bonferroni's multiple comparisons between vehicle and RU486, $p > 0.05$; $n = 8$; Panel F: two-way ANOVA; RU486, $p = 0.13$; genotype, $p < 0.0001$; interaction, $p = 0.91$; Bonferroni's multiple comparisons between vehicle and RU486, $p > 0.05$; $n = 8$).

B.2 Cp1 KNOCKDOWN IN ALL CNS GLIA ALTERS ALCOHOL SEDATION WITHOUT INFLUENCING INTERNAL ALCOHOL LEVELS

Flies with pan-glial Gal4 (*repo*-Gal4) driven expression of two different *Cp1* RNAi transgenes (*Cp1* RNAi #1 (v13959) and *Cp1* RNAi #2 (HMS00725), tested individually) had significantly decreased sedation time 50 (ST50) values compared to control flies containing the Gal4 or the respective RNAi transgene alone (Fig 4.3A, 4.3B). For reasons that are unclear, constitutive expression of a third RNAi transgene (*Cp1* RNAi #3 (v110619)) in all glia did not consistently alter alcohol sedation (Fig 4.4A). To determine if Cp1 influenced alcohol metabolism, we measured the internal alcohol levels in these same genotypes after a 30-minute alcohol exposure (approximating the ST50). We found no significant difference in the internal alcohol concentrations between flies expressing *Cp1* RNAi transgenes in glia compared to controls (Fig 4.3C, 4.3D), indicating that Cp1 might influence a pharmacodynamic mechanism that impinges on alcohol sedation. Interestingly, despite Cp1 being endogenously expressed in neurons[239], pan-neuronal expression (via *elav*-Gal4) of the *Cp1* RNAi #1 transgene did not alter ST50 values compared to Gal4 and RNAi transgene controls (Fig 4.5A). Taken together, these results suggest that Cp1 influences alcohol sedation via a role in glia. Although our studies are consistent with the hypothesis that Cp1 function in neurons might not play a major role in alcohol sedation, further studies would be required to formally assess this possibility.

The principal RNAi transgenes used in this study (Cp1 RNAi #1, #2) are predicted to target all four mRNA transcripts of *Cp1* (Fig 4.6) and have no predicted off-target effects[245-247]. We used whole brain immunofluorescence to address whether the

RNAi transgenes knockdown Cp1 expression in specific tissues. Overall Cp1 immunofluorescence was substantially reduced (*Cp1* RNAi #1: 55%; *Cp1* RNAi #2: 62%) in brains from flies with pan-glial expression of *Cp1* RNAi transgenes (Fig 4.3F, 4.3H) compared to brains from flies with the *Cp1* RNAi transgenes alone (Fig 4.3E, 4.3G). The remaining Cp1 immunofluorescence is consistent with Cp1 expression in neurons, which should not be impacted by expression of *Cp1* RNAi in glia. Additionally, overall Cp1 immunofluorescence was reduced 29% in brains expressing the Cp1 RNAi #1 transgene pan-neuronally (Fig 4.5C) compared to brains containing the Cp1 RNAi #1 transgene alone (Fig 4.5B). The remaining Cp1 immunofluorescence is consistent with Cp1 expression in glia. These results confirm that expression of the *Cp1* RNAi transgenes knocked down Cp1 as expected in both glia and neurons.

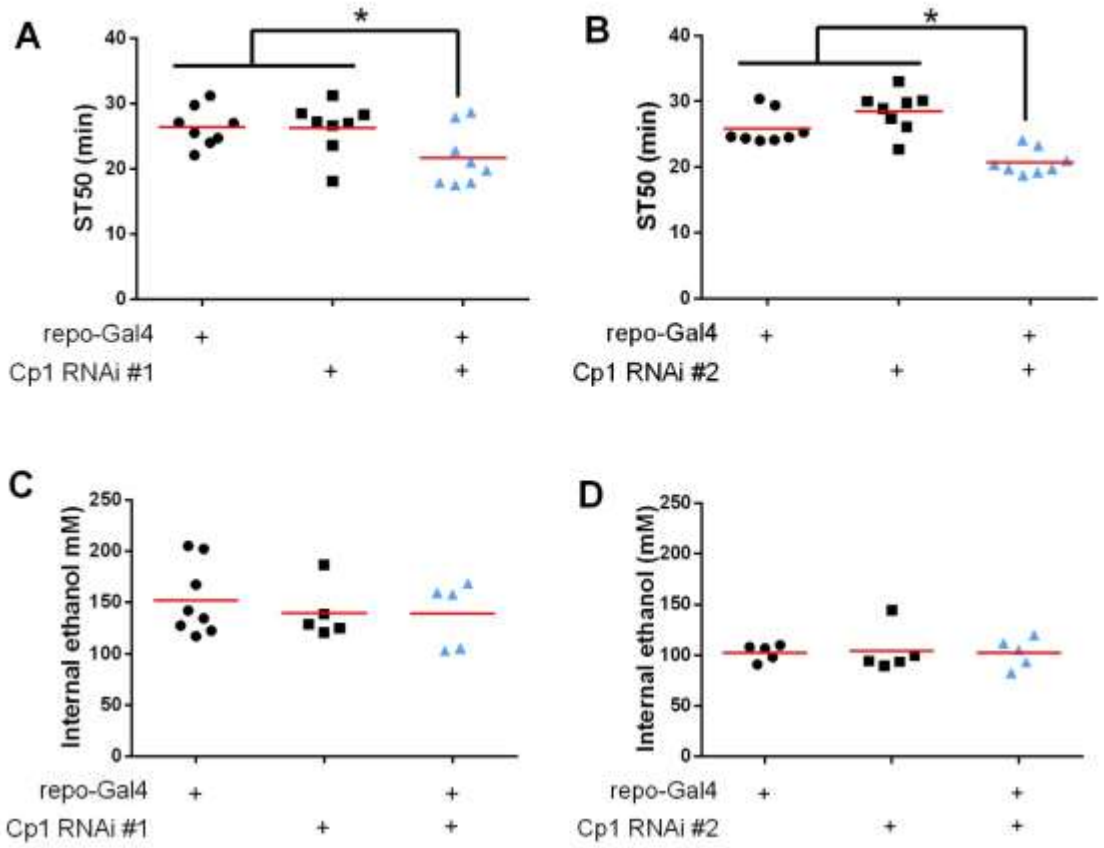
A
B
*
*
ST50 (min)
ST50 (min)
0
10
20
30
40
repo-Gal4 + +
Cp1 RNAi #1 + +
repo-Gal4 + +
Cp1 RNAi #2 + +
C
D
Internal ethanol mM)
Internal ethanol (mM)
0
50
100
150
200
250
repo-Gal4 + +
Cp1 RNAi #1 + +
repo-Gal4 + +
Cp1 RNAi #2 + +

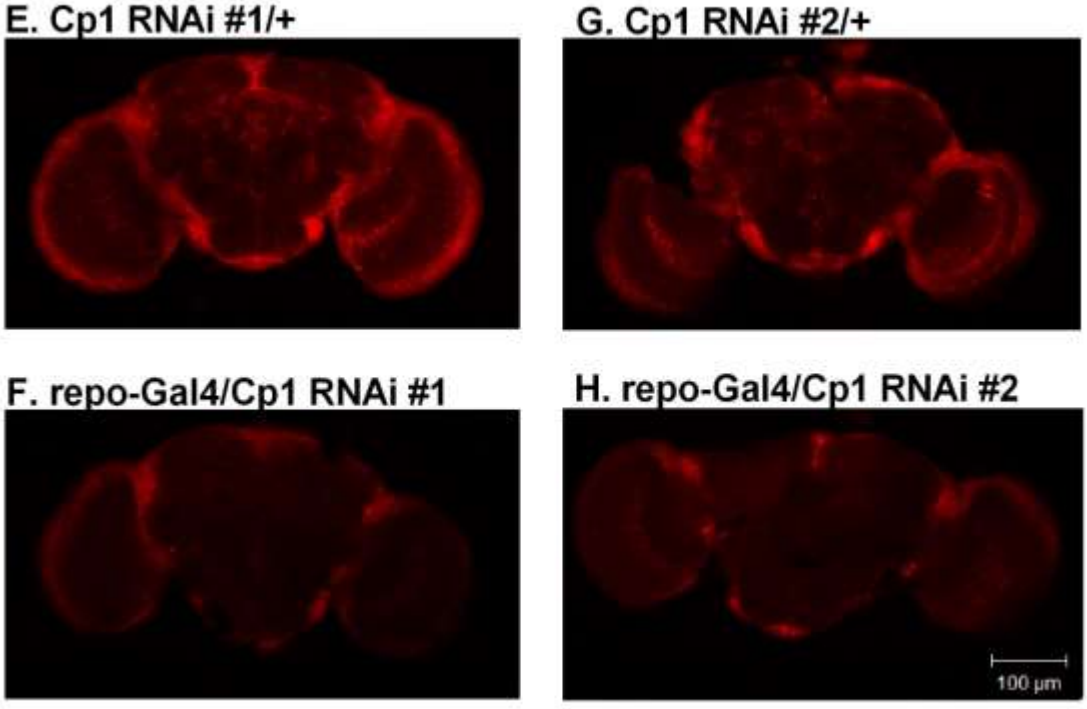
E. Cp1 RNAi #1/+
G. Cp1 RNAi #2/+
F. repo-Gal4/Cp1 RNAi #1
H. repo-Gal4/Cp1 RNAi #2
100 µm

Figure 4.3. Cp1 knockdown in CNS glia alters ethanol sedation sensitivity without affecting internal ethanol levels. (**A, B**) ST50 values were reduced in flies expressing *Cp1* RNAi transgenes in glia (blue bars: *repo*-Gal4/*Cp1* RNAi #1, panel a; *repo*-Gal4/*Cp1* RNAi #2, panel b) compared to control flies with either *repo*-Gal4 alone (black bars: *repo*-Gal4/+) or the RNAi transgenes alone (black bars: *Cp1* RNAi #1/+ and *Cp1* RNAi #2/+) (Panel A: one-way ANOVA, $p = 0.0352$; *Bonferroni's multiple comparison vs controls, $p < 0.05$; $n = 8$; Panel B: one-way ANOVA, $p < 0.0001$; *Bonferroni's multiple comparison vs control, $p < 0.05$; $n = 8$). (**C, D**) Expression of *Cp1* RNAi transgenes in CNS glia (blue bars: *Cp1* RNAi #1, panel C; *Cp1* RNAi #2, panel D) did not alter internal ethanol levels compared to controls with either *repo*-Gal4 or the RNAi transgenes alone (black bars) (individual one-way ANOVAs, $p > 0.05$; $n = 8$). (**E-H**) Whole mount brain images immunolabeled for Cp1 expression. Whole brain Cp1 detection was reduced in flies expressing *Cp1* RNAi transgenes in glia (**F,H**) compared to brains from RNAi transgene control animals (**E,G**). (Anti-Cp1 1:250, Alexa 568 1:1000). Representative images, 10X.

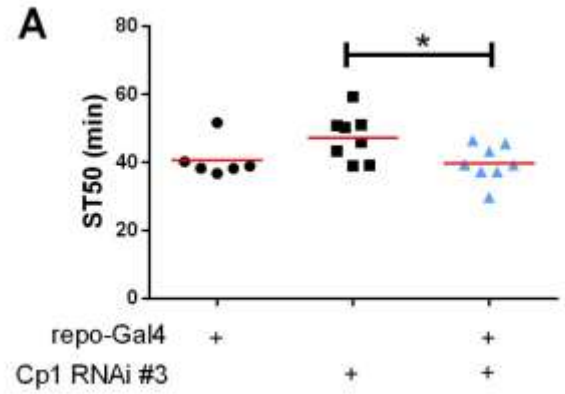
A
ST50 (min)
80
60
40
20
0
*
repo-Gal4
Cp1 RNAi #3
+
+
+

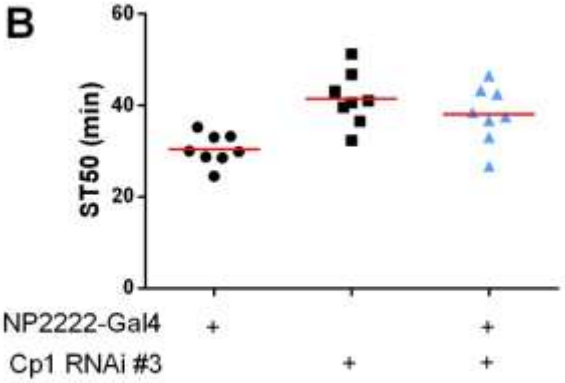
B
ST50 (min)
60
40
20
0
NP2222-Gal4
Cp1 RNAi #3
+
+
+

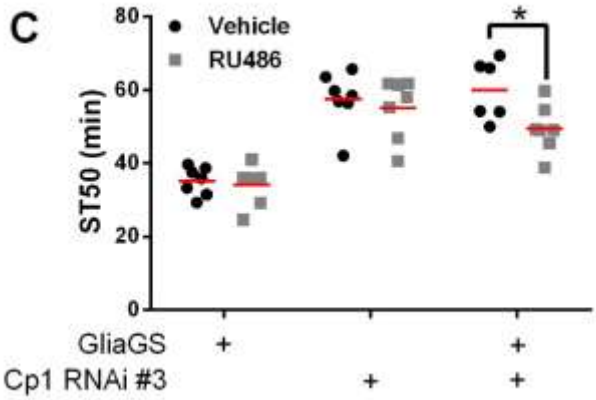
C
Vehicle
RU486
ST50 (min)
80
60
40
20
0
*
GliaGS
Cp1 RNAi #3
+
+
+

Figure 4.4. Ethanol sedation sensitivity in flies expressing *Cp1* RNAi #3 in glia. (**A**) ST50 values were influenced by overall genotype and reduced in flies expressing the *Cp1* RNAi #3 transgene in all CNS glia (blue triangles: *repo*-Gal4/*Cp1* RNAi #3) compared to one control group (black squares: *Cp1* RNAi #3/+), but not the other control group (black circles, repo-Gal4/+) (one-way ANOVA, $p = 0.0465$; *Bonferroni's multiple comparisons, *Cp1* RNAi #3/+ vs. *repo*-Gal4/*Cp1* RNAi #3, $p < 0.05$; $n = 8$). (**B**) ST50 values were influenced by overall genotype (one-way ANOVA, $p = 0.0015$, $n=8$) but were not detectably different in planned comparisons between flies expressing *Cp1* RNAi #3 transgene in cortex glia (blue triangles: *NP2222*-Gal4/*Cp1* RNAi #3) and control flies containing the NP2222-Gal4 alone (black circles) or the RNAi transgene alone (black squares) (**C**) Expression of *Cp1* RNAi in CNS glia during adulthood increased ethanol sedation sensitivity. Compared to vehicle-treated controls, treatment with 1 mM RU486 for 6 days decreased ST50 values in flies with the GliaGS driver and *Cp1* RNAi #3 transgene (GliaGS/*Cp1* RNAi #3), but not in control flies with either GliaGS or the RNAi transgene alone (two-way ANOVA; RU486, $p = 0.0341$; genotype, $p < 0.0001$; interaction, n.s.; *Bonferroni's multiple comparisons between vehicle and RU486, $p < 0.05$; $n = 8$).

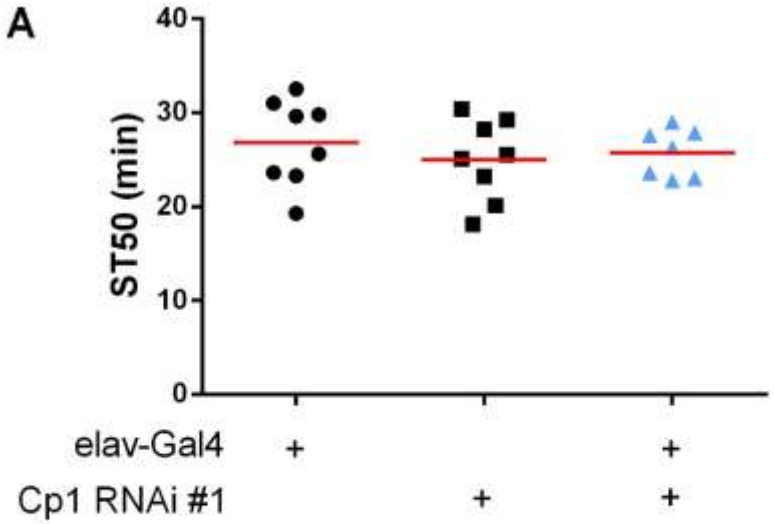

B. v13959/Cp1 RNAi #1

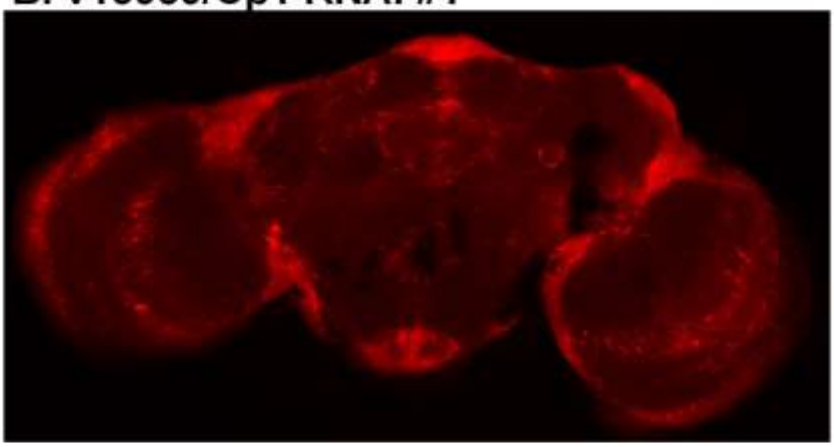

C. elav-Gal4/Cp1 RNAi #1

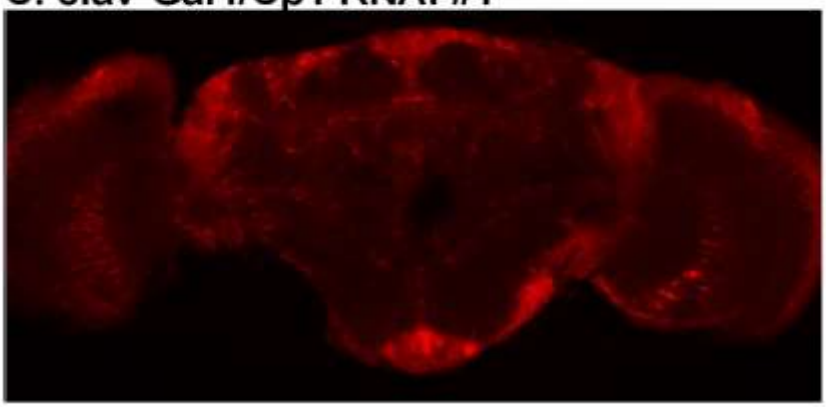

Figure 4.5. Expression of *Cp1* RNAi in neurons did not influence ethanol sedation sensitivity. (A) ST50 values were not changed in flies expressing the *Cp1* RNAi #1 transgene in neurons (blue triangles: *elav*-Gal4/*Cp1* RNAi #1) compared to control flies with either *elav*-Gal4 alone (black circles: elav-Gal4/+) or the RNAi transgene alone (black squares: *Cp1* RNAi/+) (one-way ANOVA, p = 0.6508; n = 8). **(B, C)** Whole mount brains immunolabeled for Cp1 detection (Anti-Cp1 1:250, Alexa 568 1:1000). Cp1 fluorescence was reduced 29% in flies with the *Cp1* RNAi #1 transgene expressed pan-neuronally (via *elav*-Gal4) (panel C) compared to flies that had the *Cp1* RNAi transgene alone (panel B). Microscope settings were optimized for *Cp1* RNAi #1/+ brains. Mean fluorescence intensity was calculated using Image J, n = 5. 10X, representative images.

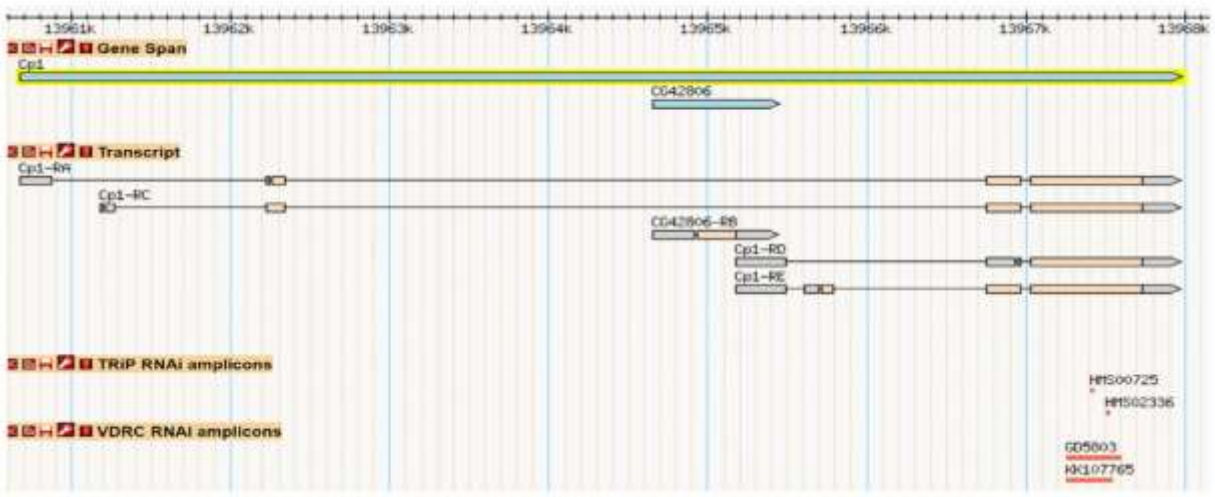

Figure 4.6. The *Cp1* region. Transcription is from left to right. Complementary sequences for UAS-*Cp1* RNAi transgenes - *Cp1* RNAi #1 (labeled as GD5803), *Cp1* RNAi #2 (labeled as HMS00725) and *Cp1* RNAi #3 (labeled as KK107765) - are shown below the predicted transcripts. All 3 RNAis are predicted to cleave all 4 *Cp1* transcripts. Image taken from the FlyBase genome browser (www.FlyBase.org).

B.3 EXPRESSION OF *DROSOPHILA PSEUDOOBSCURA* Cp1 RESCUES ALCOHOL SEDATION SENSITIVITY DUE TO KNOCKDOWN OF ENDOGENOUS *DROSOPHILA MELANOGASTER* Cp1 IN GLIA

When expressed in glia, both of the main Cp1 RNAi transgenes used in our studies (*Cp1* RNAi #1 and #2) make flies sensitive to alcohol sedation and knockdown Cp1 expression (Fig 4.3). The target sequence of *Cp1* RNAi #2 is wholly encompassed by that of *Cp1* RNAi #1 (Fig 4.6), raising the possibility that the sensitivity to alcohol sedation in flies expressing *Cp1* RNAi might be due to knockdown of *Cp1* or another, unidentified, gene. To address this possibility, we determined whether expression of a Cp1 orthologue from *Drosophila pseudoobscura* in glia could rescue the alcohol sedation sensitivity in flies expressing RNAi against endogenous melanogaster Cp1 also in glia[218]. We choose the *Drosophila pseudoobscura* Cp1 orthologue (GA25021) for these studies because (i) its primary amino acid sequence is 70-92 % similar to the four *Drosophila melanogaster* Cp1 isoforms and (ii) the *Cp1* RNAi #2 siRNA target sequence is poorly conserved between *Cp1* and *GA25021* – there are 6 base pair mismatches (Fig 4.7). Taken together, these findings suggested that GA25021 protein would have a similar function to Cp1, but importantly the GA25021 mRNA would largely escape RNAi-mediated degradation by *Cp1* RNAi #1. We therefore postulated that expression of GA25021 might rescue the alcohol sedation sensitivity observed in flies expressing RNAi against melanogaster Cp1 in glia.

We generated UAS-GA25021 transgenic flies via P-element transgenesis and screened seven lines (i.e. flies with UAS-GA25021 inserted into different locations in the genome) to determine whether or not the expression of the individual UAS-GA25021

transgenes in glia altered ST50. Out of the seven lines screened, expression of UAS-GA25021 #1, #3, #5, #6 and #7 in glia (via *repo*-Gal4) did not alter ST50 compared to control flies with either the respective UAS-GA25021 transgene or the *repo*-Gal4 transgene alone (Fig 4.8). However, expression of UAS-GA25021 #2 and #4 in glia (via *repo*-Gal4) significantly decreased ST50 compared to control flies with either the respective UAS-GA25021 transgene or the *repo*-Gal4 transgene alone (Fig 4.8). We moved forward with the five transgenic lines (UAS-GA25021 #1, #3, #5, #6, #7) that didn't impact ST50 values in the absence or presence of *repo*-Gal4.

We assessed whether expression of UAS-GA25021 transgenes rescued alcohol sensitivity in constitutive glial Cp1 knockdown flies. *repo*-Gal4/+ flies were used as a representative control in our subsequent rescue experiments because their ST50 values were not significantly different from other control flies that had the RNAi transgene alone, the UAS-GA25021 transgene alone, or *repo*-Gal4 driven expression of a UAS-GA25021 transgene (Fig 4.8; Fig 4.9A, 4.9C). Consistent with the data in Figure 4.3B, flies that constitutively expressed the *Cp1* RNAi #2 transgene in all glia (via *repo*-Gal4) had significantly decreased ST50 values compared to control flies with *repo*-Gal4 alone (Fig 4.9B, 4.9D). In contrast, flies with pan-glial expression of both the *Cp1* RNAi #2 transgene and a UAS-GA25021 transgene had (i) significantly increased ST50 values compared to flies expressing only the Cp1 RNAi #2 transgene and (ii) statistically indistinguishable ST50 values compared to control flies with *repo*-Gal4 alone (Fig 4.9B, 4.9D). In total, we tested five UAS-GA25021 transformants. The transgenes in four of the transformants rescued the glial Cp1 RNAi alcohol sedation phenotype, while one of the transgenes did not (Fig 4.9; Fig 4.10A-C). Additionally, we determined whether this

behavioral rescue was due to the Gal4 dilution phenomenon, which theorizes that a Gal4 driver cannot express two UAS-transgenes as efficiently as one UAS-transgene. If this were true, we would hypothesize that the addition of any UAS-transgene in the presence of *repo*-Gal4 and the *Cp1* RNAi #2 transgene would lead to behavioral rescue. However, flies with pan-glial expression of both the *Cp1* RNAi #2 transgene and a UAS-LacZ transgene had (i) similar ST50 values compared to flies expressing only the Cp1 RNAi #2 transgene and (ii) significantly decreased ST50 values compared to control flies with *repo*-Gal4 alone (Fig 4.10D). Taken together, these data demonstrate the ability of *Drosophila pseudoobscura Cp1* to rescue alcohol sedation sensitivity due to knockdown of *melanogaster Cp1*, and strongly supports a role for Cp1 in glia in alcohol sedation.

We used whole brain immunofluorescence to address whether the UAS-GA25021 transgenes expressed detectable levels of immunoreactive Cp1-like protein. Endogenous Cp1 was readily detectable in control *repo*-Gal4/+ brains (Fig. 4.9E). This signal was reduced substantially by expression of the *Cp1* RNAi #2 transgene in all glia (Fig. 4.9F; decreased 68%) and increased by expression of UAS-GA25021 transgene #1 in all glia (Fig. 4.9G; increased 37%). Expression of this same UAS-GA25021 transgene concurrently with the *Cp1* RNAi #2 transgene substantially increased the Cp1 signal compared to brains that expressed only *Cp1* RNAi #2 in all glia (Fig. 4.9H; increased 331%). Similarly, expression of UAS-GA25021 transgene #3 in all glia increased the Cp1 signal (Fig. 4.9I; increased 32% compared to *repo*-Gal4 alone) and expression of this same UAS-GA25021 transgene concurrently with the *Cp1* RNAi #2 transgene substantially increased the Cp1 signal compared to brains that expressed

only *Cp1* RNAi #2 in all glia (Fig. 4.9J; 188%). Although we were surprised by— and do not at this time understand—the difference in Cp1 signal in flies with concurrent expression of GA25021 and *Cp1* RNAi #2, these data indicate that the UAS-GA25021 transgenes are functional and expressed at the protein expression level in the presence of the *Cp1* RNAi transgene.

Figure 4.7. *Cp1* RNAi #2 siRNA target region on *Drosophila melanogaster* Cp1 and *Drosophila pseudoobscura* GA25021 alignment. The *Drosophila melanogaster* Cp1 transcript is “Query 1” and the *Drosophila pseudoobscura* GA25021 transcript is “Sbjct 1”. The *Cp1* RNAi #2 siRNA target sequence on the Cp1 transcript is boxed in red. Comparing this region between Cp1 and GA25021, 6 base pairs are mismatched.

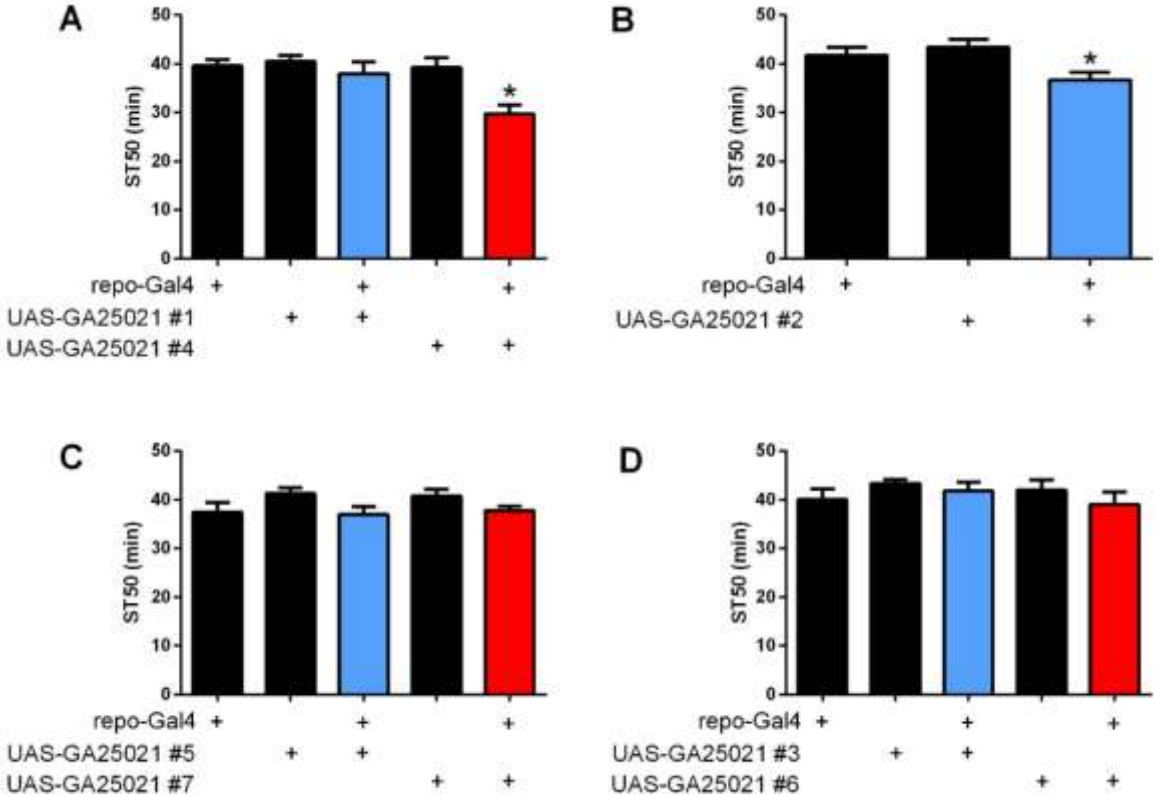
A
ST50 (min)
50
40
30
20
10
0
*
repo-Gal4 + + +
UAS-GA25021 #1 + +
UAS-GA25021 #4 + +
B
ST50 (min)
50
40
30
20
10
0
*
repo-Gal4 + +
UAS-GA25021 #2 + +
C
ST50 (min)
50
40
30
20
10
0
repo-Gal4 + + +
UAS-GA25021 #5 + +
UAS-GA25021 #7 + +
D
ST50 (min)
50
40
30
20
10
0
repo-Gal4 + + +
UAS-GA25021 #3 + +
UAS-GA25021 #6 + +

Figure 4.8. Expression of the *Drosophila pseudoobscura* UAS-GA25021 transgenes in glia. (**A**) ST50 values were not changed in flies expressing both the UAS-GA25021 #1 transgene and *repo*-Gal4 (blue bar: *repo*-Gal4/UAS-GA25021 #1) compared to control flies with either *repo*-Gal4 alone (black bar: *repo*-Gal4/+) or the UAS-GA25021 #1 transgene alone (black bar: UAS-GA25021 #1/+). ST50 values were decreased in flies expressing both the UAS-GA25021 #4 transgene and *repo*-Gal4 (red bar: *repo*-Gal4/UAS-GA25021 #4) compared to control flies with either *repo*-Gal4 alone (black bar: *repo*-Gal4/+) or the UAS-GA25021 #4 transgene alone (UAS-GA25021 #4/+) (one-way ANOVA, $p = 0.0008$; *Bonferroni's multiple comparison vs controls, $p < 0.05$; $n = 8$). (**B**) ST50 values were decreased in flies expressing both the UAS-GA25021 #2 transgene and *repo*-Gal4 (red bar: *repo*-Gal4/UAS-GA25021 #2) compared to control flies with either *repo*-Gal4 alone (black bar: *repo*-Gal4/+) or the UAS-GA25021 #2 transgene alone (UAS-GA25021 #2/+) (one-way ANOVA, $p = 0.022$; *Bonferroni's multiple comparison vs controls, $p < 0.05$; $n = 8$). (**C, D**) ST50 values were not changed in flies expressing both a UAS-GA25021 transgene and *repo*-Gal4 (Panel C, blue bar: *repo*-Gal4/UAS-GA25021 #5, red bar: *repo*-Gal4/UAS-GA25021 #7; Panel D, blue bar: *repo*-Gal4/UAS-GA25021 #3, red bar: *repo*-Gal4/UAS-GA25021 #6) compared to control flies with either *repo*-Gal4 alone or the respective UAS-GA25021 transgene alone (black bars). (Panel C: one-way ANOVA, $p = 0.12$; $n = 8$; Panel D: two-way ANOVA, $p = 0.57$; $n = 8$).

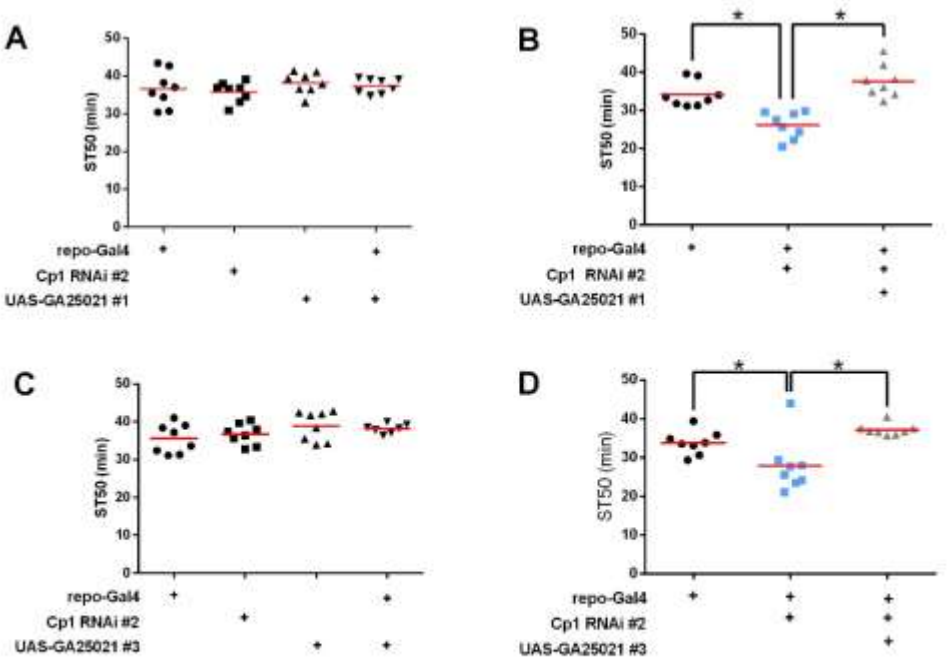
A
B
C
D
ST50 (min)
repo-Gal4
Cp1 RNAi #2
UAS-GA25021 #1
UAS-GA25021 #3
*
*

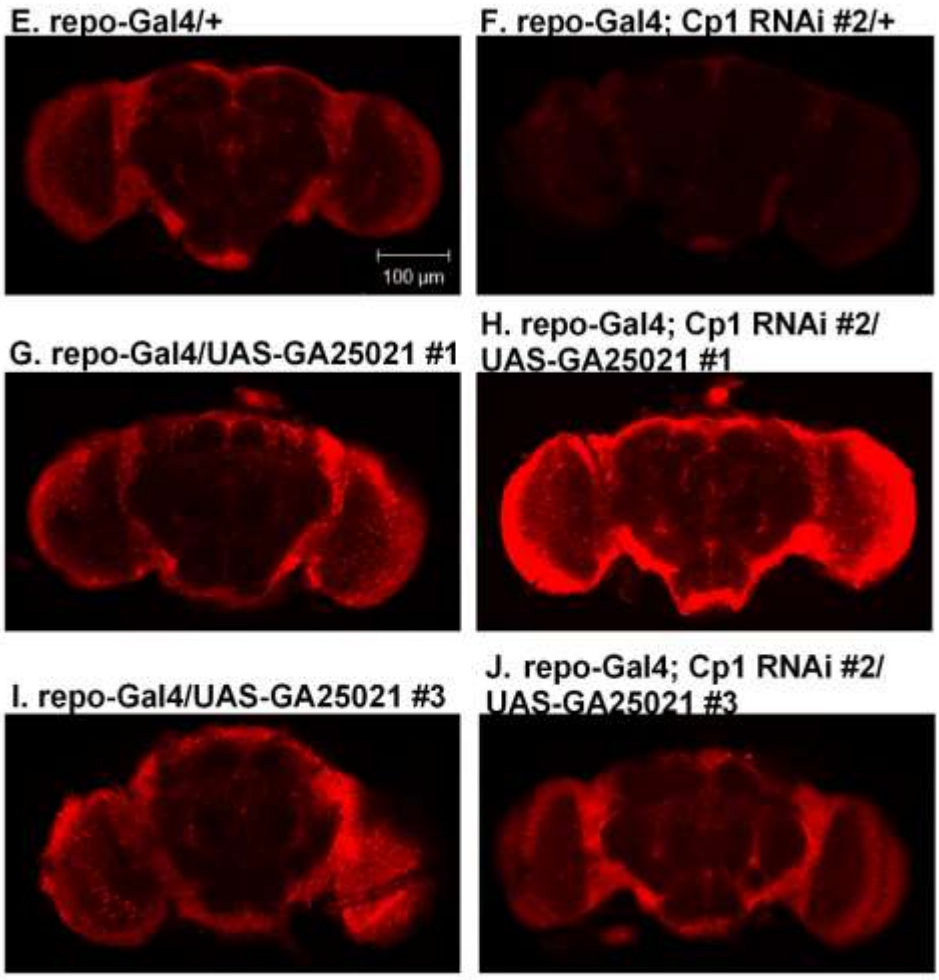
E. repo-Gal4/+
F. repo-Gal4; Cp1 RNAi #2/+
100 µm
G. repo-Gal4/UAS-GA25021 #1
H. repo-Gal4; Cp1 RNAi #2/
UAS-GA25021 #1
I. repo-Gal4/UAS-GA25021 #3
J. repo-Gal4; Cp1 RNAi #2/
UAS-GA25021 #3

Figure 4.9. Cross-species rescue of alcohol sedation in Cp1 RNAi flies. (**A, C**) Ethanol sedation in flies with repo-Gal4 alone, *Cp1* RNAi #2 alone, UAS-GA25021 transgenes alone, and repo-Gal4 with UAS-GA25021. Genotype did not impact ST50 values (Panel A: one-way ANOVA, p = 0.4855, n = 8; Panel C: one-way ANOVA, p = 0.1683, n = 8). (**B, D**) Ethanol sedation in flies with concurrent expression of Cp1 RNAi and UAS-GA25021. ST50 values were decreased in flies constitutively expressing the *Cp1* RNAi #2 transgene in all glia via *repo*-Gal4 (blue squares) compared to control flies containing *repo*-Gal4 alone (black circles). ST50 values in flies that expressed a UAS-GA25021 transgene and *Cp1* RNAi #2 transgene in all glia via *repo*-Gal4 (grey triangles: UAS-GA25021 #1, Panel B; UAS-GA25021 #3, Panel D) were significantly elevated compared to flies expressing only *Cp1* RNAi #2 in glia (blue squares: UAS-GA25021 #1, Panel B; UAS-GA25021 #3, Panel D), but were not different than control flies containing *repo*-Gal4 alone (black circles) (Panel B: one-way ANOVA, p <0.0001, n=8, *Bonferroni's multiple comparison vs repo-Gal4;*Cp1* RNAi #2 flies, p<0.05; Panel D: one-way ANOVA, p = 0.0019; *Bonferroni's multiple comparison vs repo-Gal4;*Cp1* RNAi #2 flies, p<0.05). (**E-J**) Whole mount brain images immunolabeled for Cp1. Whole brain fluorescence was reduced in flies constitutively expressing the *Cp1* RNAi #2 transgene in all glia via *repo*-Gal4 (F) compared to brains that contained *repo*-Gal4 alone (E). Compared to brains that contained *repo*-Gal4 alone (E), whole brain fluorescence was increased when a UAS-GA25021 transgene was expressed in all glia via *repo*-Gal4 (UAS-GA25021 #1, panel G; UAS-GA25021 #3, panel I). Compared to brains that expressed the *Cp1* RNAi #2 transgene in all glia via *repo*-Gal4 (F), whole brain fluorescence was increased when a UAS-GA25021 transgene was expressed with the *Cp1* RNAi #2 transgene in all glia via *repo*-Gal4 (UAS-GA25021 #1, panel H; UAS-GA25021 #3, panel J). Representative images from middle sections of adult brains, 10X (Anti-Cp1 1:250; Alexa 568 1:1000).

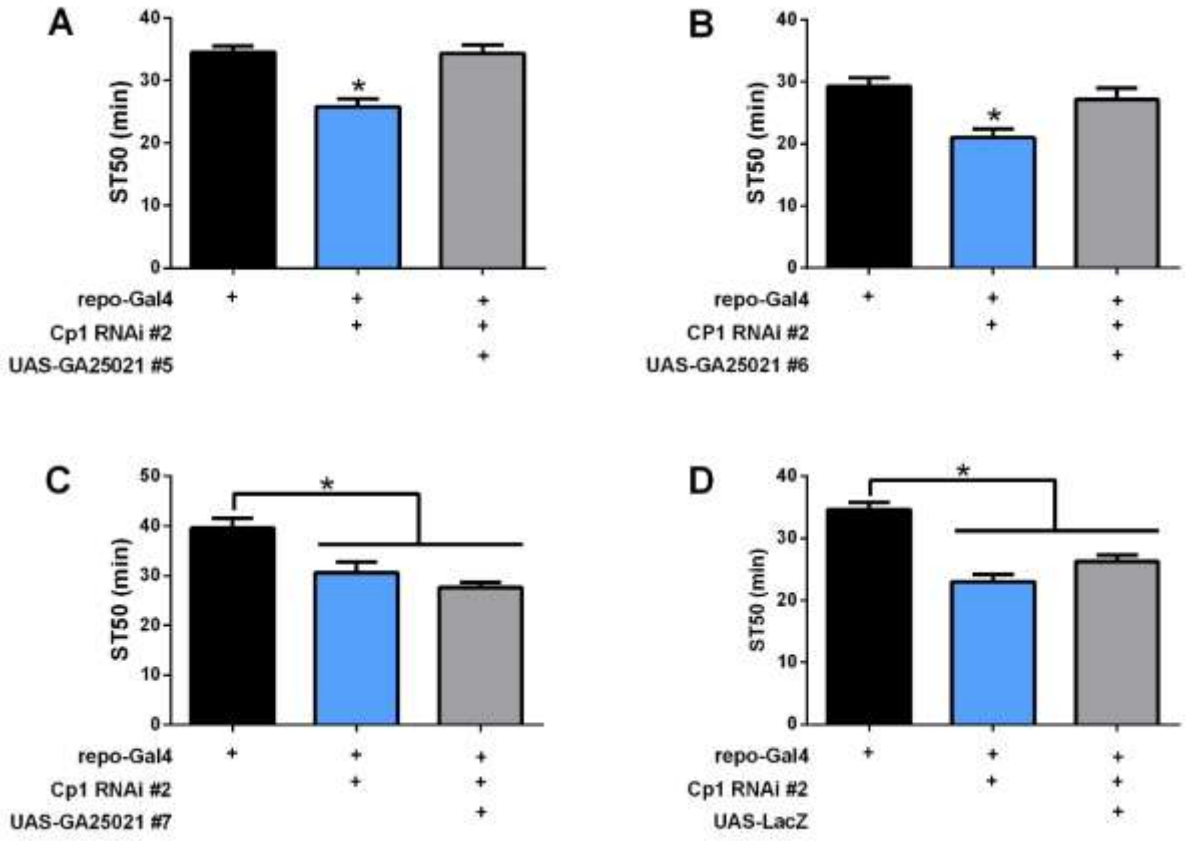
A
ST50 (min)
40
30
20
10
0
*
repo-Gal4 + + +
Cp1 RNAi #2 + +
UAS-GA25021 #5 +
B
ST50 (min)
40
30
20
10
0
*
repo-Gal4 + + +
CP1 RNAi #2 + +
UAS-GA25021 #6 +
C
ST50 (min)
50
40
30
20
10
0
*
repo-Gal4 + + +
Cp1 RNAi #2 + +
UAS-GA25021 #7 +
D
ST50 (min)
40
30
20
10
0
*
repo-Gal4 + + +
Cp1 RNAi #2 + +
UAS-LacZ +

Figure 4.10. Cross-species rescue of alcohol sedation in Cp1 RNAi flies. (**A, B**) ST50 values were decreased in flies constitutively expressing the *Cp1* RNAi #2 transgene in all glia via *repo*-Gal4 (blue bar) compared to control flies containing *repo*-Gal4 alone (black bar). ST50 values in flies that expressed a UAS-GA25021 transgene (Panel A: UAS-GA25021 #5; Panel B: UAS-GA25021 #6) and *Cp1* RNAi #2 transgene in all glia via *repo*-Gal4 (grey bar) were significantly elevated compared to flies expressing only *Cp1* RNAi #2 in glia (blue bar), but were not different than control flies containing *repo*-Gal4 alone (black bar) (Panel A: one-way ANOVA, $p < 0.0001$; *Bonferroni's multiple comparison vs repo-Gal4;*Cp1* RNAi #2 flies, $p<0.05$; n = 8; Panel B: one-way ANOVA, $p = 0.003$; *Bonferroni's multiple comparison vs repo-Gal4;*Cp1* RNAi #2 flies, $p<0.05$; n = 8). (**C**) ST50 values were decreased in flies constitutively expressing the *Cp1* RNAi #2 transgene in all glia via *repo*-Gal4 (blue bar) compared to control flies containing *repo*-Gal4 alone (black bar). ST50 values in flies that expressed the UAS-GA25021 #7 transgene and *Cp1* RNAi #2 transgene in all glia via *repo*-Gal4 (grey bar) were similar to flies expressing only *Cp1* RNAi #2 in glia (blue bar), and were decreased compared to control flies containing *repo*-Gal4 alone (black bar) (one-way ANOVA, $p = 0.0003$; *Bonferroni's multiple comparison vs repo-Gal4;*Cp1* RNAi #2 flies, $p<0.05$; n = 8). (**D**) ST50 values were decreased in flies constitutively expressing the *Cp1* RNAi #2 transgene in all glia via *repo*-Gal4 (blue bar) compared to control flies containing *repo*-Gal4 alone (black bar). ST50 values in flies that expressed the UAS-LacZ transgene and *Cp1* RNAi #2 transgene in all glia via *repo*-Gal4 (grey bar) were similar to flies expressing only *Cp1* RNAi #2 in glia (blue bar), and were decreased compared to control flies containing *repo*-Gal4 alone (black bar) (one-way ANOVA, $p < 0.0001$; *Bonferroni's multiple comparison vs repo-Gal4;*Cp1* RNAi #2 flies, $p<0.05$; n = 8).

B.4 Cp1 EXPRESSION SPECIFICALLY IN CORTEX GLIA REGULATES ALCOHOL SEDATION

Adult *Drosophila* have five CNS glial subtypes: astrocytes, ensheathing cells, cortex glia, subperineural glia and perineural glia[40]. To address the possibility that Cp1 influences alcohol sedation by functioning within one or more specific glial subtypes, we determined whether expression of *Cp1* RNAi transgenes in individual glial subtypes (via a series of Gal4 drivers) altered alcohol sedation sensitivity. Flies expressing *Cp1* RNAi #1 or *Cp1* RNAi #2 transgenes in cortex glia (via *NP2222*-Gal4[36] or CtxGlia Split-Gal4[39]) had significantly decreased ST50 values compared to control flies with the Gal4 and RNAi transgenes alone (NP2222-Gal4: Fig 4.11A, 11B; CtxGlia Split-Gal4: Fig 4.12). Flies expressing the *Cp1* RNAi #3 transgene in cortex glia (via-NP2222-Gal4) had inconsistent results (Fig 4.4B). Additionally, ST50 values were not altered by expression of *Cp1* RNAi #1 in the four other CNS glial subtypes (astrocytes, ensheathing cells, subperineural glia and perineural glia via *Alrm*-Gal4[40], *TIFR*-Gal4[36], *mz0709*-Gal4[36], *Gli*-Gal4[248] and *Indy*-Gal4[212]) (Table 4.4). The simplest interpretation of these data is that Cp1 influences alcohol sedation by functioning in cortex glia.

We used whole brain immunofluorescence to determine if Cp1 is expressed in adult *Drosophila* cortex glia. Utilizing flies that constitutively express mCD8::GFP in cortex glia via *NP2222*-Gal4, we found that Cp1 immunofluorescence colocalized with GFP (Fig 4.11C-D). When quantified using Volocity™ 3D image analysis software, greater than 60% of the red and green pixels overlapped (average Pearson's correlation = 0.622; n = 6). This result indicated that endogenous Cp1 is expressed in cortex glia, consistent with a role for Cp1 in acute alcohol sedation sensitivity.

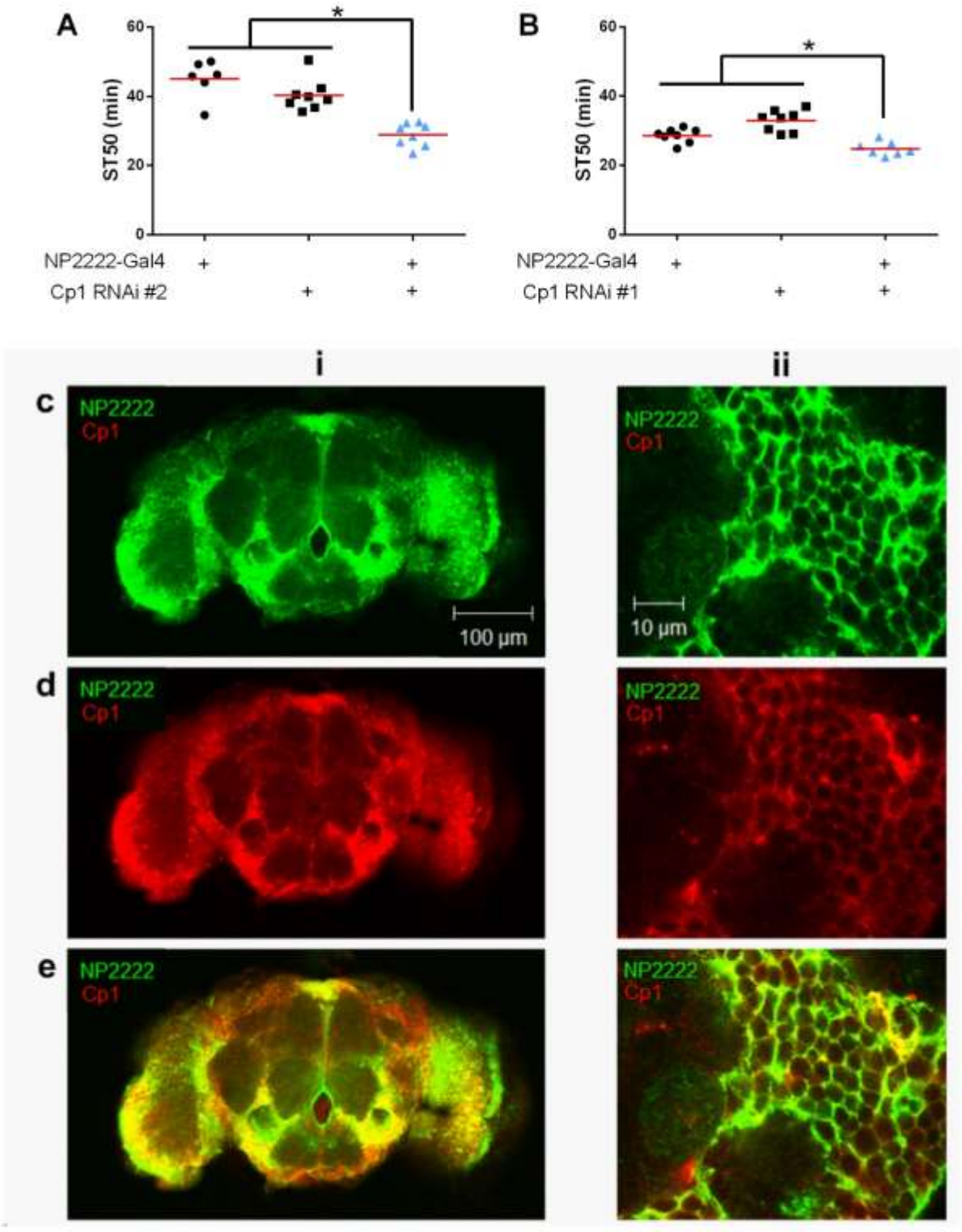
A
B
ST50 (min)
60
40
20
0
*
NP2222-Gal4
Cp1 RNAi #2
Cp1 RNAi #1
+
i
ii
c
d
e
NP2222
Cp1
100 µm
10 µm

Figure 4.11. Cp1 expression in cortex glia is required for normal ethanol sedation. (**A,B**) ST50 values were decreased in flies expressing *Cp1* RNAi transgenes in cortex glia (blue bars: *NP2222*-Gal4/*Cp1* RNAi #1, panel A; *NP2222*-Gal4/*Cp1* RNAi #2, panel B) compared to control flies containing either the cortex glia Gal4 driver (black bars: *NP2222*-Gal4/+) or the RNAi transgenes (black bars: *Cp1* RNAi #1/+ or *Cp1* RNAi #2/+) alone (individual one-way ANOVAs, $p \leq 0.0001$; *Bonferroni's multiple comparisons vs controls, $p < 0.05$; $n = 8$). (**C-E**) Cp1 is expressed in cortex glia. (**C**) Whole brain expression of UAS-GFP (green) driven by *NP2222*. (**D**) Endogenous Cp1 expression labeled red (anti-Cp1 1:250, Alexa 568 1:1000). (**E**) Merged image of panel C and panel D; GFP and Cp1 co-localization is yellow. Representative images from whole brain at 10X (i) and 63X oil immersion (ii).

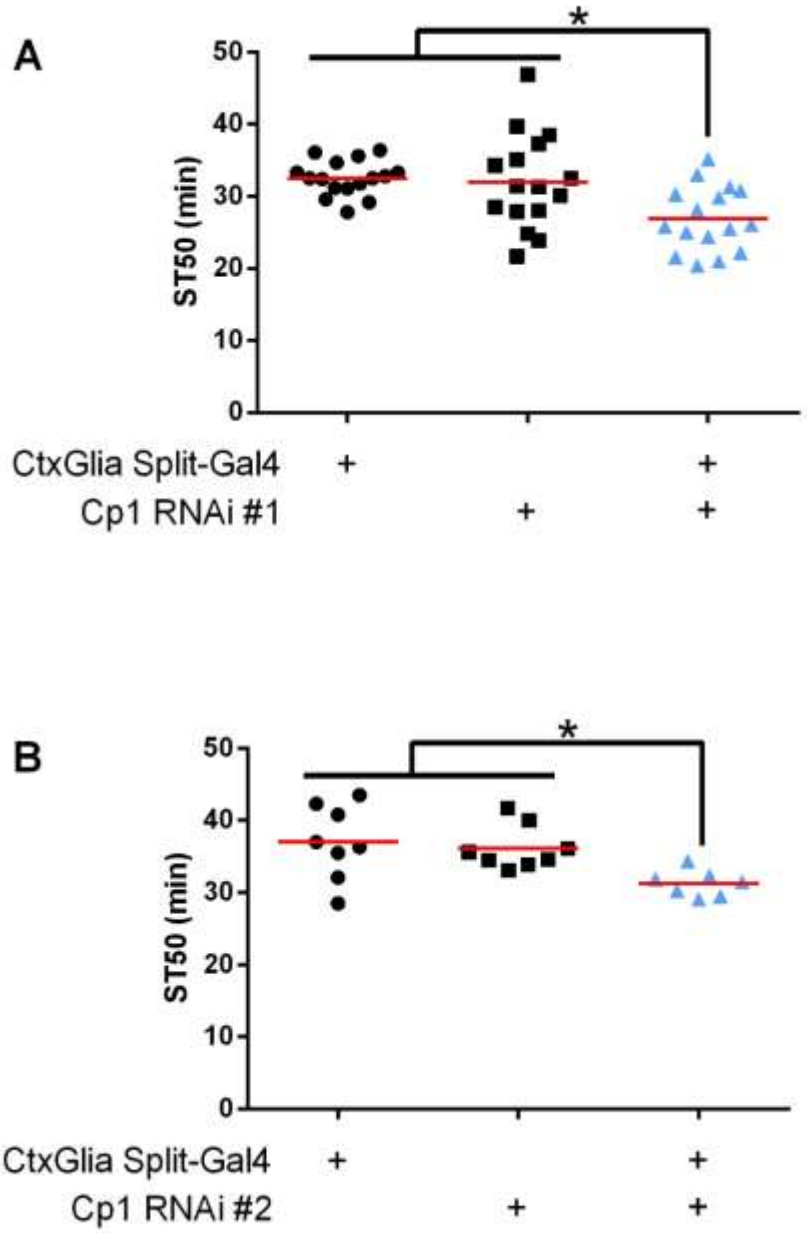

Figure 4.12. Cp1 expression in cortex glia is required for normal ethanol sedation. (**A, B**) ST50 values were decreased in flies expressing *Cp1* RNAi transgenes in cortex glia (blue triangles: CtxGlia Split-Gal4/*Cp1* RNAi #1, panel A; CtxGlia Split-Gal4/*Cp1* RNAi #2, panel B) compared to control flies containing either the cortex glia Gal4 driver (black circles: CtxGlia Split-Gal4/+) or the RNAi transgenes (black squares: *Cp1* RNAi #1/+ or *Cp1* RNAi #2/+) alone (Panel A: one-way ANOVA, $p = 0.0029$; *Bonferroni's multiple comparisons vs controls, $p < 0.05$; $n = 16$; Panel B: one-way ANOVA, $p = 0.0156$; Bonferroni's multiple comparisons vs controls, $p < 0.05$; $n = 8$).

Table 4.4. Expression of *Cp1* RNAi in each glial cell subtype individually.

Glial subtype Gal4	Group	ST50	ANOVA	Bonferonni mult. comparisons (to Gal4/RNAi)
Ensheathing cells (TIFR)	Gal4/+	36.86 ± 3.833 (7)	F (2,18) = 3.893, p = 0.0393	p > 0.05
	RNAi/+	31.10 ± 3.624 (7) $		p > 0.05
	Gal4/RNAi	35.23 ± 4.437 (7)		n/a
Subperineural glia (Gli)	Gal4/+	33.67 ± 3.185 (7)	F (2,18) = 1.564, p = 0.236	n/a
	RNAi/+	31.10 ± 3.624 (7) $		n/a
	Gal4/RNAi	31.66 ± 3.185 (7)		n/a
Astrocytes (Alrm3)	Gal4/+	26.6 ± 1.241 (8)	F (2,21) = 0.381 , p = 0.687	n/a
	RNAi/+	25.96 ± 1.066 (8) #		n/a
	Gal4/RNAi	25.66 ± 3.430 (8)		n/a
Ensheathing cells (mz0709)	Gal4/+	32.56 ± 4.084 (8)	F (2,21) = 10.85, p = 0.0006	p < 0.05
	RNAi/+	25.96 ± 1.066 (8) #		p > 0.05
	Gal4/RNAi	26.26 ± 3.592 (8)		n/a
Perineural glia (Indy)	Gal4/+	34.6 ± 1.262 (8)	F(2,21) = 0.1931, p = 0.825	n/a
	RNAi/+	33.34 ± 1.645 (8)		n/a
	Gal4/RNAi	34.03 ± 1.382 (8)		n/a

Expression of the *Cp1* RNAi #1 transgene in ensheathing cells (via *TIFR*-Gal4 and *mz0709*-Gal4), subperineural glia (via *Gli*-Gal4), astrocytes (via *Alrm*-Gal4) and perineural glia (via *Indy*-Gal4) did not consistently alter alcohol sedation compared to both Gal4 driver (Gal4/+) and RNAi transgene (RNAi/+) controls. Results from individual one-way ANOVAs and (when appropriate) Bonferroni's multiple comparisons are reported. $ and # represent common RNAi/+ controls.

B.5 Cp1 IN RAPID TOLERANCE DEVELOPMENT

Flies develop rapid tolerance to alcohol, defined as increased ST50 values during a second alcohol exposure after recovering from a first alcohol exposure[214]. To determine whether Cp1 influences this aspect of alcohol behavior through its function in CNS glia, we expressed the *Cp1* RNAi #1 transgene in all glia (via *repo*-Gal4) and then assessed rapid tolerance development. As anticipated, pan-glial knock down of Cp1 via the *Cp1* RNAi #1 transgene significantly decreased ST50 values during the first ethanol exposure (black bars, E1) as compared to Gal4 and RNAi transgene alone controls (Fig 4.13A). In contrast, ST50 values during the second alcohol exposure (grey bars, E2) were not affected by Cp1 knockdown (Fig 4.13A). When quantified as the ratio between the second and first ST50 values[214], flies with Cp1 knocked down in all glia had an increase in the development of rapid tolerance compared to controls (Fig 4.13B). As we found during the first alcohol exposure (Fig 4.3C), there was no effect of knocking-down Cp1 in all glia on internal alcohol levels during the second alcohol exposure (Fig 4.13E). Knockdown of Cp1 specifically in cortex glia (via *NP2222*-Gal4) also reduced ST50 values during the first, but not the second, alcohol exposure (Fig 4.13C), leading to an apparent increase in development of rapid tolerance compared to controls (Fig 4.13D). Given that Cp1 knockdown does not significantly impact ST50 values during the second alcohol exposure (Fig 4.13A and 4.13C), the most parsimonious interpretation of these data is that the increased development of rapid tolerance is likely a mathematical product of the enhanced sensitivity to alcohol during the first exposure. We therefore did not further investigate the potential role of Cp1 in rapid tolerance.

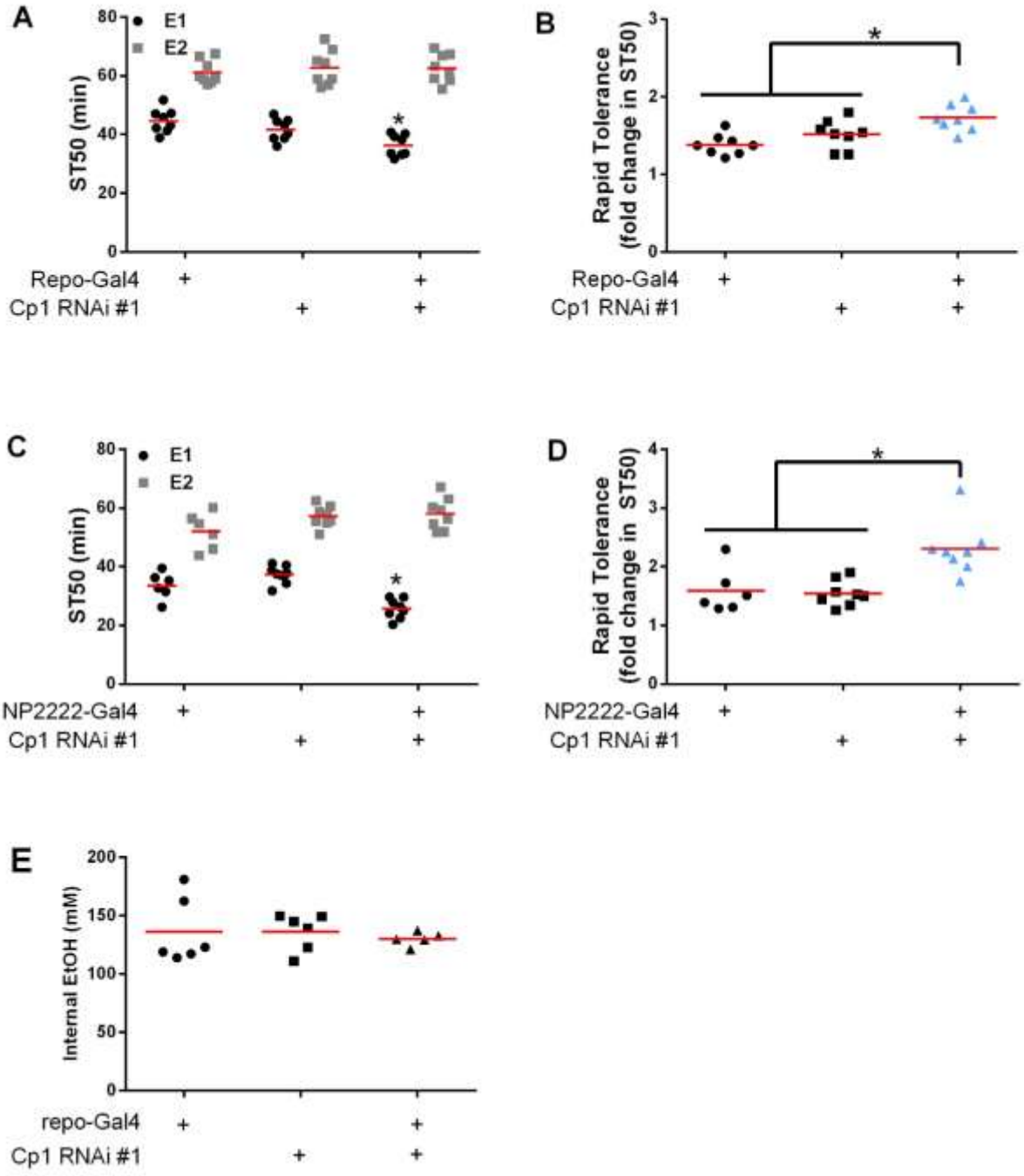
A
E1
E2
ST50 (min)
80
60
40
20
0
*
Repo-Gal4 + +
Cp1 RNAi #1 + +
B
Rapid Tolerance (fold change in ST50)
3
2
1
0
*
Repo-Gal4 + +
Cp1 RNAi #1 + +
C
E1
E2
ST50 (min)
80
60
40
20
0
*
NP2222-Gal4 + +
Cp1 RNAi #1 + +
D
Rapid Tolerance (fold change in ST50)
4
3
2
1
0
*
NP2222-Gal4 + +
Cp1 RNAi #1 + +
E
Internal EtOH (mM)
200
150
100
50
0
repo-Gal4 + +
Cp1 RNAi #1 + +

Figure 4.13. Cp1 in rapid tolerance development. (**A**) ST50 values from the first (E1) and second (E2) ethanol exposure when Cp1 is knocked down in all CNS glia. Compared to controls (*repo*-Gal4/+ and *Cp1* RNAi #1/+), expression of *Cp1* RNAi in CNS glia (*repo*-Gal4/*Cp1* RNAi #1) decreased ST50 values during E1, but not during E2 (two-way ANOVA; genotype, n.s.; ethanol exposure, $p < 0.0001$; interaction, $p = 0.015$; *Bonferroni's multiple comparisons vs controls for each ethanol exposure, $p < 0.05$; $n = 8$). (**B**) Development of rapid tolerance (fold change in ST50 from E1 to E2) quantified from the data in panel A. Expression of *Cp1* RNAi in glia (blue bar: *repo*-Gal4/*Cp1* RNAi #1) increased rapid tolerance development compared to controls (black bars: *repo*-Gal4/+, *Cp1* RNAi #1/+) (one-way ANOVA, $p = 0.0014$; *Bonferroni's multiple comparisons vs controls, $p < 0.05$; $n = 8$). (**C**) ST50 values from the first (E1) and second (E2) ethanol exposure when Cp1 is knocked down in cortex glia. Compared to controls (*NP2222*-Gal4/+ and *Cp1* RNAi #1/+), expression of *Cp1* RNAi in cortex glia (*NP2222*-Gal4/*Cp1* RNAi #1) decreased ST50 during E1, but not during E2 (two-way ANOVA; ethanol exposure, $p < 0.0001$; genotype, $p = 0.0034$; interaction, $p = 0.0001$; *Bonferroni's multiple comparisons vs controls for each ethanol exposure, $p < 0.05$; $n = 8$). (**D**) Development of rapid tolerance (fold change in ST50 from E1 to E2) quantified from the data in panel C. Expression of *Cp1* RNAi in cortex glia (blue bar: *NP2222*-Gal4/*Cp1* RNAi #1) increased rapid tolerance development compared to controls (black bars: *NP2222*-Gal4/+, *Cp1* RNAi #1/+) (one-way ANOVA, $p = 0.0009$; *Bonferroni's multiple comparisons vs controls, $p < 0.05$; $n = 8$). (**E**) Expression of *Cp1* RNAi transgenes in CNS glia (blue triangles: *repo*-Gal4/*Cp1* RNAi #1) did not alter internal ethanol levels compared to controls with either *repo*-Gal4 alone (black circles: *repo*-Gal4/+) or the RNAi transgenes alone (black squares: *Cp1* RNAi #1/+) (one-way ANOVA, $p = 0.85$; $n = 6$).

B.6 Cp1 KNOCKDOWN IN CNS GLIA DURING ADULTHOOD ALTERS ALCOHOL SEDATION

To determine if Cp1 expression in glia during adulthood is important for alcohol sedation, we used the steroid-inducible pan-glial driver, GliaGS[29]. Flies with both the GliaGS driver and a *Cp1* RNAi transgene, and control flies with either GliaGS or the RNAi transgene alone, were reared to adulthood in the absence of the steroid mifepristone (RU486) and then switched to food medium containing steroid (RU486) or vehicle for 6 days. In this experimental design, the *Cp1* RNAi transgene should be induced in RU486-exposed adult flies harboring both a GeneSwitch Gal4 driver and an RNAi transgene[29], thereby allowing Cp1 knockdown during adulthood. Compared to vehicle control animals of the same genotype, flies expressing the GliaGS transgene and a *Cp1* RNAi transgene fed RU486 had significantly decreased ST50 values (*Cp1* RNAi #1 and #2: Fig. 4.14A and 4.14B; *Cp1* RNAi #3: Fig. 4.4C). Exposure to RU486 in flies with either the GliaGS alone or the respective Cp1 RNAi transgenes alone did not alter ST50 values (Fig. 4.14A, 4.14B; Fig. 4.4C). Manipulation of Cp1 in glia during adulthood was therefore sufficient to increase alcohol sedation. Interestingly, substantial overexpression of Cp1^{238} (87%, quantified via immunofluorescence) in glia during adulthood did not change ST50 values (Fig. 4.15). These results are consistent with a model in which endogenous, physiological levels of Cp1 in glia are required and sufficient for normal alcohol sedation in flies, suggesting that biologically relevant levels of Cp1 in glia contribute to alcohol behaviors.

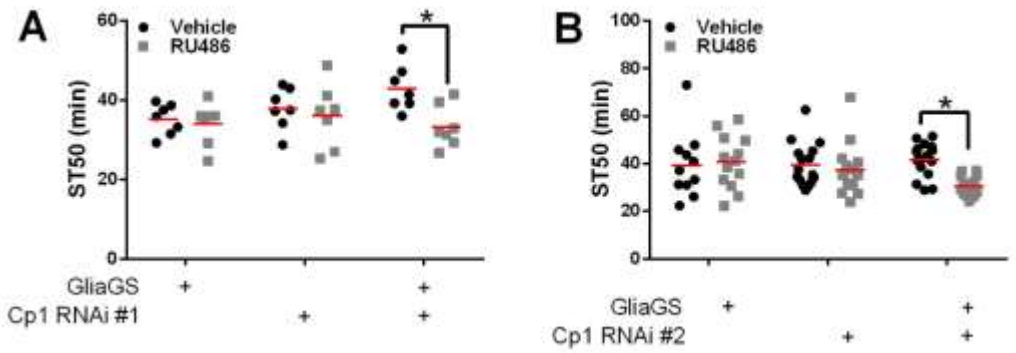

Figure 4.14. Cp1 knockdown in CNS glia during adulthood increased ethanol sedation sensitivity. Compared to vehicle, treatment with 1 mM RU486 for 6 days decreased ST50 values in flies with the GliaGS driver and a Cp1 *RNAi* transgene (GliaGS/*Cp1* RNAi #1, panel A; GliaGS/*Cp1* RNAi #2, panel B), but not in control flies with either GliaGS or an RNAi transgene alone (Panel A: two-way ANOVA; RU486, $p = 0.0247$; genotype, n.s.; interaction, n.s.; *Bonferroni's multiple comparisons between vehicle and RU486, $p < 0.05$; $n = 8$; Panel B: two-way ANOVA; RU486, n.s.; genotype, n.s.; interaction, $p = 0.0411$; *Bonferroni's multiple comparisons between vehicle and RU486, $p < 0.05$; $n = 16$).

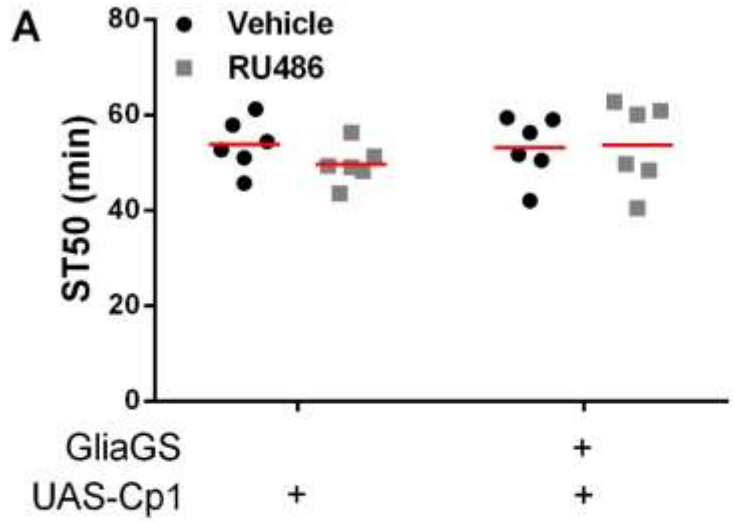

B. UAS-Cp1/+

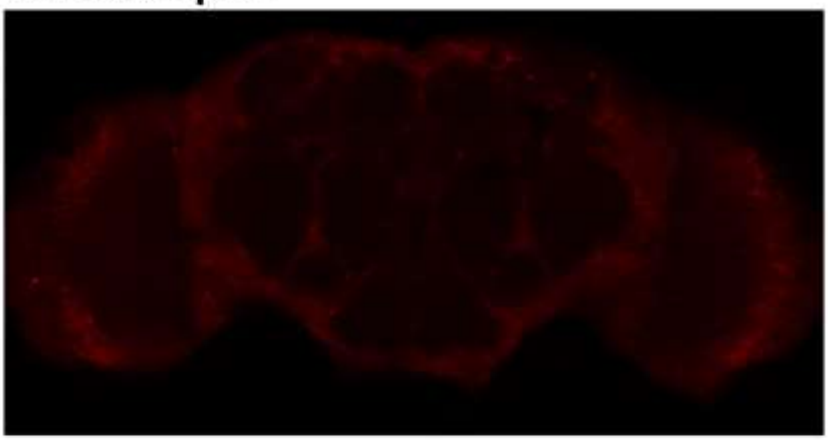

C. repo-Gal4/UAS-Cp1

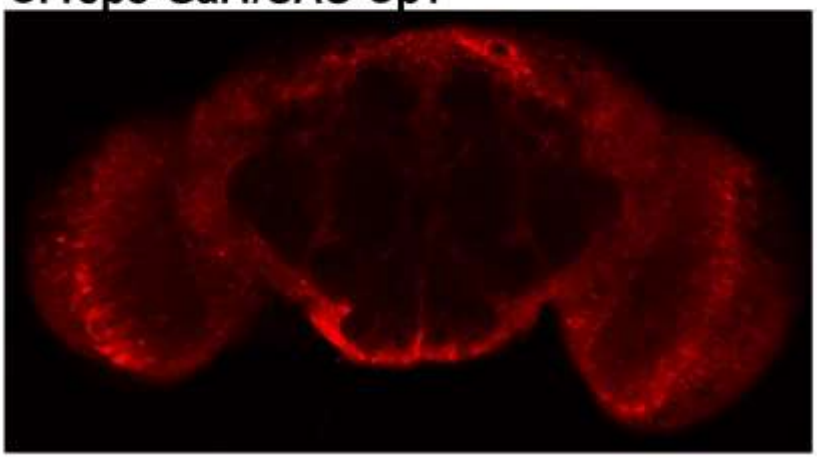

Figure 4.15. Over-expression of Cp1 in CNS glia during adulthood did not alter ethanol sedation sensitivity. (A) Over-expression of Cp1 in CNS glia during adulthood via UAS-*Cp1* did not change ethanol sedation sensitivity. Compared to vehicle-treated controls, treatment with 1 mM RU486 for 6 days did not alter ST50 values in flies with the GliaGS driver and a UAS-*Cp1* transgene (GliaGS/UAS-*Cp1*). Control flies with the UAS-*Cp1* transgene alone also had no change in ST50 between vehicle and RU486 treatment (UAS-*Cp1*/+) (two-way ANOVA; RU486, n.s.; genotype, n.s.; interaction, n.s; all Bonferroni's multiple comparisons between vehicle and RU486, $p > 0.05$; $n = 8$). **(B, C)** Whole mount brains immunolabeled for Cp1 (Anti-Cp1 1:250, Alexa 568 1:1000). Brains from flies with the UAS-*Cp1* and *repo*-Gal4 transgenes had increased fluorescence (89%) compared to brains from flies with the UAS-*Cp1* transgene alone. Microscope settings were optimized for *repo*-Gal4/UAS-*Cp1* brains to avoid over-saturation in the image analysis. Mean fluorescence intensity was calculated using Image J, n = 5-6. 10X, representative images.

C. DISCUSSION

Our understanding of the molecular-genetic basis for alcohol-related behavior in *Drosophila* and other model systems is based primarily on the results of studies that have focused on neuronal genes and mechanisms[226]. The nervous systems of flies and mammals also contain numerous classes of glia with conserved cellular-molecular activities. Given that mammalian glia respond to alcohol administration[249-251], that rodent astrocytes in the nucleus accumbens influence the motivation for alcohol consumption, and that surface glia influence alcohol sedation and tolerance in flies[183,211,212], it is likely that glia play direct—but underappreciated—roles in behavioral responses to alcohol.

Here, we used tissue specific RNAi-mediated knock down and trans-species rescue of RNAi to explore this possibility. Pan-glial Cp1 knockdown via RNAi significantly increased alcohol sedation. Expression of an orthologous gene, *Drosophila pseudoobscura* GA25021, in all glia rescued the alcohol sedation phenotype due to knockdown of endogenous Cp1. Taken together, these results indicate that Cp1 expression in glia regulates alcohol sedation. Additionally, our studies found that Cp1 expression specifically in cortex glia, and probably not other CNS glia, influences alcohol sedation. The magnitude and direction of change in alcohol sedation observed when Cp1 was knocked down in all glia versus only cortex glia were similar, suggesting that cortex glia are the principal cell type in which Cp1 functions to regulate alcohol sedation. These results reveal a novel role for Cp1 and cortex glia in *Drosophila* alcohol sedation. Thus, perineural glia[211,212] and cortex glia (our results) influence behavioral responses to alcohol in Drosophila.

Glia have prominent roles in nervous system development in flies[39,234]. Major changes in *Drosophila* nervous system development—in response to altered glial cell function—could, in principle, alter alcohol sedation sensitivity. Our data indicate that manipulation of Cp1 in glia during adulthood is sufficient to alter alcohol sedation in flies. Our findings are therefore consistent with a model in which Cp1 dynamically regulates adult glial cell function, and those changes in adult glial cell function influence the response of the nervous system to alcohol.

To date, a few studies have investigated the role of *Drosophila* cortex glia in behavior. One study suggests that innexin2 expression in cortex glia is required for normal sleep patterns[58], and two studies have indicated that cortex glia function contributes to seizures[133,139]. Additionally, cortex glia morphology influences larval locomotor behaviors[39]. The results reported here add to the emerging literature on cortex glia and behavior by showing that cortex glia, via Cp1 function, influence alcohol sedation. It could be important to explore the role of cortex glia, in conjunction with Cp1 and other candidate pathways, in behavioral responses to other drugs of abuse.

Cp1 knockdown in glia, specifically cortex glia, appeared to enhance alcohol rapid tolerance development. However, glial Cp1 knock down influenced sedation during the first exposure to alcohol only. These results suggest that Cp1 function in glia selectively influences alcohol sedation during an initial exposure to the drug and any interpretations regarding the role of Cp1 in rapid tolerance should be made with considerable caution. Importantly, though, since Cp1 knock down in glia did not influence alcohol sedation during a second alcohol exposure or alter locomotor abilities in the absence of alcohol (Fig. 4.16), it seems unlikely that the initial sedation sensitivity

of flies with Cp1 knockdown in glia is related to global sluggishness, a lack of overall behavioral fitness, or other experimental artifacts. We therefore posit that glial Cp1 plays a direct role in response of the central nervous system to alcohol.

Cp1 cleaves, and thereby activates, the transcription factor cut[239]. Additionally, the protein crammer binds to and inactivates the Cp1 protein[233]. We consequently predicted that altered expression of cut or crammer might alter sedation sensitivity. Surprisingly, constitutive expression of RNAi against *cut* or *crammer* in cortex glia or adult-specific expression of RNAi in all glia failed to substantively alter alcohol sedation (Fig. 4.17 and 4.18). Additionally, a recent study identified that Cp1 is required for synaptic vesicle degradation, and that this Cp1-mediated degradation was dependent on neuronal synaptobrevin (n-syb)[252]. Therefore, we tested whether expression of RNAi against *n-syb* in all glia altered alcohol sedation to investigate whether Cp1 and n-syb may be functioning similarly in glia to mediate alcohol sedation. Constitutive expression of *n-syb* RNAi in glia did not alter alcohol sedation (Fig 4.19), suggesting that Cp1 and n-syb are not functioning together in glia to influence alcohol sedation. However, it is possible that Cp1 and a glial version of syb may be functioning together, and this possibility would have to be investigated further. Although additional follow-up studies would be required to formally rule out a role for cut, crammer and n-syb in Cp1-dependent alcohol sedation, our data suggest that Cp1 influences alcohol sedation independently of these three known genes.

Cp1 is structurally and functionally homologous to mammalian Cathepsin L[240]. Cathepsins are powerful hydrolytic cysteine proteases and are inactively stored in the lysosomes of most tissues in mammalian cells[253]. When released from lysosomes in

their active form, they play roles in many physiological processes[253]. Although Cathepsin L has not been directly implicated in alcohol-related behaviors in mammals, Cathepsin L contributes to alcohol-induced cellular and/or organ damage. For example, Cathepsin L mediates alcohol-induced pancreatic damage and alcoholic liver fibrosis[254,255]. Following alcohol administration, Cathepsin L is activated in pancreatic lysosomes[254,256] and down-regulated in the cellular matrix in the liver[255], contributing to disease pathologies. However, it is unlikely that altered alcohol sedation in Cp1 knockdown flies is caused by over-all cathepsin-related glial cell damage because (i) flies with Cp1 knockdown have normal locomotor responses in the absence of alcohol (Fig. 4.16), (ii) Cp1 knockdown selectively alters alcohol sedation during a first, but not a second, exposure to the drug (Fig. 4.13) and (iii) Cp1 overexpression in all glia during adulthood does not alter alcohol sedation (Fig. 4.15). Although our results do not rule out the possibility that Cp1 is involved in glial cell damage, they do suggest that alcohol sedation sensitivity in Cp1 knockdown animals is unrelated to cellular damage that potentially may be occurring.

Cathepsin L also functions in secretory vesicles as a proneuropeptide processing[257]. Cathepsin L knockdown resulted in an 80-90% reduction of Neuropeptide Y (NPY) production in mammals[257]. Interestingly, NPY is synthesized in glia during development and adulthood in mammals. During adulthood, glial NPY is postulated to provide trophic support to neurons[258]. Mammalian NPY is homologous to *Drosophila* Neuropeptide F (NPF), which influences alcohol sedation in *Drosophila*[23,259]. While a role for Cp1 in NPF maturation in flies is possible, it seems unlikely that glial Cp1 influences alcohol sedation via processing of NPF. When NPF synthesis was ablated in

all NPF-producing cells, alcohol sedation was blunted[23], whereas knockdown of Cp1, which would also be predicted to decrease NPF production, increased alcohol sedation in our studies. These contradictory results make it very unlikely that Cp1 and NPF are working in conjunction to mediate alcohol sedation in *Drosophila*. Thus, additional studies, potentially involving approaches grounded in proteomics, are required to begin elucidating the molecular mechanisms involved in Cp1-dependent modulation of alcohol sedation in flies.

In summary, our results indicate a novel and potentially direct role for *Drosophila* glia in alcohol-related behaviors and that Cp1 represents a functional entry point for further understanding of cortex glial mechanisms that underlie alcohol sedation. Given that *Drosophila* Cp1 is orthologous to mammalian Cathepsin L, and that fly cortex glia are functionally similar to mammalian protoplasmic astrocytes, our findings have the potential to be translatable to mammalian systems. Our findings also raise the possibility that glial cysteine proteinases might mediate behavioral responses to other drugs of abuse in both flies and mammals.

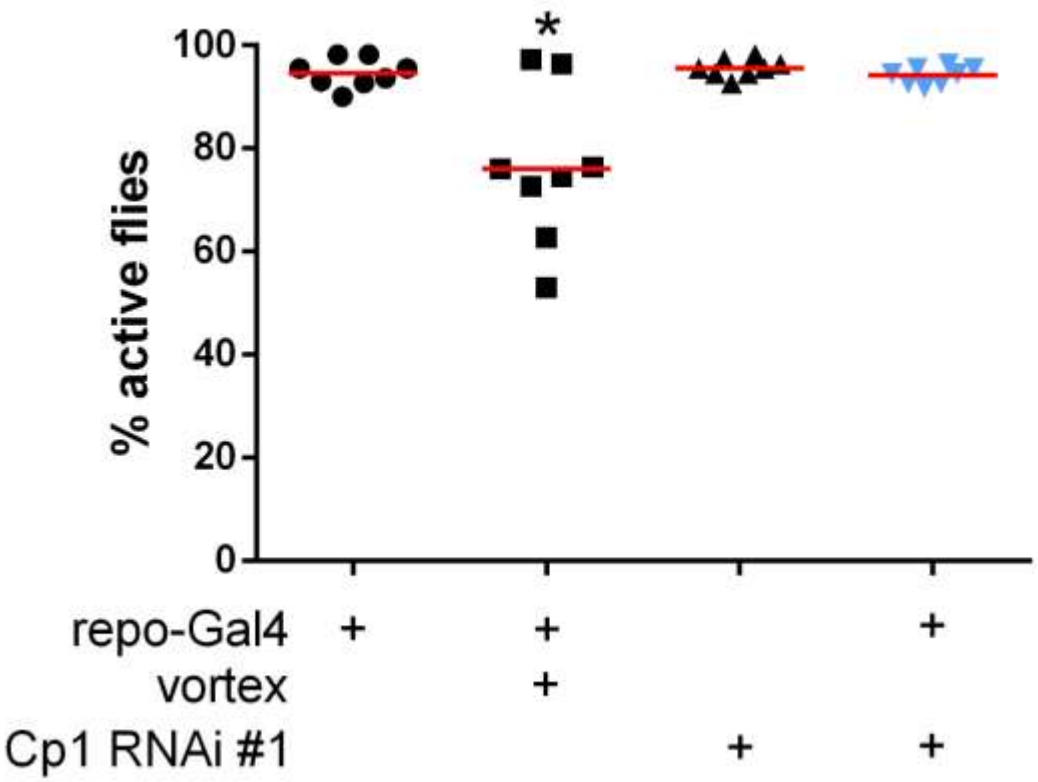

Figure 4.16. Expression of *Cp1* RNAi in CNS glia did not alter locomotion. Expression of the *Cp1* RNAi #1 transgene in CNS glia (via *repo*-Gal4) did not alter the percentage of active flies compared to controls with either *repo*-Gal4 or the RNAi transgene alone. Vortexing the *repo*-Gal4 control for 4 minutes reduced the percentage of active flies compared to the other groups (one-way ANOVA, $p < 0.001$; * Bonferronni's multiple comparison, $p < 0.05$; $n = 8$)

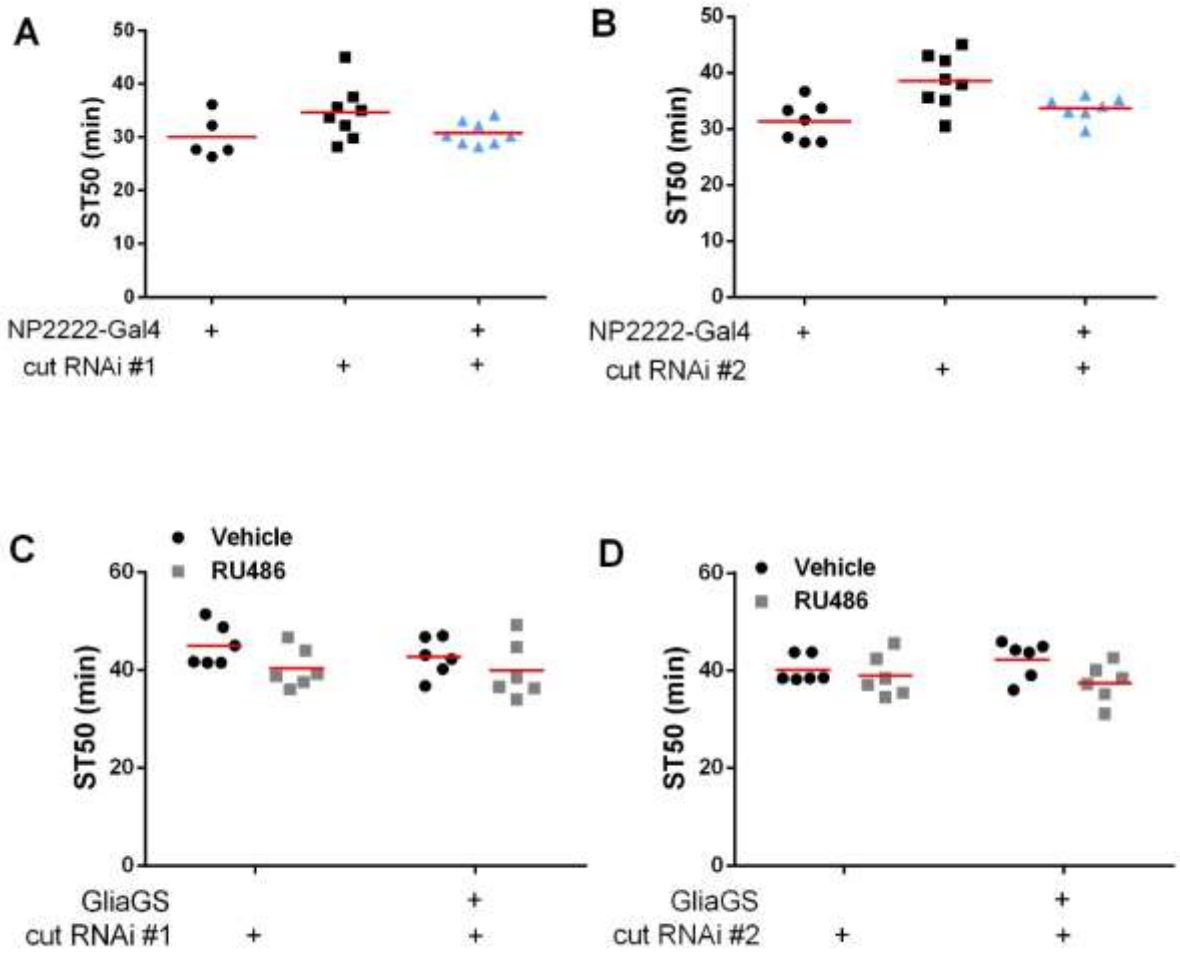

Figure 4.17. Expression of *cut* RNAi in cortex glia and CNS glia during adulthood did not alter alcohol sedation sensitivity. (**A, B**) ST50 values were not changed in flies expressing *cut* RNAi transgenes in cortex glia (blue triangles: *NP2222*-Gal4/*cut* RNAi #1, panel A; blue triangles: *NP2222*-Gal4/*cut* RNAi #2, panel B) compared to control flies containing either the cortex glia Gal4 driver (black circles: *NP2222*-Gal4/+) or the RNAi transgenes (black squares: *cut* RNAi #1/+ or *cut* RNAi #2/+) alone (Panel A: one-way ANOVA, $p > 0.05$; $n = 8$; Panel B: one-way ANOVA, $p = 0.0041$; all Bonferroni's multiple comparisons vs controls, $p > 0.05$; $n = 8$). (**C, D**) Expression of *cut* RNAi in CNS glia during adulthood did not alter ethanol sedation sensitivity. Compared to vehicle-treated controls, treatment with 1 mM RU486 for 6 days did not change ST50 values in flies with the GliaGS driver and a *cut* RNAi transgene (GliaGS/*cut* RNAi #1, panel C; GliaGS/*cut* RNAi #2, panel D). Control flies with the RNAi transgene alone also had no change in ST50 between vehicle and RU486 treatment (individual two-way ANOVAs; RU486, n.s.; genotype, n.s.; interaction, n.s.; all Bonferroni's multiple comparisons between vehicle and RU486, $p > 0.05$; $n = 8$).

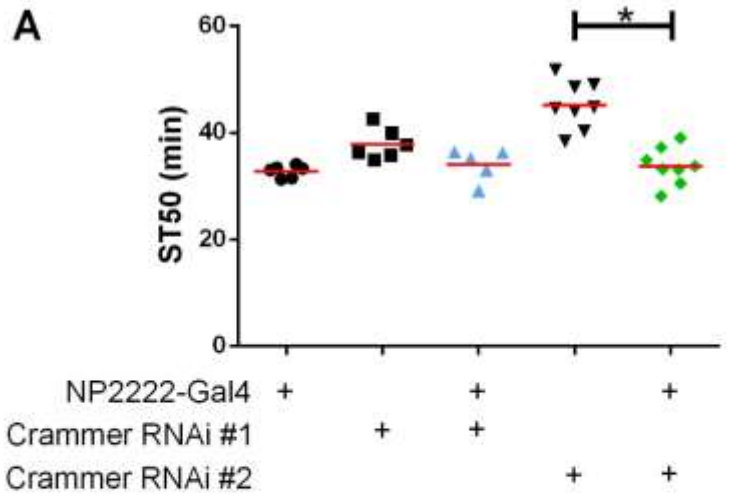
A
ST50 (min)
60
40
20
0
*
NP2222-Gal4 + + +
Crammer RNAi #1 + +
Crammer RNAi #2 + +

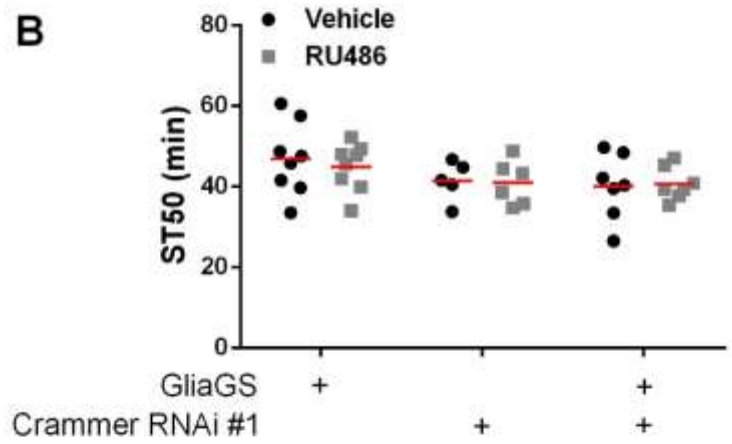
B
Vehicle
RU486
ST50 (min)
80
60
40
20
0
GliaGS + +
Crammer RNAi #1 + +

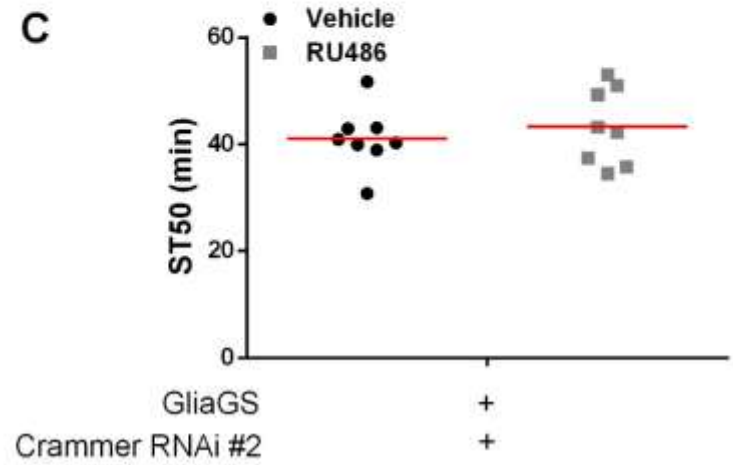
C
Vehicle
RU486
ST50 (min)
60
40
20
0
GliaGS +
Crammer RNAi #2 +

Figure 4.18. Expression of *crammer* RNAi in cortex glia and CNS glia during adulthood did not alter alcohol sedation sensitivity. (**A**) ST50 values were significantly decreased between flies expressing the *crammer* RNAi #2 transgene in cortex glia (blue triangles: *NP2222*-Gal4/*crammer* RNAi #2) compared to the RNAi alone (*crammer* RNAi #2/+) control. However, ST50 values were not changed in flies expressing *crammer* RNAi transgenes in cortex glia (blue triangles diamonds: *NP2222*-Gal4/*crammer* RNAi #1; green diamonds: *NP2222*-Gal4/*crammer* RNAi #2) compared to control flies containing either the cortex glia Gal4 driver (black circles: *NP2222*-Gal4/+) or the appropriate RNAi transgene alone (one-way ANOVA, $p < 0.0001$; *Bonferroni's multiple comparisons vs controls, $p < 0.05$; $n = 8$). (**B, C**) Expression of *crammer* RNAi in CNS glia during adulthood does not alter ethanol sedation sensitivity. (**B**) Compared to vehicle-treated controls, treatment with 1 mM RU486 for 6 days did not alter ST50 values in flies with the GliaGS driver and the *crammer* RNAi #1 transgene (GliaGS/*crammer* RNAi #1). Control flies with either GliaGS or the RNAi transgene alone also had no differences in ST50 between vehicle and RU486 treatment (two-way ANOVA; interaction, n.s.; genotype, $p = 0.0302$; RU486, n.s.; all Bonferroni's multiple comparisons between vehicle and RU486, $p > 0.05$; $n = 3$-8). (**C**) Compared to vehicle-treated controls, treatment with 1 mM RU486 for 6 days did not alter ST50 values in flies with the GliaGS driver and the *crammer* RNAi #2 transgene (GliaGS/*crammer* RNAi #2). (Student’s t-test, $p > 0.05$; $n = 8$).

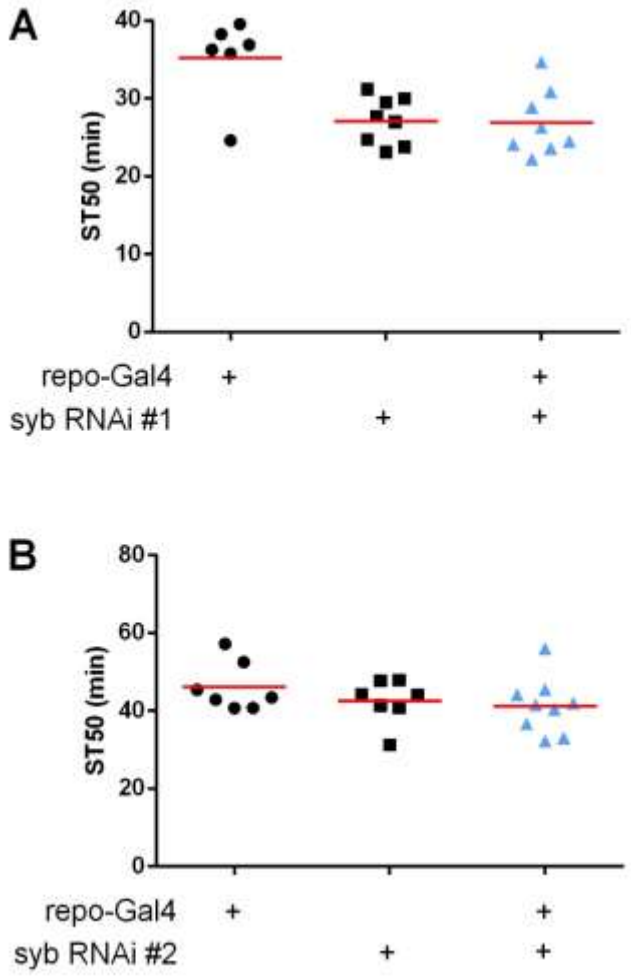

Figure 4.19. Expression of *n-syb* RNAi in all glia did not alter alcohol sedation sensitivity. (**A**) ST50 values were significantly decreased between flies expressing the *syb* RNAi #1 transgene in all glia via *repo*-Gal4 (blue triangles: *NP2222*-Gal4/*syb* RNAi #1) compared to control flies expressing *repo*-Gal4 alone (black circles: repo-Gal4/+). However, ST50 values were not changed in flies expressing *syb* RNAi #1 transgene in all glia via *repo*-Gal4 (blue triangles) compared to control flies expressing the RNAi transgene alone (black squares: *syb* RNAi #1/+) (one-way ANOVA, $p = 0.003$; *Bonferroni's multiple comparisons vs controls, $p < 0.05$; $n = 6$-8). (**B**) ST50 values were similar between flies expressing the *syb* RNAi #2 transgene in all glia via *repo*-Gal4 (blue triangles: *syb* RNAi #2/*repo*-Gal4) compared to control flies that had either the Gal4 alone (black circles: *repo*-Gal4/+) or the RNAi transgene alone (black squares: *syb* RNAi #2/+) (one-way ANOVA, $p = 0.34$; $n = 7$-8).

CHAPTER 5: TYRAMINE SYNTHESIS, VESICULAR PACKAGING AND THE SNARE COMPLEX FUNCTION COORDINATELY IN ASTROCYTES TO REGULATE DROSOPHILA ALCOHOL SEDATION

A. INTRODUCTION

Alcohol abuse impacts and is impacted by central nervous system (CNS) function[5]. There is consequently a large, continuing effort to use model organisms to identify mechanisms underlying alcohol-related behaviors to better understand the role of the CNS in alcohol abuse. Although the central nervous system contains both glia and neurons as principal cell types, the preponderance of research to date has focused on the role of neuronal mechanisms in alcohol-related behaviors. Thus, there is likely much to be learned by investigating the role of glia in behavioral responses to alcohol.

Despite the somewhat limited focus on glia and alcohol, several studies offer intriguing insights into the effect of alcohol on these cells and the roles these cells play in alcohol-related behavior. For example, calcium signaling genes are upregulated in astrocytes after chronic alcohol administration in mice[178], expression of the glial cytoskeletal protein GFAP can be altered by alcohol exposure in rodents and humans[159,260], cultured astrocytes, in the presence of alcohol, can induce interferon expression in neurons[190] and alcohol exposure correlates with increased hemichannel opening in mouse hippocampal astrocytes[182]. These studies indicate that glia are responding to alcohol administration and suggest that these responses might be required for normal alcohol-related behaviors. Consistent with the possibility that glia

are directly involved in behavioral responses to alcohol, increasing intracellular calcium in astrocytes via designer receptors exclusively activated by designer drugs (DREADDs) decreased motivation for alcohol after a 3-week abstinence period in rats[183], mutation of the gene *moody* in flies, which is expressed in surface glia, blunts alcohol-induced loss of postural control[211], and *Drosophila* perineural glia influence alcohol tolerance[212]. Thus, there is good evidence that glia respond to and are involved in the behavioral responses to alcohol.

Here, we report the results of studies using the fruit fly, *Drosophila melanogaster*, to further explore the role of glia in alcohol-related behavior. Flies are a leading model for investigating the molecular-genetics of behavioral responses to alcohol for many reasons including (i) they have conserved behavioral responses to alcohol[13], (ii) there is a large suite of genetic tools available to manipulate gene expression in flies[24,261], and (iii) many genes that impact fly alcohol behavior have been implicated in various aspects of alcohol abuse in humans[16,226]. Flies are also emerging as a powerful model for studying the contribution of glia to physiology and disease. Flies have several glial cell subtypes in the central nervous system (astrocytes, cortex glia, ensheathing cells, perineural glia and subperineural glia) that collectively share many morphological and functional attributes of mammalian glia. For example, fly astrocytes maintain ion homeostasis, remove neurotransmitters from the synapse, have hemichannels and gap junctions, produce Ca^{2+} oscillations and release gliotransmitters like their mammalian counterparts[40,140,153]. Flies are therefore well-suited for investigating the contribution of astrocytes to behavioral responses to alcohol.

We identified the gene *tyramine decarboxylase 2* (*Tdc2*) as a regulator of alcohol sedation in flies. Tdc2 is a brain-specific enzyme that converts the amino acid tyrosine to the catecholamine tyramine in invertebrates[262]. Manipulation of Tdc2 expression in all glia, selectively in astrocytes, or conditionally in glia during adulthood altered ethanol sedation. Additionally, manipulation of the vesicular monoamine transporter (VMAT) and the SNARE complex in all glia, astrocytes and in adult glia also influenced ethanol sedation by functioning downstream of Tdc2. Our studies support a model in which Tdc2 produces tyramine in astrocytes which is packaged into vesicles and released via the SNARE complex, thereby mediating alcohol sedation in *Drosophila.*

B. RESULTS

B.1 Tdc2 FUNCTIONS IN CNS GLIA, SPECIFICALLY ASTROCYTES, TO REGULATE ALCOHOL SEDATION SENSITIVITY

To identify candidate genes that could influence alcohol-related behaviors by functioning in glia, we compiled a list of genes known to be expressed in *Drosophila* CNS glial cells[263,264]. We then determined whether manipulation of 33 of these genes individually in all CNS glia influenced alcohol sedation in *Drosophila* (Table 5.1). Flies with pan-glial Gal4 (via *repo*-Gal4) driven expression of two unique *Tdc2* RNAi transgenes (*Tdc2* RNAi #1 and #2) had significantly decreased sedation time 50 (ST50) values compared to control flies containing the Gal4 or RNAi transgene alone (Fig. 5.1A, 5.1B), suggesting that Tdc2 might regulate alcohol sedation by functioning in glia.

Tdc2 could, in principle, influence alcohol sedation through the collective effect of its role in all CNS glia or by a role in a single glial cell subtype. We consequently

assessed whether manipulating *Tdc2* expression individually in astrocytes, ensheathing cells, cortex glia, perineural glia and subperineural glia impacted ST50 values. We found that expression of *Tdc2* RNAi in astrocytes (via *alrm*-Gal4) significantly decreased ST50 values compared to controls (Fig. 5.1C, 5.1D; Table 5.2). Expression of *Tdc2* RNAi in other glial cell subtypes did not alter ST50 values (Table 5.2). Additionally, *Tdc2* RNAi expression in neurons did not alter ST50 values compared to controls (Fig. 5.2). Taken together, these data suggest that Tdc2 plays a role in alcohol sedation by functioning within astrocytes, but not other glial cell subtypes or neurons.

We performed immunofluorescence studies to determine (i) whether the *Tdc2* RNAi transgenes we used knocked down expression of Tdc2 and (ii) whether Tdc2 is expressed in CNS glia. Consistent with a previous report[265], we found that Tdc2 is robustly expressed throughout the brain (Fig. 5.3A, 5.3B). Additionally, the Tdc2 immunofluorescence signal was significantly decreased by pan-neuronal *elav*-Gal4-driven expression of *Tdc2* RNAi transgenes (Figs. 5.3), confirming that Tdc2 is expressed in neurons[265] and that the RNAi transgenes knockdown expression of Tdc2.

Tdc2 is known to be expressed in astrocytes, as characterized by TRAP-seq studies[264]. To confirm these results, we labeled astrocytes through mCD8:GFP expression driven by *alrm*-Gal4 and detected endogenous Tdc2 via immunofluorescence. GFP driven by *alrm*-Gal4 was found in astrocytes throughout the brain (Fig. 5.4A), as expected[40]. Endogenous Tdc2 was also expressed throughout the brain as expected (Fig. 2B). Using Manders colocalization coefficient[266], we found that approximately 12% of the GFP (astrocytes) and red (Tdc2) pixels were colocalized (n = 6), indicating that a subpopulation of astrocytes express Tdc2 (Fig 5.4). Collectively, the

data in Figs. 5.1, 5.3 and 5.4 indicate that Tdc2 influences alcohol sedation in Drosophila by functioning in astrocytes.

Table 5.1. Identifying glial genes that regulate alcohol sedation

Gene	reagent (identifier)	Drug Treatment	ST50	two-way ANOVA	Bonferonni mult. comparisons (to Gal4/RNAi)
Sod 1	RNAi (24493)#	Vehicle	39.78	#Interaction, F (3 39) = 1.969, p = 0.13; Genotype, F (3 , 39) = 9.162, p = 0.0001; Drug treatment, F (3, 39) = 4.144, p = 0.04	p = 0.02
		RU486	51.85		
	RNAi (v31552)#	Vehicle	32.64		p > 0.9999
		RU486	36.55		
Sod2	RNAi (Sod2IR15)#	Vehicle	46.15		p > 0.9999
		RU486	49.26		
	RNAi (Sod2IR24)#	Vehicle	38.3		p > 0.9999
		RU486	36.3		
AdoR	RNAi (1385)$	Vehicle	35.16	$Interaction, F (2, 42) = 0.65, p = 0.52; Genotype, F (2, 42) = 6.32, p = 0.004; Drug treatment, F (1, 42) = 1.85, p = 0.17	p > 0.9999
		RU486	37.71		
	RNAi (1386)$	Vehicle	40.5		p = 0.31
		RU486	46.92		
Nos	UAS (56829)$	Vehicle	45.55		p > 0.9999
		RU486	45.76		
src42a	UAS(6410)%	Vehicle	43.32	%Interaction, F (3, 35) = 0.87, p = 0.46; Genotype, F (3, 35) = 5.64, p = 0.003; Drug treatment, F (3, 35) = 4.04, p = 0.05	p > 0.9999
		RU486	44.33		
Eaat1	UAS (8202)%	Vehicle	41.43		p = 0.37
		RU486	49.65		
nrg	UAS (24169)%	Vehicle	36.3		p > 0.9999
		RU486	36.83		
	UAS (24172)%	Vehicle	43.05		p = 0.42
		RU486	49.02		
Htl	DN (5366)&	Vehicle	36.88	&Interaction, F (3, 40) = 1.15, p = 0.34; Genotype, F (2, 40) = 4.94, p = 0.005; Drug treatment, F(1, 40) = 0.07, p = 0.79	p > 0.9999
		RU486	36.05		
serca	UAS (63228)&	Vehicle	42.33		p > 0.9999
		RU486	46.12		
Rab27	DN (23267)&	Vehicle	46.07		p = 0.88
		RU486	40.03		
mor	DN (59074)&	Vehicle	30.07		p > 0.9999
		RU486	35.72		
pros	UAS (32244)~	Vehicle	34.47	~Interaction, F (3, 40) = 0.26, p = 0.85; Genotype, F (3, 40) = 2.07, p = 0.11; Drug treatment, F (1, 40) = 0.83, p = 0.37	n/a
		RU486	29.78		
Gαi	UAS (44600)~	Vehicle	26.9		n/a
		RU486	25.73		
RabX4	DN (9849)~	Vehicle	32.42		n/a
		RU486	32.12		
	DN (9850)~	Vehicle	30.05		n/a
		RU486	29.13		
syx1A	UAS (51518)+	Vehicle	27.5	+Interaction, F (2, 30) = 1.72, p = 0.19; Genotype, F (2, 30) = 1.81, p = 0.18; Drug treatment, F (1, 30) = 20.29, p < 0.0001	p = 0.503
		RU486	30.38		
Tdc2	UAS (9315)+	Vehicle	28.73		p = 0.07
		RU486	33.58		
	UAS (9316)+	Vehicle	24.55		p = 0.001
		RU486	32.73		

Genes were manipulated either by over-expression (UAS), dominant negative or RNAi transgenes. Manipulations were made in all glia during adulthood using GliaGS. ST50 values for the GliaGS/transgene either fed RU486 or vehicle are reported. #, $, %, &, ~ and + represent genotypes that were tested together, and were therefore statistically compared in the two-way ANOVA. When appropriate, Bonferonni multiple comparisons adjusted p-values are reported.

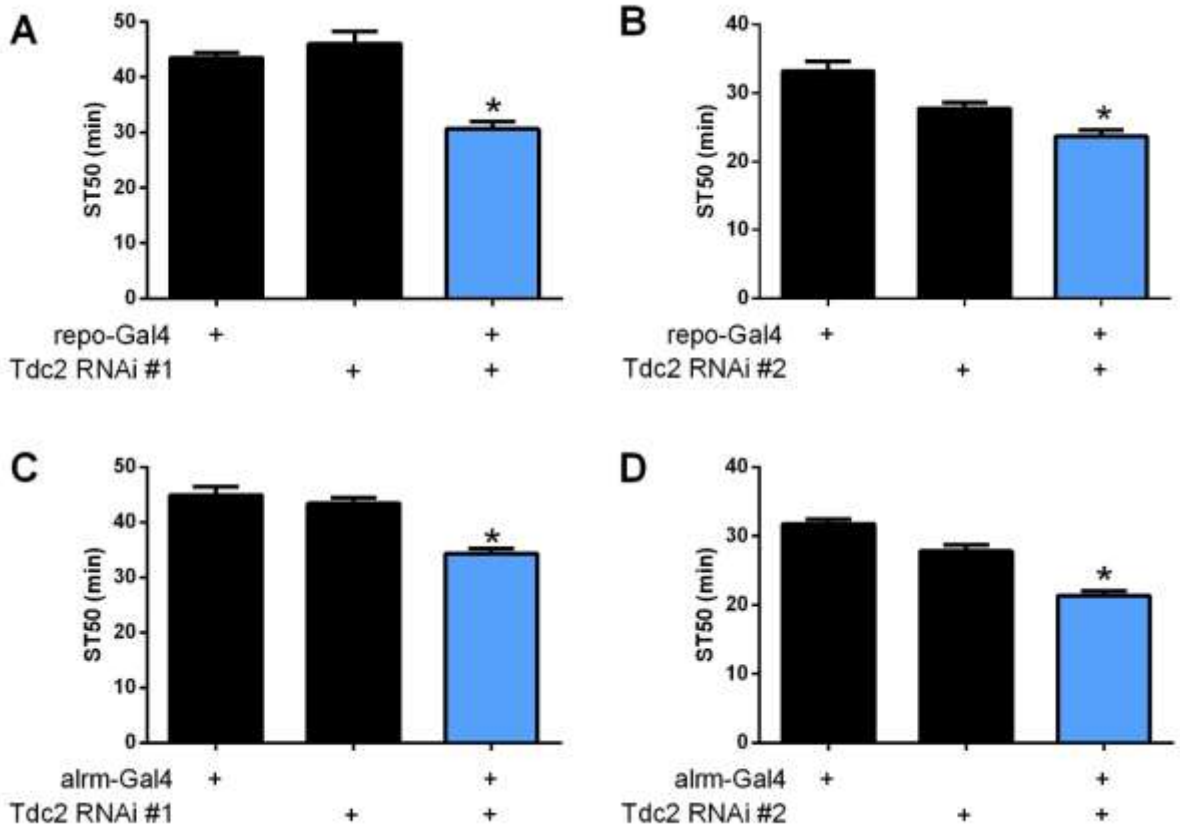

Figure 5.1. Manipulating Tdc2 expression constitutively in all glia or specifically in astrocytes alters alcohol sedation. (**A, B**) ST50 values were reduced in flies with the pan-glial driver *repo*-Gal4 and a *Tdc2* RNAi transgene (blue bars: *repo*-Gal4/*Tdc2* RNAi #1, panel A; *repo*-Gal4/*Tdc2* RNAi #2, panel B) compared to control flies with either *repo*-Gal4 alone (black bars: *repo*-Gal4/+) or the respective RNAi transgene alone (black bars: *Tdc2* RNAi #1/+ and *Tdc2* RNAi #2/+) (Panel A: one-way ANOVA, $p < 0.0001$; *Bonferroni's multiple comparison vs controls, $p < 0.05$; $n = 8$; Panel B: one-way ANOVA, $p < 0.0001$; *Bonferroni's multiple comparison vs controls, $p < 0.05$; $n = 16$). (**C, D**) ST50 values were decreased in flies expressing the astrocyte-specific driver *alrm*-Gal4 and a *Tdc2* RNAi transgene (blue bars: *alrm*-Gal4/*Tdc2* RNAi #1, panel C; *alrm*-Gal4/*Tdc2* RNAi #2, panel D) compared to control flies containing either the astrocyte Gal4 driver (black bars: *arlm*-Gal4) or the respective RNAi transgene (black bars: *Tdc2* RNAi #1/+, panel C; *Tdc2* RNAi #2, panel D) alone (Panel C: one-way ANOVA, $p < 0.0001$; *Bonferroni's multiple comparison vs controls, $p < 0.05$; $n = 8$; Panel D: one-way ANOVA, $p < 0.0001$; *Bonferroni's multiple comparison vs controls, $p < 0.05$; $n = 16$).

Table 5.2. Manipulating expression of Tdc2 in each glial cell subtype individually

Glial subtype Gal4	Group	ST50	ANOVA	Multiple comparisons (to Gal4/RNAi)
Astrocytes (Alrm)	Gal4/+	36.99 ± 0.97	F (2,21) = 18.31, p < 0.0001*	p = 0.0005*
	RNAi/+	36.94 ± 1.85		p < 0.0001*
	Gal4/RNAi	27.55 ± 0.67		
Ensheathing (TIFR)	Gal4/+	29.84 ± 1.71	F (2,21) = 1.07, p = 0.36	n/a
	RNAi/+	32.13 ± 0.55$		n/a
	Gal4/RNAi	32.03 ± 1.21		
Ensheathing (Mz0709)	Gal4/+	36.20 ± 1.82	F (2,21) = 2.88, p = 0.07	n/a
	RNAi/+	41.65 ± 1.19		n/a
	Gal4/RNAi	38.38 ± 1.76		
Cortex Glia (NP2222)	Gal4/+	30.01 ± 0.96	F (2,21) = 20.01, p < 0.0001*	p > 0.9999
	RNAi/+	40.93 ± 2.19		p < 0.0001*
	Gal4/RNAi	28.98 ± 0.91		
Subperineural glia (Gli)	Gal4/+	31.46 ± 1.27	F (2,21) = 0.41, p = 0.67	n/a
	RNAi/+	32.13 ± 0.55$		n/a
	Gal4/RNAi	32.80 ± 1.15		
Perineural glia (Indy)	Gal4/+	37.66 ± 0.49	F (2,21) = 1.795, p = 0.19	n/a
	RNAi/+	36.09 ± 1.46		n/a
	Gal4/RNAi	34.7 ± 1.14		

Expression of the *Tdc2* RNAi #1 transgene in astrocytes (via alrm-Gal4) consistently altered alcohol sedation compared to both the Gal4 driver (Gal4/+) and RNAi transgene (RNAi/+) controls. Expression of the *Tdc2* RNAi #1 transgene in ensheathing cells (via *TIFR*-Gal4 and *mz0709*-Gal4), cortex glia (via NP2222-Gal4), subperineural glia (via *Gli*-Gal4) and perineural glia (via *Indy*-Gal4) did not consistently alter alcohol sedation compared to both the Gal4 driver (Gal4/+) and RNAi transgene (RNAi/+) controls. Results from individual one-way ANOVAs and (when appropriate) Bonferroni's multiple comparisons are reported. $ represent common RNAi/+ controls.

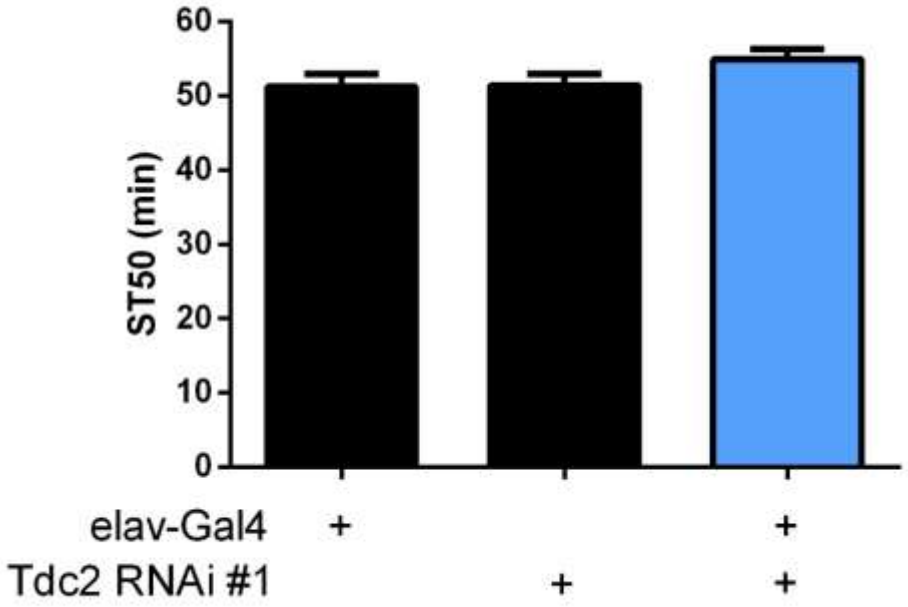

Figure 5.2. Tdc2 knockdown in neurons does not alter alcohol sedation. ST50 values were not altered in flies containing both the pan-neuronal driver *elav*-Gal4 and the *Tdc2* RNAi #1 transgene (blue bar: *elav*-Gal4/*Tdc2* RNAi #1) compared to control flies containing either *elav*-Gal4 or the *Tdc2* RNAi #1 transgene alone (black bars) (one-way ANOVA, p = 0.189, n = 8).

A. Tdc2 RNAi #1/+

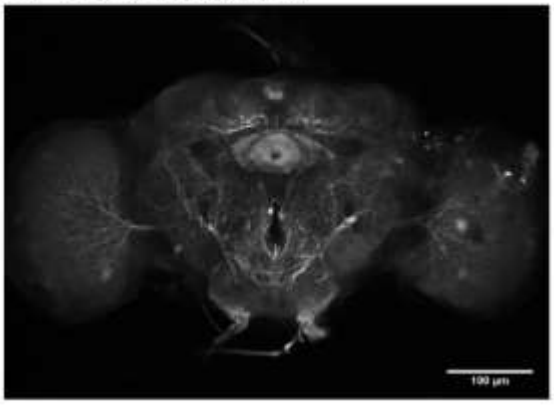

B. Tdc2 RNAi #2/+

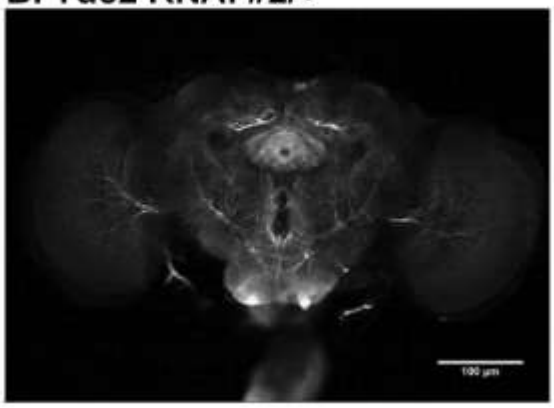

C. elav-Gal4/Tdc2 RNAi #1

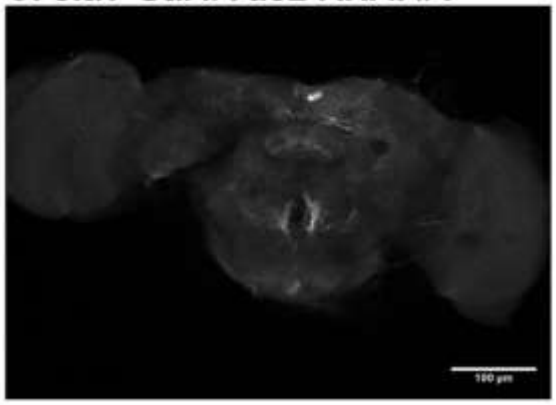

D. elav-Gal4/Tdc2 RNAi #2

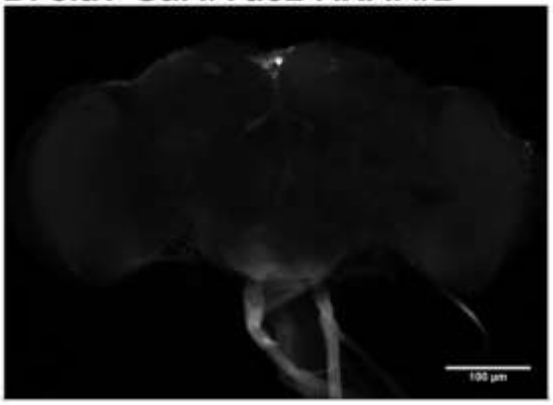

E

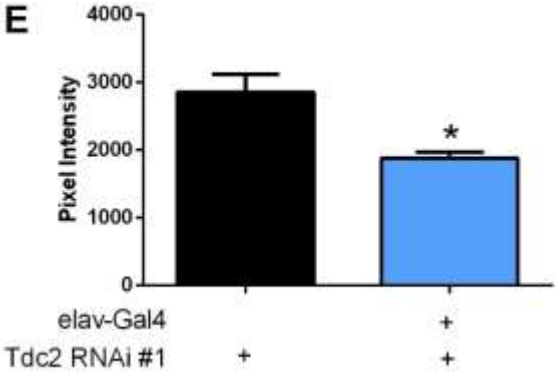

F

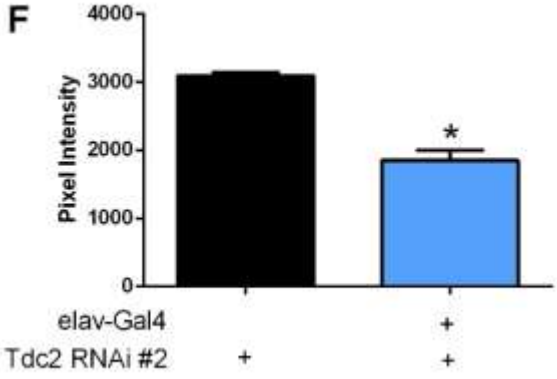

Figure 5.3. Tdc2 RNAi knocks down Tdc2 expression. Whole mount brain images immunolabeled for Tdc2 expression (anti-Tdc2 1:200, Alexa-647 1:1000). All representative images, 10X. (**A, B**) Tdc2 expression in brains of flies with a *Tdc2* RNAi transgene alone. (**C, D**) Tdc2 expression in brains of flies with the pan-neuronal driver *elav*-Gal4 and a *Tdc2* RNAi. (**E, F**) Brains with both the *elav*-Gal4 and a *Tdc2* RNAi transgene had significantly lower pixel intensity compared to control flies with the *Tdc2* RNAi transgene alone (Panel E: students t test, $p = 0.0059$, $n = 4$-5; Panel F: students t test, $p = 0.0002$, $n = 4$).

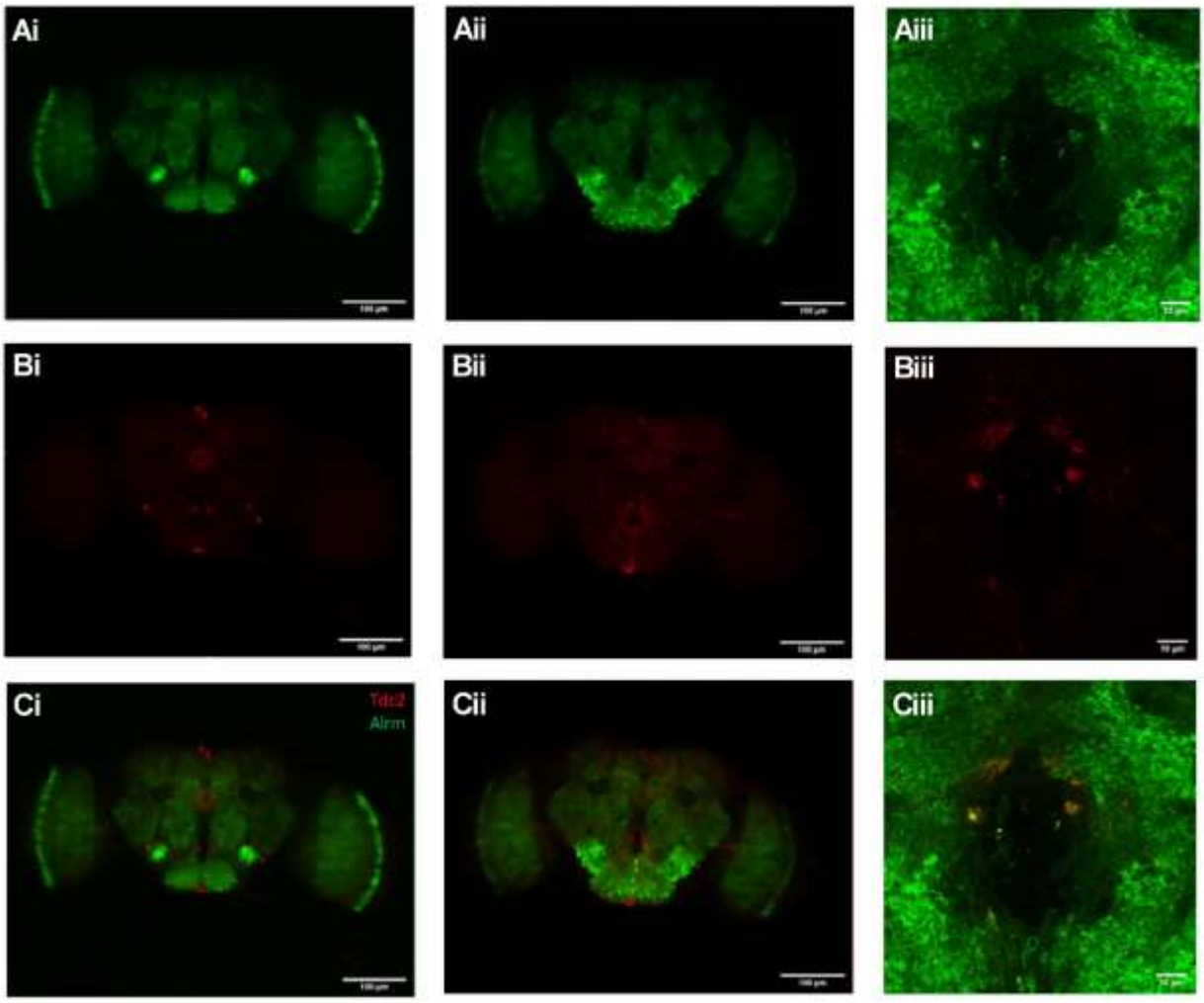

Figure 5.4. Tdc2 expression in astrocytes. (**A**) Expression of UAS-GFP (green) driven by *alrm*-Gal4. (**B**) Endogenous Tdc2 expression labeled red (anti-Tdc2 1:200, Alexa 647 1:1000). (**C**) Overlay and colocalization. Column i and ii are representative 10X Z-stack slices from the same whole brain. Column iii is representative 63X oil immersion.

B.2 Tdc2 REGULATES ALCOHOL SEDATION SENSITIVITY IN CNS GLIA DURING ADULTHOOD THROUGH A PHARMACODYNAMIC MECHANISM

To determine if *Tdc2* expression in glia during adulthood is important for alcohol sedation, we used GliaGS to conditionally express UAS-transgenes. GliaGS is a steroid (mifepristone, RU486)-inducible pan-glial Gal4 driver[29]. Compared to vehicle, induction of the two independent *Tdc2* RNAi transgenes in all glia during adulthood (i.e. in flies with GliaGS and a Tdc2 RNAi transgene fed RU486) significantly decreased ST50 values (Fig. 5.5A, 5.5B). Conversely, conditional overexpression of *Tdc2* via two independent, previously validated[267], transgenes in all glia during adulthood (i.e. in flies with GliaGS and a UAS-*Tdc2* transgene fed RU486) significantly increased ST50 values (Fig. 5.5C). Treatment with RU486 did not significantly alter ST50 values in control flies with either the GliaGS driver, the *Tdc2* RNAi transgenes or the UAS-*Tdc2* transgenes alone (Fig. 5.5). Additionally, internal alcohol levels were not altered by adult-specific *Tdc2* knockdown or over-expression in glia (Fig. 5.6A). Thus, knocking down or overexpressing *Tdc2* in glia during adulthood respectively decreased or increased ST50 values without altering the net uptake or metabolism of alcohol. Therefore, the level of *Tdc2* expression in adult glia is a key regulator of alcohol sedation in flies.

Interestingly, overexpressing Tdc2 (via UAS-*Tdc2*) constitutively in all glia (via *repo*-Gal4) and constitutively in astrocytes (via *alrm*-Gal4) caused developmental lethality. To determine if Tdc2 overexpression in astrocytes alters alcohol sedation, we utilized Gal80ts, an inducible temperature sensitive Gal4 repressor[28], to express UAS-*Tdc2* in astrocytes during adulthood. Flies developed in the Gal80ts permissive temperature (18˚C), repressing UAS-*Tdc2* expression during development (i.e. Gal80ts on, *alrm*-

Gal4 off, UAS-*Tdc2* off). During adulthood, flies were switched to the Gal80ts restrictive temperature (30˚C), which allows UAS-*Tdc2* to be expressed in astrocytes via *alrm*-Gal4 (i.e. Gal80ts off, *alrm*-Gal4 on, UAS-*Tdc2* on). Switching flies to the restrictive temperature (30˚C), and consequently overexpressing Tdc2 in astrocytes during adulthood, significantly increased ST50 compared to control flies that experienced the same temperature shift (30C, Fig 5.7). However, for reasons that we do not understand, rearing flies in the permissive temperature (18˚C), and not switching temperatures (no 30°C exposure), differentially altered flies behavioral responses to alcohol (18C, Fig 5.7). While difficult to fully interpret, these data begin to suggest that overexpressing *Tdc2* in astrocytes during adulthood also alters alcohol sedation in flies.

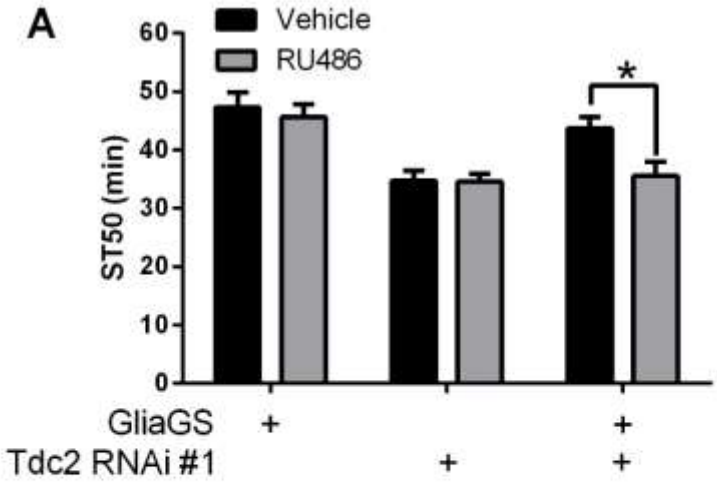
A
Vehicle
RU486
ST50 (min)
60
50
40
30
20
10
0
*
GliaGS + +
Tdc2 RNAi #1 + +

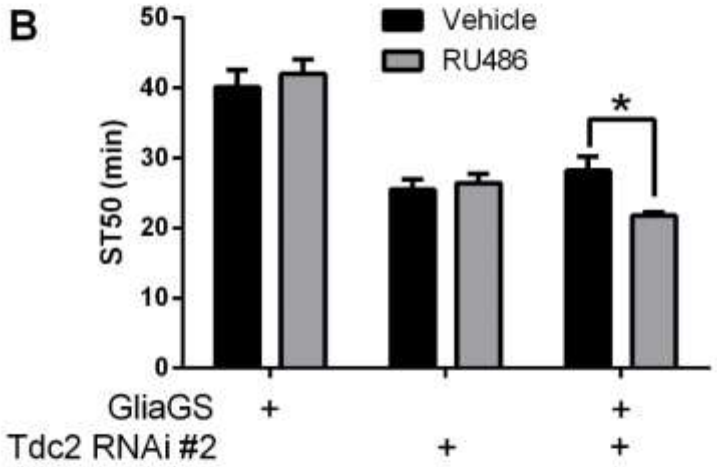
B
Vehicle
RU486
ST50 (min)
50
40
30
20
10
0
*
GliaGS + +
Tdc2 RNAi #2 + +

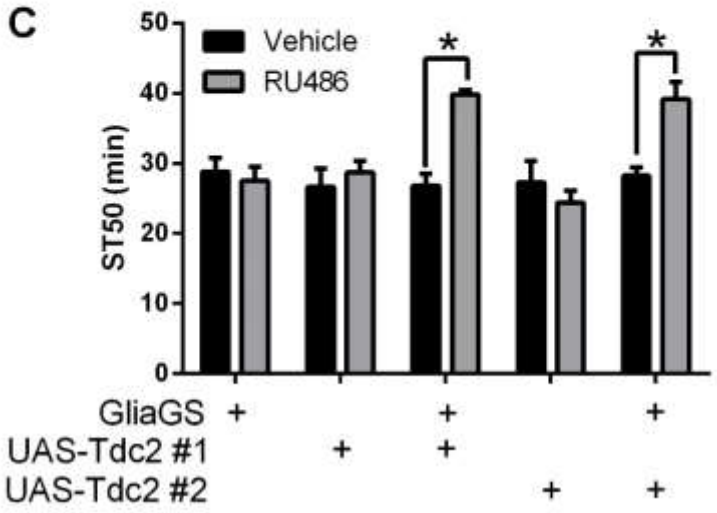
C
Vehicle
RU486
ST50 (min)
50
40
30
20
10
0
*
*
GliaGS + + +
UAS-Tdc2 #1 + +
UAS-Tdc2 #2 + +

Figure 5.5. Manipulating Tdc2 expression in all glia during adulthood influences alcohol sedation. (**A, B**) Compared to vehicle, treatment with RU486 decreased ST50 values in flies with the GliaGS driver and a *Tdc2* RNAi transgene (GliaGS/*Tdc2* RNAi #1, panel A; GliaGS/*Tdc2* RNAi #2, panel B), but not in control flies with either GliaGS or the respective RNAi transgene alone (Panel A: two-way ANOVA; RU486, $p = 0.059$; genotype, $p < 0.0001$; interaction, $p = 0.13$; *Bonferroni's multiple comparisons between vehicle and RU486, $p < 0.05$; $n = 8$; Panel B: two-way ANOVA; RU486, $p = 0.4$; genotype, $p < 0.0001$; interaction, $p = 0.045$; *Bonferroni's multiple comparisons between vehicle and RU486, $p < 0.05$; $n = 8$). (**C**) Compared to vehicle, treatment with RU486 increased ST50 values in flies with the GliaGS driver and a UAS-*Tdc2* transgene (GliaGS/UAS-*Tdc2* #1 and GliaGS/UAS-*Tdc2* #2), but not in control flies with either GliaGS or the UAS-*Tdc2* transgene alone (two-way ANOVA; RU486, $p = 0.0012$; genotype, $p = 0.0004$; interaction, $p = 0.0003$; *Bonferroni's multiple comparisons between vehicle and RU486, $p < 0.05$; $n = 6$-7).

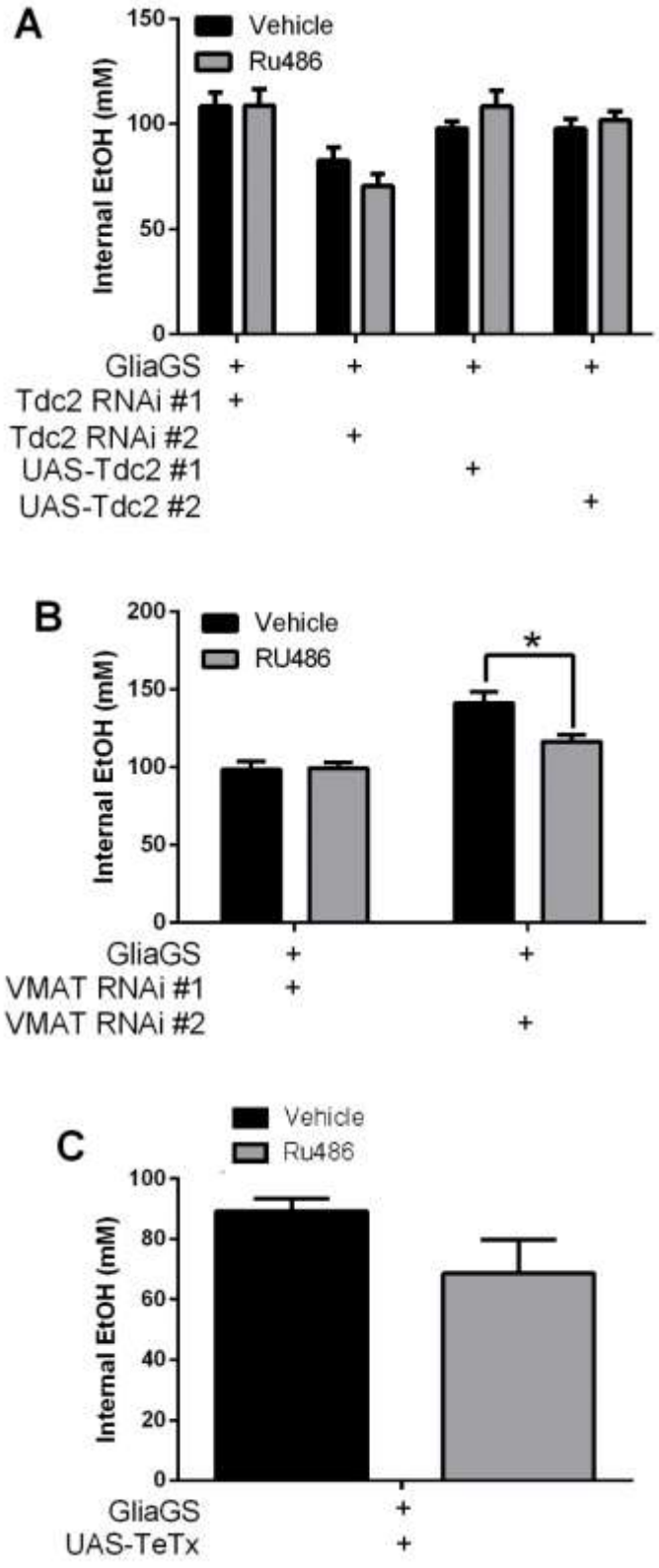
A
Vehicle
Ru486
Internal EtOH (mM)
150
100
50
0
GliaGS + + + +
Tdc2 RNAi #1 +
Tdc2 RNAi #2 +
UAS-Tdc2 #1 +
UAS-Tdc2 #2 +
B
Vehicle
RU486
*
Internal EtOH (mM)
200
150
100
50
0
GliaGS + +
VMAT RNAi #1 +
VMAT RNAi #2 +
C
Vehicle
Ru486
Internal EtOH (mM)
100
80
60
40
20
0
GliaGS +
UAS-TeTx +

Figure 5.6. Internal ethanol concentrations. (**A**) Compared to vehicle, treatment with RU486 did not alter internal ethanol levels in flies with the GliaGS driver and the *Tdc2* RNAi transgenes (GliaGS/*Tdc2* RNAi #1; GliaGS/*Tdc2* RNAi #2) or in flies with the GliaGS driver and the UAS-*Tdc2* transgenes (GliaGS/UAS-*Tdc2* #1; GliaGS/UAS-*Tdc2* #2) (two-way ANOVA; RU486, $p = 0.871$; genotype, $p < 0.0001$; interaction, $p = 0.286$; Bonferroni's multiple comparisons between vehicle and RU486, $p = 0.66$-0.9999; $n = 5$-6). (**B**) Compared to vehicle, treatment with RU486 did not alter internal ethanol levels in flies with the GliaGS driver and the *VMAT* RNAi #1 transgene (GliaGS/*VMAT* RNAi #1), but RU486 treatment decreased internal ethanol levels in flies with the GliaGS driver and the *VMAT* RNAi #2 transgene (GliaGS/*VMAT* RNAi #2) (two-way ANOVA; RU486, $p = 0.035$; genotype, $p < 0.0001$; interaction, $p = 0.022$; *Bonferroni's multiple comparisons between vehicle and RU486, $p < 0.05$; $n = 5$-6). (**C**) Compared to vehicle, treatment with RU486 did not alter internal ethanol levels in flies with the GliaGS driver and the UAS-TeTx transgene (GliaGS/UAS-TeTx) (student's t test, $p = 0.126$; $n = 5$).

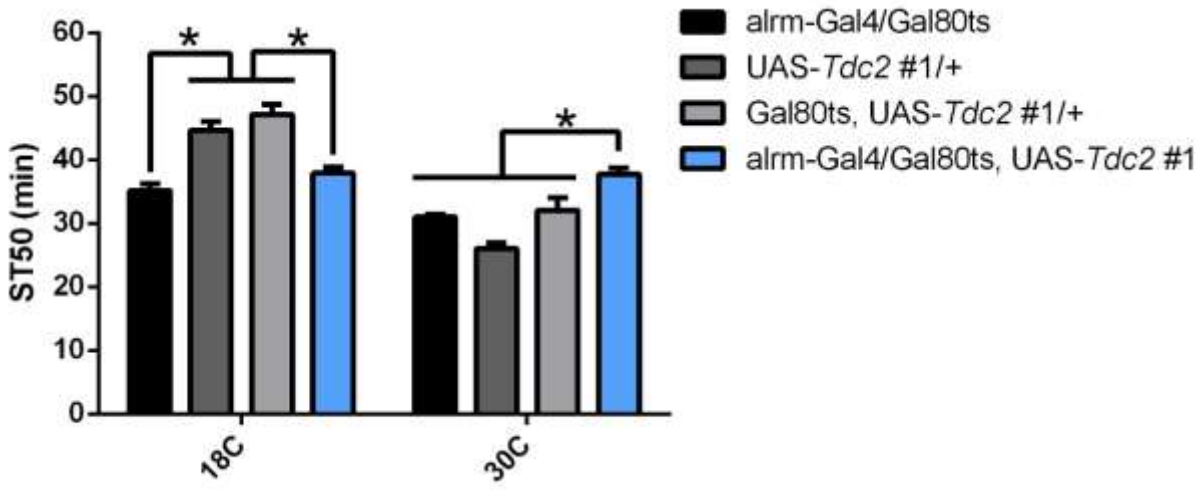

Figure 5.7. Tdc2 overexpression in astrocytes alters alcohol sedation. Gal80ts represses Gal4 in 18C and is permissive to Gal4 in 30C. Compared to controls within the same temperature treatment, exposure to 30C significantly increased ST50 values in *alrm*-Gal4/Gal80ts, UAS-*Tdc2* flies (blue bars). A second group of flies, which did not experience a temperature shift, also served as a control (labeled 18C). UAS-*Tdc2*/+ (dark grey bar) and Gal80ts, UAS-*Tdc2*/+ (light grey bar) flies had significantly increased ST50 values compared to *alrm*-Gal4/Gal80ts (black bars) and *alrm*-Gal4/Gal80ts, UAS-*Tdc2* flies (blue bars) (two-wat ANOVA; temperature, $p < 0.0001$; genotype, $p < 0.0001$; interaction, $p < 0.0001$; *Bonferroni's multiple comparisons between vehicle and RU486, $p < 0.05$; $n = 8$).

B.3 MANIPULATION OF TYRAMINE SYNTHESIS IN ASTROCYTES IMPACTS ALCOHOL SEDATION

Tyrosine is converted to tyramine by Tdc2 and to dopamine by tyrosine hydroxylase (Th). Tyramine produced by Tdc2 can be converted to octopamine by tyramine β-hydroxylase (Tbh)[262] (Fig 5.8). We postulated that manipulation of Tdc2 might influence alcohol sedation by impacting tyramine levels directly or through secondary effects on dopamine or octopamine synthesis. To test this, we targeted *Tbh* and *Th* expression in glia during adulthood using GliaGS and previously validated RNAi and UAS transgenes[109,268-272]. Induction of *Tbh* RNAi or UAS transgenes (Fig. 5.9) and induction of *Th* RNAi or UAS transgenes (Fig. 5.10) individually in all glia during adulthood did not alter ST50 values. While follow-up studies would be needed to fully rule out a role for glial Tbh and Th in alcohol sedation, our results support the hypothesis that manipulation of Tdc2 expression in glia influences alcohol sedation by altering tyramine levels.

If *Tdc2* impacts alcohol sedation through tyramine synthesis, we predicted that alcohol sedation sensitivity in *Tdc2* knockdown flies might be rescued by supplementation with dietary tyramine. In vehicle-fed (i.e. no tyramine supplementation) flies, expression of *Tdc2* RNAi in astrocytes via *alrm*-Gal4 decreased ST50 values (Fig. 5.11A, 5.11B), consistent with our previous studies (Fig. 5.1C, 5.1D). Providing flies with a diet supplemented with tyramine eliminated (Fig. 5.11A) or partially reversed (Fig. 5.11B) the effect of *Tdc2* knockdown in astrocytes on ST50 values. Collectively, the data in Figs. 5.9, 5.10 and 5.11 are consistent with a model in which tyramine produced in astrocytes by Tdc2 regulates alcohol sedation.

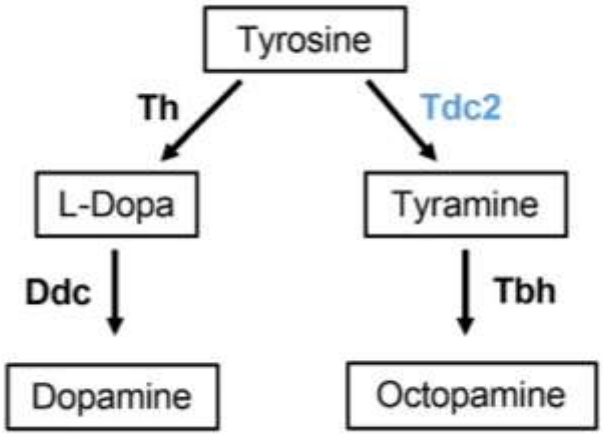

Figure 5. 8. The invertebrate catecholamine synthesis pathway. The amino acid tyrosine can be converted to L-Dopa by tyramine hydroxylase (Th, also known as pale). L-Dopa is converted to dopamine by dopamine decarboxylase (Ddc). Tyrosine can also be converted to tyramine by tyramine decarboxylase 2 (Tdc2). Tyramine can be converted to octopamine by tyramine β hydroxylase (Tbh). Adapted from Cole, 2005[262].

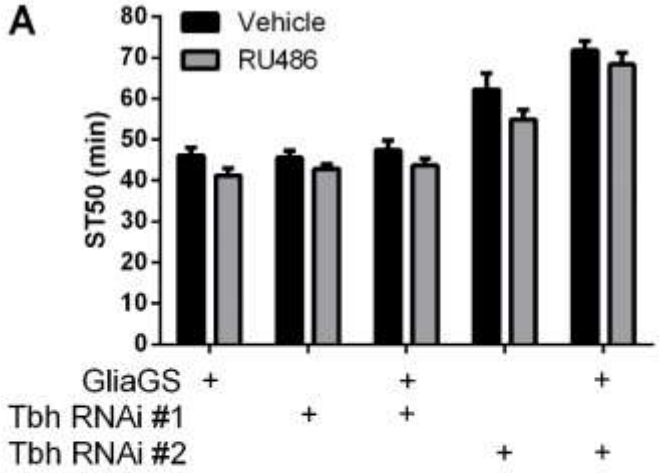
A
Vehicle
RU486
ST50 (min)
80
70
60
50
40
30
20
10
0
GliaGS + + +
Tbh RNAi #1 + +
Tbh RNAi #2 + +

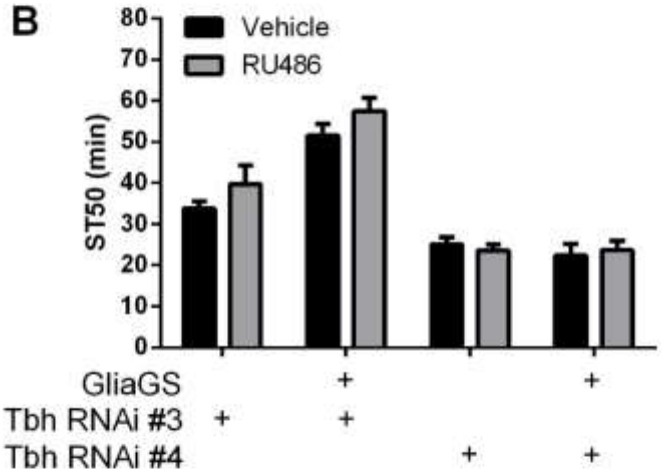
B
Vehicle
RU486
ST50 (min)
80
70
60
50
40
30
20
10
0
GliaGS + +
Tbh RNAi #3 + +
Tbh RNAi #4 + +

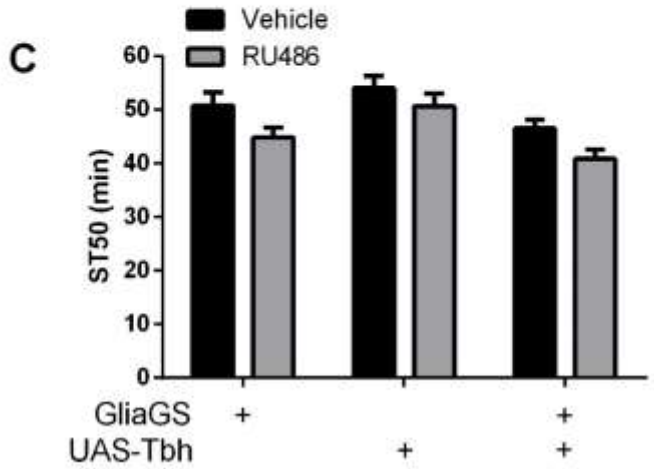
C
Vehicle
RU486
ST50 (min)
60
50
40
30
20
10
0
GliaGS + +
UAS-Tbh + +

Figure 5.9. Manipulation of Tbh in glia does not alter normal alcohol sedation. (**A, B**) Compared to vehicle, treatment with RU486 did not alter ST50 values in flies with the GliaGS driver and a *Tbh* RNAi transgene (panel A: GliaGS/*Tbh* RNAi #1, GliaGS/*Tbh* RNAi #2; panel B: GliaGS/*Tbh* RNAi #3, GliaGS/*Tbh* RNAi #4) or in control flies with either GliaGS or the *Tbh* RNAi transgene alone (Panel A: two-way ANOVA; RU486, $p = 0.003$; genotype, $p < 0.0001$; interaction, $p = 0.875$; Bonferroni's multiple comparisons between vehicle and RU486, $p = 0.15$-0.9999; $n = 8$; Panel B: two-way ANOVA; RU486, $p = 0.147$; genotype, $p < 0.0001$; interaction, $p = 0.48$; Bonferroni's multiple comparisons between vehicle and RU486, $p = 0.55$-0.9999; $n = 6$). (**C**) Compared to vehicle, treatment with RU486 did not alter ST50 values in flies with the GliaGS driver and the UAS-*Tbh* transgene (GliaGS/UAS-*Tbh*) or in control flies with either GliaGS or the UAS-*Tbh* transgene alone (two-way ANOVA; RU486, $p = 0.005$; genotype, $p = 0.0009$; interaction, $p = 0.81$; Bonferroni's multiple comparisons between vehicle and RU486, $p = 0.16$-0.77; $n = 8$).

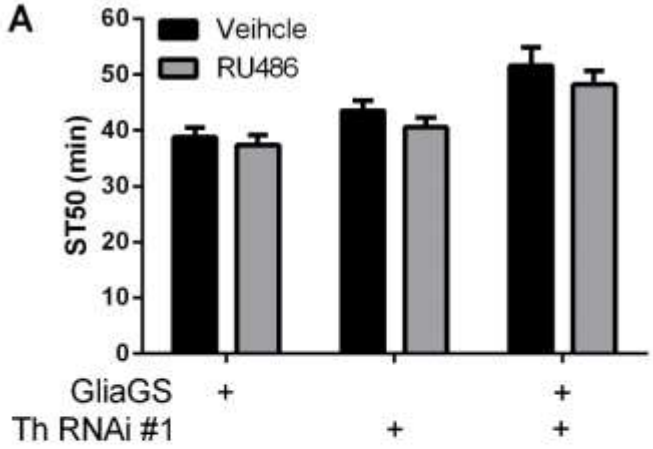
A
Veihcle
RU486
ST50 (min)
60
50
40
30
20
10
0
GliaGS + +
Th RNAi #1 + +

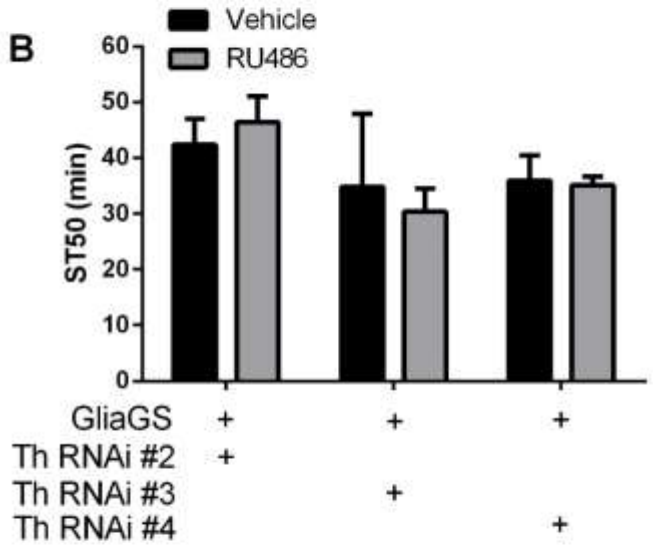
B
Vehicle
RU486
ST50 (min)
60
50
40
30
20
10
0
GliaGS + + +
Th RNAi #2 +
Th RNAi #3 +
Th RNAi #4 +

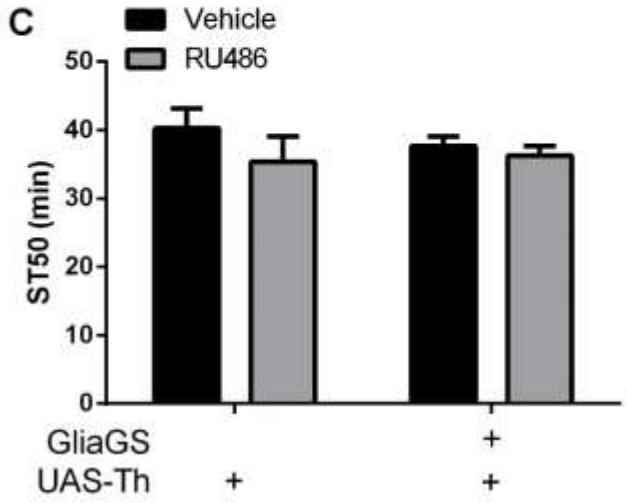
C
Vehicle
RU486
ST50 (min)
50
40
30
20
10
0
GliaGS +
UAS-Th + +

Figure 5.10. Manipulation of Th in glia does not alter alcohol sedation. (**A, B**) Compared to vehicle, treatment with RU486 did not alter ST50 values in flies with the GliaGS driver and a *Th* RNAi transgene (panel A: GliaGS/*Th* RNAi #1; panel B: GliaGS/*Th* RNAi #2, GliaGS/*Th* RNAi #3, GliaGS/*Th* RNAi #4) or in control flies with either GliaGS or the *Th* RNAi transgene alone (Panel A: two-way ANOVA; RU486, $p = 0.16$; genotype, $p < 0.0001$; interaction, $p = 0.902$; Bonferroni's multiple comparisons between vehicle and RU486, $p = 0.86$-0.9999; $n = 8$; Panel B: two-way ANOVA; RU486, $p = 0.885$; genotype, $p = 0.007$; interaction, $p = 0.503$; Bonferroni's multiple comparisons between vehicle and RU486, $p > 0.9999$; $n = 6$). (**C**) Compared to vehicle, treatment with RU486 did not alter ST50 values in flies with the GliaGS driver and the UAS-*Th* transgene (GliaGS/UAS-*Th*) or in control flies with either GliaGS or the UAS-*Th* transgene alone (two-way ANOVA; RU486, $p = 0.23$; genotype, $p = 0.749$; interaction, $p = 0.504$; $n = 6$).

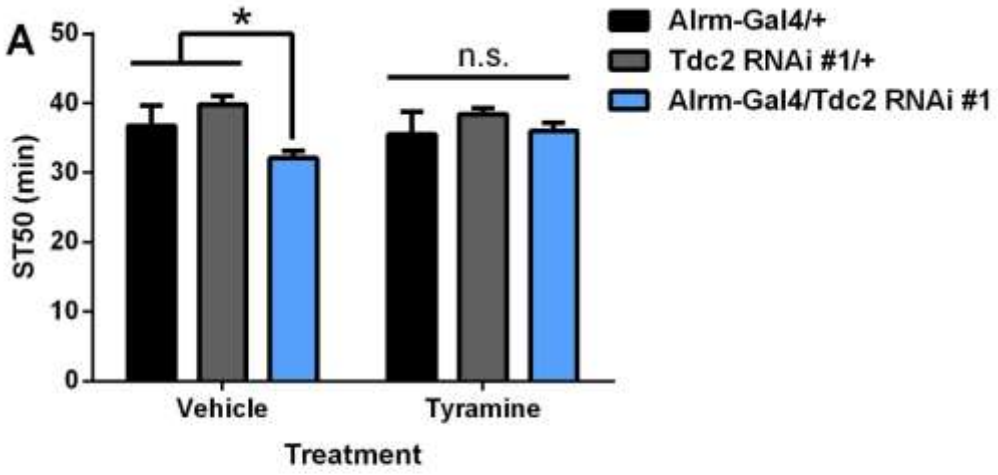
A
*
n.s.
Alrm-Gal4/+
Tdc2 RNAi #1/+
Alrm-Gal4/Tdc2 RNAi #1
ST50 (min)
50
40
30
20
10
0
Vehicle
Tyramine
Treatment

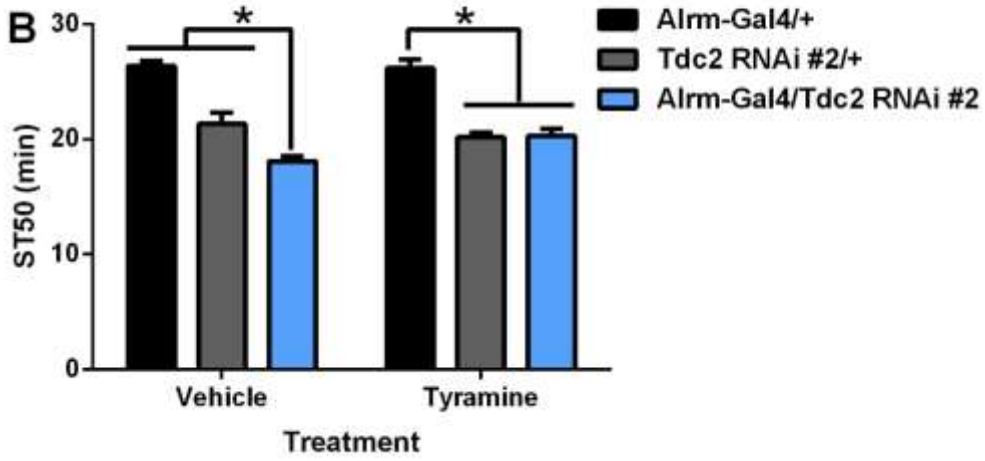
B
*
*
Alrm-Gal4/+
Tdc2 RNAi #2/+
Alrm-Gal4/Tdc2 RNAi #2
ST50 (min)
30
20
10
0
Vehicle
Tyramine
Treatment

Figure 5.11. Tyramine feeding rescues Tdc2 RNAi-associated alcohol sedation sensitivity. (**A**) ST50 values were decreased in vehicle-fed flies expressing the astrocyte specific driver *alrm*-Gal4 and the *Tdc2* RNAi #1 transgene (blue bar: *alrm*-Gal4/*Tdc2* RNAi #1) compared to vehicle-fed control flies containing either the astrocyte Gal4 driver (black bar: *arlm*-Gal4) or the RNAi transgene (grey bar: *Tdc2* RNAi #1/+) alone. ST50 values were not different in tyramine-fed flies expressing *alrm*-Gal4 and *Tdc2* RNAi transgene #1 (blue bar: *alrm*-Gal4/*Tdc2* RNAi #1) compared to tyramine-fed control flies containing either the astrocyte Gal4 driver (black bar: *arlm*-Gal4) or the *Tdc2* RNAi transgene alone (grey bar: *Tdc2* RNAi #1/+) (two-way ANOVA; tyramine treatment, $p = 0.77$; genotype, $p = 0.029$; interaction, $p = 0.28$; *Bonferroni's multiple comparisons within treatments, $p < 0.05$; n = 14-16). (**B**) ST50 values were decreased in vehicle-fed flies expressing the astrocyte specific driver *alrm*-Gal4 and the *Tdc2* RNAi #2 transgene (blue bar: *alrm*-Gal4/*Tdc2* RNAi #2) compared to vehicle-fed control flies containing either the astrocyte Gal4 driver (black bar: *arlm*-Gal4) or the RNAi transgene (grey bar: *Tdc2* RNAi #2/+) alone. ST50 values were not different in tyramine-fed flies expressing *alrm*-Gal4 and the *Tdc2* RNAi transgene #2 (blue bar: *alrm*-Gal4/*Tdc2* RNAi #2) compared to tyramine-fed control flies containing the *Tdc2* RNAi transgene alone (grey bar: *Tdc2* RNAi #2/+). ST50 values were higher in tyramine-fed control flies with the astrocyte Gal4 driver alone (black bar: *alrm*-Gal4/+) compared to tyramine-fed flies containing the *Tdc2* RNAi transgene alone (grey bar: *Tdc2* RNAi #2/+) and flies containing both *alrm*-Gal4 and *Tdc2* RNAi transgene (blue bar: *alrm*-Gal4/*Tdc2* RNAi #2) (two-way ANOVA; tyramine treatment, $p = 0.57$; genotype, $p < 0.0001$; interaction, $p = 0.02$; *Bonferroni's multiple comparisons within treatments, $p < 0.05$; n = 8).

B.4 ALCOHOL SEDATION IS INFLUENCED BY VESICULAR PACKAGING AND RELEASE MACHINERY IN GLIA

In fly neurons, tyramine is released into the synapse through vesicular exocytosis and then functions as a neurotransmitter[27,267,273]. If tyramine production in glia mediates alcohol sedation, we predicted that manipulating the vesicular packaging machinery might have the same effect on alcohol sedation as *Tdc2* knockdown. We therefore assessed whether the vesicular monoamine transporter (VMAT) in glia regulates alcohol sedation because this transporter (i) packages monoamines, including tyramine, into vesicles in neurons[274], (ii) is expressed in mammalian astrocytes[76] and (iii) is expressed in fly glia[275,276]. Constitutive expression of two unique *VMAT* RNAi transgenes individually in all glia via *repo*-Gal4 significantly decreased ST50 (Fig. 5.12A, 5.12B). Similarly, flies expressing *VMAT* RNAi in astrocytes (via *alrm*-Gal4) had significantly decreased ST50s compared to controls (Fig. 5.12C, 5.12D). RU486-induced expression of *VMAT* RNAi in all glia during adulthood significantly decreased ST50s, whereas treatment with RU486 had no effect in control genotypes (Fig. 5.12E, 5.12F). Internal alcohol levels were not consistently altered by expression of *VMAT* RNAi transgenes (Fig. 5.6B), indicating that that VMAT is mediating alcohol sedation through a pharmacodynamic mechanism. Expression of the RNAi transgenes used in these experiments in neurons significantly decreased the detection of VMAT in whole fly brains (Fig 5.13), indicating that the transgenes are capable of knocking down VMAT expression. Thus, knocking down Tdc2 (Figs. 5.1 and 5.5) and VMAT (Fig. 5.12), using three different expression strategies targeting all glia, astrocytes or adult glia, have similar effects on alcohol sedation.

Given that manipulation of *Tdc2* and *VMAT* in glia produced similar changes in alcohol sedation, we postulated that they might function in the same pathway. To address this possibility, we assessed alcohol sedation in flies with *Tdc2* over-expressed and *VMAT* knocked down using three approaches: pan-glial expression via *repo*-Gal4, astrocyte-specific expression using *alrm*-Gal4, and adult-induced expression in all glia using GliaGS. Over-expression of *Tdc2* in all glia and in astrocytes was lethal (missing bars in Fig. 5.14A, 5.14B). Expression of *VMAT* RNAi in all glia (Fig. 5.14A) or in astrocytes (Fig. 5.14B) significantly decreased ST50 values as described above (Fig. 5.12). Interestingly, expression of only the *VMAT* RNAi, and not a UAS-GFP transgene, suppressed the lethality associated with *Tdc2* over-expression (quantified for *repo*-Gal4 in Table 5.3). More importantly, the ST50 values in flies over-expressing *Tdc2* in conjunction with the *VMAT* RNAi were statistically indistinguishable from flies expressing only *VMAT* RNAi (Fig. 5.14A, all glia; Fig. 5.14B, astrocytes). Similarly, RU486-induced over-expression of *Tdc2* during adulthood increased ST50 values, expression of *VMAT* RNAi decreased ST50 values, and flies with concomitant over-expression of *Tdc2* and *VMAT* RNAi had decreased ST50s that were comparable to ST50s in flies expressing only *VMAT* RNAi (Fig. 5.14C). Taken together, these data strongly support a model in which knockdown of *VMAT* is epistatic to over-expression of *Tdc2*, thereby placing VMAT biochemically downstream of Tdc2 and suggesting that alcohol sedation might be influenced by tyramine packaging into vesicles within glia.

Synaptic vesicles loaded with transmitters dock to the plasma membrane prior to releasing their contents into the synapse[102]. This process is, in part, mediated by the SNARE complex in both glia and neurons[102,252,277]. We therefore reasoned that the

SNARE complex in glia might be required for normal alcohol sedation and that this complex might function downstream of Tdc2. We used two expression strategies to test these possibilities: constitutive expression in astrocytes via *alrm*-Gal4 and RU486-induced expression in glia during adulthood via GliaGS. Additionally, we used tetanus toxin, which cleaves synaptobrevin, to inhibit the SNARE complex and block synaptic transmission[278]. Expression of tetanus toxin (UAS-TeTx) in astrocytes (Fig. 5.15A) and adult glia (Fig. 5.15B) decreased ST50 values. Internal ethanol levels were not altered by expressing UAS-TeTx in glia during adulthood (Fig. 5.6C), suggesting that the SNARE complex in glia influences alcohol sedation through a pharmacodynamic mechanism. However, ST50 was not altered when RNAi expression for individual components of vesicular release machinery was induced in glia during adulthood (Table 5.4). While surprising, this may suggest that compensatory mechanisms occur in response to the RNAi expression to keep vesicular exocytosis in glia occurring. Nonetheless, the effect of expressing the tetanus toxin in astrocytes and in adult glia was similar to that of knocking down *Tdc2* (Figs. 5.1, 5.5), suggesting that the SNARE complex might function in the same pathway as *Tdc2*. To formally address this possibility, we assessed alcohol sedation in flies with *Tdc2* over-expression and tetanus toxin expression. Expression of tetanus toxin in astrocytes suppressed the lethality due to *Tdc2* over-expression and these flies had significantly decreased ST50s. Additionally, the ST50 value of these flies was indistinguishable from flies that expressed tetanus toxin alone in astrocytes (Fig. 5.15C). Similarly, RU486-induced over-expression of *Tdc2* in adult glia increased ST50s, expression of tetanus toxin decreased ST50s, and flies with concomitant over-expression of *Tdc2* and expression of tetanus toxin had

decreased ST50s that were indistinguishable from that of flies expressing tetanus toxin alone (Fig. 5.15D). Taken together, these data strongly support a role for the SNARE complex regulating alcohol sedation by functioning within astrocytes and adult glia. Additionally, these data argue that SNARE-dependent vesicle-mediated release is functionally downstream of Tdc2 in glia within the context of alcohol sedation.

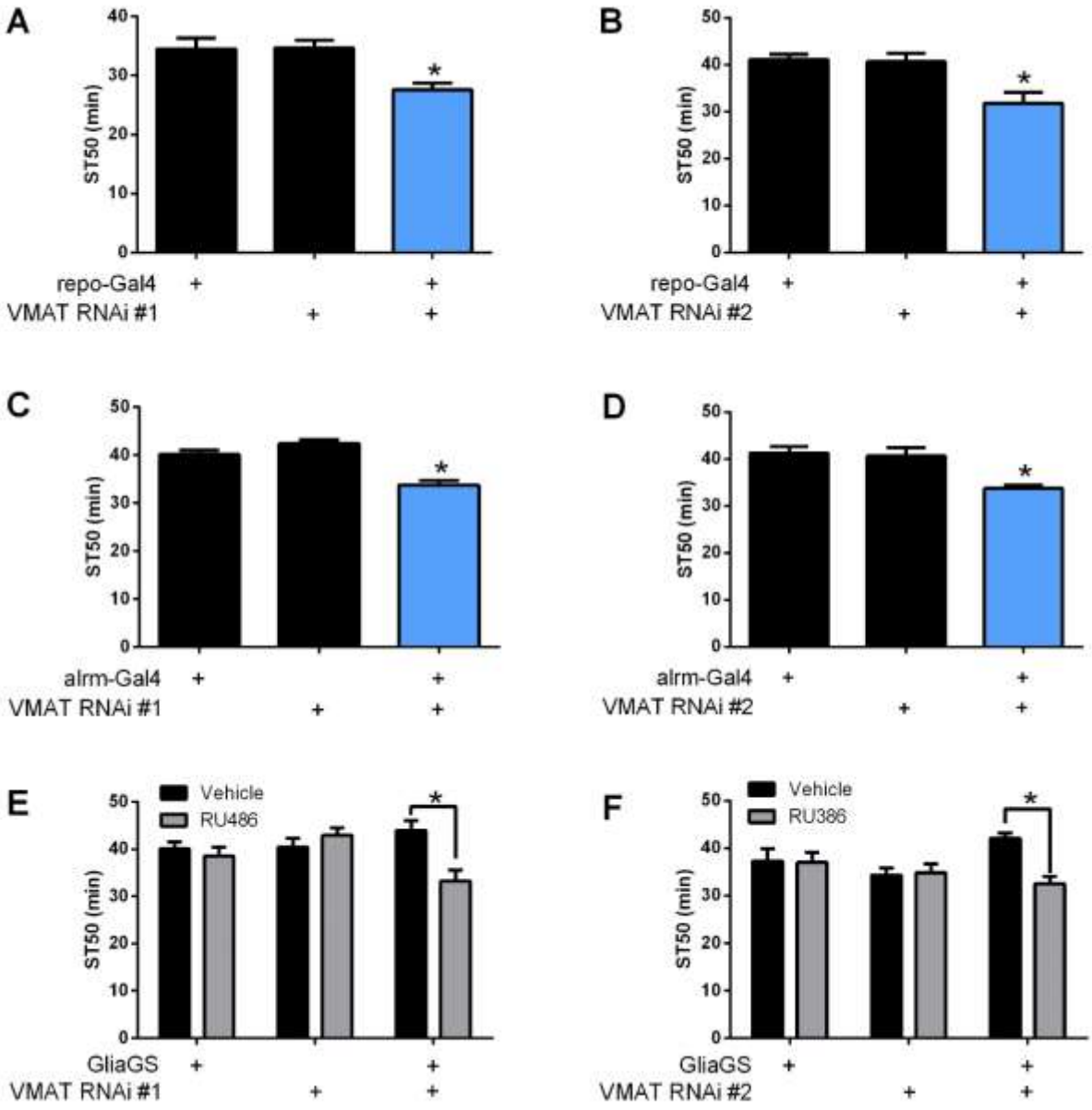
A
ST50 (min)
repo-Gal4
VMAT RNAi #1
B
ST50 (min)
repo-Gal4
VMAT RNAi #2
C
ST50 (min)
alrm-Gal4
VMAT RNAi #1
D
ST50 (min)
alrm-Gal4
VMAT RNAi #2
E
Vehicle
RU486
ST50 (min)
GliaGS
VMAT RNAi #1
F
Vehicle
RU386
ST50 (min)
GliaGS
VMAT RNAi #2

Figure 5.12. VMAT expression in glia is required for normal alcohol sedation. (**A, B**) ST50 values were reduced in flies with the pan-glial driver *repo*-Gal4 and a *VMAT* RNAi transgene (blue bars: *repo*-Gal4/*VMAT* RNAi #1, panel A; *repo*-Gal4/*VMAT* RNAi #2, panel B) compared to control flies with either *repo*-Gal4 alone (black bars: *repo*-Gal4/+) or the respective RNAi transgene alone (black bars: *VMAT* RNAi #1/+ and *VMAT* RNAi #2/+) (Panel A: one-way ANOVA, $p = 0.003$; *Bonferroni's multiple comparison vs controls, $p < 0.05$; $n = 8$; Panel B: one-way ANOVA, $p = 0.002$; *Bonferroni's multiple comparison vs controls, $p < 0.05$; $n = 8$). (**C, D**) ST50 values were decreased in flies expressing the astrocyte-specific driver *alrm*-Gal4 and a *VMAT* RNAi transgene (blue bars: *alrm*-Gal4/*VMAT* RNAi #1, panel C; *alrm*-Gal4/*VMAT* RNAi #2, panel D) compared to control flies containing either the astrocyte Gal4 driver (black bars: *arlm*-Gal4) or the respective RNAi transgene (black bars: *VMAT* RNAi #1/+, panel C; *VMAT* RNAi #2, panel D) alone (Panel C: one-way ANOVA, $p < 0.001$; *Bonferroni's multiple comparison vs controls, $p < 0.05$; $n = 8$; Panel D: one-way ANOVA, $p = 0.0001$; *Bonferroni's multiple comparison vs controls, $p < 0.05$; $n = 8$). (**E, F**) Compared to vehicle, treatment with RU486 decreased ST50 values in flies with the GliaGS driver and a *VMAT* RNAi transgene (GliaGS/*VMAT* RNAi #1, panel E; GliaGS/*VMAT* RNAi #2, panel F), but not in control flies with either GliaGS or the respective RNAi transgene alone (Panel E: two-way ANOVA; RU486, $p = 0.04$; genotype, $p = 0.23$; interaction, $p = 0.003$; *Bonferroni's multiple comparisons between vehicle and RU486, $p < 0.05$; $n = 8$; Panel F: two-way ANOVA; RU486, $p = 0.051$; genotype, $p = 0.284$; interaction, $p = 0.018$; *Bonferroni's multiple comparisons between vehicle and RU486, $p < 0.05$; $n = 8$).

A. VMAT RNAi #1/+

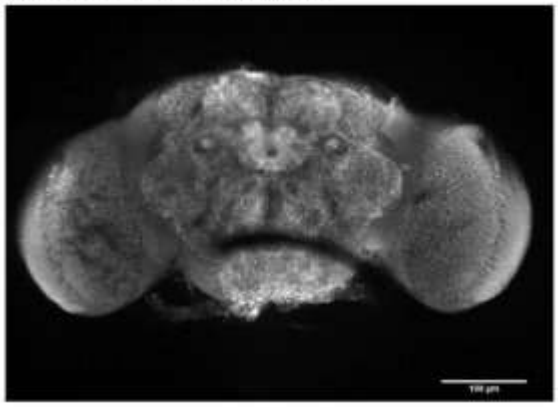

B. VMAT RNAi #2/+

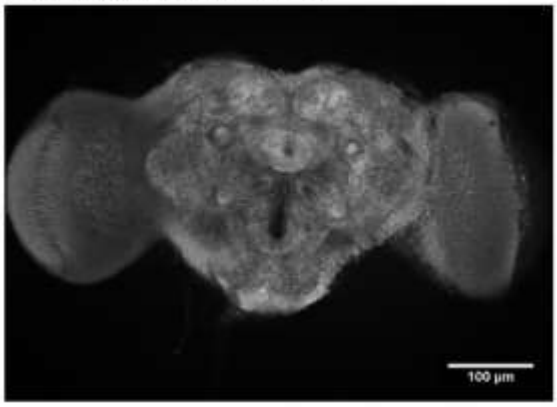

C. elav-Gal4/VMAT RNAi #1

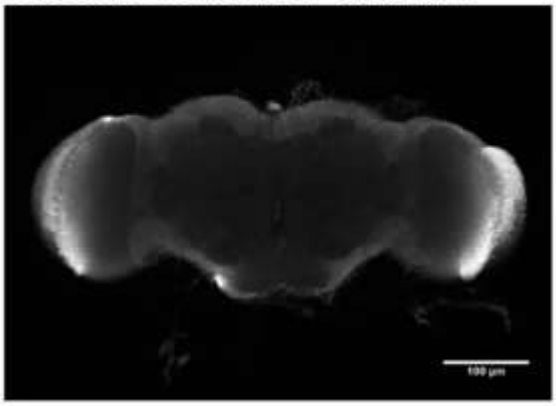

D. elav-Gal4/VMAT RNAi #2

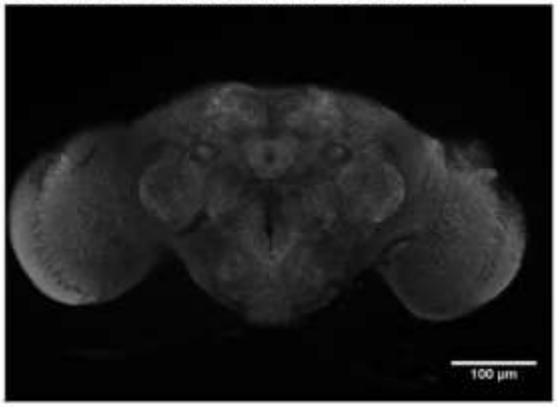

E

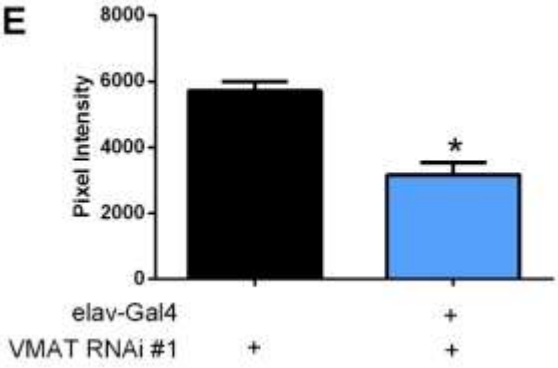

F

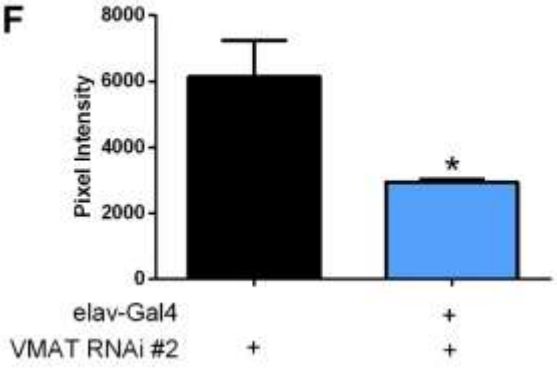

Figure 5.13. VMAT RNAi knocks down VMAT expression. Whole mount brain images immunolabeled for VMAT expression (anti-VMAT 1:2000, Alexa-647 1:1000). All representative images, 10X. (**A, B**) VMAT expression in brains of flies with a *VMAT* RNAi transgene alone. (**C, D**) VMAT expression in brains of flies with the pan-neuronal driver *elav*-Gal4 and a *VMAT* RNAi. (**E, F**) Brains with both the *elav*-Gal4 and a *VMAT* RNAi transgene had significantly lower pixel intensity compared to control brains of flies with the *VMAT* RNAi transgene alone (Panel E: students t test, $p = 0.0005$, $n = 5\text{-}6$; Panel F: students t test, $p = 0.0448$, $n = 4$).

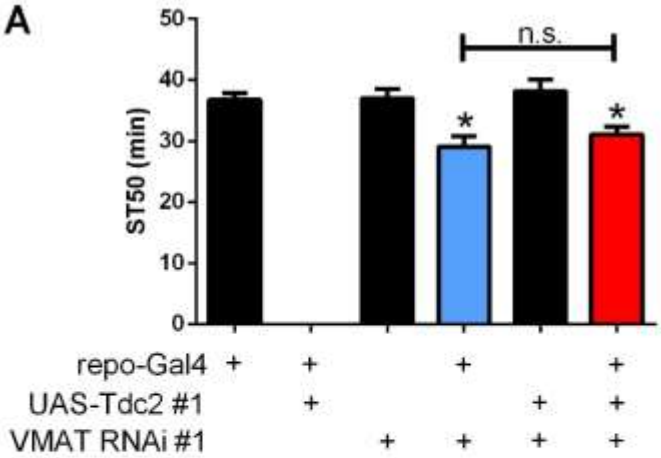
A
ST50 (min)
50
40
30
20
10
0
n.s.
*
*
repo-Gal4 + + + +
UAS-Tdc2 #1 + + +
VMAT RNAi #1 + + + +

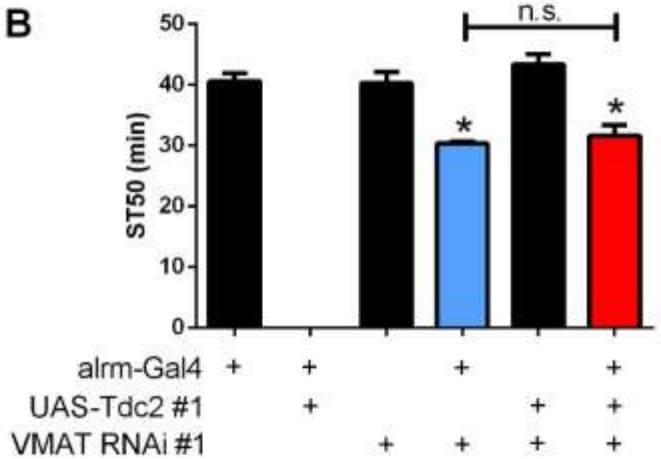
B
ST50 (min)
50
40
30
20
10
0
n.s.
*
*
alrm-Gal4 + + + +
UAS-Tdc2 #1 + + +
VMAT RNAi #1 + + + +

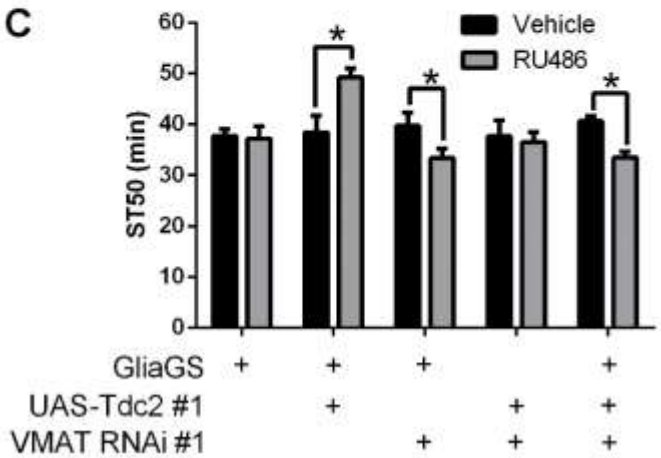
C
ST50 (min)
60
50
40
30
20
10
0
Vehicle
RU486
*
*
*
GliaGS + + + +
UAS-Tdc2 #1 + + +
VMAT RNAi #1 + + +

Figure 5.14. VMAT functions downstream of Tdc2. (**A**) ST50 values were decreased in flies with the pan-glial driver *repo*-Gal4 and a *VMAT* RNAi transgene (blue bar: *repo*-Gal4/*VMAT* RNAi #1) and in flies with *repo*-Gal4, the *VMAT* RNAi and the UAS-*Tdc2* transgenes (red bar: *repo*-Gal4/*VMAT* RNAi #1; UAS-*Tdc2* #1) compared to control flies (black bars). ST50 values were not different between flies with the *repo*-Gal4 and the *VMAT* RNAi transgenes (blue bar: *repo*-Gal4/*VMAT* RNAi #1) and flies with the *repo*-Gal4, the *VMAT* RNAi and the UAS-*Tdc2* transgenes (red bar: *repo*-Gal4/*VMAT* RNAi #1; UAS-*Tdc2* #1) (one-way ANOVA, $p = 0.003$; *Bonferroni's multiple comparison vs controls, $p < 0.05$; $n = 8$). Flies with both the pan-glial driver *repo*-Gal4 and the UAS-*Tdc2* transgene did not emerge as adults (no bar: *repo*-Gal4/UAS-*Tdc2* #1). (**B**) ST50 values were decreased in flies with the astrocyte-specific driver *alrm*-Gal4 and the *VMAT* RNAi transgene (blue bar: *alrm*-Gal4/*VMAT* RNAi #1) and in flies with *alrm*-Gal4, the *VMAT* RNAi transgene and the UAS-*Tdc2* transgene (red bar: *alrm*-Gal4/*VMAT* RNAi #1; UAS-*Tdc2* #1) compared to control flies (black bars). ST50 values were not different between flies with the *alrm*-Gal4 and the *VMAT* RNAi transgenes (blue bar: *alrm*-Gal4/*VMAT* RNAi #1) and flies with the *alrm*-Gal4, the *VMAT* RNAi and the UAS-*Tdc2* transgenes (red bar: *alrm*-Gal4/*VMAT* RNAi #1; UAS-*Tdc2* #1) (one-way ANOVA, $p < 0.0001$; *Bonferroni's multiple comparison vs controls, $p < 0.05$; $n = 8$). Flies expressing both *alrm*-Gal4 and UAS-*Tdc2* transgenes did not emerge as adults (no bar: *alrm*-Gal4/UAS-*Tdc2* #1). (**C**) Compared to vehicle, treatment with RU486 increased ST50 values in flies with the GliaGS driver and a UAS-*Tdc2* transgene (GliaGS/UAS-*Tdc2* #1), decreased ST50 values in flies with the GliaGS driver and a *VMAT* RNAi transgene (GliaGS/*VMAT* RNAi #1) and decreased ST50 values in flies with the GliaGS driver, a *VMAT* RNAi transgene and a UAS-*Tdc2* transgene (GliaGS/*VMAT* RNAi #1; UAS-*Tdc2* #1). Treatment with RU486 did not alter ST50 in control flies with GliaGS alone (GliaGS/+) or both the *VMAT* RNAi and the UAS-*Tdc2* transgenes (*VMAT* RNAi #1; UAS-*Tdc2* #1/+) compared to controls (two-way ANOVA; RU486, $p = 0.543$; genotype, $p = 0.006$; interaction, $p = 0.0007$; *Bonferroni's multiple comparisons between vehicle and RU486, $p < 0.05$; $n = 8$).

Table 5.3. Lethality associated with UAS-Tdc2 expression in glia

Group	Cross	Progeny Genotype	Observed n	Observed Genotype Percentage	Group Compared to	Expected n	Chi-Square	Significance
A	repo-Gal4 X wA	TM3SB/+	260	34%	n/a	n/a	n/a	n/a
		repo-Gal4/+	504	66%				
B	repo-Gal4 X VMAT RNAi	TM3SB/+	318	38%	A	283	3.19	p = 0.074
		repo-Gal4/VMAT RNAi	513	62%		548		
C	repo-Gal4 X UAS-Tdc2	TM3SB/+	1072	100%	A	365	1054	p < 0.0001
		repo-Gal4/UAS-Tdc2	0	0%		704		
D	repo-Gal4 X UAS-Tdc2;VMAT RNAi	TM3SB/+	356	40%	C	886	753.175	p < 0.0001
		repo-Gal4/UAS-Tdc2;VMAT RNAi	530	60%		0		
E	repo-Gal4; GFP X UAS-Tdc2	TM3SB/+	864	100%	C	864	0	p = 1
		repo-Gal4; GFP/UAS-Tdc2	0	0%		0		

Progeny from the indicated crosses were counted and recorded as the “observed n”. The “observed genotype percentage” was calculated by dividing the number of flies of each genotype by the total number of flies from the indicated cross. The “expected n” was used for the comparison between that group (observed) and the group indicated in the “Group Compared to” column (expected). It was calculated by multiplying the total number of progeny by the expected percentage of the genotype from the cross being compared to. The chi-square statistic compared the “expected n” and the “observed n” to determine if they were different. All chi-square values and their associated p-values are reported (df = 3). Driving VMAT RNAi with *repo*-Gal4 (Group B) did not impact lethality, whereas expression of Tdc2 (Group C) was 100% lethal. Expression of VMAT RNAi significantly suppressed the lethality due to Tdc2 expression (Group D). Expression of UAS-GFP did not suppress the lethality due to Tdc2 expression (Group E)

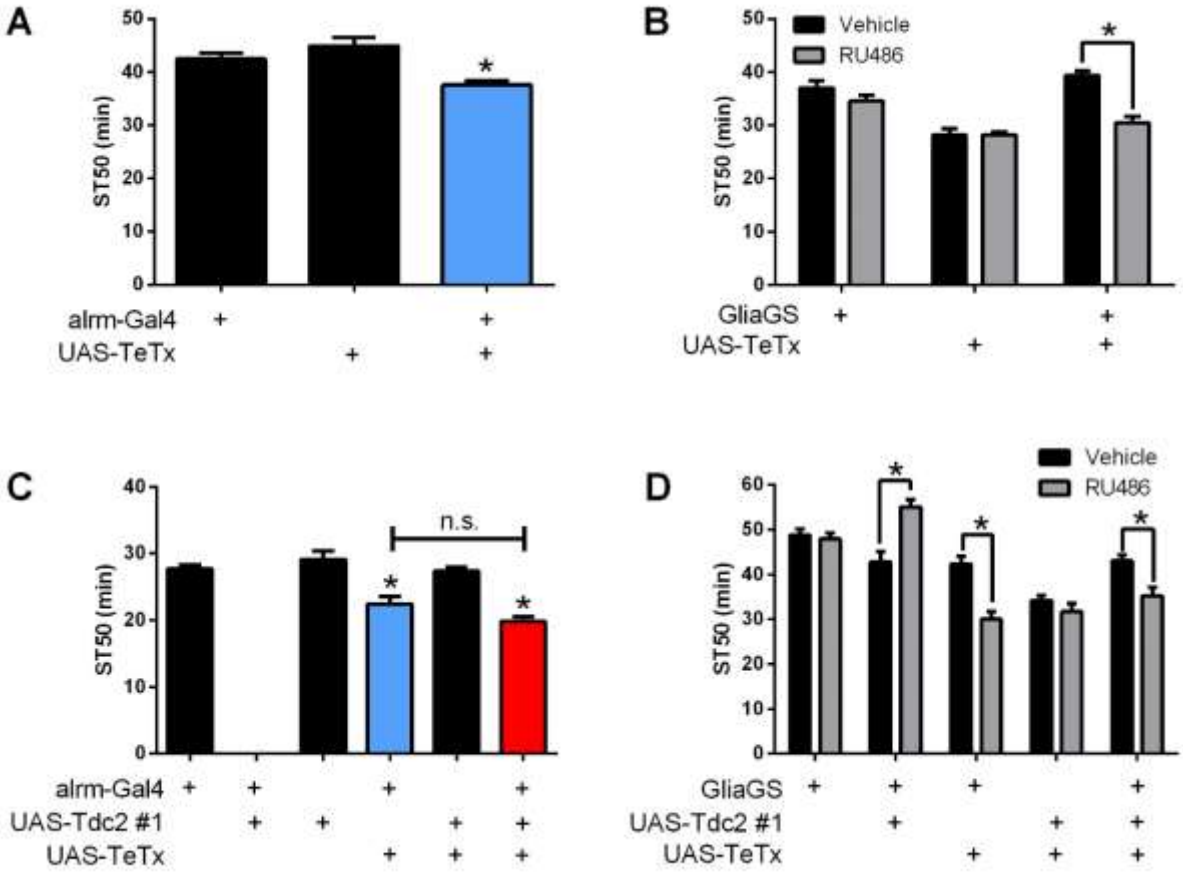
A
ST50 (min)
50
40
30
20
10
0
*
alrm-Gal4 + +
UAS-TeTx + +
B
Vehicle
RU486
ST50 (min)
*
GliaGS + +
UAS-TeTx + +
C
ST50 (min)
n.s.
*
*
alrm-Gal4 + + + +
UAS-Tdc2 #1 + + + +
UAS-TeTx + + +
D
Vehicle
RU486
ST50 (min)
*
*
*
GliaGS + + + +
UAS-Tdc2 #1 + + +
UAS-TeTx + + +

Figure 5.15. Expression of tetanus toxin in glia alters alcohol sedation and is epistatic to of Tdc2. (**A**) ST50 values were decreased in flies expressing the astrocyte-specific driver *alrm*-Gal4 and the UAS-TeTx transgene (blue bar: *alrm*-Gal4/UAS-TeTx) compared to control flies containing either the astrocyte Gal4 driver (black bar: *arlm*-Gal4/+) or the UAS-TeTx transgene (black bar: UAS-TeTx/+) alone (one-way ANOVA, $p = 0.0004$; *Bonferroni's multiple comparison vs controls, $p < 0.05$; $n = 15$-16). (**B**) Compared to vehicle, treatment with RU486 decreased ST50 values in flies with the GliaGS driver and the UAS-TeTx transgene (GliaGS/UAS-TeTx), but not in control flies with either GliaGS or the UAS-TeTx transgene alone (two-way ANOVA; RU486, $p = 0.0002$; genotype, $p < 0.0001$; interaction, $p = 0.0009$; *Bonferroni's multiple comparisons between vehicle and RU486, $p < 0.05$; $n = 8$) (**C**) ST50 values were decreased in flies with the astrocyte-specific driver *alrm*-Gal4 and the UAS-TeTx transgene (blue bar: *alrm*-Gal4/UAS-TeTx) and in flies with *alrm*-Gal4, the UAS-TeTx transgene and the UAS-*Tdc2* transgene (red bar: *alrm*-Gal4/UAS-TeTx; UAS-*Tdc2* #1) compared to control flies (black bars). ST50 values were not different between flies containing the *alrm*-Gal4 and the UAS-TeTx transgenes (blue bar: *alrm*-Gal4/UAS-TeTx) and flies containing the *alrm*-Gal4, the UAS-TeTx and the UAS-*Tdc2* transgenes (red bar: *alrm*-Gal4/UAS-TeTx; UAS-*Tdc2* #1) (one-way ANOVA, $p < 0.0001$; *Bonferroni's multiple comparison vs controls, $p < 0.05$; $n = 8$). Flies expressing both *alrm*-Gal4 and UAS-*Tdc2* transgenes did not emerge as adults (no bar: *alrm*-Gal4/UAS-*Tdc2* #1). (**D**) Compared to vehicle, treatment with RU486 increased ST50 values in flies with the GliaGS driver and a UAS-*Tdc2* transgene (GliaGS/UAS-*Tdc2* #1), decreased ST50 values in flies with the GliaGS driver and the UAS-TeTx transgene (GliaGS/UAS-TeTx) and decreased ST50 values in flies with the GliaGS driver, the UAS-TeTx transgene and a UAS-*Tdc2* transgene (GliaGS/UAS-TeTx; UAS-*Tdc2* #1). Compared to vehicle, treatment with RU486 did not alter ST50 in control flies with GliaGS alone (GliaGS/+) or both the UAS-TeTx and the UAS-*Tdc2* transgenes (UAS-TeTx; UAS-*Tdc2* #1/+) (two-way ANOVA; RU486, $p = 0.036$; genotype, $p < 0.0001$; interaction, $p < 0.0001$; *Bonferroni's multiple comparisons between vehicle and RU486, $p < 0.05$; $n = 6$-8).

Table 5.4. Expressing RNAi against individual components of the vesicular release machinery in adult glia does not alter alcohol sedation

Gene	reagent (identifier)	Drug Treatment	ST50	two-way ANOVA	Bonferonni mult. comparisons (to Gal4/RNAi)
syt1	RNAi (31289)[@]	Vehicle	31.62	[@]Interaction, F (1, 20) = 0.27, p = 0.61; Genotype, F (1, 20) = 15.22, p = 0.0009; Drug treatment, F (1, 20) = 0.009, p = 0.92	p > 0.9999
		RU486	30.56		
	RNAi (v100608)[@]	Vehicle	37.36		p > 0.9999
		RU486	38.08		
SNAP25	RNAi (27306)[#]	Vehicle	37.75	[#]Interaction, F (1, 20) = 0.35, p = 0.56; Genotype, F (1, 20) = 18.96, p = 0.0003; Drug treatment, F (1, 20) = 0.09, p = 0.76	p > 0.9999
		RU486	35.37		
	RNAi (34377)[#]	Vehicle	47.6		p > 0.9999
		RU486	48.35		
syx1	RNAi (25811)[$]	Vehicle	31.28	[$]Interaction, F (1, 20) = 0.34, p = 0.57; Genotype, F (1, 20) = 0.91, p = 0.35; Drug treatment, F (1, 20) = 0.69, p = 0.42	n/a
		RU486	30.82		
	RNAi (v33112)[$]	Vehicle	30.58		n/a
		RU486	27.93		
Syb	RNAi (38234)[%]	Vehicle	49.68	[%]Interaction, F (2, 27) = 0.01, p = 0.98; Genotype, F (2, 27) = 2.05, p = 0.15; Drug treatment, F (1, 27) = 0.06, p = 0.8	n/a
		RU486	48.66		
	RNAi (44014)[%]	Vehicle	46.7		n/a
		RU486	46.66		
Rob	RNAi (28929)%	Vehicle	41.7		n/a
		RU486	40.26		
ykt6	RNAi (51925)[&]	Vehicle	29.35	[&]Interaction, F (1, 14) = 0.36, p = 0.55; Genotype, F (1, 14) = 35.52, p < 0.0001; Drug treatment, F (1, 14) = 1.589, p = 0.23	p = 0.59
		RU486	27.53		
	RNAi (50937)[&]	Vehicle	23.2		p > 0.9999
		RU486	22.56		
snapin	RNAi (38314)[~]	Vehicle	22.72	[~]Interaction, F (1, 20) = 0.58, p = 0.45; Genotype, F (1, 20) = 0.68, p = 0.68; Drug treatment, F (1, 20) = 0.87, p = 0.36	n/a
		RU486	20.73		
	RNAi (40837)[~]	Vehicle	21.33		n/a
		RU486	21.13		
ykt6	RNAi (v19329)[+]	Vehicle	43.36	[+]Interaction, F (2, 28) = 0.04, p = 0.96; Genotype, F (2, 28) = 6.34, p = 0.005; Drug treatment, F (1, 28) = 1.13, p = 0.29	p > 0.9999
		RU486	39.94		
	RNAi (v105648)[+]	Vehicle	53.13		p > 0.9999
		RU486	51.42		
syt4	RNAi (26730)[+]	Vehicle	51.25		p > 0.9999
		RU486	48.46		
	RNAi (v33317)[+]	Vehicle	44.72	[=]Interaction, F (1, 19) = 2.088, p = 0.16; Genotype, F (1, 19) = 9.72, p = 0.006; Drug treatment, F (1, 19) = 1.09, p = 0.31	p = 0.17
		RU486	38.02		
syb	RNAi (39067)[=]	Vehicle	32.44		p > 0.9999
		RU486	33.51		

Manipulations were made in all glia during adulthood using GliaGS. ST50 values for the GliaGS/transgene either fed RU486 or vehicle are reported. @, #, $, %, &, ~, +, = represent genotypes that where tested together, and therefore were statistically compared in the two-way ANOVA. When appropriate, Bonferonni multiple comparision adjusted p-values are reported

B.5 THE TYRAMINE RECEPTOR IS IMPORTANT FOR ALCOHOL SEDATION

When tyramine is released from neurons, it binds to a tyramine receptor on a post-synaptic membrane[273]. Three tyramine receptor subtypes exist in the fly: TyrR, TyrRII and TAR1 (also known as Oct-TyrR)[279]. If tyramine production in glia mediates alcohol sedation, we predicted that pharmacologically antagonizing the tyramine receptors might have the same effect on alcohol sedation as *Tdc2* knockdown. We utilized the drug Yohimbine, which efficiently blocks all tyramine receptors[280]. Flies fed Yohimbine had a decreased ST50 compared to vehicle fed flies, suggesting that the tyramine receptors are important for alcohol sedation (Fig 5.16). Thus knocking down Tdc2 (Fig 5.1) and antagonizing tyramine receptors (Fig 5.16) have similar effects on alcohol sedation.

Tyramine could, in principle, influence alcohol sedation through the collective effect of binding to each tyramine receptor subtype or by a role in a binding to an individual receptor subtype. Since the tyramine receptors are expressed on both neurons and glia[279], we consequently expressed RNAi against each tyramine receptor individually in neurons and glia via *elav*- and *repo*-Gal4, respectively. Expression of multiple RNAi against *TyrR*, *TyrRll* and *TAR1* in neurons (via *elav*-Gal4) did not alter alcohol sedation and expression of one RNAi (identifier 27670) against *TyrRII* significantly increased ST50 compared to controls (Table 5.5). Given that Tdc2 knockdown in glia decreased ST50 (Fig 5.1), these data suggest that (i) the tyramine receptors on neurons are not regulating alcohol sedation or (ii) TyrRII may be regulating alcohol sedation independently of glial tyramine. Interestingly, expression of RNAi against *TAR1* (identifier v26876) in glia (via *repo*-Gal4) significantly decreased ST50

compared to controls, while expression of a second RNAi (identifier 28332) did not alter ST50 values (Table 5.6). Glial expression of RNAi against *TyrR* either significantly decreased, significantly increased, or did not alter ST50 compared to control (Table 5.6). Expression of RNAi against *TyrRII* in glia did not alter ST50 compared to controls (Table 5.6). Taken together, these data suggest that expression of TAR1 on glia may regulate alcohol sedation, while the expression of TyrR and TyrRII on glia may not mediate alcohol sedation. Since individual expression of RNAi against *Tdc2* and *TAR1* in glia (via *repo*-Gal4) lead to significant decreases in ST50, it is possible that glial tyramine is binding to a glial TAR1 receptor to mediate alcohol sedation. Additional studies are needed to formally assess this possibility.

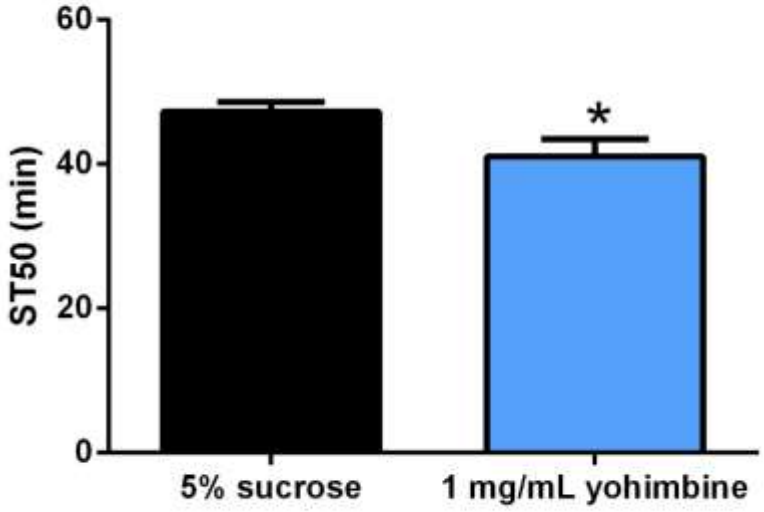

Figure 5.16. Antagonizing tyramine receptors with Yohimbine alters alcohol sedation sensitivity. Our labs standard fly, w[A], was fed Yohimbine or vehicle (5% sucrose). Flies fed Yohimbine (blue bar) had a significantly decreased ST50 compared to vehicle control (black bar) (Students t test, $p = 0.039$, $n = 8$).

Table 5.5. Pan-neuronal expression of RNAi's against each tyramine receptor subtype

Tyramine receptor	Reagent (Identifier)	Group	ST50	one-way ANOVA	Multiple comparisons (to Gal4/RNAi)
TyrR	RNAi (v2857)	Gal4/+	36.59 ± 1.16 @	F (2, 20) = 0.69, p = 0.51	n/a
		RNAi/+	39.21 ± 1.56		n/a
		Gal4/RNAi	41.63 ± 1.32		
	RNAi (25857)	Gal4/+	40.45 ± 1.78 #	F (2, 21) = 2.07, p = 0.15	n/a
		RNAi/+	36.23 ± 2.41		n/a
		Gal4/RNAi	41.80 ± 1.81		
	RNAi (57496)	Gal4/+	40.45 ± 1.78 #	F (2, 21) = 7.74, p = 0.003	p > 0.9999
		RNAi/+	51.40 ± 7.44		p = 0.006*
		Gal4/RNAi	40.68 ± 2.25		
TyrRII	RNAi (v51387)	Gal4/+	36.59 ± 1.16 @	F (2, 21) = 4.3, p = 0.02	p = 0.027*
		RNAi/+	43.18 ± 2.37		p > 0.9999
		Gal4/RNAi	44.09 ± 2.16		
	RNAi (27670)	Gal4/+	37.35 ± 0.78 %	F (2, 21) = 16.84, p < 0.0001	p < 0.0001*
		RNAi/+	41.71 ± 1.91		p = 0.004*
		Gal4/RNAi	48.65 ± 1.23		
	RNAi (64964)	Gal4/+	39.85 ± 1.15	F (2, 21) = 4.28, p = 0.03	p = 0.02*
		RNAi/+	44.8 ± 2.43		p = 0.54
		Gal4/RNAi	47.98 ± 2.13		
TAR1	RNAi (v26876)	Gal4/+	28.75 ± 0.94	F (2, 21) = 1.023, p = 0.38	n/a
		RNAi/+	38.35 ± 1.42		n/a
		Gal4/RNAi	38.48 ± 0.94		
	RNAi (28332)	Gal4/+	37.35 ± 0.78 %	F (2, 21) = 0.0008, p = 0.999	n/a
		RNAi/+	37.38 ± 1.68		n/a
		Gal4/RNAi	37.30 ± 1.36		

Expression of RNAi against *TyrR, TyrRII* and *TAR1* in neurons (via *elav*-Gal4) did not consistently alter alcohol sedation compared to both the Gal4 driver (Gal4/+) and RNAi transgene (RNAi/+) controls. Only expression of the 27670 RNAi transgene against TyrRII had a significantly increased ST50 compared to controls. Results from individual one-way ANOVAs and (when appropriate) Bonferroni's multiple comparisons are reported. @, # and % represent common Gal4/+ controls.

Table 5.6. Pan-glial expression of RNAi's against each tyramine receptor subtype

Tyramine receptor	Reagent (Identifier)	Group	ST50	one-way ANOVA	Multiple comparisons (to Gal4/RNAi)
TyrR	RNAi (v2857)	Gal4/+	-	lethal	n/a
		RNAi/+	-		n/a
		Gal4/RNAi	-		
	RNAi (25857)	Gal4/+	33.23 ± 0.86 #	F (2, 21) = 5.803, p = 0.009	p = 0.007*
		RNAi/+	31.78 ± 1.23		p = 0.048*
		Gal4/RNAi	27.68 ± 1.42		
	RNAi (57496)	Gal4/+	37.33 ± 1.21	F (2, 21) = 24.64, p < 0.0001	p < 0.0001*
		RNAi/+	44.06 ± 2.04		p = 0.0012*
		Gal4/RNAi	53.26 ± 1.47		
TyrRII	RNAi (v51387)	Gal4/+	32.00 ± 1.27	F (2, 19) = 1.36, p = 0.28	n/a
		RNAi/+	33.81 ± 1.22		n/a
		Gal4/RNAi	31.08 ± 1.48		
	RNAi (27670)	Gal4/+	45.15 ± 1.93 @	F (2, 21) = 0.63, p = 0.54	n/a
		RNAi/+	48.88 ± 2.09		n/a
		Gal4/RNAi	47.70 ± 3.03		
	RNAi (64964)	Gal4/+	45.15 ± 1.93 @	F (2, 21) = 0.73, p = 0.49	n/a
		RNAi/+	46.11 ± 2.46		n/a
		Gal4/RNAi	48.58 ± 1.77		
TAR1	RNAi (v26876)	Gal4/+	29.56 ± 56	F (2, 21) = 6.76, p = 0.005	p = 0.02*
		RNAi/+	30.49 ± 0.73		p = 0.004*
		Gal4/RNAi	26.05 ± 0.97		
	RNAi (28332)	Gal4/+	33.23 ± 0.86 #	F (2, 21) = 3.09, p = 0.06	n/a
		RNAi/+	33.56 ± 1.05		n/a
		Gal4/RNAi	36.64 ± 1.25		

Expression of RNAi against *TyrR, TyrRII* and *TAR1* in glia (via *repo*-Gal4) did not consistently alter alcohol sedation compared to both the Gal4 driver (Gal4/+) and RNAi transgene (RNAi/+) controls. Expression of the TyrR RNAi 25857 significantly decreased ST50 compared to controls, while expression of the TyrR RNAi 57496 significantly increased ST50 compared to controls. Expression of the TAR1 RNAi v26876 significantly decreased ST50 compared to controls. Results from individual one-way ANOVAs and (when appropriate) Bonferroni's multiple comparisons are reported. @ and # represent common Gal4/+ controls.

C. DISCUSSION

A more detailed understanding of the genes and mechanisms that influence behavioral responses to alcohol could ultimately facilitate the development of novel diagnostic and treatment options for individuals that abuse the drug. Understandably, much of the genetic analysis of alcohol behavior in model organisms (mainly mice, flies and worms) has focused on genes that function in neurons, leaving mechanisms driven by other cell types largely unexplored. Our studies on Tdc2, glia and fly alcohol sedation help fill this gap. Here, we show that (i) knockdown and overexpression of Tdc2 in glia makes flies sensitive and resistant, respectively, to alcohol sedation, (ii) feeding flies tyramine can rescue the ethanol sedation sensitivity in *Tdc2* knockdown flies, (iii) VMAT and the SNARE complex influence alcohol sedation by functioning in glia, (iv) VMAT and the SNARE complex impact alcohol sedation by functioning downstream of Tdc2 in glia, and (v) these findings map to astrocytes and adulthood. Our data support a model in which astrocytes, during adulthood, influence alcohol sedation by synthesizing and releasing tyramine into the synapse through SNARE-dependent vesicular exocytosis. Given that resistance to alcohol responses is linked to the propensity to abuse it[225], our findings raise the possibility that astrocytes may be key contributors to AUD and problematic alcohol consumption through their role in mediating alcohol sensitivity through synthesis and release of transmitters.

Although synaptic vesicle exocytosis is a slower process in astrocytes than in neurons, the SNARE complex is used by both cell types to release synaptic vesicle contents[101]. Whether vesicular exocytosis is a physiologically relevant mechanism in astrocytes, however, is somewhat controversial. Our studies on VMAT and the SNARE

complex strongly suggest that synaptic vesicle loading and release within astrocytes are required for normal alcohol sedation in flies, thereby supporting the hypothesis that synaptic vesicle exocytosis in astrocytes could have important physiological roles.

Our data suggest that a small fraction of astrocytes expresses Tdc2 and synthesize/release tyramine, potentially as a gliotransmitter. The presence of or level of expression of Tdc2 could therefore represent astrocyte heterogeneity, which could be relevant for normal behavioral responses to alcohol. Given that the fly brain contains approximately 4,600 astrocytes total [125], it is intriguing to speculate how a minor fraction of such a small number of cells could impact alcohol sedation in an organism whose brain contains roughly 100,000 neurons [281]. One possibility is that the astrocytes engaged in tyramine synthesis are physically associated with numerous neurons involved in regulating alcohol sedation, and the tyramine released from the astrocytes binds to G protein-coupled tyramine receptors on neurons [279], thereby influencing the response of those neurons to alcohol. Another possibility is that tyramine released from a minor fraction of astrocytes permeates the brain as a whole, thereby influencing the physiological properties of nearby, as well as distant, neurons. However, these possibilities seem unlikely since expression of RNAi again the tyramine receptors in neurons did not produce a consistent alcohol sedation response (Table 5.5). Additionally, tyramine released from a minor fraction of astrocytes could function as an autocrine/paracrine factor to alter calcium signaling within nearby astrocytes, influencing their physiology, which can lead to altered responses of neurons to alcohol. This possibility is supported by our findings, since expressing TAR1 RNAi in glia significantly decreased ST50 (Table 5.6). Yet another possibility is that astrocytes contain direct

pharmacological targets of alcohol, and the binding of ethanol to these targets alters the release of tyramine which influences alcohol sedation. Although these models are speculative (and not mutually exclusive), they emphasize the need for additional studies to better understand the role of astrocytes in behavioral responses to ethanol.

Glia in flies and rodents, as well as in human alcoholic post-mortem tissue, are molecularly and morphologically altered by the presence of alcohol [158,159,211,212,249,282]. In flies, surface glia can regulate initial alcohol sedation and rapid tolerance development [211,212]. In rodents, blocking astrocyte hemichannels, increasing astrocyte intracellular calcium, and increasing astrocyte cytokine release has been associated with changes in alcohol related behaviors [183,194]. This study, however, is the first to identify an astrocyte molecular pathway that directly influences any alcohol-related behavior in any model organism. While research has demonstrated that astrocytes respond to alcohol administration and can influence behavioral responses after alcohol administration [182,183,190,194], but none of these identify a molecular pathway responsible for the changes. Given that astrocytes are major regulators of the synaptic environment, this finding is not particularly surprising. However, since alcohol use disorder is a disease of the central nervous system [5], our data stress the importance to consider both neurons and glia when investigating the genetic and molecular contributions to alcohol-related behaviors.

CHAPTER 6: DISCUSSION

A. SUMMARY AND FUTURE DIRECTIONS

Studies in model organisms, such as the worm, fly and rodents, have led to the discovery of many novel genes and pathways that regulate alcohol-related behaviors[226]. A majority of this work has focused on neurons, leaving glial contributions to alcohol-related behaviors overlooked. However, previous research using human alcohol post-mortem tissue, as well as rodents and flies, has demonstrated that glial cells do respond to alcohol administration and can influence alcohol related behaviors. For this reason, we hypothesized that glia are important and direct regulators of alcohol related behavior. Since flies and mammals have conserved behavioral responses to alcohol, as well as conserved glial cell function, we used *Drosophila melanogaster* as a model to fill this gap in the alcohol field[13]. *Drosophila* have an expansive toolkit to manipulate genes in specific tissues and cell types, including all glia as well as each glial cell subtype individually[24,125]. However, prior to this research, no pan-glial steroid-inducible GeneSwitch transgenic fly had been characterized. By measuring B-galactosidase activity, and using immunohistochemistry, we characterized a fly that induces robust transgene expression in adult CNS glia, and termed it GliaGS (Chapter 3). Using these glial gene manipulation methods, we conducted targeted screens to identify genes whose expression in glia is important for the alcohol-related behavior, sedation. From

these screens, we investigated the genes *Cysteine proteinase 1* (Chapter 4) and *Tyramine decarboxylase 2* (Chapter 5) further.

Our data suggests that expression of Cp1 in cortex glia during adulthood regulates alcohol sedation sensitivity and possibly rapid tolerance development to alcohol. This was the first research to associate Cp1, as well as cortex glia, with an alcohol-related behavior. Although the role of Cp1 in glia had not been studied previously, Cp1 function in neurons had. We used this data to try to identify pathways Cp1 was functioning within to mediate alcohol sedation, and specifically screened the transcription factor cut, the Cp1 inhibitor crammer, and the synaptic vesicle marker neuronal-synaptobrevin[233,239,252]. Unfortunately, manipulating these genes in glia did not alter alcohol sedation, suggesting that they were not functioning in the same pathway as Cp1 to mediate this response. Given that Cp1 is involved in protein degradation[241], it is possible that Cp1 is interacting with different proteins in cortex glia to regulate alcohol sedation. To identify these proteins, future studies should utilize mass spectrometry.

Additionally, our data suggests that Tdc2 is synthesizing tyramine in astrocytes during adulthood, and that tyramine is being release through vesicular exocytosis to regulate alcohol sedation. This was the first research to identify a molecular pathway within astrocytes that directly influences an alcohol related behavior. Additionally, these data suggest that astrocyte vesicular exocytosis is physiologically relevant, and that astrocyte heterogeneity may exist within the fly. Interestingly, our preliminary data suggests that a tyramine receptor on astrocytes (TAR1, also referred to the Oct-TyrR) may be involved in this pathway. While additional studies are necessary, this result invites the speculation that astrocytic tyramine may be functioning in an

autocrine/paracrine loop to regulate alcohol sedation, since it is known that astrocytes can communicate with each other through GTs[32]. Future studies should investigate this, as well as determine how glial TAR1 is regulating alcohol sedation. Previous literature has demonstrated that activating TAR1 on astrocytes leads to an increase in intracellular calcium and adenosine release, which inhibits nearby dopaminergic neurons[27]. Since dopamine is heavily involved in addiction, and has been previously implicated in fly alcohol-related behaviors[5,6], this may be an interesting pathway to pursue.

B. TRANSLATABILITY TO MAMMALS

Cp1 is orthologous to mammalian Cathepsin L, which has been previous implicated in alcohol-induced tissue damage and is known to be expressed in astrocytes and microglia[283,284]. Our data suggest that glial Cathepsin L may have a role in mediating the behavior response to an acute dose of alcohol. Interestingly, chronic alcohol administration leads to neurodegeneration[191], and Cathepsin L is involved in alcohol-induced cell damage outside the CNS[253]. Given that glial cell damage or death can lead to neurodegeneration[32], future studies in mammals should investigate whether glial Cathepsin L contributes to alcohol-induced neurodegeneration, which is a hallmark feature in severe alcoholic brains[163]. If true, then glial Cathepsin L may mediate both acute behavioral responses to alcohol, as well as CNS changes due to chronic alcohol administration.

Invertebrate tyramine is functionally homologous to mammalian norepinephrine, and the tyramine receptors are closely related to the vertebrate adrenergic receptors[279].

Both molecules have been associated with the “fight or flight” or arousal response, which can be measured as aggression and courtship in flies[285]. To date, norepinephrine has not been identified as a GT, but it has been implicated in alcohol dependence. Specifically, norepinephrine is elevated during alcohol withdrawal in mice and humans[286], and blocking norepinephrine neurotransmission also blunts alcohol withdrawal symptoms in mice. This result suggests that norepinephrine may regulate the negative emotional state associated with alcohol dependence, which is a criteria for AUD diagnosis in humans[287]. In our research, overexpressing Tdc2, and presumably overexpressing tyramine, leads to alcohol sedation resistance. Given that there is an inverse correlation between initial sensitivity and risk of alcohol dependence in humans[225], our data suggests that increases in tyramine, and therefore norepinephrine, may correlate with alcohol dependence development. Taken together, this suggests that increased norepinephrine levels are associated with alcohol dependence risk and progression.

Interestingly, tyramine is a trace amine in mammals. Trace amines are endogenously found monoamines in mammals, and are approximately 100-fold less abundant than catecholamines[288]. Trace amines have been implicated in many disorders, such as schizophrenia, bipolar disorder, depression, addiction and narcolepsy[289]. However, the invertebrate and mammalian receptors for tyramine are evolutionarily distinct, suggesting that tyramine in invertebrates and mammals is also functionally distinct[289]. For this reason, tyramine research in invertebrates is not translatable to tyramine function in mammals.

The principle cell types implicated in this research are *Drosophila* cortex glia and astrocytes. As described earlier, these cell types are morphologically and functionally similar to mammalian astrocytes (Chapter 1C). While previous literature has demonstrated that the mammalian orthologue of Cp1 functions in astrocytes[283], it is unknown whether the enzyme responsible for norepinephrine synthesis does. However, utilizing human RNA-sequencing data, this enzyme, Dopamine β-hydroxylase (DBH), is expressed in mature astrocytes[290]. Taken together, this suggests that our results studying Cp1 and Tdc2 in fly cortex glia and astrocytes may be translatable to mammalian astrocytes.

Based on the assumption that our studies in the fly are wholly translatable to mammals, it is possible that DBH and Cathepsin L may be functioning together in mammalian astrocytes to regulate alcohol-related behaviors. Our studies suggest that astrocytes contain synaptic vesicles that release norepinephrine, and that the release of these vesicles is important for alcohol sedation. Previous literature has demonstrated that Cp1 is required for synaptic vesicle degradation[252]. Therefore, it is possible that the synthesis and release of norepinephrine via DBH and the degradation of the vesicles that contain norepinephrine via Cathepsin L are functioning together in astrocytes to influence alcohol sedation. Degraded synaptic vesicles can be processed into new synaptic vesicles[252], therefore allowing norepinephrine to be released from the astrocyte though vesicular exocytosis. In flies, knocking down Cp1 (i.e. blocking synaptic vesicle degradation) and knocking down Tdc2 (i.e. blocking tyramine synthesis) produced the same behavioral effect: decreased ST50, or increased alcohol sedation sensitivity. It is possible that the studies looking at a relationship between Cp1 and neuronal-

synaptobrevin in cortex glia did not work because fly cortex glia do not have synaptic vesicles. However, in mammals, Cp1 (i.e. Cathepsin L) would be expressed in a cell type where this interaction could occur. Future studies in mammals would be needed to test this possibility.

Our data suggests that glia are important regulators of alcohol sedation in *Drosophila melanogaster*. Given that alcohol use, abuse and dependence effects the central nervous system, future research within the field should consider both neuronal and glial contributions. Since glia and neuron function is reliant on the other, it seems likely that differences in behavioral responses to alcohol may, in part, be due to impairments in the synchrony of glia and neurons. This impairment can lead to overall CNS dysfunction, which over time may contribute to alcohol dependence development.

REFERENCES

1 Park-Lee, E., Lipari, R. N., Hedden, S. L., Kroutil, L. A. & Porter, J. D. in *CBHSQ Data Review* 1-35 (Substance Abuse and Mental Health Services Administration (US), 2012).

2 The global burden of disease attributable to alcohol and drug use in 195 countries and territories, 1990-2016: a systematic analysis for the Global Burden of Disease Study 2016. *The lancet. Psychiatry* **5**, 987-1012, doi:10.1016/s2215-0366(18)30337-7 (2018).

3 American Psychiatric, A. *Diagnostic and statistical manual of mental disorders*. 5 edn, (American Psychiatric Publishing, 2013).

4 Mason, B. J. Emerging pharmacotherapies for alcohol use disorder. *Neuropharmacology* **122**, 244-253, doi:10.1016/j.neuropharm.2017.04.032 (2017).

5 Edenberg, H. J. & Foroud, T. Genetics and alcoholism. *Nature reviews.Gastroenterology & hepatology* **10**, 487-494, doi:10.1038/nrgastro.2013.86 [doi] (2013).

6 Wolf, F. W., Rodan, A. R., Tsai, L. T. & Heberlein, U. High-resolution analysis of ethanol-induced locomotor stimulation in Drosophila. *The Journal of neuroscience : the official journal of the Society for Neuroscience* **22**, 11035-11044 (2002).

7 Babor, T. F., Berglas, S., Mendelson, J. H., Ellingboe, J. & Miller, K. Alcohol, affect, and the disinhibition of verbal behavior. *Psychopharmacology* **80**, 53-60 (1983).

8 Bhandari, P., Kendler, K. S., Bettinger, J. C., Davies, A. G. & Grotewiel, M. An assay for evoked locomotor behavior in Drosophila reveals a role for integrins in ethanol sensitivity and rapid ethanol tolerance. *Alcoholism, clinical and experimental research* **33**, 1794-1805, doi:10.1111/j.1530-0277.2009.01018.x [doi] (2009).

9 Berger, K. H., Heberlein, U. & Moore, M. S. Rapid and chronic: two distinct forms of ethanol tolerance in Drosophila. *Alcoholism, clinical and experimental research* **28**, 1469-1480 (2004).

10 Kosten, T. R. & O'Connor, P. G. Management of drug and alcohol withdrawal. *The New England journal of medicine* **348**, 1786-1795, doi:10.1056/NEJMra020617 (2003).

11 Ghezzi, A., Krishnan, H. R. & Atkinson, N. S. Susceptibility to ethanol withdrawal seizures is produced by BK channel gene expression. *Addiction biology* **19**, 332-337, doi:10.1111/j.1369-1600.2012.00465.x (2014).

12 Devineni, A. V. & Heberlein, U. Preferential ethanol consumption in Drosophila models features of addiction. *Current biology : CB* **19**, 2126-2132, doi:10.1016/j.cub.2009.10.070 (2009).

13 Devineni, A. V. & Heberlein, U. The evolution of Drosophila melanogaster as a model for alcohol research. *Annual review of neuroscience* **36**, 121-138, doi:10.1146/annurev-neuro-062012-170256 (2013).

14 David, J. R., Bocquet, C., Arens, M. F. & Fouillet, P. Biological role of alcohol dehydrogenase in the tolerance of Drosophila melanogaster to aliphatic alochols: utilization of an ADH-null mutant. *Biochemical genetics* **14**, 989-997 (1976).

15 Fry, J. D. & Saweikis, M. Aldehyde dehydrogenase is essential for both adult and larval ethanol resistance in Drosophila melanogaster. *Genetical research* **87**, 87-92, doi:10.1017/s0016672306008032 (2006).

16 Scholz, H. & Mustard, J. A. in *Behavioral Neurobiology of Alcohol Addiction* (eds Wolfgang H. Sommer & Rainer Spanagel) 433-457 (Springer Berlin Heidelberg, 2013).

17 Ogueta, M., Cibik, O., Eltrop, R., Schneider, A. & Scholz, H. The influence of Adh function on ethanol preference and tolerance in adult Drosophila melanogaster. *Chemical senses* **35**, 813-822, doi:10.1093/chemse/bjq084 (2010).

18 Dzitoyeva, S., Dimitrijevic, N. & Manev, H. Gamma-aminobutyric acid B receptor 1 mediates behavior-impairing actions of alcohol in Drosophila: adult RNA interference and pharmacological evidence. *Proceedings of the National Academy of Sciences of the United States of America* **100**, 5485-5490, doi:10.1073/pnas.0830111100 (2003).

19 Colombo, G. *et al.* Role of GABA(B) receptor in alcohol dependence: reducing effect of baclofen on alcohol intake and alcohol motivational properties in rats and amelioration of alcohol withdrawal syndrome and alcohol craving in human alcoholics. *Neurotoxicity research* **6**, 403-414 (2004).

20 Kong, E. C. *et al.* A pair of dopamine neurons target the D1-like dopamine receptor DopR in the central complex to promote ethanol-stimulated locomotion in Drosophila. *PloS one* **5**, e9954, doi:10.1371/journal.pone.0009954 (2010).

21 Heinz, A. Dopaminergic dysfunction in alcoholism and schizophrenia--psychopathological and behavioral correlates. *European psychiatry : the journal of the Association of European Psychiatrists* **17**, 9-16 (2002).

22 Thorsell, A. Neuropeptide Y (NPY) in alcohol intake and dependence. *Peptides* **28**, 480-483, doi:10.1016/j.peptides.2006.11.017 (2007).

23 Wen, T., Parrish, C. A., Xu, D., Wu, Q. & Shen, P. Drosophila neuropeptide F and its receptor, NPFR1, define a signaling pathway that acutely modulates alcohol sensitivity. *Proceedings of the National Academy of Sciences of the United States of America* **102**, 2141-2146, doi:0406814102 [pii] (2005).

24 Brand, A. H. & Perrimon, N. Targeted gene expression as a means of altering cell fates and generating dominant phenotypes. *Development (Cambridge, England)* **118**, 401-415 (1993).

25 Yagi, R., Mayer, F. & Basler, K. Refined LexA transactivators and their use in combination with the Drosophila Gal4 system. *Proceedings of the National Academy of Sciences of the United States of America* **107**, 16166-16171, doi:10.1073/pnas.1005957107 (2010).

26 Potter, C. J., Tasic, B., Russler, E. V., Liang, L. & Luo, L. The Q system: a repressible binary system for transgene expression, lineage tracing, and mosaic analysis. *Cell* **141**, 536-548, doi:10.1016/j.cell.2010.02.025 (2010).

27 Ma, Z., Stork, T., Bergles, D. E. & Freeman, M. R. Neuromodulators signal through astrocytes to alter neural circuit activity and behaviour. *Nature* **539**, 428-432, doi:10.1038/nature20145 [doi] (2016).

28 Suster, M. L., Seugnet, L., Bate, M. & Sokolowski, M. B. Refining GAL4-driven transgene expression in Drosophila with a GAL80 enhancer-trap. *Genesis (New York, N.Y.: 2000)* **39**, 240-245, doi:10.1002/gene.20051 [doi] (2004).

29 Nicholson, L. *et al.* Spatial and temporal control of gene expression in Drosophila using the inducible GeneSwitch GAL4 system. I. Screen for larval nervous system drivers. *Genetics* **178**, 215-234, doi:10.1534/genetics.107.081968 [doi] (2008).

30 Saab, A. S., Tzvetanova, I. D. & Nave, K. A. The role of myelin and oligodendrocytes in axonal energy metabolism. *Current opinion in neurobiology* **23**, 1065-1072, doi:10.1016/j.conb.2013.09.008 [doi] (2013).

31 Barcia, C., Guillemin, G. J., Curtin, J. F. & Zirger, J. M. Editorial: Glial Cells: Managers of Neuro-Immunity. *Frontiers in cellular neuroscience* **10**, 60, doi:10.3389/fncel.2016.00060 (2016).

32 Mederos, S., Gonzalez-Arias, C. & Perea, G. Astrocyte-Neuron Networks: A Multilane Highway of Signaling for Homeostatic Brain Function. *Frontiers in synaptic neuroscience* **10**, 45, doi:10.3389/fnsyn.2018.00045 (2018).

33 Hindle, S. J. *et al.* Evolutionarily Conserved Roles for Blood-Brain Barrier Xenobiotic Transporters in Endogenous Steroid Partitioning and Behavior. *Cell reports* **21**, 1304-1316, doi:10.1016/j.celrep.2017.10.026 (2017).

34 Peco, E. *et al.* Drosophila astrocytes cover specific territories of the CNS neuropil and are instructed to differentiate by Prospero, a key effector of Notch. *Development (Cambridge, England)* **143**, 1170-1181, doi:10.1242/dev.133165 (2016).

35 Otto, N. *et al.* The sulfite oxidase Shopper controls neuronal activity by regulating glutamate homeostasis in Drosophila ensheathing glia. *Nature communications* **9**, 3514, doi:10.1038/s41467-018-05645-z (2018).

36 Doherty, J., Logan, M. A., Tasdemir, O. E. & Freeman, M. R. Ensheathing glia function as phagocytes in the adult Drosophila brain. *The Journal of neuroscience : the official journal of the Society for Neuroscience* **29**, 4768-4781, doi:10.1523/JNEUROSCI.5951-08.2009 [doi] (2009).

37 Dutta, S., Rieche, F., Eckl, N., Duch, C. & Kretzschmar, D. Glial expression of Swiss cheese (SWS), the Drosophila orthologue of neuropathy target esterase (NTE), is required for neuronal ensheathment and function. *Disease models & mechanisms* **9**, 283-294, doi:10.1242/dmm.022236 [doi] (2016).

38 Kazama, H., Yaksi, E. & Wilson, R. I. Cell death triggers olfactory circuit plasticity via glial signaling in Drosophila. *The Journal of neuroscience : the official journal of the Society for Neuroscience* **31**, 7619-7630, doi:10.1523/JNEUROSCI.5984-10.2011 [doi] (2011).

39 Coutinho-Budd, J. C., Sheehan, A. E. & Freeman, M. R. The secreted neurotrophin Spatzle 3 promotes glial morphogenesis and supports neuronal survival and function. *Genes & development* **31**, 2023-2038, doi:10.1101/gad.305888.117 [doi] (2017).

40 Freeman, M. R. Drosophila Central Nervous System Glia. *Cold Spring Harbor perspectives in biology* **7**, 10.1101/cshperspect.a020552, doi:10.1101/cshperspect.a020552 [doi] (2015).

41 Dent, K. A. *et al.* Oligodendrocyte birth and death following traumatic brain injury in adult mice. *PloS one* **10**, e0121541, doi:10.1371/journal.pone.0121541 (2015).

42 Armstrong, R. C., Mierzwa, A. J., Sullivan, G. M. & Sanchez, M. A. Myelin and oligodendrocyte lineage cells in white matter pathology and plasticity after traumatic brain injury. *Neuropharmacology* **110**, 654-659, doi:10.1016/j.neuropharm.2015.04.029 (2016).

43 Raghupathi, R., Graham, D. I. & McIntosh, T. K. Apoptosis after traumatic brain injury. *Journal of neurotrauma* **17**, 927-938, doi:10.1089/neu.2000.17.927 (2000).

44 Sofroniew, M. V. & Vinters, H. V. Astrocytes: biology and pathology. *Acta Neuropathologica* **119**, 7-35, doi:10.1007/s00401-009-0619-8 [doi] (2010).

45 Oberheim, N. A. *et al.* Uniquely hominid features of adult human astrocytes. *The Journal of neuroscience : the official journal of the Society for Neuroscience* **29**, 3276-3287, doi:10.1523/jneurosci.4707-08.2009 (2009).

46 Fernandez, B., Suarez, I. & Gonzalez, G. Topographical distribution of the astrocytic lamellae in the hypothalamus. *Anatomischer Anzeiger* **156**, 31-37 (1984).

47 Escartin, C. *et al.* Activation of astrocytes by CNTF induces metabolic plasticity and increases resistance to metabolic insults. *The Journal of neuroscience : the official journal of the Society for Neuroscience* **27**, 7094-7104, doi:10.1523/jneurosci.0174-07.2007 (2007).

48 Plata, A. *et al.* Astrocytic Atrophy Following Status Epilepticus Parallels Reduced Ca(2+) Activity and Impaired Synaptic Plasticity in the Rat Hippocampus. *Frontiers in molecular neuroscience* **11**, 215, doi:10.3389/fnmol.2018.00215 (2018).

49 Bedner, P. *et al.* Astrocyte uncoupling as a cause of human temporal lobe epilepsy. *Brain : a journal of neurology* **138**, 1208-1222, doi:10.1093/brain/awv067 (2015).

50 Cornell-Bell, A. H., Finkbeiner, S. M., Cooper, M. S. & Smith, S. J. Glutamate induces calcium waves in cultured astrocytes: long-range glial signaling. *Science (New York, N.Y.)* **247**, 470-473 (1990).

51 Semyanov, A. Spatiotemporal pattern of calcium activity in astrocytic network. *Cell calcium* **78**, 15-25, doi:10.1016/j.ceca.2018.12.007 (2018).

52 Rusakov, D. A., Bard, L., Stewart, M. G. & Henneberger, C. Diversity of astroglial functions alludes to subcellular specialisation. *Trends in neurosciences* **37**, 228-242, doi:10.1016/j.tins.2014.02.008 (2014).

53 Borden, L. A. GABA transporter heterogeneity: pharmacology and cellular localization. *Neurochemistry international* **29**, 335-356 (1996).

54 Bergles, D. E. & Jahr, C. E. Synaptic activation of glutamate transporters in hippocampal astrocytes. *Neuron* **19**, 1297-1308 (1997).

55 Danbolt, N. C. Glutamate uptake. *Progress in neurobiology* **65**, 1-105 (2001).

56 Verkhratsky, A. & Nedergaard, M. Physiology of Astroglia. *Physiological reviews* **98**, 239-389, doi:10.1152/physrev.00042.2016 (2018).

57 Huang, Y. H., Sinha, S. R., Tanaka, K., Rothstein, J. D. & Bergles, D. E. Astrocyte glutamate transporters regulate metabotropic glutamate receptor-mediated excitation of hippocampal interneurons. *The Journal of neuroscience : the official journal of the Society for Neuroscience* **24**, 4551-4559, doi:10.1523/jneurosci.5217-03.2004 (2004).

58 Farca Luna, A. J., Perier, M. & Seugnet, L. Amyloid Precursor Protein in Drosophila Glia Regulates Sleep and Genes Involved in Glutamate Recycling. *The Journal of neuroscience : the official journal of the Society for Neuroscience* **37**, 4289-4300, doi:10.1523/JNEUROSCI.2826-16.2017 [doi] (2017).

59 Beenhakker, M. P. & Huguenard, J. R. Astrocytes as gatekeepers of GABAB receptor function. *The Journal of neuroscience : the official journal of the Society for Neuroscience* **30**, 15262-15276, doi:10.1523/jneurosci.3243-10.2010 (2010).

60 Doengi, M. *et al.* GABA uptake-dependent Ca(2+) signaling in developing olfactory bulb astrocytes. *Proceedings of the National Academy of Sciences of the United States of America* **106**, 17570-17575, doi:10.1073/pnas.0809513106 (2009).

61 Seifert, G. *et al.* Analysis of astroglial K+ channel expression in the developing hippocampus reveals a predominant role of the Kir4.1 subunit. *The Journal of neuroscience : the official journal of the Society for Neuroscience* **29**, 7474-7488, doi:10.1523/jneurosci.3790-08.2009 (2009).

62 Seifert, G., Henneberger, C. & Steinhauser, C. Diversity of astrocyte potassium channels: An update. *Brain research bulletin* **136**, 26-36, doi:10.1016/j.brainresbull.2016.12.002 (2018).

63 Haj-Yasein, N. N. *et al.* Evidence that compromised K+ spatial buffering contributes to the epileptogenic effect of mutations in the human Kir4.1 gene (KCNJ10). *Glia* **59**, 1635-1642, doi:10.1002/glia.21205 (2011).

64 Nagelhus, E. A. *et al.* Immunogold evidence suggests that coupling of K+ siphoning and water transport in rat retinal Muller cells is mediated by a coenrichment of Kir4.1 and AQP4 in specific membrane domains. *Glia* **26**, 47-54 (1999).

65 Larsen, B. R. *et al.* Contributions of the Na(+)/K(+)-ATPase, NKCC1, and Kir4.1 to hippocampal K(+) clearance and volume responses. *Glia* **62**, 608-622, doi:10.1002/glia.22629 (2014).

66 Ransom, C. B., Ransom, B. R. & Sontheimer, H. Activity-dependent extracellular K+ accumulation in rat optic nerve: the role of glial and axonal Na+ pumps. *The Journal of physiology* **522 Pt 3**, 427-442 (2000).

67 Shigetomi, E., Jackson-Weaver, O., Huckstepp, R. T., O'Dell, T. J. & Khakh, B. S. TRPA1 channels are regulators of astrocyte basal calcium levels and long-term potentiation via constitutive D-serine release. *The Journal of neuroscience : the official journal of the Society for Neuroscience* **33**, 10143-10153, doi:10.1523/jneurosci.5779-12.2013 (2013).

68 Reyes, R. C., Verkhratsky, A. & Parpura, V. TRPC1-mediated Ca2+ and Na+ signalling in astroglia: differential filtering of extracellular cations. *Cell calcium* **54**, 120-125, doi:10.1016/j.ceca.2013.05.005 (2013).

69 Grimaldi, M., Maratos, M. & Verma, A. Transient receptor potential channel activation causes a novel form of [Ca 2+]I oscillations and is not involved in capacitative Ca 2+ entry in glial cells. *The Journal of neuroscience : the official journal of the Society for Neuroscience* **23**, 4737-4745 (2003).

70 Shibasaki, K., Ikenaka, K., Tamalu, F., Tominaga, M. & Ishizaki, Y. A novel subtype of astrocytes expressing TRPV4 (transient receptor potential vanilloid 4) regulates neuronal excitability via release of gliotransmitters. *The Journal of biological chemistry* **289**, 14470-14480, doi:10.1074/jbc.M114.557132 (2014).

71 Butenko, O. *et al.* The increased activity of TRPV4 channel in the astrocytes of the adult rat hippocampus after cerebral hypoxia/ischemia. *PloS one* **7**, e39959, doi:10.1371/journal.pone.0039959 (2012).

72 Ho, K. S., TN; Lamber, WS; Calkins, DJ. Age and Elevated Pressure Increase Astrocyte Expression of TRPV1 in Retina and Optic Nerve of the DBA2J Mouse Model of Glaucoma. *investigative ophthalmology & visual science* **52** (2011).

73 Wang, H. *et al.* Brain temperature and its fundamental properties: a review for clinical neuroscientists. *Frontiers in neuroscience* **8**, 307, doi:10.3389/fnins.2014.00307 (2014).

74 Marrone, M. C. *et al.* TRPV1 channels are critical brain inflammation detectors and neuropathic pain biomarkers in mice. *Nature communications* **8**, 15292, doi:10.1038/ncomms15292 (2017).

75 Letellier, M. *et al.* Astrocytes regulate heterogeneity of presynaptic strengths in hippocampal networks. *Proceedings of the National Academy of Sciences of the United States of America* **113**, E2685-2694, doi:10.1073/pnas.1523717113 (2016).

76 Zhang, Y. *et al.* An RNA-sequencing transcriptome and splicing database of glia, neurons, and vascular cells of the cerebral cortex. *The Journal of neuroscience : the official journal of the Society for Neuroscience* **34**, 11929-11947, doi:10.1523/jneurosci.1860-14.2014 (2014).

77 Willis, M. *et al.* L-type calcium channel CaV 1.2 in transgenic mice overexpressing human AbetaPP751 with the London (V717I) and Swedish

(K670M/N671L) mutations. *Journal of Alzheimer's disease : JAD* **20**, 1167-1180, doi:10.3233/jad-2010-091117 (2010).

78 Westenbroek, R. E. *et al.* Upregulation of L-type Ca2+ channels in reactive astrocytes after brain injury, hypomyelination, and ischemia. *The Journal of neuroscience : the official journal of the Society for Neuroscience* **18**, 2321-2334 (1998).

79 Carmignoto, G., Pasti, L. & Pozzan, T. On the role of voltage-dependent calcium channels in calcium signaling of astrocytes in situ. *The Journal of neuroscience : the official journal of the Society for Neuroscience* **18**, 4637-4645 (1998).

80 Kirischuk, S., Parpura, V. & Verkhratsky, A. Sodium dynamics: another key to astroglial excitability? *Trends in neurosciences* **35**, 497-506, doi:10.1016/j.tins.2012.04.003 (2012).

81 Durkee, C. A. & Araque, A. Diversity and Specificity of Astrocyte-neuron Communication. *Neuroscience* **396**, 73-78, doi:10.1016/j.neuroscience.2018.11.010 (2019).

82 Bekar, L. K., He, W. & Nedergaard, M. Locus coeruleus alpha-adrenergic-mediated activation of cortical astrocytes in vivo. *Cerebral cortex (New York, N.Y. : 1991)* **18**, 2789-2795, doi:10.1093/cercor/bhn040 (2008).

83 Paukert, M. *et al.* Norepinephrine controls astroglial responsiveness to local circuit activity. *Neuron* **82**, 1263-1270, doi:10.1016/j.neuron.2014.04.038 (2014).

84 Jennings, A. *et al.* Dopamine elevates and lowers astroglial Ca(2+) through distinct pathways depending on local synaptic circuitry. *Glia* **65**, 447-459, doi:10.1002/glia.23103 (2017).

85 Kim, J. G. *et al.* Leptin signaling in astrocytes regulates hypothalamic neuronal circuits and feeding. *Nature neuroscience* **17**, 908-910, doi:10.1038/nn.3725 (2014).

86 Palygin, O., Lalo, U., Verkhratsky, A. & Pankratov, Y. Ionotropic NMDA and P2X1/5 receptors mediate synaptically induced Ca2+ signalling in cortical astrocytes. *Cell calcium* **48**, 225-231, doi:10.1016/j.ceca.2010.09.004 (2010).

87 Finch, E. A., Turner, T. J. & Goldin, S. M. Calcium as a coagonist of inositol 1,4,5-trisphosphate-induced calcium release. *Science (New York, N.Y.)* **252**, 443-446 (1991).

88 Dupont, G. & Goldbeter, A. One-pool model for Ca2+ oscillations involving Ca2+ and inositol 1,4,5-trisphosphate as co-agonists for Ca2+ release. *Cell calcium* **14**, 311-322 (1993).

89 Kirischuk, S., Kirchhoff, F., Matyash, V., Kettenmann, H. & Verkhratsky, A. Glutamate-triggered calcium signalling in mouse bergmann glial cells in situ: role of inositol-1,4,5-trisphosphate-mediated intracellular calcium release. *Neuroscience* **92**, 1051-1059 (1999).

90 Nakahara, K., Okada, M. & Nakanishi, S. The metabotropic glutamate receptor mGluR5 induces calcium oscillations in cultured astrocytes via protein kinase C phosphorylation. *Journal of neurochemistry* **69**, 1467-1475 (1997).

91 Kastritsis, C. H., Salm, A. K. & McCarthy, K. Stimulation of the P2Y purinergic receptor on type 1 astroglia results in inositol phosphate formation and calcium mobilization. *Journal of neurochemistry* **58**, 1277-1284 (1992).

92 Xu, T. & Pandey, S. C. Cellular localization of serotonin(2A) (5HT(2A)) receptors in the rat brain. *Brain research bulletin* **51**, 499-505 (2000).

93 Porter-Stransky, K. A. *et al.* Noradrenergic Transmission at Alpha1-Adrenergic Receptors in the Ventral Periaqueductal Gray Modulates Arousal. *Biological psychiatry* **85**, 237-247, doi:10.1016/j.biopsych.2018.07.027 (2019).

94 Rizzuto, R., De Stefani, D., Raffaello, A. & Mammucari, C. Mitochondria as sensors and regulators of calcium signalling. *Nature reviews. Molecular cell biology* **13**, 566-578, doi:10.1038/nrm3412 (2012).

95 Santo-Domingo, J. & Demaurex, N. Calcium uptake mechanisms of mitochondria. *Biochimica et biophysica acta* **1797**, 907-912, doi:10.1016/j.bbabio.2010.01.005 (2010).

96 Williams, G. S., Boyman, L., Chikando, A. C., Khairallah, R. J. & Lederer, W. J. Mitochondrial calcium uptake. *Proceedings of the National Academy of Sciences of the United States of America* **110**, 10479-10486, doi:10.1073/pnas.1300410110 (2013).

97 Agarwal, A. *et al.* Transient Opening of the Mitochondrial Permeability Transition Pore Induces Microdomain Calcium Transients in Astrocyte Processes. *Neuron* **93**, 587-605.e587, doi:10.1016/j.neuron.2016.12.034 (2017).

98 Perea, G. & Araque, A. Glial calcium signaling and neuron-glia communication. *Cell calcium* **38**, 375-382, doi:10.1016/j.ceca.2005.06.015 (2005).

99 Shigetomi, E., Bowser, D. N., Sofroniew, M. V. & Khakh, B. S. Two forms of astrocyte calcium excitability have distinct effects on NMDA receptor-mediated slow inward currents in pyramidal neurons. *The Journal of neuroscience : the official journal of the Society for Neuroscience* **28**, 6659-6663, doi:10.1523/jneurosci.1717-08.2008 (2008).

100 Savtchouk, I. & Volterra, A. Gliotransmission: Beyond Black-and-White. *The Journal of neuroscience : the official journal of the Society for Neuroscience* **38**, 14-25, doi:10.1523/jneurosci.0017-17.2017 (2018).

101 Zorec, R., Verkhratsky, A., Rodriguez, J. J. & Parpura, V. Astrocytic vesicles and gliotransmitters: Slowness of vesicular release and synaptobrevin2-laden vesicle nanoarchitecture. *Neuroscience* **323**, 67-75, doi:10.1016/j.neuroscience.2015.02.033 (2016).

102 Schwarz, Y., Zhao, N., Kirchhoff, F. & Bruns, D. Astrocytes control synaptic strength by two distinct v-SNARE-dependent release pathways. *Nature neuroscience* **20**, 1529-1539, doi:10.1038/nn.4647 (2017).

103 Rossi, D. J., Oshima, T. & Attwell, D. Glutamate release in severe brain ischaemia is mainly by reversed uptake. *Nature* **403**, 316-321, doi:10.1038/35002090 (2000).

104 Abudara, V., Retamal, M. A., Del Rio, R. & Orellana, J. A. Synaptic Functions of Hemichannels and Pannexons: A Double-Edged Sword. *Frontiers in molecular neuroscience* **11**, 435, doi:10.3389/fnmol.2018.00435 (2018).

105 Ambrosi, C. *et al.* Pannexin1 and Pannexin2 channels show quaternary similarities to connexons and different oligomerization numbers from each other. *The Journal of biological chemistry* **285**, 24420-24431, doi:10.1074/jbc.M110.115444 (2010).

106 Saez, J. C., Berthoud, V. M., Branes, M. C., Martinez, A. D. & Beyer, E. C. Plasma membrane channels formed by connexins: their regulation and functions. *Physiological reviews* **83**, 1359-1400, doi:10.1152/physrev.00007.2003 (2003).

107 Dahl, G. ATP release through pannexon channels. *Philosophical transactions of the Royal Society of London. Series B, Biological sciences* **370**, doi:10.1098/rstb.2014.0191 (2015).

108 Contreras, J. E., Saez, J. C., Bukauskas, F. F. & Bennett, M. V. Gating and regulation of connexin 43 (Cx43) hemichannels. *Proceedings of the National Academy of Sciences of the United States of America* **100**, 11388-11393, doi:10.1073/pnas.1434298100 (2003).

109 (!!! INVALID CITATION !!! {}).

110 Fujii, Y., Maekawa, S. & Morita, M. Astrocyte calcium waves propagate proximally by gap junction and distally by extracellular diffusion of ATP released from volume-regulated anion channels. *Scientific reports* **7**, 13115, doi:10.1038/s41598-017-13243-0 (2017).

111 Harris, A. L. Connexin channel permeability to cytoplasmic molecules. *Progress in biophysics and molecular biology* **94**, 120-143, doi:10.1016/j.pbiomolbio.2007.03.011 (2007).

112 Kumar, N. M. & Gilula, N. B. The gap junction communication channel. *Cell* **84**, 381-388 (1996).

113 Zhang, Y. & Barres, B. A. Astrocyte heterogeneity: an underappreciated topic in neurobiology. *Current opinion in neurobiology* **20**, 588-594, doi:10.1016/j.conb.2010.06.005 (2010).

114 Lanjakornsiripan, D. *et al.* Layer-specific morphological and molecular differences in neocortical astrocytes and their dependence on neuronal layers. *Nature communications* **9**, 1623, doi:10.1038/s41467-018-03940-3 (2018).

115 Takata, N. & Hirase, H. Cortical layer 1 and layer 2/3 astrocytes exhibit distinct calcium dynamics in vivo. *PloS one* **3**, e2525, doi:10.1371/journal.pone.0002525 (2008).

116 Tang, X., Taniguchi, K. & Kofuji, P. Heterogeneity of Kir4.1 channel expression in glia revealed by mouse transgenesis. *Glia* **57**, 1706-1715, doi:10.1002/glia.20882 (2009).

117 John Lin, C. C. *et al.* Identification of diverse astrocyte populations and their malignant analogs. *Nature neuroscience* **20**, 396-405, doi:10.1038/nn.4493 (2017).

118 Morel, L. *et al.* Molecular and Functional Properties of Regional Astrocytes in the Adult Brain. *The Journal of neuroscience : the official journal of the Society for Neuroscience* **37**, 8706-8717, doi:10.1523/jneurosci.3956-16.2017 (2017).

119 Clarke, L. E. *et al.* Normal aging induces A1-like astrocyte reactivity. *Proceedings of the National Academy of Sciences of the United States of America* **115**, E1896-e1905, doi:10.1073/pnas.1800165115 (2018).

120 Chai, H. *et al.* Neural Circuit-Specialized Astrocytes: Transcriptomic, Proteomic, Morphological, and Functional Evidence. *Neuron* **95**, 531-549.e539, doi:10.1016/j.neuron.2017.06.029 (2017).

121 Xin, W. *et al.* Ventral midbrain astrocytes display unique physiological features and sensitivity to dopamine D2 receptor signaling. *Neuropsychopharmacology : official publication of the American College of Neuropsychopharmacology* **44**, 344-355, doi:10.1038/s41386-018-0151-4 (2019).

122 Liddelow, S. A. *et al.* Neurotoxic reactive astrocytes are induced by activated microglia. *Nature* **541**, 481-487, doi:10.1038/nature21029 (2017).

123 Miller, S. J. Astrocyte Heterogeneity in the Adult Central Nervous System. *Frontiers in cellular neuroscience* **12**, 401, doi:10.3389/fncel.2018.00401 (2018).

124 Awasaki, T., Lai, S. L., Ito, K. & Lee, T. Organization and postembryonic development of glial cells in the adult central brain of Drosophila. *The Journal of neuroscience : the official journal of the Society for Neuroscience* **28**, 13742-13753, doi:10.1523/JNEUROSCI.4844-08.2008 [doi] (2008).

125 Kremer, M. C., Jung, C., Batelli, S., Rubin, G. M. & Gaul, U. The glia of the adult Drosophila nervous system. *Glia* **65**, 606-638, doi:10.1002/glia.23115 [doi] (2017).

126 Stork, T., Bernardos, R. & Freeman, M. R. Analysis of glial cell development and function in Drosophila. *Cold Spring Harbor protocols* **2012**, 1-17, doi:10.1101/pdb.top067587 (2012).

127 Speder, P. & Brand, A. H. Systemic and local cues drive neural stem cell niche remodelling during neurogenesis in Drosophila. *eLife* **7**, doi:10.7554/eLife.30413 (2018).

128 Volkenhoff, A. *et al.* Glial Glycolysis Is Essential for Neuronal Survival in Drosophila. *Cell metabolism* **22**, 437-447, doi:10.1016/j.cmet.2015.07.006 [doi] (2015).

129 Delgado, M. G. *et al.* Chaski, a novel Drosophila lactate/pyruvate transporter required in glia cells for survival under nutritional stress. *Scientific reports* **8**, 1186, doi:10.1038/s41598-018-19595-5 (2018).

130 Lee, Y. *et al.* Oligodendroglia metabolically support axons and contribute to neurodegeneration. *Nature* **487**, 443-448, doi:10.1038/nature11314 [doi] (2012).

131 Suzuki, A. *et al.* Astrocyte-neuron lactate transport is required for long-term memory formation. *Cell* **144**, 810-823, doi:10.1016/j.cell.2011.02.018 (2011).

132 Newman, L. A., Korol, D. L. & Gold, P. E. Lactate produced by glycogenolysis in astrocytes regulates memory processing. *PloS one* **6**, e28427, doi:10.1371/journal.pone.0028427 (2011).

133 Melom, J. E. & Littleton, J. T. Mutation of a NCKX eliminates glial microdomain calcium oscillations and enhances seizure susceptibility. *The Journal of neuroscience : the official journal of the Society for Neuroscience* **33**, 1169-1178, doi:10.1523/JNEUROSCI.3920-12.2013 [doi] (2013).

134 Li, X. F. *et al.* Importance of K+-dependent Na+/Ca2+-exchanger 2, NCKX2, in motor learning and memory. *The Journal of biological chemistry* **281**, 6273-6282, doi:10.1074/jbc.M512137200 (2006).

135 Schnetkamp, P. P. The SLC24 Na+/Ca2+-K+ exchanger family: vision and beyond. *Pflugers Archiv : European journal of physiology* **447**, 683-688, doi:10.1007/s00424-003-1069-0 (2004).

136 Tashiro, A., Goldberg, J. & Yuste, R. Calcium oscillations in neocortical astrocytes under epileptiform conditions. *Journal of neurobiology* **50**, 45-55 (2002).

137 Gomez-Gonzalo, M. *et al.* An excitatory loop with astrocytes contributes to drive neurons to seizure threshold. *PLoS biology* **8**, e1000352, doi:10.1371/journal.pbio.1000352 (2010).

138 Tian, G. F. *et al.* An astrocytic basis of epilepsy. *Nature medicine* **11**, 973-981, doi:10.1038/nm1277 (2005).

139 Kunduri, G. *et al.* Defective cortex glia plasma membrane structure underlies light-induced epilepsy in cpes mutants. *Proceedings of the National Academy of Sciences of the United States of America* **115**, E8919-e8928, doi:10.1073/pnas.1808463115 (2018).

140 Yildirim, K., Petri, J., Kottmeier, R. & Klambt, C. Drosophila glia: Few cell types and many conserved functions. *Glia* **67**, 5-26, doi:10.1002/glia.23459 (2019).

141 MacNamee, S. E. *et al.* Astrocytic glutamate transport regulates a Drosophila CNS synapse that lacks astrocyte ensheathment. *The Journal of comparative neurology* **524**, 1979-1998, doi:10.1002/cne.24016 [doi] (2016).

142 Freeman, M. R., Delrow, J., Kim, J., Johnson, E. & Doe, C. Q. Unwrapping glial biology: Gcm target genes regulating glial development, diversification, and function. *Neuron* **38**, 567-580, doi:S0896627303002897 [pii] (2003).

143 Stork, T., Sheehan, A., Tasdemir-Yilmaz, O. E. & Freeman, M. R. Neuron-glia interactions through the Heartless FGF receptor signaling pathway mediate morphogenesis of Drosophila astrocytes. *Neuron* **83**, 388-403, doi:10.1016/j.neuron.2014.06.026 [doi] (2014).

144 Rival, T. *et al.* Decreasing glutamate buffering capacity triggers oxidative stress and neuropil degeneration in the Drosophila brain. *Current biology : CB* **14**, 599-605, doi:10.1016/j.cub.2004.03.039 (2004).

145 Cho, S., Muthukumar, A. K., Stork, T., Coutinho-Budd, J. C. & Freeman, M. R. Focal adhesion molecules regulate astrocyte morphology and glutamate transporters to suppress seizure-like behavior. *Proceedings of the National Academy of Sciences of the United States of America* **115**, 11316-11321, doi:10.1073/pnas.1800830115 (2018).

146 Zhang, Y. V., Ormerod, K. G. & Littleton, J. T. Astrocyte Ca2+ Influx Negatively Regulates Neuronal Activity. *eNeuro* **4**, 10.1523/ENEURO.0340-1516.2017. eCollection 2017 Mar-Apr, doi:ENEURO.0340-16.2017 [pii] (2017).

147 Muthukumar, A. K., Stork, T. & Freeman, M. R. Activity-dependent regulation of astrocyte GAT levels during synaptogenesis. *Nature neuroscience* **17**, 1340-1350, doi:10.1038/nn.3791 (2014).

148 Jen, J. C., Wan, J., Palos, T. P., Howard, B. D. & Baloh, R. W. Mutation in the glutamate transporter EAAT1 causes episodic ataxia, hemiplegia, and seizures. *Neurology* **65**, 529-534, doi:10.1212/01.wnl.0000172638.58172.5a (2005).

149 Carvill, G. L. *et al.* Mutations in the GABA Transporter SLC6A1 Cause Epilepsy with Myoclonic-Atonic Seizures. *American journal of human genetics* **96**, 808-815, doi:10.1016/j.ajhg.2015.02.016 (2015).

150 Danjo, R., Kawasaki, F. & Ordway, R. W. A tripartite synapse model in Drosophila. *PloS one* **6**, e17131, doi:10.1371/journal.pone.0017131 [doi] (2011).

151 Ding, F. *et al.* alpha1-Adrenergic receptors mediate coordinated Ca2+ signaling of cortical astrocytes in awake, behaving mice. *Cell calcium* **54**, 387-394, doi:10.1016/j.ceca.2013.09.001 (2013).

152 Srinivasan, R. *et al.* Ca(2+) signaling in astrocytes from Ip3r2(-/-) mice in brain slices and during startle responses in vivo. *Nature neuroscience* **18**, 708-717, doi:10.1038/nn.4001 (2015).

153 Holcroft, C. E. *et al.* Innexins Ogre and Inx2 are required in glial cells for normal postembryonic development of the Drosophila central nervous system. *Journal of cell science* **126**, 3823-3834, doi:10.1242/jcs.117994 (2013).

154 Li, Y. X., Sibon, O. C. M. & Dijkers, P. F. Inhibition of NF-kappaB in astrocytes is sufficient to delay neurodegeneration induced by proteotoxicity in neurons. *Journal of neuroinflammation* **15**, 261, doi:10.1186/s12974-018-1278-2 (2018).

155 Yang, Y. & Jackson, R. Astrocyte identity: evolutionary perspectives on astrocyte functions and heterogeneity. *Current opinion in neurobiology* **56**, 40-46, doi:10.1016/j.conb.2018.11.006 (2018).

156 Edwards, T. N., Nuschke, A. C., Nern, A. & Meinertzhagen, I. A. Organization and metamorphosis of glia in the Drosophila visual system. *The Journal of comparative neurology* **520**, 2067-2085, doi:10.1002/cne.23071 (2012).

157 Richier, B., Vijandi, C. M., Mackensen, S. & Salecker, I. Lapsyn controls branch extension and positioning of astrocyte-like glia in the Drosophila optic lobe. *Nature communications* **8**, 317, doi:10.1038/s41467-017-00384-z (2017).

158 Korbo, L. Glial cell loss in the hippocampus of alcoholics. *Alcoholism, clinical and experimental research* **23**, 164-168 (1999).

159 Miguel-Hidalgo, J. J. *et al.* Glia pathology in the prefrontal cortex in alcohol dependence with and without depressive symptoms. *Biological psychiatry* **52**, 1121-1133 (2002).

160 Miguel-Hidalgo, J. J. Withdrawal from free-choice ethanol consumption results in increased packing density of glutamine synthetase-immunoreactive astrocytes in the prelimbic cortex of alcohol-preferring rats. *Alcohol and Alcoholism (Oxford, Oxfordshire)* **41**, 379-385, doi:agl006 [pii] (2006).

161 Cullen, K. M. & Halliday, G. M. Chronic alcoholics have substantial glial pathology in the forebrain and diencephalon. *Alcohol and alcoholism (Oxford, Oxfordshire). Supplement* **2**, 253-257 (1994).

162 Miguel-Hidalgo, J. J. *et al.* Reduced connexin 43 immunolabeling in the orbitofrontal cortex in alcohol dependence and depression. *Journal of psychiatric research* **55**, 101-109, doi:10.1016/j.jpsychires.2014.04.007 (2014).

163 Lewohl, J. M. *et al.* Gene expression in human alcoholism: microarray analysis of frontal cortex. *Alcoholism, clinical and experimental research* **24**, 1873-1882 (2000).

164 Liu, J. *et al.* Patterns of gene expression in the frontal cortex discriminate alcoholic from nonalcoholic individuals. *Neuropsychopharmacology : official publication of the American College of Neuropsychopharmacology* **31**, 1574-1582, doi:10.1038/sj.npp.1300947 (2006).

165 Mayfield, R. D. *et al.* Patterns of gene expression are altered in the frontal and motor cortices of human alcoholics. *Journal of neurochemistry* **81**, 802-813 (2002).

166 Aschner, M., Mutkus, L. A. & Allen, J. W. Amino acid uptake and release in primary astrocyte cultures exposed to ethanol. *Annals of the New York Academy of Sciences* **939**, 23-27 (2001).

167 Smith, T. L. & Navratilova, E. Increased calcium/calmodulin protein kinase activity in astrocytes chronically exposed to ethanol: influences on glutamate transport. *Neuroscience letters* **269**, 145-148 (1999).

168 Smith, T. L. & Navratilova, E. The effect of ethanol exposure on mitogen-activated protein kinase activity and expression in cultured rat astrocytes. *Neuroscience letters* **341**, 91-94 (2003).

169 Aal-Aaboda, M., Alhaddad, H., Osowik, F., Nauli, S. M. & Sari, Y. Effects of (R)-(-)-5-methyl-1-nicotinoyl-2-pyrazoline on glutamate transporter 1 and cysteine/glutamate exchanger as well as ethanol drinking behavior in male,

alcohol-preferring rats. *Journal of neuroscience research* **93**, 930-937, doi:10.1002/jnr.23554 (2015).

170 Sari, Y. Potential therapeutic role of glutamate transporter 1 for the treatment of alcohol dependence. *OA alcohol* **1**, 6 (2013).

171 Zink, M., Schmitt, A., Vengeliene, V., Henn, F. A. & Spanagel, R. Ethanol induces expression of the glutamate transporters EAAT1 and EAAT2 in organotypic cortical slice cultures. *Alcoholism, clinical and experimental research* **28**, 1752-1757 (2004).

172 Karlsson, R. M. *et al.* Reduced alcohol intake and reward associated with impaired endocannabinoid signaling in mice with a deletion of the glutamate transporter GLAST. *Neuropharmacology* **63**, 181-189, doi:10.1016/j.neuropharm.2012.01.027 (2012).

173 Smith, K. L. *et al.* Exploring the role of central astrocytic glutamate uptake in ethanol reward in mice. *Alcoholism, clinical and experimental research* **38**, 1307-1314, doi:10.1111/acer.12361 (2014).

174 Lebourgeois, S., Gonzalez-Marin, M. C., Jeanblanc, J., Naassila, M. & Vilpoux, C. Effect of N-acetylcysteine on motivation, seeking and relapse to ethanol self-administration. *Addiction biology* **23**, 643-652, doi:10.1111/adb.12521 (2018).

175 Hakami, A. Y. & Sari, Y. beta-Lactamase inhibitor, clavulanic acid, attenuates ethanol intake and increases glial glutamate transporters expression in alcohol preferring rats. *Neuroscience letters* **657**, 140-145, doi:10.1016/j.neulet.2017.08.013 (2017).

176 Alhaddad, H. *et al.* Effects of MS-153 on chronic ethanol consumption and GLT1 modulation of glutamate levels in male alcohol-preferring rats. *Frontiers in behavioral neuroscience* **8**, 366, doi:10.3389/fnbeh.2014.00366 (2014).

177 Sari, Y., Toalston, J. E., Rao, P. S. S. & Bell, R. L. Effects of ceftriaxone on ethanol, nicotine or sucrose intake by alcohol-preferring (P) rats and its association with GLT-1 expression. *Neuroscience* **326**, 117-125, doi:10.1016/j.neuroscience.2016.04.004 (2016).

178 Erickson, E. K., Farris, S. P., Blednov, Y. A., Mayfield, R. D. & Harris, R. A. Astrocyte-specific transcriptome responses to chronic ethanol consumption. *The pharmacogenomics journal* **18**, 578-589, doi:10.1038/s41397-017-0012-2 (2018).

179 Allen, J. W., Mutkus, L. A. & Aschner, M. Chronic ethanol produces increased taurine transport and efflux in cultured astrocytes. *Neurotoxicology* **23**, 693-700, doi:10.1016/s0161-813x(02)00027-x (2002).

180 Allansson, L., Khatibi, S., Olsson, T. & Hansson, E. Acute ethanol exposure induces [Ca2+]i transients, cell swelling and transformation of actin cytoskeleton in astroglial primary cultures. *Journal of neurochemistry* **76**, 472-479 (2001).

181 Locovei, S., Wang, J. & Dahl, G. Activation of pannexin 1 channels by ATP through P2Y receptors and by cytoplasmic calcium. *FEBS letters* **580**, 239-244, doi:10.1016/j.febslet.2005.12.004 (2006).

182 Gomez, G. I. *et al.* Heavy Alcohol Exposure Activates Astroglial Hemichannels and Pannexons in the Hippocampus of Adolescent Rats: Effects on Neuroinflammation and Astrocyte Arborization. *Frontiers in cellular neuroscience* **12**, 472, doi:10.3389/fncel.2018.00472 (2018).

183 Bull, C. *et al.* Rat nucleus accumbens core astrocytes modulate reward and the motivation to self-administer ethanol after abstinence. *Neuropsychopharmacology : official publication of the American College of Neuropsychopharmacology* **39**, 2835-2845, doi:10.1038/npp.2014.135 [doi] (2014).

184 Franklin, K. M. *et al.* P2X4 receptors (P2X4Rs) represent a novel target for the development of drugs to prevent and/or treat alcohol use disorders. *Frontiers in neuroscience* **8**, 176, doi:10.3389/fnins.2014.00176 (2014).

185 Wu, J., Lee, M. R., Choi, S., Kim, T. & Choi, D. S. ENT1 regulates ethanol-sensitive EAAT2 expression and function in astrocytes. *Alcoholism, clinical and experimental research* **34**, 1110-1117, doi:10.1111/j.1530-0277.2010.01187.x (2010).

186 Alfonso-Loeches, S., Pascual-Lucas, M., Blanco, A. M., Sanchez-Vera, I. & Guerri, C. Pivotal role of TLR4 receptors in alcohol-induced neuroinflammation and brain damage. *The Journal of neuroscience : the official journal of the Society for Neuroscience* **30**, 8285-8295, doi:10.1523/jneurosci.0976-10.2010 (2010).

187 Blanco, A. M., Pascual, M., Valles, S. L. & Guerri, C. Ethanol-induced iNOS and COX-2 expression in cultured astrocytes via NF-kappa B. *Neuroreport* **15**, 681-685 (2004).

188 Blanco, A. M., Valles, S. L., Pascual, M. & Guerri, C. Involvement of TLR4/type I IL-1 receptor signaling in the induction of inflammatory mediators and cell death induced by ethanol in cultured astrocytes. *Journal of immunology (Baltimore, Md. : 1950)* **175**, 6893-6899 (2005).

189 Avila, D. V. *et al.* Phosphodiesterase 4b expression plays a major role in alcohol-induced neuro-inflammation. *Neuropharmacology* **125**, 376-385, doi:10.1016/j.neuropharm.2017.08.011 (2017).

190 Lawrimore, C. J., Coleman, L. G. & Crews, F. T. Ethanol induces interferon expression in neurons via TRAIL: role of astrocyte-to-neuron signaling. *Psychopharmacology*, doi:10.1007/s00213-018-5153-8 (2019).

191 Erickson, E. K., Grantham, E. K., Warden, A. S. & Harris, R. A. Neuroimmune signaling in alcohol use disorder. *Pharmacology, biochemistry, and behavior* **177**, 34-60, doi:10.1016/j.pbb.2018.12.007 (2019).

192 Kane, C. J. *et al.* Effects of ethanol on immune response in the brain: region-specific changes in aged mice. *Journal of neuroinflammation* **10**, 66, doi:10.1186/1742-2094-10-66 (2013).

193 Kane, C. J. *et al.* Effects of ethanol on immune response in the brain: region-specific changes in adolescent versus adult mice. *Alcoholism, clinical and experimental research* **38**, 384-391, doi:10.1111/acer.12244 (2014).

194 Bray, J. G., Roberts, A. J. & Gruol, D. L. Transgenic mice with increased astrocyte expression of CCL2 show altered behavioral effects of alcohol. *Neuroscience* **354**, 88-100, doi:10.1016/j.neuroscience.2017.04.009 (2017).

195 Tang, Y. & Le, W. Differential Roles of M1 and M2 Microglia in Neurodegenerative Diseases. *Molecular neurobiology* **53**, 1181-1194, doi:10.1007/s12035-014-9070-5 (2016).

196 He, J. & Crews, F. T. Increased MCP-1 and microglia in various regions of the human alcoholic brain. *Experimental neurology* **210**, 349-358, doi:10.1016/j.expneurol.2007.11.017 (2008).

197 Henriques, J. F. *et al.* Microglia and alcohol meet at the crossroads: Microglia as critical modulators of alcohol neurotoxicity. *Toxicology letters* **283**, 21-31, doi:10.1016/j.toxlet.2017.11.002 (2018).

198 Barton, E. A., Baker, C. & Leasure, J. L. Investigation of Sex Differences in the Microglial Response to Binge Ethanol and Exercise. *Brain sciences* **7**, doi:10.3390/brainsci7100139 (2017).

199 Zhao, Y. N. *et al.* Activated microglia are implicated in cognitive deficits, neuronal death, and successful recovery following intermittent ethanol exposure. *Behavioural brain research* **236**, 270-282, doi:10.1016/j.bbr.2012.08.052 [doi] (2013).

200 McCarthy, G. M., Farris, S. P., Blednov, Y. A., Harris, R. A. & Mayfield, R. D. Microglial-specific transcriptome changes following chronic alcohol consumption. *Neuropharmacology* **128**, 416-424, doi:10.1016/j.neuropharm.2017.10.035 (2018).

201 Marshall, S. A. *et al.* Microglial activation is not equivalent to neuroinflammation in alcohol-induced neurodegeneration: The importance of microglia phenotype. *Neurobiology of disease* **54**, 239-251, doi:10.1016/j.nbd.2012.12.016 (2013).

202 Fernandez-Lizarbe, S., Montesinos, J. & Guerri, C. Ethanol induces TLR4/TLR2 association, triggering an inflammatory response in microglial cells. *Journal of neurochemistry* **126**, 261-273, doi:10.1111/jnc.12276 (2013).

203 Qin, L. & Crews, F. T. NADPH oxidase and reactive oxygen species contribute to alcohol-induced microglial activation and neurodegeneration. *Journal of neuroinflammation* **9**, 5, doi:10.1186/1742-2094-9-5 (2012).

204 Agrawal, R. G., Hewetson, A., George, C. M., Syapin, P. J. & Bergeson, S. E. Minocycline reduces ethanol drinking. *Brain, behavior, and immunity* **25 Suppl 1**, S165-169, doi:10.1016/j.bbi.2011.03.002 (2011).

205 Gajbhiye, S. V., Tripathi, R. K., Petare, A., Potey, A. V. & Shankar, A. Minocycline in Alcohol Withdrawal Induced Anxiety and Alcohol Relapse in Rats. *Current clinical pharmacology* **13**, 65-72, doi:10.2174/1574884713666180228110310 (2018).

206 Walter, T. J., Vetreno, R. P. & Crews, F. T. Alcohol and Stress Activation of Microglia and Neurons: Brain Regional Effects. *Alcoholism, clinical and experimental research* **41**, 2066-2081, doi:10.1111/acer.13511 (2017).

207 Miguel-Hidalgo, J. J. Molecular Neuropathology of Astrocytes and Oligodendrocytes in Alcohol Use Disorders. *Frontiers in molecular neuroscience* **11**, 78, doi:10.3389/fnmol.2018.00078 (2018).

208 Lewohl, J. M., Wixey, J., Harper, C. G. & Dodd, P. R. Expression of MBP, PLP, MAG, CNP, and GFAP in the Human Alcoholic Brain. *Alcoholism, clinical and experimental research* **29**, 1698-1705 (2005).

209 Samantaray, S. *et al.* Chronic intermittent ethanol induced axon and myelin degeneration is attenuated by calpain inhibition. *Brain research* **1622**, 7-21, doi:10.1016/j.brainres.2015.06.014 (2015).

210 Coutts, D. J. & Harrison, N. L. Acetaldehyde, not ethanol, impairs myelin formation and viability in primary mouse oligodendrocytes. *Alcoholism, clinical and experimental research* **39**, 455-462, doi:10.1111/acer.12642 (2015).

211 Bainton, R. J. *et al.* moody encodes two GPCRs that regulate cocaine behaviors and blood-brain barrier permeability in Drosophila. *Cell* **123**, 145-156, doi:S0092-8674(05)00760-9 [pii] (2005).

212 Parkhurst, S. J. *et al.* Perineurial Barrier Glia Physically Respond to Alcohol in an Akap200-Dependent Manner to Promote Tolerance. *Cell reports* **22**, 1647-1656, doi:10.1016/j.celrep.2018.01.049 (2018).

213 Stork, T. *et al.* Organization and function of the blood-brain barrier in Drosophila. *The Journal of neuroscience : the official journal of the Society for Neuroscience* **28**, 587-597, doi:10.1523/JNEUROSCI.4367-07.2008 [doi] (2008).

214 Chan, R. F. *et al.* Contrasting influences of Drosophila white/mini-white on ethanol sensitivity in two different behavioral assays. *Alcoholism, clinical and experimental research* **38**, 1582-1593, doi:10.1111/acer.12421 [doi] (2014).

215 Sandhu, S., Kollah, A. P., Lewellyn, L., Chan, R. F. & Grotewiel, M. An inexpensive, scalable behavioral assay for measuring ethanol sedation sensitivity and rapid tolerance in Drosophila. *Journal of visualized experiments : JoVE* **(98). doi**, 10.3791/52676, doi:10.3791/52676 [doi] (2015).

216 Wu, J. S. & Luo, L. A protocol for dissecting Drosophila melanogaster brains for live imaging or immunostaining. *Nature protocols* **1**, 2110-2115, doi:nprot.2006.336 [pii] (2006).

217 Martin, I. *et al.* Sod2 knockdown in the musculature has whole-organism consequences in Drosophila. *Free radical biology & medicine* **47**, 803-813, doi:10.1016/j.freeradbiomed.2009.06.021 [doi] (2009).

218 Kondo, S., Booker, M. & Perrimon, N. Cross-species RNAi rescue platform in Drosophila melanogaster. *Genetics* **183**, 1165-1173, doi:10.1534/genetics.109.106567 (2009).

219 Kim, J. H. *et al.* Functional role of the polymorphic 647 T/C variant of ENT1 (SLC29A1) and its association with alcohol withdrawal seizures. *PloS one* **6**, e16331, doi:10.1371/journal.pone.0016331 [doi] (2011).

220 Vetreno, R. P. & Crews, F. T. Adolescent binge drinking increases expression of the danger signal receptor agonist HMGB1 and Toll-like receptors in the adult prefrontal cortex. *Neuroscience* **226**, 475-488, doi:10.1016/j.neuroscience.2012.08.046 [doi] (2012).

221 Song, C. & Zhang, H. TARV: tree-based analysis of rare variants identifying risk modifying variants in CTNNA2 and CNTNAP2 for alcohol addiction. *Genetic epidemiology* **38**, 552-559, doi:10.1002/gepi.21843 [doi] (2014).

222 Bai, L. *et al.* A Conserved Circadian Function for the Neurofibromatosis 1 Gene. *Cell reports* **22**, 3416-3426, doi:10.1016/j.celrep.2018.03.014 (2018).

223 Ford, D. *et al.* Alteration of Drosophila life span using conditional, tissue-specific expression of transgenes triggered by doxycyline or RU486/Mifepristone. *Experimental gerontology* **42**, 483-497, doi:10.1016/j.exger.2007.01.004 (2007).

224 Yamada, R. *et al.* Mifepristone Reduces Food Palatability and Affects Drosophila Feeding and Lifespan. *The journals of gerontology. Series A, Biological sciences and medical sciences* **72**, 173-180, doi:10.1093/gerona/glw072 (2017).

225 Schuckit, M. A. Low level of response to alcohol as a predictor of future alcoholism. *The American journal of psychiatry* **151**, 184-189, doi:10.1176/ajp.151.2.184 [doi] (1994).

226 Grotewiel, M. & Bettinger, J. C. Drosophila and Caenorhabditis elegans as Discovery Platforms for Genes Involved in Human Alcohol Use Disorder. *Alcoholism, clinical and experimental research* **39**, 1292-1311, doi:10.1111/acer.12785 [doi] (2015).

227 Park, A., Ghezzi, A., Wijesekera, T. P. & Atkinson, N. S. Genetics and genomics of alcohol responses in Drosophila. *Neuropharmacology* **122**, 22-35, doi:S0028-3908(17)30038-2 [pii] (2017).

228 Ou, J., Gao, Z., Song, L. & Ho, M. S. Analysis of Glial Distribution in Drosophila Adult Brains. *Neuroscience bulletin* **32**, 162-170, doi:10.1007/s12264-016-0014-0 [doi] (2016).

229 Logan, M. A. Glial contributions to neuronal health and disease: new insights from Drosophila. *Current opinion in neurobiology* **47**, 162-167, doi:S0959-4388(17)30072-7 [pii] (2017).

230 Limmer, S., Weiler, A., Volkenhoff, A., Babatz, F. & Klambt, C. The Drosophila blood-brain barrier: development and function of a glial endothelium. *Frontiers in neuroscience* **8**, 365, doi:10.3389/fnins.2014.00365 [doi] (2014).

231 Pereanu, W., Spindler, S., Cruz, L. & Hartenstein, V. Tracheal development in the Drosophila brain is constrained by glial cells. *Developmental biology* **302**, 169-180, doi:S0012-1606(06)01223-1 [pii] (2007).

232 Liu, H. *et al.* Astrocyte-like glial cells physiologically regulate olfactory processing through the modification of ORN-PN synaptic strength in Drosophila. *The European journal of neuroscience* **40**, 2744-2754, doi:10.1111/ejn.12646 [doi] (2014).

233 Deshapriya, R. M. *et al.* Drosophila CTLA-2-like protein (D/CTLA-2) inhibits cysteine proteinase 1 (CP1), a cathepsin L-like enzyme. *Zoological Science* **24**, 21-30, doi:JST.JSTAGE/zsj/24.21 [pii] (2007).

234 Fernandes, V. M., Chen, Z., Rossi, A. M., Zipfel, J. & Desplan, C. Glia relay differentiation cues to coordinate neuronal development in Drosophila. *Science (New York, N.Y.)* **357**, 886-891, doi:10.1126/science.aan3174 [doi] (2017).

235 Isaacman-Beck, J. & Clandinin, T. R. Glia put visual map in sync. *Science (New York, N.Y.)* **357**, 867-868, doi:10.1126/science.aao2991 [doi] (2017).

236 Zwarts, L., Van Eijs, F. & Callaerts, P. Glia in Drosophila behavior. *Journal of comparative physiology.A, Neuroethology, sensory, neural, and behavioral physiology* **201**, 879-893, doi:10.1007/s00359-014-0952-9 [doi] (2015).

237 Dong, Q., Brenneman, B., Fields, C. & Srivastava, A. A Cathepsin-L is required for invasive behavior during Air Sac Primordium development in Drosophila melanogaster. *FEBS letters* **589**, 3090-3097, doi:10.1016/j.febslet.2015.08.036 [doi] (2015).

238 Kinser, R. D. & Dolph, P. J. Cathepsin proteases mediate photoreceptor cell degeneration in Drosophila. *Neurobiology of disease* **46**, 655-662, doi:10.1016/j.nbd.2012.03.004 [doi] (2012).

239 Lyons, G. R., Andersen, R. O., Abdi, K., Song, W. S. & Kuo, C. T. Cysteine proteinase-1 and cut protein isoform control dendritic innervation of two distinct sensory fields by a single neuron. *Cell reports* **6**, 783-791, doi:10.1016/j.celrep.2014.02.003 [doi] (2014).

240 Tryselius, Y. & Hultmark, D. Cysteine proteinase 1 (CP1), a cathepsin L-like enzyme expressed in the Drosophila melanogaster haemocyte cell line mbn-2. *Insect molecular biology* **6**, 173-181 (1997).

241 Gray, Y. H., Sved, J. A., Preston, C. R. & Engels, W. R. Structure and associated mutational effects of the cysteine proteinase (CP1) gene of Drosophila melanogaster. *Insect molecular biology* **7**, 291-293 (1998).

242 Mohamed, M. M. & Sloane, B. F. Cysteine cathepsins: multifunctional enzymes in cancer. *Nature reviews.Cancer* **6**, 764-775, doi:nrc1949 [pii] (2006).

243 Schwartz, M. K. Tissue cathepsins as tumor markers. *Clinica chimica acta; international journal of clinical chemistry* **237**, 67-78, doi:0009-8981(95)06065-L [pii] (1995).

244 Cermak, S. *et al.* Loss of Cathepsin B and L Leads to Lysosomal Dysfunction, NPC-Like Cholesterol Sequestration and Accumulation of the Key Alzheimer's Proteins. *PloS one* **11**, e0167428, doi:10.1371/journal.pone.0167428 [doi] (2016).

245 Dietzl, G. *et al.* A genome-wide transgenic RNAi library for conditional gene inactivation in Drosophila. *Nature* **448**, 151-156, doi:nature05954 [pii] (2007).

246 Perkins, L. A. *et al.* The Transgenic RNAi Project at Harvard Medical School: Resources and Validation. *Genetics* **201**, 843-852, doi:10.1534/genetics.115.180208 [doi] (2015).

247 Gramates, L. S. *et al.* FlyBase at 25: looking to the future. *Nucleic acids research* **45**, D663-D671, doi:10.1093/nar/gkw1016 [doi] (2017).

248 Schmidt, I. *et al.* Kinesin heavy chain function in Drosophila glial cells controls neuronal activity. *The Journal of neuroscience : the official journal of the Society for Neuroscience* **32**, 7466-7476, doi:10.1523/jneurosci.0349-12.2012 (2012).

249 Adermark, L. & Bowers, M. S. Disentangling the Role of Astrocytes in Alcohol Use Disorder. *Alcoholism, clinical and experimental research* **40**, 1802-1816, doi:10.1111/acer.13168 [doi] (2016).

250 Blednov, Y. A. *et al.* Neuroimmune regulation of alcohol consumption: behavioral validation of genes obtained from genomic studies. *Addiction biology* **17**, 108-120, doi:10.1111/j.1369-1600.2010.00284.x [doi] (2012).

251 Miguel-Hidalgo, J., Shoyama, Y. & Wanzo, V. Infusion of gliotoxins or a gap junction blocker in the prelimbic cortex increases alcohol preference in Wistar rats. *Journal of psychopharmacology (Oxford, England)* **23**, 550-557, doi:10.1177/0269881108091074 [doi] (2009).

252 Jin, E. J. *et al.* Live Observation of Two Parallel Membrane Degradation Pathways at Axon Terminals. *Current biology : CB* **28**, 1027-1038.e1024, doi:10.1016/j.cub.2018.02.032 (2018).

253 Conus, S. & Simon, H. U. Cathepsins: key modulators of cell death and inflammatory responses. *Biochemical pharmacology* **76**, 1374-1382, doi:10.1016/j.bcp.2008.07.041 [doi] (2008).

254 Kanbak, G. *et al.* Preventive role of gallic acid on alcohol dependent and cysteine protease-mediated pancreas injury. *Molecular biology reports* **39**, 10249-10255, doi:10.1007/s11033-012-1901-8 [doi] (2012).

255 Mir, R. A. & Chauhan, S. S. Down regulation of a matrix degrading cysteine protease cathepsin L, by acetaldehyde: role of C/EBPalpha. *PloS one* **6**, e20768, doi:10.1371/journal.pone.0020768 [doi] (2011).

256 Thrower, E. C., Gorelick, F. S. & Husain, S. Z. Molecular and cellular mechanisms of pancreatic injury. *Current opinion in gastroenterology* **26**, 484-489, doi:10.1097/MOG.0b013e32833d119e [doi] (2010).

257 Funkelstein, L., Beinfeld, M., Minokadeh, A., Zadina, J. & Hook, V. Unique biological function of cathepsin L in secretory vesicles for biosynthesis of neuropeptides. *Neuropeptides* **44**, 457-466, doi:10.1016/j.npep.2010.08.003 [doi] (2010).

258 Ubink, R., Calza, L. & Hokfelt, T. 'Neuro'-peptides in glia: focus on NPY and galanin. *Trends in neurosciences* **26**, 604-609, doi:S0166-2236(03)00285-6 [pii] (2003).

259 Shohat-Ophir, G., Kaun, K. R., Azanchi, R., Mohammed, H. & Heberlein, U. Sexual deprivation increases ethanol intake in Drosophila. *Science (New York, N.Y.)* **335**, 1351-1355, doi:10.1126/science.1215932 [doi] (2012).

260 Bull, C., Syed, W. A., Minter, S. C. & Bowers, M. S. Differential response of glial fibrillary acidic protein-positive astrocytes in the rat prefrontal cortex following

ethanol self-administration. *Alcoholism, clinical and experimental research* **39**, 650-658, doi:10.1111/acer.12683 [doi] (2015).

261 McGuire, S. E., Roman, G. & Davis, R. L. Gene expression systems in Drosophila: a synthesis of time and space. *Trends in genetics : TIG* **20**, 384-391, doi:10.1016/j.tig.2004.06.012 [doi] (2004).

262 Cole, S. H. *et al.* Two functional but noncomplementing Drosophila tyrosine decarboxylase genes: distinct roles for neural tyramine and octopamine in female fertility. *The Journal of biological chemistry* **280**, 14948-14955, doi:M414197200 [pii] (2005).

263 Ng, F. S. & Jackson, F. R. The ROP vesicle release factor is required in adult Drosophila glia for normal circadian behavior. *Frontiers in cellular neuroscience* **9**, 256, doi:10.3389/fncel.2015.00256 [doi] (2015).

264 Ng, F. S. *et al.* TRAP-seq Profiling and RNAi-Based Genetic Screens Identify Conserved Glial Genes Required for Adult Drosophila Behavior. *Frontiers in molecular neuroscience* **9**, 146, doi:10.3389/fnmol.2016.00146 [doi] (2016).

265 Huang, Y., Ainsley, J. A., Reijmers, L. G. & Jackson, F. R. Translational profiling of clock cells reveals circadianly synchronized protein synthesis. *PLoS biology* **11**, e1001703, doi:10.1371/journal.pbio.1001703 [doi] (2013).

266 McDonald, J. H. & Dunn, K. W. Statistical tests for measures of colocalization in biological microscopy. *Journal of microscopy* **252**, 295-302, doi:10.1111/jmi.12093 (2013).

267 Hardie, S. L., Zhang, J. X. & Hirsh, J. Trace amines differentially regulate adult locomotor activity, cocaine sensitivity, and female fertility in Drosophila melanogaster. *Developmental neurobiology* **67**, 1396-1405, doi:10.1002/dneu.20459 (2007).

268 Wu, C. L., Shih, M. F., Lee, P. T. & Chiang, A. S. An octopamine-mushroom body circuit modulates the formation of anesthesia-resistant memory in Drosophila. *Current biology : CB* **23**, 2346-2354, doi:10.1016/j.cub.2013.09.056 [doi] (2013).

269 Ohhara, Y. *et al.* Autocrine regulation of ecdysone synthesis by beta3-octopamine receptor in the prothoracic gland is essential for Drosophila metamorphosis. *Proceedings of the National Academy of Sciences of the United States of America* **112**, 1452-1457, doi:10.1073/pnas.1414966112 (2015).

270 Schneider, A. *et al.* Neuronal basis of innate olfactory attraction to ethanol in Drosophila. *PloS one* **7**, e52007, doi:10.1371/journal.pone.0052007 (2012).

271 Pathak, T., Agrawal, T., Richhariya, S., Sadaf, S. & Hasan, G. Store-Operated Calcium Entry through Orai Is Required for Transcriptional Maturation of the

Flight Circuit in Drosophila. *The Journal of neuroscience : the official journal of the Society for Neuroscience* **35**, 13784-13799, doi:10.1523/jneurosci.1680-15.2015 (2015).

272 Riemensperger, T. *et al.* A single dopamine pathway underlies progressive locomotor deficits in a Drosophila model of Parkinson disease. *Cell reports* **5**, 952-960, doi:10.1016/j.celrep.2013.10.032 (2013).

273 Huang, J., Liu, W., Qi, Y. X., Luo, J. & Montell, C. Neuromodulation of Courtship Drive through Tyramine-Responsive Neurons in the Drosophila Brain. *Current biology : CB* **26**, 2246-2256, doi:10.1016/j.cub.2016.06.061 [doi] (2016).

274 Martin, C. A. & Krantz, D. E. Drosophila melanogaster as a genetic model system to study neurotransmitter transporters. *Neurochemistry international* **73**, 71-88, doi:10.1016/j.neuint.2014.03.015 [doi] (2014).

275 Romero-Calderon, R. *et al.* A glial variant of the vesicular monoamine transporter is required to store histamine in the Drosophila visual system. *PLoS genetics* **4**, e1000245, doi:10.1371/journal.pgen.1000245 [doi] (2008).

276 Croset, V., Treiber, C. D. & Waddell, S. Cellular diversity in the Drosophila midbrain revealed by single-cell transcriptomics. *eLife* **7**, doi:10.7554/eLife.34550 (2018).

277 Yoon, E. J., Jeong, Y. T., Lee, J. E., Moon, S. J. & Kim, C. H. Tubby domain superfamily protein is required for the formation of the 7S SNARE complex in Drosophila. *Biochemical and biophysical research communications* **482**, 814-820, doi:S0006-291X(16)31991-X [pii] (2017).

278 Sweeney, S. T., Broadie, K., Keane, J., Niemann, H. & O'Kane, C. J. Targeted expression of tetanus toxin light chain in Drosophila specifically eliminates synaptic transmission and causes behavioral defects. *Neuron* **14**, 341-351 (1995).

279 El-Kholy, S. *et al.* Expression analysis of octopamine and tyramine receptors in Drosophila. *Cell and tissue research* **361**, 669-684, doi:10.1007/s00441-015-2137-4 [doi] (2015).

280 Brembs, B., Christiansen, F., Pfluger, H. J. & Duch, C. Flight initiation and maintenance deficits in flies with genetically altered biogenic amine levels. *The Journal of neuroscience : the official journal of the Society for Neuroscience* **27**, 11122-11131, doi:10.1523/jneurosci.2704-07.2007 (2007).

281 Zheng, Z. *et al.* A Complete Electron Microscopy Volume of the Brain of Adult Drosophila melanogaster. *Cell* **174**, 730-743.e722, doi:10.1016/j.cell.2018.06.019 (2018).

282 Miguel-Hidalgo, J. J. The Role of Glial Cells in Drug Abuse. *Current drug abuse reviews* **2**, 76-82 (2009).

283 Xu, M. *et al.* Inhibition of cysteine cathepsin B and L activation in astrocytes contributes to neuroprotection against cerebral ischemia via blocking the tBid-mitochondrial apoptotic signaling pathway. *Glia* **62**, 855-880, doi:10.1002/glia.22645 [doi] (2014).

284 Lee, H. M., Kang, J., Lee, S. J. & Jo, E. K. Microglial activation of the NLRP3 inflammasome by the priming signals derived from macrophages infected with mycobacteria. *Glia* **61**, 441-452, doi:10.1002/glia.22448 [doi] (2013).

285 Pereira, T. D. & Murthy, M. To Fight or Not to Fight. *Neuron* **95**, 986-988, doi:10.1016/j.neuron.2017.08.029 (2017).

286 Fitzgerald, P. J. Elevated Norepinephrine may be a Unifying Etiological Factor in the Abuse of a Broad Range of Substances: Alcohol, Nicotine, Marijuana, Heroin, Cocaine, and Caffeine. *Substance abuse : research and treatment* **7**, 171-183, doi:10.4137/sart.S13019 (2013).

287 Koob, G. F. Neurocircuitry of alcohol addiction: synthesis from animal models. *Handbook of clinical neurology* **125**, 33-54, doi:10.1016/b978-0-444-62619-6.00003-3 (2014).

288 Berry, M. D. Mammalian central nervous system trace amines. Pharmacologic amphetamines, physiologic neuromodulators. *Journal of neurochemistry* **90**, 257-271, doi:10.1111/j.1471-4159.2004.02501.x (2004).

289 Gainetdinov, R. R., Hoener, M. C. & Berry, M. D. Trace Amines and Their Receptors. *Pharmacological reviews* **70**, 549-620, doi:10.1124/pr.117.015305 (2018).

290 Zhang, Y. *et al.* Purification and Characterization of Progenitor and Mature Human Astrocytes Reveals Transcriptional and Functional Differences with Mouse. *Neuron* **89**, 37-53, doi:10.1016/j.neuron.2015.11.013 (2016).

APPENDIX

Basic Fly Handling and Husbandry

A. Standard Fly Lab Lingo:

1. Stock or strain: a culture of flies with a particular genotype. Balanced stocks have a special chromosome called a balancer that is marked with a dominant phenotype and suppresses recombination on the corresponding sister chromosome. Balanced stocks are often weak (i.e. grow poorly).

2. Seeding: putting adult flies into a new bottle or vial. Also called 'setting-up'.

3. Transfer: moving flies without anesthesia from one vial or bottle to another. One-to-one transfer means moving flies from one bottle/vial to one new bottle/vial. Two-to-one transfer means moving flies from 2 vials/bottles to 1 new vial/bottle. Also called 'flipping'.

4. Clearing: removing all of the adults from a bottle or vial. Can be done with or without anesthesia.

5. Anesthesia: CO_2 used to temporarily immobilize flies.

6. Brood: refers to the number of times a set of adults has been used to seed bottles. Using flies for 2 broods is common, with 3 broods being possible in some cases.

7. white plus (w^+): indicates eye color. white minus (w^-) flies have white eyes. w^+ flies have eyes that can vary from light peach to deep red.

8. Food: All of our fly food currently has antibiotics on it (ampicillin, tetracycline and chloramphenicol, ATC). Yeasted (Y) food vials and bottles have live yeast on added. Yeasted food should be used for seeding new vials and bottles for *growing* flies. Nonyeasted (NY) food has no yeast on it and should be used to *house* flies prior to behavioral studies and for *storing* virgin females and males prior to setting-up crosses.

B. Standard Fly Husbandry

1. Remove necessary number of yeasted bottles or vials from the cold room. Use bottles to grow lots of flies for behavioral, stress or other large experiments. Use vials for smaller numbers of flies in limited scale crosses or other small scale experiments.

2. Before putting in new flies, bottles and vials must be dried 2 hours to overnight in the environmental chamber so that all condensation on the walls evaporates. The food will pull away from the wall of the bottle or vial if they are over-dried. It is poor practice to use over-dried food.

3. Turn on the CO_2. Clean microscope, CO_2 pad and counter with ethanol. Clean before starting, between each genotype and after you are finished. Be sure the CO_2 is on before putting ethanol on the pad.

4. Open CO_2 to pipette, invert bottle or vial, insert pipette along cotton plug and tap bottle/vial gently. Flies will become anesthetized quickly and should fall onto the plug and/or the neck of the bottle/vial.

5. Clic off CO_2 to pipette, remove CO_2 pipette from vial/bottle. Hold inverted bottle/vial over CO_2 pad. Remove plug and gently shake/tap flies onto pad into a pile. Return plug to bottle/vial and set aside.

6. Place anesthetized flies in a row and sort flies according to needs. Short CO_2 times are important. For collecting flies that will be used in behavioral studies, goals are (1) all genotypes experience the same CO_2 exposure and (2) all flies are anesthetized for less than 5 minutes.

7. Set-up new bottles/vials by putting sorted flies from step 6 into dried bottles/vials. Anesthetized flies should be kept on the wall of the bottle/vial. If they fall into the food, many of them will stick there and die. Robust strains such as w[A], CS, etc. will do well with 10 females (♀, see below) per bottle or 3 females per vial. It is good practice to include a comparable number of males (♂, see below). Weaker stocks will need more females, up to as many as 50 per bottle and 15 per vial. When working with a stock that is new to you it is good practice to seed bottles or vials with a range of females (10-25/bottle for example) and then use an optimum number thereafter based on how the various bottles/vials grow.

8. Insert cotton plug, invert new bottle/vial and tap anesthetized flies onto the plug. Lay the bottle/vial on its side, label with genotype and date. First broods (i.e. bottles or vials in which the flies are new parents) are marked with a single slash.

9. Wait for flies to regain locomotor activity. Turn bottles/vials upright and place in environmental chamber to grow.

10. Beginning at around 4 days after seeding, check bottles/vials daily for larval activity. When larval activity is obvious, transfer adults to new bottles/vials (dried appropriately). Label second brood with genotype, date and two slashes.

11. Beginning at around 4 days after seeding the second brood, check bottles/vials daily for larval activity. Discard adults when larval activity is obvious. If necessary, a third brood is possible in some cases.

12. You should expect to see obvious larval activity 4 to 7 days after seeding and obvious pupae 5-10 days after seeding. New adults should begin emerging ~10 days after seeding. Some strains, especially balanced strains, can take up to 4 additional days to emerge. Perfectly seeded bottle/vials will have robust larval activity followed by large numbers of pupae that populate the bottom three-fourths of the wall. Pupae will not typically be in the food or on the plug in these bottles. Large numbers of healthy adults suitable for experiments will emerge from perfectly seeded bottles/vials.

13. Common Problems: If your bottles/vials are too dry or wet (as described below), the resulting adults should not be used for behavioral, stress or gene expression studies. The resulting adults are fine genotype-wise and reproduction-wise, though, and can be used to set-up new bottles/vials as necessary.

a. Food too dry after 4-7 days of new adults in bottle/vial: The food should not be so dry that it detaches from the wall of the bottle of vial and the pupae are in the food. In cases like this, the food was either over-dried, there were not enough females placed in the bottle/vial, or possibly both. If this occurs across several strains that have grown well in the past, it is likely due to over-drying. If it occurs with a subset of strains, it is more likely due to insufficient numbers of females being used for those specific strains. The appropriate fixes are to decrease drying time, add more females, or both.

When you transfer flies from the first to second brood or when clearing the second brood, note the quality of the culture and food. If the food in some bottle/vials is detached from the wall after 7 days, go ahead and transfer/clear the adults and then add ddH_2O (NOT ETHANOL!) to the bottle/vial until the gap between the food and the wall is filled. In many cases this will help the larvae quite a lot and you still might get a decent yield of adults, although they might be delayed a few days due to lack of water.

b. Food too wet after 4-7 days of new adults in bottle/vial: The food should not be so wet that it runs down the wall of the bottle/vial when it is inverted and the pupae are on the plug. If this happens, the food was not dried sufficiently before adults were added, too many adults were added, or possibly both. If this occurs across several strains that have not had this problem in the past, it is likely due to under-drying the food. If it occurs with only a subset of strains, it is more likely due to too many females being added in those specific strains. The fixes are to increase the drying time for bottles/vials, decrease the number of females used, or both.

If you notice that your bottles are too wet when transferring from the first to second brood or when clearing the second brood, you can put a folded Kim wipe in the bottle/vial so that it touches both the food and the plug. This will not result in a miraculous drying of the bottle/vial, but it can convert a bottle/vial that is far too wet into one that can be managed with some care.

C. The Basics of Setting-Up Crosses

1. You will need males (♂, mated or unmated) and females (♀ with a ‘v’ on top, unmated or virgin) for your crosses. Grow bottles or vials as above for strains required to generate males and virgin females. For planning purposes, you can comfortably collect 100 males and/or 50 virgin females from a robust bottle. Likewise, you can probably count on collecting 20 males and 10 virgin females from each well-seeded vial.

2. Around day 10 after seeding, begin to collect virgin females, identified by their light body pigmentation and female genitalia (see below). Typically, one would collect virgin females first thing in the morning, again around noon, and again last thing before leaving for the day.

3. Keep virgin females in nonyeasted vials with no more than 25 females/vial. Label each vial with genotype, date and number collected. Keep collected females in environmental chamber until ready to use. One will often collect virgin females over several days or until a sufficient number of virgin females has been collected. Also, it is convenient to store virgin females in upside-down vials.

4. When sufficient numbers of virgin females have been collected (~10% more than you plan to use) or when it is obvious that you will be able to collect all the virgin females you will need, collect all males into nonyeasted vials needed for your crosses. Males are identified by their male genitalia (see below).

5. Set-out yeasted bottles or vials to warm and dry as described above. On the day of the cross, check all virgin female vials for larvae using the microscope. Any vials with larvae MUST be discarded because at least one of the females has mated. Use only virgin females from vials with no larvae.

6. To set-up a cross, anesthetize the males and check them, anesthetize the virgin females on the same plate and check them, and put appropriate numbers of males and females into yeasted bottles/vials as described in steps B7-B9 above. Handle them thereafter as described in B10-B12 above.

7. Make sure that you know what progeny to expect from your crosses before you set them up.

Simple Ethanol Sedation Assay

A. Day before assay

1. Collect flies (reared for behavioral assays) in groups of 11 (single sex) under brief CO_2 following standard procedures for behavioral assays.

2. Allow flies to recover overnight in non-yeasted food vials in the environmental chamber. It is possible to test a maximum of 24 vials of flies in a single experiment.

3. Dilute ethanol solution as necessary (85% is our standard concentration). ~250 ml of ethanol solution can be stored in a sealed 500ml bottle or other sealed container for a week without a problem. Make ethanol fresh weekly. Diluted ethanol is exothermic and should be stored overnight at room temperature before use.

B. Day of assay

1. For each vial of flies to be tested, you will need (a) a clean, empty food vial; i.e. testing vial, (b) a new Flug, (c) a silicone #4 stopper and (d) 0.9 ml of ethanol solution (85% ethanol is our standard concentration).

2. Turn on humidifier and allow relative humidity in testing room to rise to 55-65%.

3. Have someone else in the lab assign a unique code to each group of vials for each genotype and—IMPORTANTLY—record the code for later. Place coded vials with flies in testing room to acclimate.

3. Label empty testing vials with tape to match codes on fly vials from B.3.

4. Construct a testing log by entering the code for each vial into the Test Log E sheet within the Excel Sedation file SA E EE 6 min SIGMOIDAL 2015.03.02. Use a random or cycling order. Add other pertinent information (% ethanol, sex, etc.) to the Test Log worksheet and print for use during testing.

5. Using the Test Log as a guide, arrange coded food vials with flies and empty testing vials into matching arrays in the testing room. I have found that it is possible to test 6 sets of 4 vials simultaneously, so arrange 24 vials (maximum) in 6 sets or rows containing 4 vials each.

6. Transfer all flies from all food vials into matched/labeled testing vials one at a time and immediately insert Flugs into testing vials until Flugs are a uniform distance below the vial tops. Use the Fluginator to push Flugs down into vials.

7. Time 0 assessment: For each vial individually, grasp with thumb and forefinger, tap gently on the table three times to knock flies to the bottom of the vial, wait 30 seconds

and then count the number of flies that are immobile. Typically, this is 0 or 1 at time 0. Record the number of immobile flies for each vial at time 0 in the printed Testing Log.

8. Hereafter, each row of four vials will be handled as a set at staggered one-minute intervals.

Start timer counting up at time 0 and immediately begin adding 1 ml of ethanol to the Flug in the vials for the first row/set of 4 vials. Add ethanol to the vials at 5 second intervals in the order they will be tested. Add ethanol to the Flugs in a circular motion so that all ethanol is absorbed. When ethanol has been added to all four testing vials in the set, insert a silicone #4 plug in each vial to seal it.

At times 1, 2, 3, 4 and 5 minutes, add 1 ml of ethanol to the second, third, fourth and fifth sets of 4 vials, respectively. Continue inserting #4 stoppers after adding ethanol to each set of 4 vials.

9. At time 6 minutes, test the first set of 4 vials by grasping each vial with thumb and forefinger, tapping gently on the table three times to knock flies to the bottom of the vial, waiting 30 seconds and then counting and recording the total number of flies that are sedated. Flies are scored as sedated if they do not appear to have productive locomotion.

Handle each vial within the set at 5 second intervals. The specific schedule is:

Vial	Tap	Assess
1	6 min 0 s	6 min 30 s
2	6 min 5 s	6 min 35 s
3	6 min 10 s	6 min 40 s
4	6 min 15 s	6 min 45 s

At times 7, 8, 9, 10 and 11 minutes, test the second, third, fourth, fifth and sixth sets of vials, respectively, as done for the first set.

10. At time 12 minutes, test the first set of 4 vials again as described in B9 and continue testing the second, third, fourth, fifth and sixth sets of vials at 13, 14, 15, 16 and 17 minutes, respectively.

Continue testing flies as described in B9 and B10 for 60 minutes (single ethanol exposure) or 90 min (2 ethanol exposures, rapid tolerance).

Clean-up is (a) turn off humidifier, (b) remove #4 plugs for washing and reuse, (c) discard Flugs containing ethanol, (d) dispose of flies in morgue, (e) place testing vials on sink to be washed, (f) remove any trash from and straighten up testing room and (g) turn off light in testing room.

11. Enter the total number of flies in each vial in the Test Log within the Excel worksheet. Percent Active flies will be automatically calculated and graphed below the

Test Log. Press ‘Ctrl + s’ to calculate ST50s for each vial and sort the data by group in the Sorted Data worksheet.

12. Note any flagged data in Sorted Data worksheet. Consider excluding data that looks qualitatively poor.

Internal Ethanol Content

Use pre-chilled solutions throughout assay for consistency

1. Grow/collect flies and prepare Flugged vials as you normally would for eRING assays. Use 11 flies/vial and typically 1 vial/genotype with 3-5 vials total per test. Expose one group to ddH_2O (0 minutes) and other groups to ethanol during SSAs for 15-45 minutes or other times as appropriate.

2. After each water or ethanol exposure, transfer flies to labeled 1.5 ml snap-cap tubes and store at -70°C. Continue water and ethanol exposures until you have a complete set of frozen flies from each genotype at each time-point.

3. Homogenize frozen flies with drill/pestle in 200 µl ice-cold ddH_2O for 30 seconds. Keep flies on ice before and after homogenization.

4. Centrifuge homogenized flies at maximum speed at 4°C for 20 minutes. Prepare 25 mM standard by adding 4.37 µl of 100% ethanol (17.16 M) to 2996 µl ice-cold ddH_2O. Prepare remaining standards using the table below. Store standards on ice.

5. Transfer 100 µl of clear supernatant to new labeled 1.5 ml snap-cap tube. Lipid or other crud will stick to the outside of the pipette tip. DO NOT TOUCH PIPPETTE TIP TO NEW TUBE! Store 100 µl supernatants on ice.

6. Add 300 µl of cold ethanol reagent to 1.5 ml snap-cap tubes for each sample (in triplicate, 3 tubes/sample) and standard (in duplicate, 2 tubes/standard).

7. Add 10 µl of each sample supernatant and standard to the corresponding tube from step 6. Mix by single pulse vortexing.

8. Incubate at 30°C in heat block for 5 minutes.

9. Read absorbance of 100 µl of each reaction at 340 nm and print out results.

10. Final ethanol concentration in samples determined in Internal Ethanol BLANK Excel sheet as:

mM interpolation x (200 µl + [# flies x µl/fly])/(# flies x µl/fly)

Fly water volume in µl is determined as indicated on next page. Each vial of flies is an N of one.

Notes:

1. Standards

Standard	Volume of ddH_2O	Volume of 25 mM
0 mM	1000 µl	0
2 mM	920 µl	80 µl
4 mM	840 µl	160 µl
6 mM	760 µl	240 µl
8 mM	680 µl	320 µl
10 mM	600 µl	400 µl

2. Alcohol Reagent: Dilute per manufacturer's instructions. Good for at least 2 weeks at 4°C.
3. Reaction is maximal at ~2 minutes and has a stable product (i.e. A340) out to at least 12 minutes.
4. Use all cold reagents for consistency.
5. A 30 minute exposure to vapor from 2 mL of 50% ethanol in a SSA should lead to a final internal ethanol concentration of 100-150 mM in control flies.

Fixation Protocol for whole adult *Drosophila* brains

Dissection:

1. Anesthetize flies and place adults of the appropriate age, genotype and gender into a three well dish on ice

2. Fill another three well dish with PBT and place it under the dissecting microscope

3. Place a 0.5mL snap cap tube containing 500µL of freshly prepared 4% paraformaldehyde on ice

4. With gentle, SHARP forceps, remove the brain from the head cuticle in the PBT solution. Place it into the 4% paraformaldehyde on ice

5. Repeat for the remaining flies

Staining: 1-20 tubes at a time

Day 1 (~3 hours)

1. Place the 0.5mL tube containing brains in 4% paraformaldehyde onto a nutator. Allow the brains to fix for 20 min at room temperature

2. Remove the tube from the nutator and place it into a tube rack at room temperature. Allow the brains to settle to the bottom of the tube. Use a P-200 pipet to remove the paraformaldehyde. Dispose appropriately.

3. Add 0.5mL PBT to the tube. Close and invert the tube. Allow the brains to settle to the bottom. Remove the PBT. Repeat once more (=2 quick washes at room temp)

4. Add 0.5mL PBT to the tube. Place on nutator to wash for 20 min. Repeat twice (=3 20min washes at room temp)

5. Remove the PBT from the brains and add 0.5mL block solution (5% NGS). Place brains on nutator to block for atleast 30 min at room temp

6. Remove block solution from the brains. Add the primary antibody solution. Place on nutator at 4°C for 2 nights.
   ** can be increased to 1 week

Day 3 (~1.5 hours)

7. Remove primary antibody and store it at 4°C. The antibody can be reused roughly three more times

8. Add 0.5mL PBT to the tube. Close and invert the tube. Allow the brains to settle to the bottom. Remove the PBT. Repeat once more (=2 quick washes at room temp)

9. Add 0.5mL PBT to the tube. Place on nutator to wash for 20 min. Repeat twice (=3 20min washes at room temp)

10. Remove PBT. Add secondary antibody. Place on nutator at 4°C for 2 nights.
** can be increased to 1 week

Day 5 (~1.5 hours)

11. Remove the secondary antibody and discard

12. Add 0.5mL PBT to the tube. Close and invert the tube. Allow the brains to settle to the bottom. Remove the PBT. Repeat once more (=2 quick washes at room temp)

13. Add 0.5mL PBT to the tube. Place on nutator to wash for 20 min. Repeat twice (=3 20min washes at room temp)

** DAPI can be added to one of the 20 min washes to stain nuclei for analyses such as counting cell numbers

14. Remove PBT and add 200µL SlowFade. Allow brains to settle in SlowFade at 4°C

** brains can be left at this stage for up to 1 week at 4°C

Mount brains:

1. Use a P-200 pipet tip to transfer the brains from the tube and transfer them onto a mounting slide. Avoid adding excess SlowFade. Excess SlowFade can be removed with a P-200 pipet or kimwipe.

2. Using forceps, carefully align the brains for ease of imaging.

3. Arrange two broken coverslips on the microscope slide to form a bridge around the brains. This prevents the brains from becoming too compressed under the top coverslip. For adult brains, use broken no. 2 coverslips

4. Gently place a no. 1 coverslip on top of the bridge to cover the brains

5. Slowly pipet SlowFade, starting from one side of the coverslip, until the sample is covered.

6. Seal the edges of the coverslip with nail polish. Store at 4°C in a dark slide holder

** mounted slides are good for several months at 4°C and several years (3+) at -20 or -80°C

7. Image using multi-photon confocal microscope

Notes:

<u>0.3% (vol/vol) PBT solution</u>:
Add 1.5 Triton-X 100 to 498.5mL 1 X PB. Store at room temperature

<u>4% (vol/vol) paraformaldehyde</u>:
In a 0.5mL snap cap tube, add 100µL 20% w/v paraformaldehyde to 400µL PBT. Prepare fresh and place on ice.

<u>5% (vol/vol) normal goat serum (NGS):</u> Add 50µL normal goat serum to 950µL PBT. Store this block solution for short periods at 4°C (24 hour max)

<u>Primary antibody:</u> Dilute the primary antibody in freshly prepared 5% NGS. A 0.5mL tube requires 400µL of diluted antibody. Diluted primary antibodies can be reused up to 3 times. Store in 4°C for up to 1 month

<u>Secondary antibody</u>: Dilute the secondary antibody in freshly prepared 5% NGS. A 0.5mL tube required 400µL of diluted antibody. Prepare fresh and discard after use

Primary Antibody Information

- Stored in -80°C

Primary Antibody	Mono/Poly?	Source	Dilution - whole brain
Mouse Anti-Repo	Monoclonial	Developmental Studies Hybridoma Bank	1:100
Mouse Anti-GFP	Monoclonial	Fischer	1:100
Rat Anti-axotactin	Monoclonial	Barry Ganetzky (1999)	??
Guinea pig Anti-Cp1	Polyclonal	Dolph	1:250
Rabbit Anti-Cp1	Polyclonal	Kuo	1:20
Mouse anti-lacZ	Monoclonial	Developmental Studies Hybridoma Bank	1:20
Rabbit anti-lacZ	Polyclonal	Fischer	1:25
Rabbit anti-Tdc2	Polyclonal	Covalab (Pech,2013)	1:200
rabbit anti-VMAT	??	Krantz (Romero-Calderon, 2008)	1:2000
rabbit anti-Tbh	??	Budnik (Koon, 2011)	1:500
mouse anti-Th	Monoclonial	Developmental Studies Hybridoma Bank	??
rabbit anti-Mef2	polyclonal	Bruce Paterson	1:10,000
mouse anti-elav	Monoclonial	Developmental Studies Hybridoma Bank (supernant)	1:500

Secondary Antibody Information

- Stored in 4°C

Secondary Antibody	Fluorophore	Source	Cat. Number
Rabbit Anti-Mouse	Alexa 488 (Green)	ThermoFisher	A-11059
Goat Anti-Guinea Pig	Alexa 568 (red)	ThermoFisher	A-21450
Chicken Anti-Rabbit	Alexa 647 (red)	ThermoFisher	
Goat anti-mouse	Alexa 647 (red)	ThermoFisher	A-21235

Quantitative measurement of β-gal activity in flies

1) Homogenize (with drill/pestle in 1.5 ml snap-cap tubes) 10 lacZ-expressing flies of desired age and gender in 250 µl of extraction buffer (1X PBS with 1X protease inhibitor cocktail) for 25 seconds.
   - if using rotating spec, can only test 6 samples at a time (1 every 10 seconds for a minute)
2) Add 500 µl extraction buffer to each tube from step 1, mix by vortexing for 30 sec
3) Centrifuge extracts for 5 min at 14,000 rpm at room temperature
4) Transfer supernatants from step 3 into new labeled 1.5 ml snap-cap tubes
5) Set spectrophotometer at 562 nm.
6) Add 900 µL of 1 mM CPRG to 100 µl of water to a plastic cuvette for the blank. Set spec reference with the blank (water sample + CPRG).
7) Transfer 100 µl of each fly extract to an individual plastic cuvette. Add 900 µL of 1 mM CPRG to each of the fly extracts. Stagger the addition of CPRG to coincide with the order and timing of absorbance measurements.
8) Record absorbance of each cuvette every minute for 6 mins

<u>CPRG</u>

*CPRG is more sensitive than X-GAL and product measurement at 562 not interfered with by fly pigment

*CPRG solution is only good for 24 hours

Final volume of 1mM CPRG (mL)	CPRG added (g)
10	0.005
15	0.008
35	0.0205

<u>Protease inhibitor cocktail</u>

Stored in the -20

Sigma (P8340)

Simple Locomotor Assay

A. Day before assay

1. Collect experimental flies (reared for behavioral assays) in groups of 11 (single sex) under brief CO_2 following standard procedures for behavioral assays. A maximum of 24 vials, 6 groups of 4, can be tested during the assay. You will need to collect 4 additional vials of controls flies to be the vortexed group.

2. Allow flies to recover overnight in non-yeasted food vials in the environmental chamber.

B. Day of assay – Flugged Vial Experiment

1. Turn on humidifier(s) and allow relative humidity in testing room to become/remain between 55-65%.

2. Prior to the experiment, print the locomotor test log sheet. For each vial of flies to be tested, you will need: a clean, empty testing vial and a new Flug

3. Transfer flies from all food vials into matched testing vials one at a time and immediately insert Flugs into testing vials until the bottom of the Flugs are just below the vial tops. For vials used for vortexing, use “The Fluginator” to force Flugs further down into vials until the tape is in contact with the vial.

4. Vortex the control vials for 4 minutes. Up to four vials will be vortexed at once. In order to prevent vial destruction during the vortex, use a couple of rubber bands on each vial and a few rubber bands to hold all four vials together. (See Below)

5. Have someone else in the lab assign a unique code to each vial for each genotype and—IMPORTANTLY—record the code for later*. Place coded vials with flies in testing room to acclimate.

6. Label empty testing vials to match codes on fly vials from B5

7. Using the Test Log as a guide, arrange coded food vials with flies and empty testing vials into matching arrays in the testing room. It is possible to test 6 sets of 4 vials simultaneously, so arrange 24 vials (maximum) in 6 sets or rows containing 4 vials each. Then transfer flies from food vials to the matching testing vials.

8. Time 0 assessment (# dead): For each vial individually: grasp with thumb and forefinger, tap the vial on the table three times to knock flies to the bottom of the vial, wait 30 seconds and then count the number of flies that are dead (no movement whatsoever). Record this number of flies for each vial at time 0 in the printed Testing Log.

9. Hereafter, each row of four vials will be handled as a set at staggered one-minute intervals.

Start timer counting up at time 0 upon completion of recording the number of dead flies.

10. At time 6 minutes, test the first set of 4 vials by grasping each vial individually with thumb and forefinger, tapping on the table three times to knock flies to the bottom of the vial. Then wait 30 seconds to count and record the total number of flies that are on the bottom.

The specific schedule is:

Vial	Tap	Assess
1	6 min 0 s	6 min 35 s
2	6 min 5 s	6 min 40 s
3	6 min 10 s	6 min 45 s
4	6 min 15 s	6 min 50 s

At times 7, 8, 9, 10 and 11 minutes, test the second, third, fourth, fifth and sixth sets of vials, respectively, as done for the first set.

11. At time 12 minutes, test the first set of 4 vials again as described in B10 and continue testing the second, third, fourth, fifth and sixth sets of vials at 13, 14, 15, 16 and 17 minutes, respectively.

Continue testing flies as described in B10 and B11 for 60 minutes.

12. Record the total number of flies in each vial on the locomotor assay sheet.

13. Fill out the locomotor assay file. Percent Active flies will be automatically calculated. Compile the data as directed on the sheet to calculate aggregate percent active and fraction alive for each vial and sort the data by group in the Sorted Data worksheet.

Clean-up is (a) turn off humidifier, (b) discard vials containing flies, (c) remove any trash from and straighten up testing room, and (d) turn off light in testing room.

Tyramine feeding assay

1. Make tyramine vials. Pipet 100mL of 100 mg/mL of tyramine onto vials. Tyramine will readily dissolve in diH_20. Control vials only contain 100 mL of diH_20

2. Let vials dry in environmental chamber overnight

3. Sedation, sort and place 11 female flies in each tyramine or vehicle treated vial (as you would for a sedation assay). Store vials food-side down in environmental chamber for two nights

Yohimbine administration protocol

Day before experiment:

1. Collect flies (10-20) and place in food vials in the environment chamber

Day of experiment:

2. Place 5 pieces of Whatman filter paper in bottom of vial

3. Administer drug (400uL??) to filter paper:
    - Control = 5% sucrose
    - Drug = 5% sucrose, 10mg/mL yohimbine

4. Flip flies from food vials into vials with treatment

5. Let flies consume treatment for 2 hours

6. Test flies in sedation assay

For a 16 vial experiment: Make 8mL sucrose solution

- 5% sucrose = 8mL diH_20, 0.4g sucrose

4mL of sucrose solution = control
4mL of sucrose solution = Add 10mg/mL yohimbine

- Add 40mg yohimbine to the 4mL of 5% sucrose solution

VITA

Kristen Mary Lee was born on April 12th, 1992 in Vorhees, New Jersey and is a United States Citizen. She attended Wagner College (Staten Island, New York) from 2010 to 2014 and received her Bachelor of Science in Biopsychology, where she was awarded the Biopsychology Award and was an Academic All-American Division 1 athlete. She came to Virginia Commonwealth University in 2014 in the Biomedical Science Doctoral Portal and entered the Neuroscience Program. She joined Dr. Mike Grotewiel's laboratory, which is in the Department of Human and Molecular Genetics. She received her NRSA F31 pre-doctoral fellowship from the National Institute of Alcohol Abuse and Alcoholism in 2018.